Substrate Analogues As Mechanistic Probes For 3-Deoxy-D-*Arabino*-Heptulosonate 7-Phosphate Synthase And 3-Deoxy-D-*Manno*-Octulosonate 8-Phosphate Synthase

A dissertation presented in partial fulfillment of the requirements for the degree

of

Doctor of Philosophy

in

Biochemistry

at Massey University, Palmerston North,

New Zealand

Meekyung Ahn

2007

For Cem

ABSTRACT

Substrate analogues as mechanistic probes for 3-deoxy-D-*arabino*-heptulosonate 7-phosphate synthase and 3-deoxy-D-*manno*-octulosonate 8-phosphate synthase

3-Deoxy-D-*arabino*-heptulosonate 7-phosphate synthase (DAH7P synthase) catalyses the condensation reaction between phosphoenolpyruvate (PEP) and the four-carbon monosaccharide D-erythrose 4-phosphate (D-E4P). 3-Deoxy-D-*manno*-octulosonate 8-phosphate synthase (KDO8P synthase) catalyses a closely related reaction of PEP with the five-carbon monosaccharide D-arabinose 5-phosphate (D-A5P). These enzymes are two functionally unrelated enzymes that share many mechanistic and structural features.

D-Threose 4-phosphate (D-T4P), L-threose 4-phosphate (L-T4P), D-arabinose 5-phosphate (D-A5P), D-lyxose 5-phosphate (D-L5P), and L-xylose 5-phosphate (L-X5P) have been prepared synthetically or enzymatically to provide insights into aspects of metal requirement and substrate specificity. These compounds were different stereoisomers of natural substrates D-E4P and D-A5P. The results presented in this thesis show that D-T4P and L-T4P (C2 and C3 stereoisomers of D-E4P) are substrates for the DAH7P synthases from *E. coli* and *P. furiosus*. For *N. meningitidis* KDO8P synthase, natural substrate D-A5P and L-X5P (the C4 epimer of D-A5P) were substrates, whereas D-L5P, the C3 epimer of D-A5P, was not. These observations show that the configuration of the C2 and C3 hydroxyl groups is not important for DAH7P synthase reaction, but having the correct configuration at these positions is critical for KDO8P synthase.

The analysis of the interaction of D-T4P and L-T4P with DAH7P synthase, and D-A5P, D-R5P, and L-X5P reveals previously unrecognised mechanistic differences between the DAH7P synthase-catalysed reaction and that catalysed by the closely related enzyme, KDO8P synthase.

ACKNOWLEDGEMENTS

First of all, I would like to great thank to my supervisor, Associate Professor Emily Parker, for giving me the opportunity to study this project at Massey University. I am also grateful to her for lots of support in the synthetic chemistry lab and the molecular biology lab, and for endless encouragement during the course of this study.

I appreciate co-supervisor Professor Geoffrey Jameson's support during my study. I especially thank him for proof reading parts of this thesis in his busy time. I am particularly grateful to Dr Gillian Norris for her kindness in giving me the opportunity of working in the molecular biology lab. I also thank to Dr Gillian Norris and people in the molecular biology lab for helping me to come back to the lab during my difficult time.

I wish to thank to all members of Emily Parker's group (Shikimate Group) past and present. Dr Rachel Williamson, for her kindness when I just started the course at Massey University. Dr Charlie Matthews and Dr Mattihas Rost for sharing their knowledge and skills in the biology lab and the synthetic chemistry lab. I specially thank Dr Linley Schofield for spending her time for listening to my complaints and sharing her yummy food during my study. I am particularly grateful to Dr Linley Schofield, Dr Fiona Cochrane, and Scott Walker for proof reading parts of this thesis. Thank to Jenness Guthrie, Ben Mulchin, Amy Pietersma, and Celia Webby for such a joyful companionship.

I also would like to thank IFS for use of all equipment and facilities that have been provided during my project. I also thank to Massey University for the opportunity of a Vice Chancellor's Doctoral Scholarship during the study.

Finally, I would like to thank to my family for their endless love, support, and encouragement from Korea for the many years needed to complete this study. I also would like to be grateful to Ingeborg and Cem. I cannot find words how much I appreciate their love and support. It would not be possible to complete this thesis without the love and encouragement from my family and my friends.

SUBSTRATE ANALOGUES AS MECHANISTIC PROBES FOR 3-DEOXY-D-*ARABINO*-HEPTULOSONATE 7-PHOSPHATE SYNTHASE AND 3-DEOXY-D-*MANNO*-OCTULOSONATE 8-PHOSPHATE SYNTHASE

Table of Contents

Chapter Six: MECHANISTIC INSIGHT INTO 3-DEOXY D-*ARABINO* HEPTULOSONATE 7-PHOSPHATE SYNTHASE AND 3-DEOXY D-*MANNO*-OCTULOSONATE 8-PHOSPHATE SYNTHASE

Chapter Seven: EXPERIMENTAL

List of Figures

Chapter One: INTRODUCTION

Chapter Two: PREPARATION OF AND PRELIMINARY STUDIES WITH D-ERYTHROSE 4-PHOSPHATE AND ITS ANALOGUES

Chapter Three: PREPARATION OF D-ARABINOSE 5-PHOSPHATE AND ITS ANALOGUES

Chapter Four: INVESTIGATION INTO THE ENZYME-SPECIFIC REACTION WITH 3-DEOXY-D-*ARABINO*-HEPTULOSONATE 7-PHOSPHATE SYNTHASE USING PHOSPHORYLATED MONOSACCHARIDE ANALOGUES

List of Tables

Abbreviations

D-A5P	D-arabinose 5-phosphate
AHBA	3-amino 5-hydroxybenzoate
ATP	adenosine triphosphate
BSA	bovine serum albumin
BTE	boron trifluoride etherate
BTP	1,3-bis(tris(hydroxymethyl)-methylamino)propane
DAH7P	3-deoxy-D-*arabino*-heptulosonate 7-phosphate
D-DAO8P	3-deoxy-D-*altro*-octulosonate 8-phosphate
3-deoxyA5P	3-deoxy arabinose 5-phosphate
4-deoxyA5P	4-deoxy arabinose 5-phosphate
2-deoxyE4P	2-deoxy erythrose 4-phosphate
3-deoxyE4P	3-deoxy erythrose 4-phosphate
2-deoxyR5P	2-deoxy ribose 5-phosphate
L-DGO8P	3-deoxy-L-*gulo*-octulosonate 8-phosphate
D-DLH7P	3-deoxy-D-*lyxo*-heptulosonate 7-phosphate
L-DXH7P	3-deoxy-L-*xylo*-heptulosonate 7-phosphate
DHQ	3-dehydroquinate
DHS	3-dehydroshikimate
DPA	dipicolinic acid
DTNB	5,5′-dithio-bis(2-nitrobenzoate)
EDTA	ethylenediaminetetra acetic acid
EPSP	5-enolpyruvyl shikimate 3-phosphate
D-E4P	D-erythrose 4-phosphate
ESI	negative ion electrospray mass spectrometry
ESI-TOF MS	time-resolved electrospray ionisation mass spectrometry
EtOH	ethanol

D-F6P	D-fructose 6-phosphate
D-Gal6P	D-galactose 6-phosphate
G3P	D-glycerol 3-phosphate
G^- bacteria	Gram negative bacteria
G^+ bacteria	Gram positive bacteria
D-Glu6P	D-glucose 6-phosphate
glyphosate	N-(phosphonomethyl)glycine isopropylamine salt
GMH	L-*glycero*- D-*manno*-heptose
homophosphonate	4,5-dideoxy-5-phosphono-D-erythro-pentose
iminoE4P	imino erythrose 4-phosphate
KDO	3-deoxy- D-*manno*-octulosonate acid
KDO8P	3-deoxy-D-*manno*-octulosonate 8-phosphate
K_M	Michaelis constant
K_i	inhibition constant
LAH	lithium aluminum hydride
LPS	lipopolysaccharide
NAD^+	nicotinamide adenine dinucleotide
NADH	nicotinamide adenine dinucleotide reduced form
D-L5P	D-lyxose 5-phosphate
PABA	*para*-aminobenzoate
PEP	phosphoenolpyruvate
phosphonate	4-deoxy-4-phosphono-D-erythro-tetrose
P_i	inorganic phosphate
D-R5P	D-ribose 5-phosphate
D-T4P	D-threose 4-phosphate
L-T4P	L-threose 4-phosphate
S7P	sedoheptulose 7-phosphate
tlc	thin layer chromatography
UV	ultra-violet
THF	tetrahydrofuran
D-X5P	D-xylose 5-phosphate
L-X5P	L-xylose 5-phosphate

DAH7P synthase	3-deoxy-D-*arabino*-heptulosonate 7-phosphate synthase
DHQase	dehydroquinase
DHQS	3-dehydroquinate synthase
EPSP synthase	5-enolpyruvyl shikimate 3-phosphate synthase
G3P dehydrogenase	D-glycerol 3-phosphate dehydrogenase
KDO8P synthase	3-deoxy-D-*manno*-octulosonate 8-phosphate

A. aeolicus	*Aquifex aeolicus*
A. pyrophilus	*Aquifex pyrophilus*
B. subtilis	*Bacillus subtilis*
E. coli	*Escherichia coli*
H. pylori	*Helicobacter pylori*
M. tuberculosis	*Mycobacterium tuberculosis*
P. furiosus	*Pyrococcus furiosus*
S. cerevisiae	*Saccharomyces cerevisiae*
T. maritima	*Thermotoga maritima*
N. meningitidis	*Neisseria meningitidis*

Publication

Parts of chapters two, four, and six in this thesis have been published.

Ahn, M., Pietersma, A. L., Schofield, L. R., and Parker, E. J. Mechanistic divergence of two closely related enzyme-catalysed reaction *Organic and Biomolecular Chemistry* **2005,** 3, 4046-4049.

Chapter One

INTRODUCTION

1.1. The Shikimate Pathway

The shikimate pathway is the biosynthetic pathway responsible for producing aromatic compounds. This pathway utilises D-erythrose 4-phosphate (D-E4P) and phosphoenolpyruvate (PEP) to generate chorismate *via* seven enzyme-catalysed steps (Figure 1.1). [1,2]

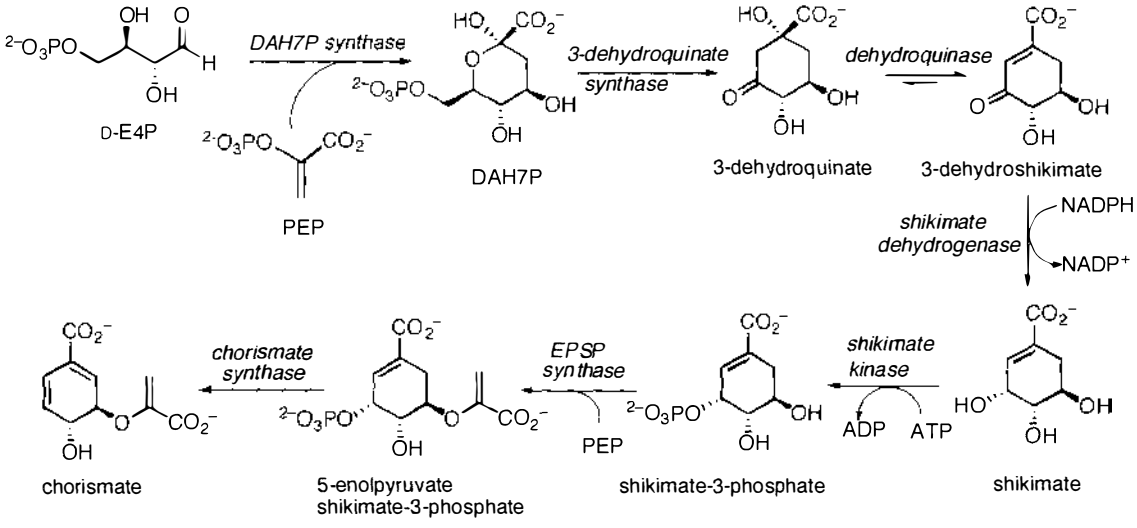

Figure 1.1. The shikimate pathway

Chorismate is the precursor for the aromatic amino acids, tryptophan, phenylalanine, and tyrosine (Figure 1.2)[1,2] and for many other important aromatic compounds, such as ubiquinone and *para*-aminobenzoate (PABA, Figure 1.2).[3] In some organisms, there is an alternative version of the shikimate pathway that uses imino-D-erythrose 4-phosphate (iminoE4P) as a starting material. This pathway gives rise to 3-amino-5-hydroxybenzoate (AHBA, Figure 1.2), the precursor of the ansamycin antibiotics.[4]

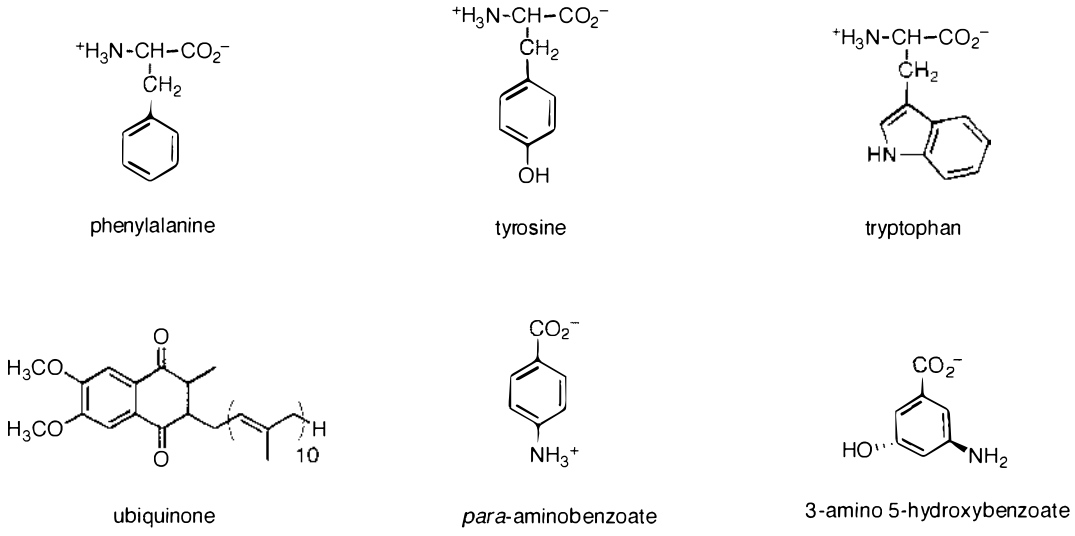

Figure 1.2. Aromatic compounds derived from the shikimate pathway

The history of the shikimate pathway

The shikimate pathway is named after shikimic acid, which was first isolated from *Illicium religiosum*, shikimi-no-ki (star anise tree) in 1885.[5] However, the structure and absolute stereochemistry of shikimic acid were not determined until the 1930s.[6-11] It was not until the 1950s that the structure of shikimic acid was noted to be similar to that of aromatic compounds and that shikimic acid was identified as an important intermediate

in aromatic biosynthesis.[12-14] 3-Dehydroquinate (DHQ),[15] 3-dehydroshikimate (DHS),[16] shikimate 3-phosphate,[17] 5-enolpyruvyl shikimate 3-phosphate (EPSP),[18] and chorismate[19] were all identified as intermediates leading to aromatic amino acids. The two starting compounds of the pathway, PEP and D-E4P, were identified by the condensation of the two compounds to give 3-deoxy-D-*arabino*-heptulosonate 7-phosphate (DAH7P) in the presence of an *Escherichia coli* cell-free extract.[20,21]

Exploration of the shikimate pathway for inhibitor design

The shikimate pathway is present in plants, microorganisms, and some parasites, but not in mammals.[1,2,22-24] Mammals obtain their aromatic compounds from their diet, whereas aromatic compounds in plants and microorganisms, including the three aromatic amino acids found in proteins, are produced *via* the shikimate pathway.[1] Due to the vital role of shikimate pathway end products in protein synthesis and other essential biological processes, inhibitors of the enzymes in the shikimate pathway may prevent growth or virulence of microorganisms or plants. An example of this is the potent action of the herbicide Roundup®. The active ingredient of Roundup® is glyphosate (*N*-(phosphonomethyl)glycine), which inhibits the sixth enzyme, 5-enolpyruvyl shikimate 3-phosphate synthase (EPSP synthase), of the shikimate pathway.[25] As well, glyphosate has been shown to inhibit the growth of several apicomplexan parasites that cause malaria and toxoplasmosis.[22] Therefore, the pathway is considered a potential target for the development of new antimicrobial and antiparasitic compounds and of non-toxic herbicides.[26]

1.2. DAH7P Synthase

The enzyme 3-deoxy-D-*arabino*-heptulosonate 7-phosphate synthase (DAH7P synthase, EC 2.1.5.54) catalyses the first committed step in the shikimate pathway.

DAH7P synthase catalyses an aldol-like condensation reaction between D-E4P and PEP to give the seven-carbon sugar, DAH7P, and inorganic phosphate (P_i) (Figure 1.3). There is a similar enzyme, 3-deoxy-D-*manno*-octulosonate 8-phosphate synthase (KDO8P synthase, EC 2.1.5.55), which catalyses a closely related reaction to DAH7P synthase. KDO8P synthase catalyses the condensation of the five-carbon sugar, D-arabinose 5-phosphate (D-A5P), and PEP to form KDO8P (Figure 1.3). More details of KDO8P synthase and its relationship to DAH7P synthase will be discussed in section 1.3.4.

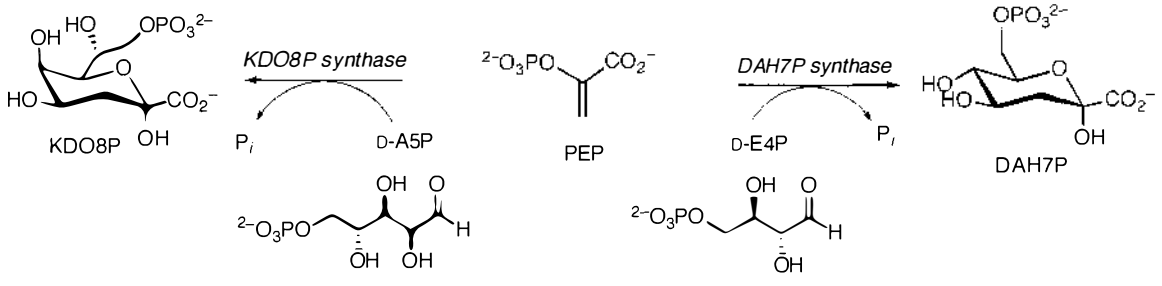

Figure 1.3. Enzymatic reactions catalysed by DAH7P and KDO8P synthases

1.2.1. Feedback regulation of DAH7P synthase

In *E. coli*, three DAH7P synthase isozymes are present and each isozyme is subject to feedback regulation by one of the three aromatic amino acids.[27-29] These three isozymes are denoted as DAH7P(Phe) synthase, DAH7P(Trp) synthase, and DAH7P(Tyr) synthase, and they are encoded by the genes *aroG*, *aroH*, and *aroF*, respectively.[30-34] Feedback inhibition of DAH7P synthase isozymes has been shown to be the major regulatory mechanism for the entire shikimate pathway.[35] Total cellular DAH7P synthase activities are not equally distributed between the three isozymes. DAH7P(Phe) synthase in *E. coli* accounts for about 79 % of the total enzyme activity, compared to DAH7P(Trp) synthase (20 %) and DAH7P(Tyr) synthase (1 %).[36] Therefore, DAH7P(Phe) synthase has been the major focus of research studies to date.[36,37] Additionally, in plants, the shikimate pathway is responsible for 20 – 30 % of the carbon flux, suggesting that the first step of the pathway, DAH7P synthase, is important in the control of cellular carbon flux through the pathway.[34]

There are some DAH7P synthase enzymes that are not inhibited by aromatic amino acids.[38] The latest functional studies of the *Pyrococcus furiosus* DAH7P synthase,[39] for instance, have found that tryptophan, phenylalanine, and tyrosine are not inhibitors of this enzyme. This enzyme, therefore, differs from the other DAH7P synthases that are inhibited by one of these amino acids.[1] The lack of feedback inhibition of the *P. furiosus* enzyme can be explained by absence of regulatory domains on the *P. furiosus* enzyme. The structural studies and phylogenetic relationship of DAH7P synthases and the similar KDO8P synthases will be described later in this chapter.

1.2.2. Metal dependence of DAH7P synthase

In early studies on metal dependency, the sensitivity of the enzyme to the presence of metal ions and to the metal chelator EDTA was noted. In these studies, some enzyme preparations were found to be inhibited by chelating agents and reactivated by metal ions,[40-42] whereas others were unaffected by either the addition of chelating agents or metals.[43,44] However, the studies were not clear and were confused due to an abundance of conflicting evidence.[45] For example, the DAH7P synthase from *Bacillus subtilis* did not appear to require a divalent metal ion but the three *E. coli* isoenzymes were activated by a metal cofactor.[45,46] In more recent studies, including those on the *B. subtilis* and *Helicobacter pylori* enzymes, it was shown that a divalent metal ion is required for enzymatic activity.[47,48] In the study of *B. subtilis*, dipicolinic acid (DPA) was used as a strong metal-chelating agent.[47] Using DPA, the metal-bound enzyme was inactivated and the inactivated enzyme could be reactivated by the addition of divalent metal ions, Zn^{2+}, Cd^{2+}, Cu^{2+}, Mg^{2+}, Fe^{2+}, Co^{2+}, Ni^{2+}, or Mn^{2+}.

While DAH7P synthase appears to have an absolute requirement for the presence of a divalent metal ion, there is considerable variation in the ability of different metal ions to activate the enzyme. In 1991, Stephens and Bauerle reported on the specific activation of the three *E. coli* isozymes with a number of divalent metal ions.[46] The order of activity of the three reactivated *E. coli* isozymes with the different metal ions was the following: $Mn^{2+} > Cd^{2+}$, $Fe^{2+} > Co^{2+} > Ni^{2+}$, Cu^{2+}, $Zn^{2+} >> Ca^{2+}$. Interestingly, although Mn^{2+} showed the highest activity with enzyme, enzyme-bound Mn^{2+} is readily

replaced by other metal ions. In contrast, the Fe^{2+}, Co^{2+}, and Zn^{2+} enzyme complexes are considerably less labile. These workers suggested that Fe^{2+} and perhaps Zn^{2+}, were the preferred metal cofactors *in vivo* based on the presence of these two metals before removal by chelation, on the high apparent affinity of the enzymes for these metal ions, and on their high bioavailability. They also observed a cooperative interaction between metal and D-E4P binding to the enzyme and a dependence of $K_M^{D\text{-}E4P}$ on the identity of the metal ion. For example, $K_M^{D\text{-}E4P}$ for the enzyme-Mn^{2+} complex was reported to be 170 μM, whereas the Fe^{2+}, Co^{2+}, and Zn^{2+} enzymes had $K_M^{D\text{-}E4P}$ values of 67 μM, 36 μM, and 16 μM, respectively. The nature of the activating metal ion appeared to have no significant effect on the interaction between PEP and DAH7P(Phe) synthase.

Recently, the *H. pylori* DAH7P synthase has been tested with a variety of divalent metals.[48] In this study, it was observed that the Co^{2+}-bound enzyme had the highest enzyme activity, whereas the Mn^{2+}, Zn^{2+}, Cd^{2+}, and Ni^{2+} enzymes had 76 %, 5 %, 2 %, and 1%, of the Co^{2+} activated enzyme activity, respectively. The results suggested that the preferred metal ion was Co^{2+} in the enzyme assay, whereas Zn^{2+}, Cd^{2+}, and Ni^{2+} were relatively poor cofactors. Thus, all DAH7P synthases characterised to date have been shown to require a divalent metal ion for enzymatic activity.

1.2.3. Mechanistic studies on DAH7P synthase

The first step of the shikimate pathway is the condensation of the four-carbon sugar D-E4P and the three-carbon compound PEP to give a seven-carbon sugar DAH7P and P_i catalysed by the enzyme DAH7P synthase (Figure 1.4).

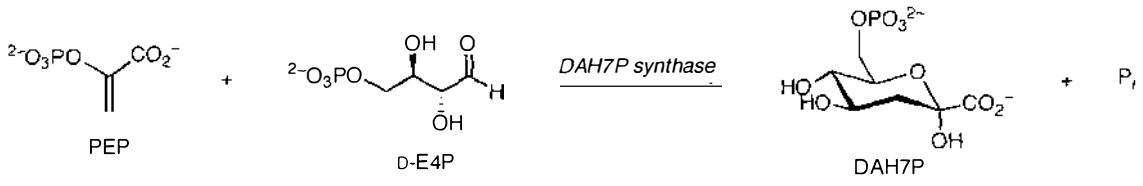

Figure 1.4. DAH7P synthase-catalysed reaction

While many details of the reaction mechanism for the DAH7P synthase condensation reaction are still unclear, several studies have provided valuable information. Analysis of the products obtained in the reaction using stereospecifically labelled PEP have shown that the addition of PEP to D-E4P proceeds stereospecifically with the *si* face of PEP attacking the *re* face of D-E4P to produce a seven-carbon deoxy sugar of the *arabino* configuration.[49,50] In addition, labelling studies have shown that, unlike many other PEP-utilising enzymes, the phosphate of PEP is directly released by breakage of the C–O bond rather than the P–O bond of PEP.[51,52] It has also been demonstrated that the reaction mechanism is ordered sequential and that PEP is the first substrate to bind to the enzyme and DAH7P is the last product to leave.[53-55] Based on these observations, several mechanisms have been proposed. Two possible mechanisms are shown in Figure 1.5. These differ by the order in which water adds to PEP and PEP adds to D-E4P.

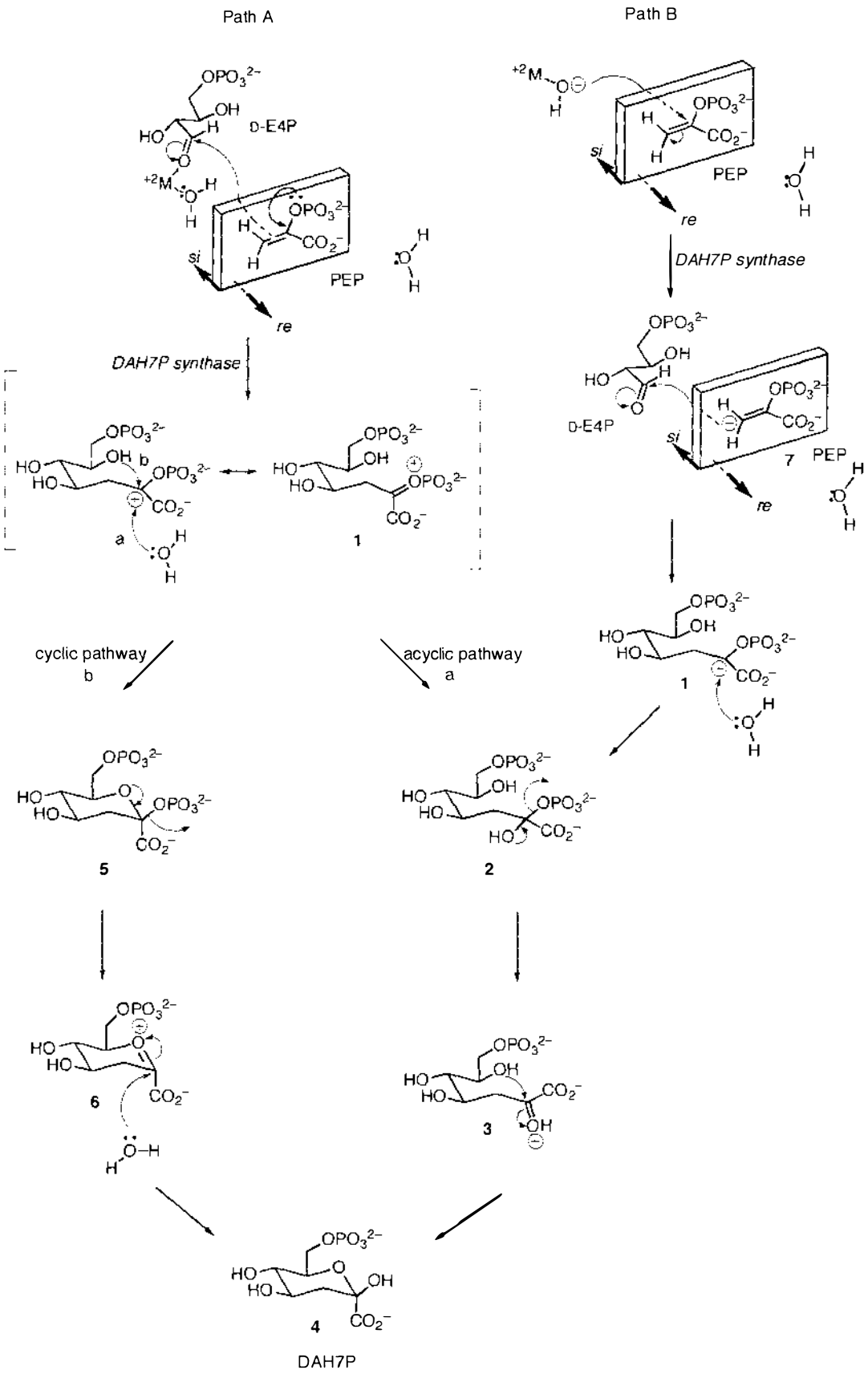

Figure 1.5. Proposed mechanisms for DAH7P synthase

In path A, the C3 of PEP attacks the metal-activated carbonyl group on D-E4P generating an oxonium ion intermediate (**1**, Figure 1.5).[34] The mechanism then diverges into two ways, an acyclic pathway (a) and a cyclic pathway (b). In the acyclic pathway, the transiently formed intermediate is attacked by a water molecule forming the labile acyclic hemiketal biphosphate (**2**, Figure 1.5). This compound then loses a phosphate group to give the open-chain form of DAH7P (**3**, Figure 1.5). DAH7P is then proposed to cyclise to the hemiacetal form of DAH7P (**4**, Figure 1.5) away from the enzyme active site. In the cyclic pathway, the C3 hydroxyl group of the D-E4P portion of the intermediate attacks the oxonium ion forming the cyclic hemiketal biphosphate (**5**, Figure 1.5). The phosphate is eliminated to form the cyclic oxonium ion (**6**, Figure 1.5), which is then attacked by a water molecule to give cyclic DAH7P (**4**, Figure 1.5).

In the proposed mechanism shown as path B,[56,57] a carbanion intermediate (**7**, Figure 1.5) is formed by the attack of a hydroxide ion produced by deprotonation of a metal-water complex. The C3 of the carbanion intermediate then attacks D-E4P forming the acyclic phosphate hydrate (**2**, Figure 1.5).

Although there have been a number of studies on the DAH7P synthase-catalysed reaction, the nature of the enzyme-bound intermediates in the reaction is not yet clear. However, formation of an acyclic intermediate and acyclic form of DAH7P is now favoured as structural studies have indicated that the C2 of PEP and the C3 hydroxyl group of D-E4P are unlikely to come into close contact.

1.2.4. Active-site studies of DAH7P synthase

Two conserved cysteines have been identified in the known microbial DAH7P synthase enzyme sequences, namely Cys61 and Cys328 [*E. coli* DAH7P(Phe) synthase numbering]. The role of both these cysteines was investigated by both chemical modification and site-directed mutagenesis.[58-61] From these studies, it was found that Cys61 was essential for catalytic activity. This residue was subsequently shown to be a metal-binding ligand when the structure of DAH7P synthase(Phe) was solved.[29] Cys328 appears to be nonessential but is involved in disulfide bond formation with Cys61 that results in loss of enzyme activity.[28,29]

Four highly conserved histidine residues, His64, His172, His207, and His268, have been identified in DAH7P synthase [*E. coli* DAH7P(Phe) synthase numbering].[62] Structural studies have shown that His268 is located at the active site and is close to PEP and also coordinates to the divalent metal.[29] His268 in DAH7P synthase is homologous to His202 in *E. coli* KDO8P synthase[62] and His202 is one of the essential histidines in *E. coli* KDO8P synthase.[63,65] His202 and His268 have been mutated to Gly in KDO8P synthase (His202Gly) and DAH7P synthase (His268Gly), respectively, from *E. coli*.[63,65] The activity of the KDO8P synthase mutant was significantly attenuated relative to the wild-type activity, whereas the DAH7P synthase mutant was inactive (Table 1.1). These studies indicated that His268 in DAH7P synthase is an essential residue for the catalytic reaction of DAH7P(Phe) synthase.

Table 1.1.
Kinetic parameters of wild-type and mutant of KDO8P synthase and of DAH7P synthase from *E. coli*.

	E. coli KDO8P synthase[65]		*E. coli* DAH7P synthase[63]	
	wild-type	His202Gly	wild-type	His268Gly
k_{cat} (s^{-1})	6.8 ± 0.5	0.016 ±0.007	32	NA[b]
$K_M^{monosaccharide}$ (μM)[c]	33 ± 6	ND[a]	86	NA[b]
$k_{cat} / K_M^{monosaccharide}$ ($s^{-1}/\mu M^{-1}$)[c]	0.2	ND[a]	0.37	NA[b]

[a] not determined.
[b] not active.
[c] K_M of D-E4P and D-A5P was measured with DAH7P synthase and KDO8P synthase from *E. coli*, respectively.

1.2.5. Phylogenetic analysis of DAH7P synthase and KDO8P synthase

DAH7P synthases can be divided into two distinct families based on amino-acid sequence similarity and molecular weight (Figure 1.6).[62,66] These two families have been denoted as type I and type II, and have also been referred to as $AroA_I$ and $AroA_{II}$.[67,68] *E. coli*, *Saccharomyces cerevisiae*, *Thermotoga maritima*, and *P. furiosus* DAH7P synthases are functionally and structurally known to be type I enzymes. Type II enzymes were originally described as similar to the high molecular weight plant enzymes (54,000 Da) and were found in several microorganisms.[66] However, as more divergent microbial enzymes have been found and sequenced, it has been shown that type II DAH7P synthases have a microbial origin and the plant DAH7P synthases form a subset within this class.[48,68-70] Whereas most of the mechanistic and structural studies have been performed on the type I DAH7P synthases from *E. coli*,[29,71,72] *S. cerevisiae*,[38,73] *T. maritima*,[57] and *P. furiosus*,[39,74] there has been comparatively less work

on type II DAH7P synthases. Recently, *H. pylori* type II DAH7P synthase has been purified and characterised,[48] and *Mycobacterium tuberculosis* type II DAH7P synthase has been crystallised and its structure has been solved.[70]

Type I DAH7P synthases are smaller than type II DAH7P synthases and were originally described as proteins with a molecular weight less than 40,000 Da. Type I DAH7P synthases can be further separated into two subfamilies, subfamily Iβ and subfamily Iβ, based on sequence similarity.[62] Subfamily Iβ DAH7P synthases have been characterised structurally and functionally from *E. coli*[29,40-44,46,75-77] and *S. cerevisiae*.[55,78] All characterised Iβ DAH7P proteins are metalloenzymes and each displays feedback regulation. In addition, the examination of the substrate specificity of *E. coli* DAH7P(Phe) synthases from subfamily Iβ showed limited enzyme activity with a range of phosphorylated five-carbon monosaccharides.[79] Subfamily Iβ consists exclusively of DAH7P synthase proteins, whereas subfamily Iβ can be further divided (Figure 1.6).[62,68] As well as containing DAH7P synthases (subfamily $I\beta_D$), subfamily Iβ contains KDO8P synthases (subfamily $I\beta_K$).

KDO8P synthase catalyses a related reaction to that catalysed by DAH7P synthase, a condensation reaction between D-A5P and PEP. Although functionally subfamily Iβ and subfamily $I\beta_D$ are equivalent to each other, catalysing the condensation of PEP and D-E4P, subfamily $I\beta_D$ proteins have more similarity to KDO8P synthases of subfamily $I\beta_K$ than to subfamily Iβ in terms of overall sequence and structure.[62] Subfamily $I\beta_D$ proteins are known to be metalloenzymes based on evidence from *T. maritima* DAH7P synthase[80] and *P. furiosus* DAH7P synthase.[39]

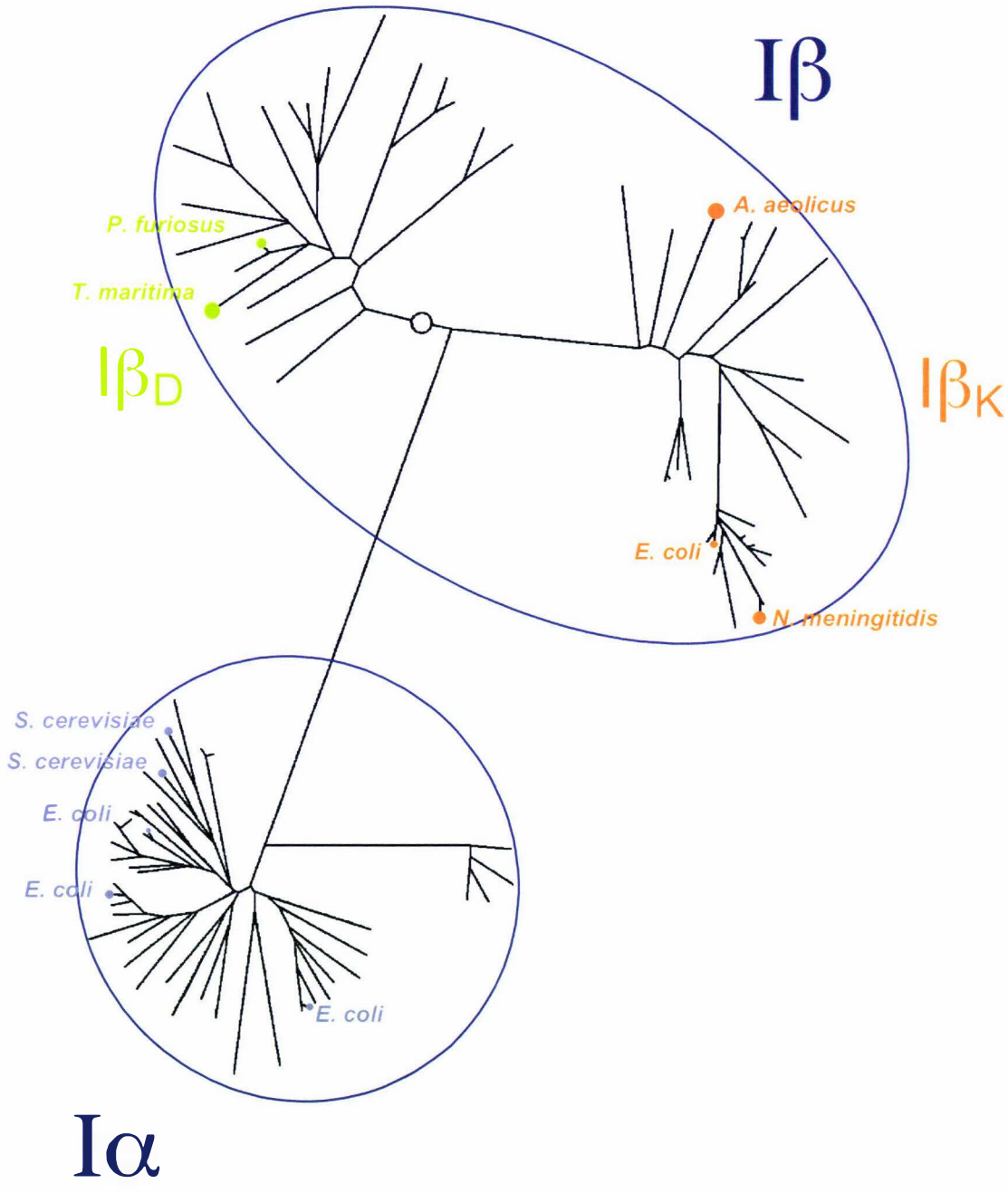

Figure 1.6. Phylogenetic tree of homology type I proteins consisting of subfamilies Iβ and Iβ modified from Jensen *et al.*[68] Subfamily Iβ contains only DAH7P synthase proteins and has feedback regulation. Subfamily Iβ consists of subfamily $I\beta_D$ and subfamily $I\beta_K$, representing DAH7P synthase and KDO8P synthase, respectively. Among structurally characterised members of subfamily Iβ, only *T. maritima* has feedback regulation. The white circle indicates the hypothetical root.

Interestingly, subfamily $I\beta_K$ contains both metalloenzymes and non-metalloenzymes as exemplified by the metal-dependent *Aquifex aeolicus* KDO8P synthase[81,82] and the metal-independent *E. coli* KDO8P synthase,[83] respectively. In addition, whereas the $I\beta_D$ DAH7P synthase from *T. maritima* is subject to feedback inhibition,[57] the $I\beta_D$ DAH7P synthase from *P. furiosus* is not, which is a feature shared by all KDO8P synthases characterised to date.[74] KDO8P synthases appear to have a very narrow substrate specificity, utilising only D-A5P.[83-85]

While the exact nature of the phylogenetic relationship between DAH7P synthase and KDO8P synthase is still under debate,[67,68,86] Subramaniam *et al.* have proposed that a DAH7P synthase is the ancestral protein in this enzyme family.[62] They have suggested that the initial ancestor was similar to the Iβ type of DAH7P synthase, which had metal dependency, had broad substrate specificity, and was not subject to feedback inhibition. However, over a long period of time, gene duplication gave a Iβ type of KDO8P synthase that lost metal dependency and gained altered substrate specificity.

The recent studies on the *P. furiosus* DAH7P synthase[39,74] have suggested that this protein may represent the closest characterised protein to the ancestral type I DAH7P synthase. *P. furiosus* DAH7P synthase is a metalloenzyme, lacks allosteric inhibition, and has a broad substrate specificity. This substrate ambiguity for *P. furiosus* DAH7P synthase has suggested that KDO8P synthase evolved from a *P. furiosus* DAH7P synthase-like ancestor by losing the ability to accept phosphorylated four-carbon monosaccharides and by tightening the specificity at the C2 hydroxyl group configuration. More details of this substrate ambiguity will be discussed in section 1.2.7 for DAH7P synthase and in section 1.3.2 for KDO8P synthase.

1.2.6. Structural studies of DAH7P synthase

The first structure of the DAH7P(Phe) synthase from *E. coli* as a Pb^{2+} and PEP complex was determined at 2.6 Å resolution by Shumilin *et al.* in 1999 (Figure 1.7).[29]

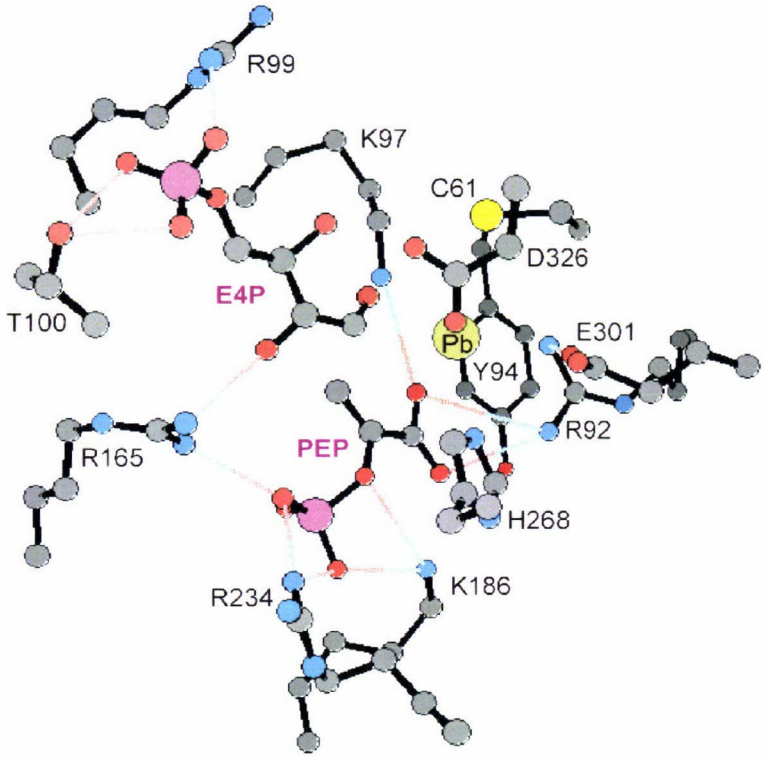

Figure 1.7. The structure of the *E. coli* DAH7P(Phe) synthase modelled by Prof. Geoffrey B Jameson based on the first DAH7P synthase structure from *E. coli* from Shumilin *et al.* Although the PEP binding site is clearly defined in this structure, the binding site of D-E4P is less well defined. D-E4P has been modelled into the active site of the structure in order to predict the key binding interactions between this enzyme and its aldose phosphate substrate. In this model, the aldehyde moiety and C3 hydroxyl group of D-E4P have been placed so as to coordinate to the metal ion, Pb^{2+}, and C61, respectively (these interactions are not shown). The phosphate functionality has been placed at a sulfate binding site in the original structure.

The enzyme crystallised as a tetramer, consistent with a tetrameric state that was predicted from solution studies.[28,75] However, closer analysis reveals that there is a tight dimer interface and the two dimers are less tightly associated. Solution studies have indicated that the tyrosine and tyrosine-sensitive *E. coli* isozymes are dimers[44,76] and the

tight dimer of DAH7P(Phe) synthase is a close structural analogue of these dimeric DAH7P synthase isoforms.[29] The monomer of DAH7P(Phe) synthase has a $(\beta/\beta)_8$-barrel formed by eight parallel β strands. The active site of the enzyme is located at the C-terminal end of the β strands of the barrel and contains the binding sites for metal, PEP, and D-E4P. This first structure of DAH7P(Phe) synthase revealed that there are four key residues that provide the stabilisation of the DAH7P(Phe) synthase tetramer: Glu24, Lys25, Arg124, and His217. In this structure, PEP is surrounded by six positively charged residues: Arg92, Lys97, Arg165, Lys186, Arg234, and His268. Moreover, it was also suggested that a SO_4^{2-} present in the active site was occupying the position of the phosphate group of D-E4P. When the phosphate group of D-E4P is located at this SO_4^{2-} binding site, D-E4P can be modelled into a channel, so that the carbonyl of D-E4P approaches the C3 of PEP (Figure 1.7).

In 2002, Shumilin *et al.* determined the crystal structure of DAH7P(Phe) synthase–Mn^{2+}–PEP in complex with its feedback inhibitor, phenylalanine, to 2.8 Å resolution.[71] The phenylalanine-binding site was shown to be in a cavity formed by residues from each monomer of the tight dimer including an N-terminal extension and two extra-barrel loops. Comparison of this structure with those determined previously reveals that the inhibitory signal from phenylalanine binding is transmitted to the active site by the movement of four adjacent segments. The movement of these segments causes changes to the tight-dimer interface and to the enzyme active site, which is immediately adjacent to this interface. These conformational changes induced by phenylalanine binding significantly alter the substrate binding properties of the active site of the enzyme. In this structure, PEP was observed to bind in a flipped orientation, such that the positions of the carboxylate and phosphate groups are interchanged

relative to previously reported structures determined in the absence of phenylalanine. It was concluded that the displacement of both Arg99 and Thr100 in the phenylalanine-bound enzyme precludes binding of D-E4P. It is these changes in the ability to bind both PEP and D-E4P that result in enzyme inhibition.

Attempts to solve the structure of a catalytically active form of the enzyme DAH7P(Phe) synthase with Mn^{2+} and PEP were reportedly confounded by unit cell disorder. However, recently, the structure of a catalytically active mutant (Glu24Gln) in complex with PEP and Mn^{2+} has been determined to 1.75 Å.[72] This mutant enzyme is reported to have similar kinetic properties to those of the wild-type enzyme but exists as a dimer in solution due to disruption, by mutation, of electrostatic interactions necessary for tetramer formation. In this structure, it was observed that the PEP bound at the active site was twisted so that its enol and carboxylate planes form a dihedral angle of 30°, whereas the phosphate group is tightly anchored with the side chains of Lys186, Arg234, and Arg165 and the main chain NH of Ala164. In addition, seven water molecules are found to be within contact distance of PEP. Two of these water molecules, one that is hydrogen bonded to the carboxylate of PEP and the other that is hydrogen bonded to Glu143, are close enough to the C2 of PEP to potentially act as a nucleophile in the reaction mechanism.

The crystal structure of the *S. cerevisiae* DAH7P(Tyr) synthase has recently been determined by König *et al.* in complex with Co^{2+}, PEP, and the D-E4P analogue, glycerol 3-phosphate (G3P) at 1.5 Å resolution.[73] In the structure, the C1 hydroxyl group in G3P, corresponding to C2 hydroxyl group of D-E4P, was hydrogen-bonded to Asp342 and the C2 hydroxyl group of G3P, corresponding to C3 hydroxyl group in D-

E4P, was hydrogen-bonded to the main-chain carbonyl group of Pro113. Pro has been found to be a conserved residue in all DAH7P synthases and is a part of a conserved LysProArgThr(Ser) motif found in all DAH7P synthases. In addition, two water molecules have observed: one is on the *si* face side of and the other one is on the *re* face side of PEP, and were close enough to the PEP to participate in the enzymic reaction. The water molecule on the *si* face side of PEP was coordinated to the metal ion and interacted with the carbonyl group of D-E4P. This observation gives a plausible reaction mechanism. In this mechanism, the metal ion is coordinated to the water molecule on the *si* face side of PEP and activates carbonyl group of D-E4P. The C3 of PEP attacks from *si* face side onto *re* face side of the metal-activated carbonyl group of D-E4P forming oxocarbenium intermediate (**1,** Figure 1.5). The intermediate is then attacked by the water molecule on the *re* face side of PEP to form the acyclic hemiketal biphosphate (**2**, Figure 1.5).

Although the PEP binding site is clearly defined in previously reported structures,[29,71,73] the binding site of D-E4P is less well defined. However, the structure of the DAH7P synthase from *T. maritima* has been determined recently with both substrates, PEP and D-E4P, as well as Cd^{2+} bound at the active site.[57] The crystals were grown at 4 °C, a temperature at which this hyperthermophilic enzyme is inactive. Although this was the first structure that contained a metal cofactor and both substrates, D-E4P and PEP, the enzyme was only partially occupied by D-E4P and this ligand was bound in an unreactive conformation. The active-site structure of *T. maritima* DAH7P synthase is similar to that of *E. coli* and *S. cerevisiae* DAH7P synthases (subfamily Iβ DAH7P synthase enzymes). However, the overall structure of *T. maritima* DAH7P synthase is more similar to those of the *E. coli* and *A. aeolicus* KDO8P synthases (subfamily $I\beta_K$

KDO8P synthases) than to those of the *E. coli* and *S. cerevisiae* DAH7P synthases. In addition, although *T. maritima* DAH7P synthase has tyrosine and phenylalanine feedback regulation, it lacks the extended loops found in the Iβ DAH7P synthase enzymes and has a different N-terminal extension suggesting a different mechanism of feedback regulation (Figure 1.8).

The structure of *P. furiosus* DAH7P synthase in complex with PEP has been determined to 2.25 Å resolution.[74] As with the *T. maritima* enzyme, *P. furiosus* DAH7P synthase had a very similar active-site structure to those reported for other DAH7P synthases (*E. coli*, *S. cerevisiae*, and *T. maritima* DAH7P synthases, Figure 1.8). *P. furiosus* DAH7P synthase has short KDO8P synthase-like loops consistent with the lack of feedback regulation as seen with type Iβ DAH7P synthases. Moreover, the *P. furiosus* DAH7P synthase lacks the 70 amino-acid ferrodoxin-like N-terminal domain that has been implicated in feedback regulation by *T. maritima* DAH7P synthase, and the 40 amino-acid N-terminal extension that is involved, along with the extended loops, in feedback inhibition by *E. coli* and *S. cerevisiae* DAH7P synthases. In the studies of the *P. furiosus* DAH7P synthase structure, the six known structures of DAH7P and KDO8P synthases were compared; two from subfamily Iβ DAH7P synthases (*E. coli* and *S. cerevisiae*), two from $I\beta_D$ DAH7P synthases (*T. maritima* and *P. furiosus*), and two from $I\beta_K$ KDO8P synthases (*E. coli* and *A. aeolicus*) (Figure 1.8). This analysis has shown that $I\beta_K$ KDO8P synthase enzymes have shorter loops than Iβ DAH7P synthase enzymes and that the overall structures of the $I\beta_D$ DAH7P synthase enzymes are closer to those of the $I\beta_K$ KDO8P synthase enzymes than to the Iβ DAH7P synthases. More details of the comparison between DAH7P and KDO8P synthases are discussed in chapter six.

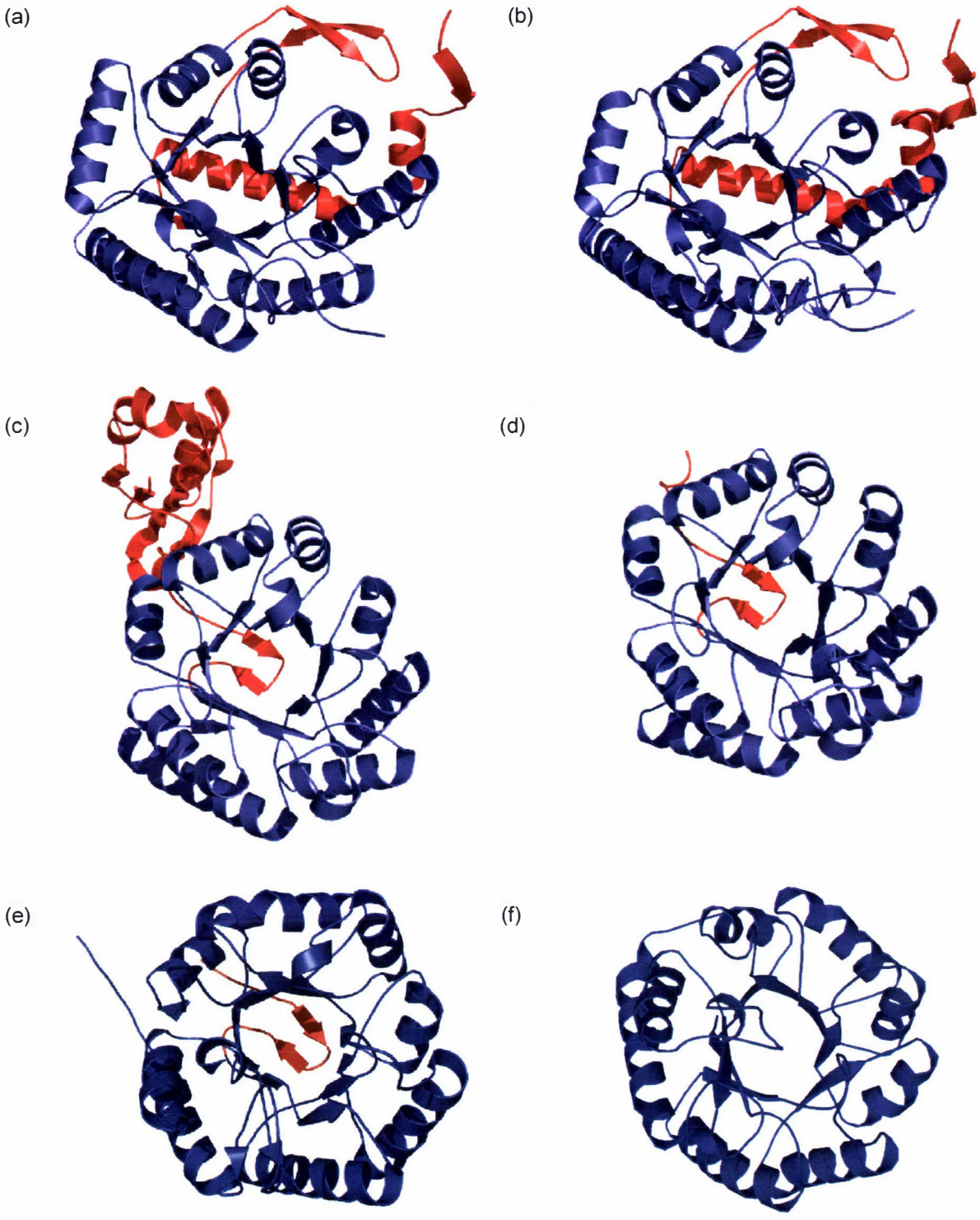

Figure 1.8. The monomer structures of (a) *E. coli* DAH7P(Phe) synthase, (b) *S. cerevisiae* DAH7P(Tyr) synthase, (c) *T. maritima* DAH7P synthase, (d) *P. furiosus* DAH7P synthase, (e) *E. coli* KDO8P synthase, and (f) *A. aeolicus* KDO8P synthase. Taken from Schofield *et al.*[74] The views of the structures are looking down their $(\beta/\beta)_8$-barrel. The overall structures of *T. maritima* and *P. furiosus* DAH7P synthases appear to be more similar to those of *E. coli* and *A. aeolicus* KDO8P synthases than those of *E. coli* and *S. cerevisiae* DAH7P synthases. The helices and loops are highlighted in blue and the N-terminal extension, along with extended loops, is highlighted in red. The extra extension and loops are implicated in feedback regulation. *P. furiosus* DAH7P synthase, and *E. coli* and *A. aeolicus* KDO8P synthases do not have feedback regulation and lack N-terminal extensions. Note that the structure of *Neisseria meningitidis* KDO8P synthase is not shown.

1.2.7. Substrates and analogues for DAH7P synthase

Substrate analogues are considered a significant tool for studying enzyme-substrate interactions and enzymatic reaction mechanisms. PEP and D-E4P are the natural substrates of DAH7P synthase. *E. coli* DAH7P(Phe) synthase has been shown to accept a number of other substrates with varying degrees of efficiency.[74,79]

Analogues of PEP

There has been significant interest in the synthesis of analogues of PEP (Figure 1.9) due to the importance of this compound as a substrate in many enzyme-catalysed reactions.

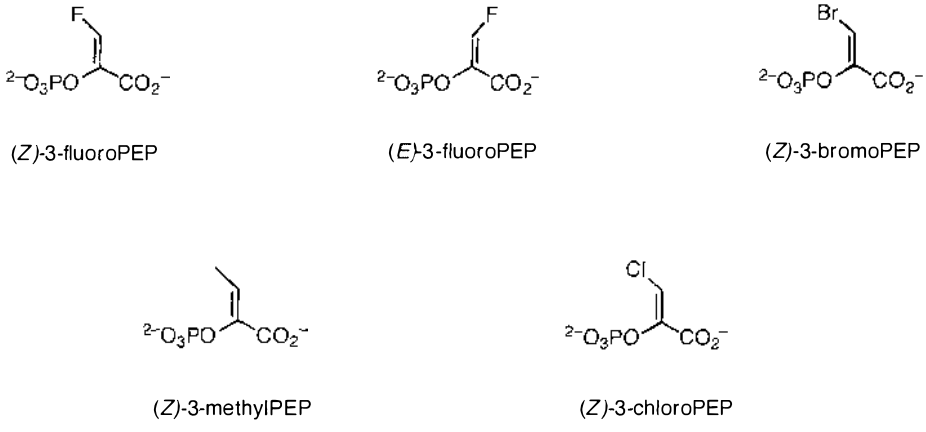

Figure 1.9. Analogues of PEP

The synthesis of a number of PEP analogues has been described in earlier studies.[88] Both isomers of 3-fluoroPEP have been shown to be substrates for the DAH7P(Phe) synthase from *E. coli*, whereas 3-bromoPEP, 3-methylPEP, and 3-chloroPEP (Figure

1.9) have been found to be reversible competitive inhibitors with respect to PEP, showing that size of substituent has a large bearing on substrate reactivity (Table 1.2).[87,88]

Table 1.2.
Kinetic parameters of analogues of PEP as substrates and inhibitors of *E. coli* DAH7P(Phe) synthase[87]

	K_M (μM)	K_i (μM)	k_{cat} (s^{-1})
PEP	2.0 ± 0.2		71 ± 3
(*Z*)-3-fluoroPEP	18 ± 1		4.1 ± 0.2
(*E*)-3-fluoroPEP	4.0 ± 0.4		1.0 ± 0.2
(*Z*)-3-chloroPEP		31 ± 6	
(*Z*)-3-methylPEP		160 ± 30	
(*Z*)-3-bromoPEP		250 ± 50	

Analogues of D-E4P

Prior to the commencement of these studies, there were two known phosphonate analogues of D-E4P that had been shown to be accepted as substrates of DAH7P(Tyr) synthase from *E. coli*: the phosphonate (4-deoxy-4-phosphono-D-*erythro*-tetrose) and the homophosphonate (4,5-dideoxy-5-phosphono-D-*erythro*-pentose) (Figure 1.10).[89] The V_{max} values determined for phosphonate and homophosphonate were approximately 5 % and 30 % of that obtained using D-E4P as a substrate, respectively.

It has also been shown that the DAH7P(Phe) synthase from *E. coli* can utilise D-ribose 5-phosphate (D-R5P), D-A5P, and 2-deoxy-ribose 5-phosphate (2-deoxyR5P) (Figure 1.10) as alternative substrates to D-E4P.[79,86] All these phosphorylated monosaccharides are one carbon unit longer than the natural substrate, D-E4P. In the recent studies, *P.*

furiosus DAH7P synthase has been shown to have a broad substrate specificity.[74,90] The *P. furiosus* enzyme accepted five-carbon phosphorylated monosaccharides, as well as 2-deoxy-erythrose 4-phosphate (2-deoxyE4P) and 3-deoxy-erythrose 4-phosphate (3-deoxyE4P) as alternative substrates (Figure 1.10). Further work on analogues of D-E4P is presented in chapter two of this thesis.

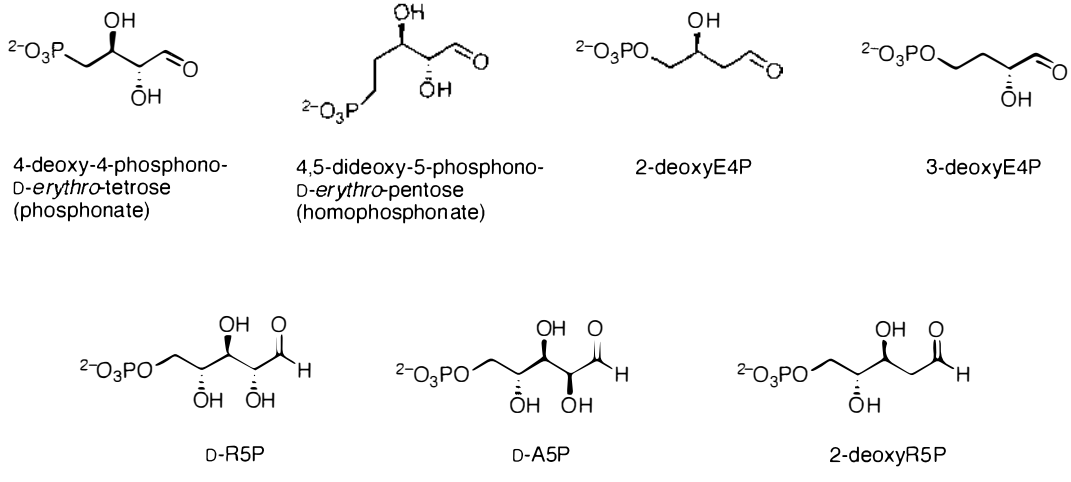

Figure 1.10. Analogues of D-E4P

1.3. KDO8P Synthase

Broadly, Gram-positive (G^+) and Gram-negative (G^-) bacteria are distinguished by the Gram stain. The difference between G^+ and G^- bacteria is in the organisation of structures outside the phospholipid bilayer plasma membrane. In G^- organisms, such as *E. coli*, the structures outside the plasma membrane constitute the cell envelope, whereas in G^+ organisms they make up the bacterial cell wall.[91] The G^- bacteria cellular

envelope contains a much smaller peptidoglycan layer than G^+ bacteria (Figure 1.11).

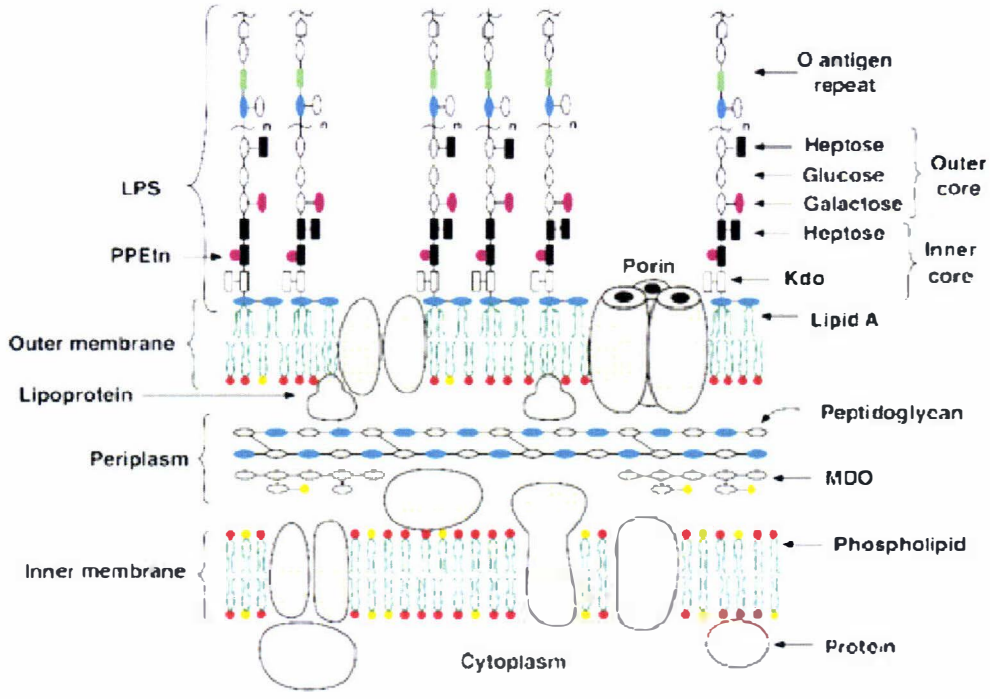

Figure 1.11. Schematic molecular model of the inner and outer membranes of *E. coli* K-12. Taken from Raetz and Whitefield.[91]

The peptidoglycan layer is surrounded by an outer membrane, which acts as a protective barrier preventing many antibiotics from reaching their site of action and thus confers a natural resistance to such agents. This outer membrane is composed of a non-symmetrical bilayer of phospholipid (interior) and lipopolysaccharide (LPS; exterior, Figure 1.11). The unique LPS layer, also referred to as bacterial endotoxin, is responsible for G^- infections causing pathophysiological disease.[91] LPS is an amphipathic molecule consisting of a hydrophobic head called lipid A (Figure 1.12), which possesses most of the biological activities of LPS, and a hydrophilic

polysaccharide tail. Since the biosynthesis of LPS is known to be unique to G⁻ bacteria, and G⁻ bacteria require LPS for their growth and virulence, LPS biosynthesis has been identified as a target for the development of novel antibacterial agents.[92,93]

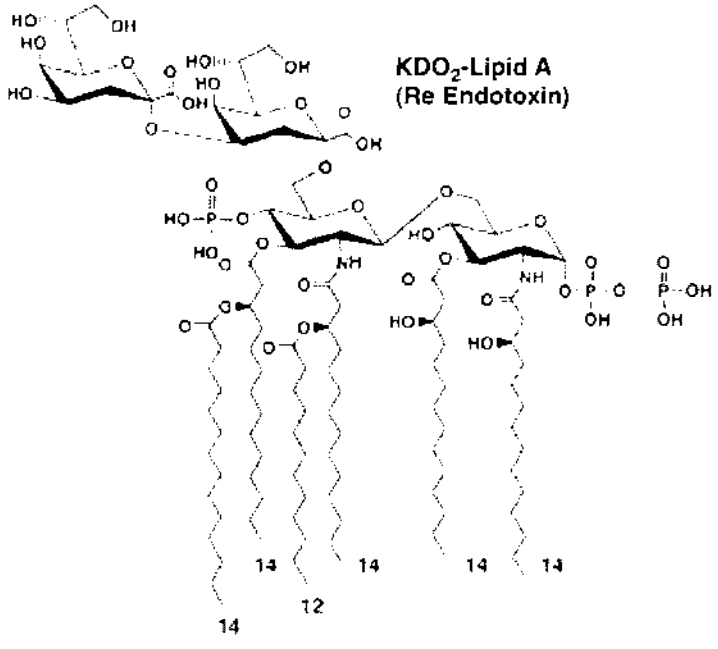

Figure 1.12. Structure of KDO_2-Lipid A in *E. coli* K-12. The numbers denote the number of carbon atoms of the fatty acid. Taken from Raetz and Whitefield.[91]

There are four unique components in the structure of LPS: i) lipid A, ii) *R*-3-hydroxymyristate in the lipid A region, iii) L-*glycero*-D-*manno*-heptose (GMH) in the core polysaccharide region, and iv) 3-deoxy-D-*manno*-octulosonic acid (KDO) in the core polysaccharide region.[94] Inhibition of the biosynthesis of KDO is an excellent chemotherapeutic target, since KDO is a site-specific molecule found in G⁻ organisms and is required for lipid A maturation and cellular growth.[94] Thus, synthetic inhibitors of KDO biosynthesis have been designed.[94-96] The biosynthesis and utilisation of KDO can be envisioned as an essential minor branched pathway in carbohydrate metabolism in G⁻

bacteria. Most of the enzymes in the pathway have been isolated and purified to homogeneity, and some elementary inhibition studies have been initiated.[94]

KDO8P synthase is the key enzyme in the biosynthesis of LPS in the majority of G$^-$ organisms and for controlling the carbon flow in the biosynthetic formation of KDO.[95-98] KDO8P synthase catalyses the condensation of D-A5P and PEP to give KDO8P (Figure 1.13). KDO8P is dephosphorylated by the next enzyme in the pathway to generate KDO.

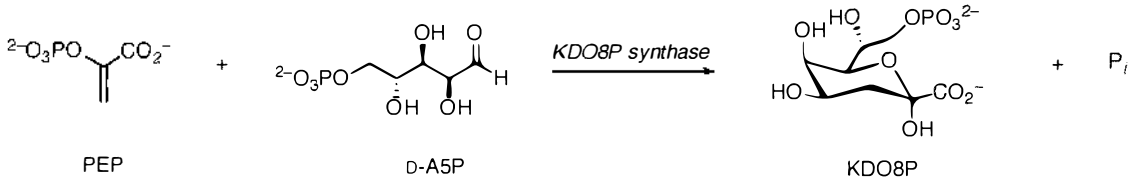

Figure 1.13. KDO8P synthase-catalysed reaction

All KDO8P synthases were initially thought to be non-metalloenzymes, as the *E. coli* enzyme does not require a divalent metal ion for catalysis. However, recent studies have shown that *A. aeolicus*, *H. pylori*, and *Aquifex pyrophilus* KDO8P synthases are metal-dependent.[48,86,99,100] In addition, these enzymes do not have any feedback inhibitors in contrast to most of the DAH7P synthases.[74] Although DAH7P synthase and KDO8P synthase belong to unrelated biosynthetic pathways, both enzymes appear to share mechanistic similarities for the condensation between PEP and an aldose phosphate.

1.3.1. Mechanistic studies of KDO8P synthase

Like DAH7P synthase, KDO8P synthase catalyses an unusual aldol-like condensation between D-A5P and PEP to give KDO8P with the release of phosphate.[83] The KDO8P synthase reaction has also been shown to follow an ordered sequential kinetic mechanism in which PEP binds first, followed by D-A5P, with P_i released prior to the final product, KDO8P.[101] From an early study using specifically labelled [^{18}O]-PEP as a substrate for KDO8P synthase in the enzymatic reaction, it is now known that the mechanism involves the C–O cleavage of PEP instead of P–O bond cleavage.[102] Additionally, the KDO8P synthase-catalysed reaction has been shown to have the same facial selectivity as the DAH7P synthase reaction where the *si* face of PEP attacks the *re* face of D-A5P from studies using the labelled 3-deutero and 3-fluoro analogues of PEP as alternative substrates for the *E. coli* KDO8P synthase. [103-108]

As for DAH7P synthase, two distinct mechanisms for the KDO8P synthase reaction have been proposed involving either the generation of a cyclic or an acyclic intermediate (Figure 1.14).[102,109] These intermediates would then give rise to the cyclic or open-chain forms of KDO8P, respectively.

The acyclic mechanism (Path A) was suggested initially by Hedstrom and Abel in 1988.[102] They proposed that the condensation of PEP and D-A5P to form KDO8P proceeds *via* attack by water at C2 of PEP and by C3 of PEP on C1 of D-A5P. They also determined that the reaction is essentially irreversible, meaning that the enzyme-bound

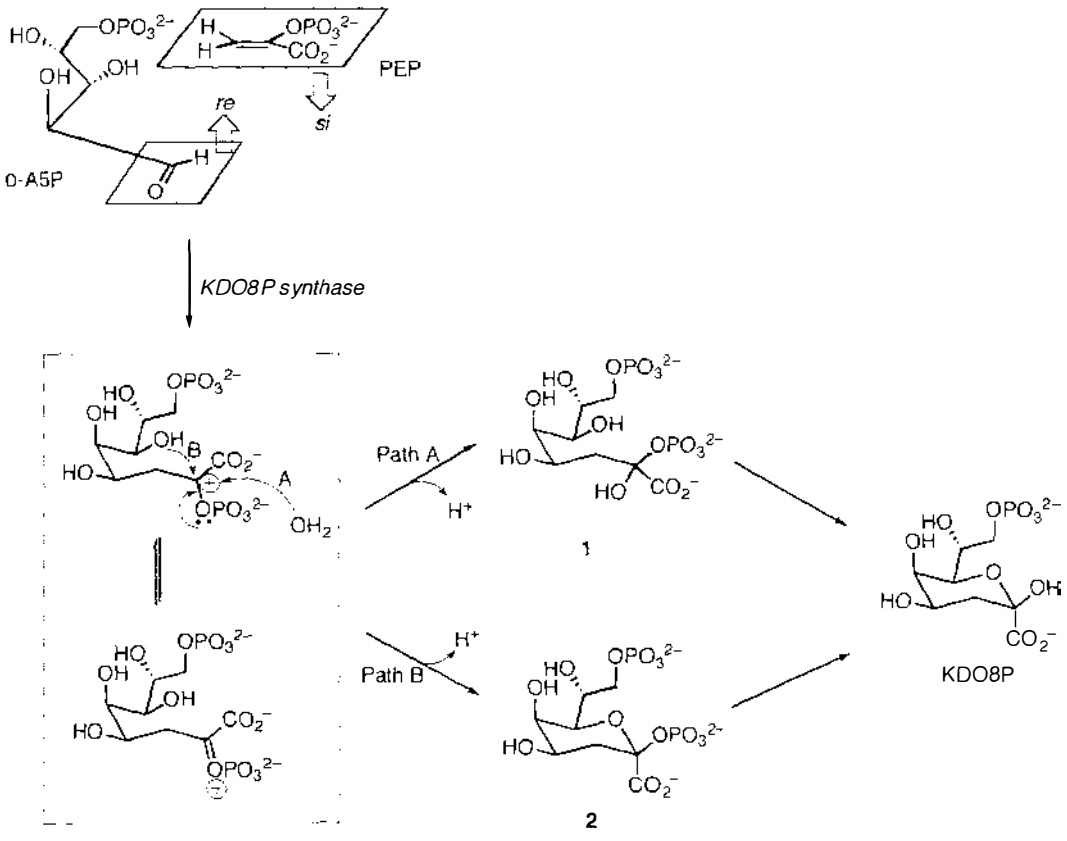

Figure 1.14. Proposed mechanism of KDO8P synthase. Note that steps involved in the loss of the phosphate are not shown. Taken from Bassov *et al.*[106]

intermediate cannot be examined under equilibrium conditions. Therefore, the mechanistic proposals have been based on the results of possible intermediate mimics and examination of reaction of the various analogues of D-A5P, analogues of PEP, and analogues of KDO8P.[94,102,105-118] One of these analogues, 4-deoxy-arabinose 5-phosphate (4-deoxyA5P, Figure 1.15), was prepared for a mechanistic study in order to determine whether the cyclic furanose form or the acyclic form of D-A5P (Figure 1.15) was the substrate for the enzyme.[111] Examination of the 4-deoxyA5P with the enzyme revealed that 4-deoxyA5P has a similar k_{cat} value (11 ± 0.4 s^{-1}) to the original substrate D-A5P (7 ± 0.4 s^{-1}), suggesting that the enzymatic reaction utilises the acyclic form of D-A5P.

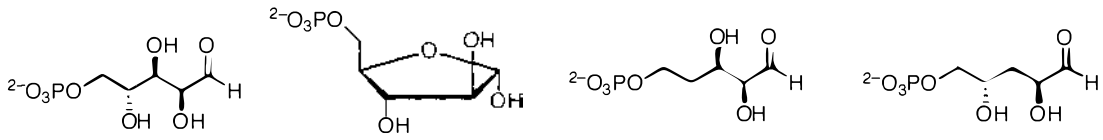

Figure 1.15. Analogues of D-A5P

A series of experiments on the *E. coli* KDO8P synthase with inhibitors and alternative substrates had favoured the cyclic mechanism (Path B in Figure 1.14).[94] The observation that 3-deoxy-arabinose 5-phosphate (3-deoxyA5P, Figure 1.15) was neither a substrate nor an inhibitor for *E. coli* KDO8P synthase led to the proposal that the reaction may pass through a cyclic intermediate (**2**, Figure 1.14).[94] In support of the cyclic mechanism, the 2-deoxy cyclic analogues (**3** and **4**, Figure 1.16) of the product both showed moderate inhibition of the enzyme (K_i values of 303 μM and 470 μM, respectively), whereas the isosteric phosphonate analogue (**5**, Figure 1.16) of the cyclic intermediate was considerably more potent (K_i = 5 μM).[113] However, when the putative

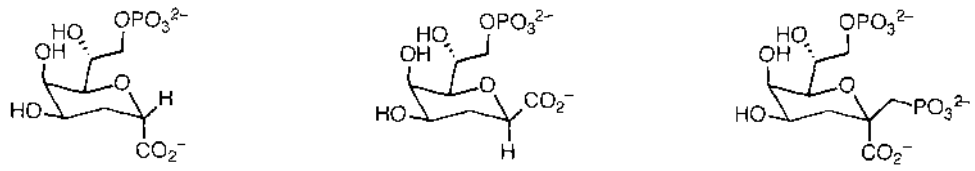

Figure 1.16. 2-Deoxy cyclic analogues and an isosteric phosphonate analogue of KDO8P

cyclic intermediate (**2**, Figure 1.14) was synthesised and examined as an alternative substrate for the enzyme, this compound was not a substrate.[113] This strongly suggests that cyclic intermediate is not involved in the enzyme-catalysed reaction and supports the acyclic mechanism originally proposed by Hedstrom and Abeles (Path A in Figure 1.14).[102] In addition, the first acyclic bisubstrate inhibitor of *E. coli* KDO8P synthase (Figure 1.17) has been synthesised and shown to be the most potent inhibitor of the enzyme reported to date (K_i = 0.42 μM).[105,115,119] This analogue mimics the positive charge of the putative acyclic oxocarbenium intermediate (Figure 1.14).

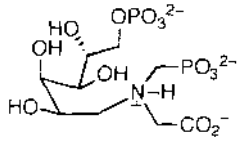

Figure 1.17. Acyclic bisubstrate inhibitor of KDO8P synthase

Despite all of the evidence for an acyclic mechanism, there is still no evidence for the existence of the acyclic intermediate as a true enzymatic intermediate. However, in recent studies, the hemiketal phosphate intermediate (**1**, Figure 1.14) has been identified using time-resolved electrospray ionisation mass spectrometry (ESI-TOF MS).[120] This experiment allows direct detection of the enzyme-intermediate complex on a very short millisecond lifetime scale. Consequently, this result has supported the acyclic mechanism for KDO8P synthase and, by analogy, it has been assumed that DAH7P synthase also catalyses its reaction through an acyclic mechanism.

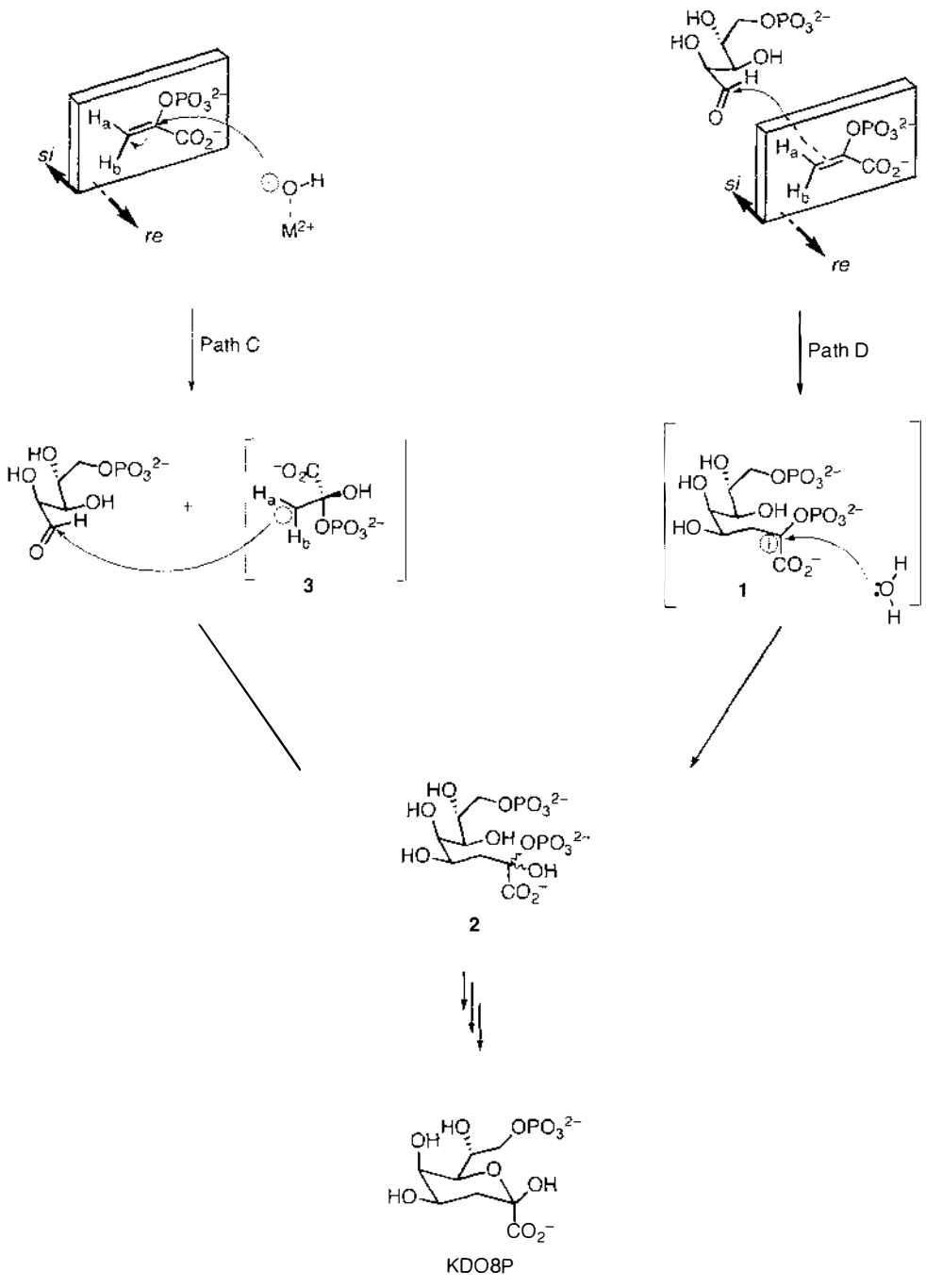

Figure 1.18. Two proposed elementary steps for the formation of a linear intermediate of KDO8P synthase. Taken from Shulami *et al.*[126]

Since the structures of two different KDO8P synthases, one metal-independent and the other metal-dependent, have been determined,[121-125] new mechanisms have been proposed depending on the presence or absence of metal at the active site (Figure 1.18). The metal-independent KDO8P synthase has been postulated to follow the linear mechanism *via* a transient oxocarbenium intermediate (Path D in Figure 1.18).[123] In this mechanism, the initial attack of the *si* face of the PEP double bond to the *re* face of the carbonyl of D-A5P gives the acyclic oxocarbenium intermediate (**1**, Figure 1.18). The cation is then attacked by a water molecule resulting in the formation of the acyclic biphosphate intermediate (**2**, Figure 1.18). In contrast, for metal-dependent KDO8P synthases (Path C in Figure 1.18),[125] a hydroxide ion produced by deprotonation of a metal-water complex attacks C2 of PEP forming a carbanion intermediate at C3 of PEP (**3**, Figure 1.18). The carbonyl of D-A5P could then attacked by the carbanion to produce a linear form of KDO8P.

More recently, it has been demonstrated that a metal-dependent KDO8P synthase can be converted to a metal-independent KDO8P synthase retaining about 10 % of wild-type maximal activity in the absence of metal ions.[126,127] This change takes place by a single mutation to the metal-binding cysteine to give an asparagine in its place. An asparagine at this position is absolutely conserved in all metal-independent KDO8P synthases. This result suggests that the metal ion is not directly involved in the metal-dependent KDO8P synthase reaction. Therefore, the suggestion that a divalent metal ion provides a hydroxide ion, which leads to the formation of the C3 carbanion (Path C in Figure 1.18),[125] might be less plausible than initially thought. These experiments and observations support a common mechanism for both metal-independent and metal-dependent KDO8P synthases in which a transient oxocarbenium intermediate forms at

C2 of PEP from combination of PEP with D-A5P. This is supported by the results and analysis presented in this thesis as described in chapter six.

1.3.2. Substrate specificity of KDO8P synthase

As KDO8P synthase appears to be highly related to DAH7P synthase, any study of DAH7P synthase needs to consider similar work on KDO8P synthase. The substrate specificity of DAH7P synthase, to date, has been examined with *E. coli* DAH7P(Phe) synthase and *P. furiosus* DAH7P synthase.[84,79] Both studies showed that KDO8P can be formed from D-A5P (or other five-carbon sugars) and PEP using DAH7P synthase, whereas *E. coli* KDO8P synthase cannot catalyse the formation of DAH7P from D-E4P and PEP.[84,85] Recently, it has been reported that D-R5P, which has the same C2 hydroxyl group configuration as D-E4P (but opposite to the C2 hydroxyl group configuration of D-A5P), is not a substrate of *A. aeolicus* KDO8P synthase.[125] Additionally, neither 2-deoxyR5P nor 3-deoxyA5P act as alternative substrates, but 4-deoxyA5P is an alternative substrate of the *E. coli* KDO8P synthase enzyme.[94,101] It has also been demonstrated that both *E. coli* and *A. aeolicus* KDO8P synthases cannot utilise either four- or six-carbon sugars as alternative substrates.[84,85,94] Collectively, these results suggest that KDO8P synthase is more substrate specific than DAH7P synthase.

1.3.3. Structural studies of KDO8P synthase

Although DAH7P synthase and KDO8P synthase are functionally unrelated enzymes, the mechanistic similarities suggest that both enzymes have a common ancestor, as described in section 1.3.1. Moreover, the structural studies of DAH7P synthase[29,56,57,71-74]

and KDO8P synthase[121-125] have revealed that the structure of DAH7P synthase (from *E. coli*, *S. cerevisiae*, *T. maritima*, and *P. furiosus*) is similar to that of KDO8P synthase (from *E. coli*, *A. aeolicus*, and *N. meningitidis*) (structures are shown in Figure 1.8). Both *E. coli* and *N. meningitidis* KDO8P synthases are metal-independent enzymes,[121-123,128] whereas *A. aeolicus* KDO8P synthase is a metal-dependent enzyme.[86,124]

The first structure of a metal-independent KDO8P synthase from *E. coli* was determined at 2.4 Å resolution in 2000.[121] This study demonstrated that KDO8P synthase is a homotetramer in which each monomer is a $(\beta/\beta)_8$-barrel. The KDO8P synthase crystals were grown in 1.4 M $(NH_4)_2SO_4$ and 0.4 M $(K/H)_3PO_4$ (pH 7.5). Two SO_4^{2-}/HPO_4^{2-} sites were found in the structure and these were proposed to represent the binding sites for the phosphate groups of D-A5P and PEP. The distance between the D-A5P and PEP phosphate groups in this model structure was 13 Å supporting the original hypothesis that KDO8P synthesis proceeds *via* an acyclic intermediate.

In 2001, Asojo *et al.* solved the crystal structures of KDO8P synthase from *E. coli* in complex with substrate PEP and in complex with a mechanism-based inhibitor (Figure 1.17) to 2.8 Å and 2.3 Å resolution, respectively.[123] The overall structures of these complexes were shown to be very similar to the structures from Radaev *et al.*,[121] confirming that KDO8P synthase is homotetramer. In the first structure, KDO8P synthase-PEP, the phosphate group of PEP was anchored to the enzyme so as to block the *si* face of PEP. The vinyl group of PEP was away from the active site cleft and is not within van der Waals contact distance of any nearby residues (His202, Lys138, Arg168,

and Gln141 on the *si* face of PEP; Arg63 and Asn62 on the *re* face of PEP). In their second structure, the KDO8P synthase-inhibitor complex, the phosphate group from the PEP moiety in the inhibitor is hydrogen-bonded to His202, Arg168, and Gln141 and the D-A5P portion of the inhibitor was stretched out along the active site cleft. Also, it was observed that whereas, in the D-A5P portion of the inhibitor, the two hydroxyl groups at C2 and C3 formed hydrogen bonds with residues Pro252, Gln205, and Gly251, the C1 and C4 hydroxyl groups did not make any close contacts with the enzyme.

The structure of the metal-dependent KDO8P synthase from *A. aeolicus* has recently been determined to 1.9 Å for substrate-free enzyme with and without Cd^{2+}.[124] The structure of the enzyme has also been solved in complex with PEP, PEP–Cd^{2+}, D-A5P–Cd^{2+}, and D-A5P–PEP–Cd^{2+}. It is noteworthy that two water molecules, one that is on the *si* face of PEP and the other one that is on the *re* face of PEP, were also found in the structures of the enzyme-PEP-Cd^{2+}, the enzyme-PEP, and the enzyme-D-A5P-PEP-Cd^{2+} complexes and were close to C2 of PEP in van der Waals contact. In the KDO8P synthase-D-A5P-PEP-Cd^{2+} complex, the water molecule on the *si* face of PEP was observed to be hydrogen-bonded to a water molecule coordinated to Cd^{2+}.

Furthermore, the structure of *A. aeolicus* KDO8P synthase in complex with D-R5P has also been determined by Wang *et al.*[125] D-R5P is not a substrate for this enzyme and has the opposite configuration at C2 to substrate D-A5P. In this structure, the water molecule hydrogen-bonded to the C2 hydroxyl group of D-A5P and coordinated to the metal is not present. The absence of this water molecule was considered to account for the inability of D-R5P to act as a substrate for KDO8P synthase. Based on these observations, Wang *et al.* proposed a possible mechanism for KDO8P synthase. In their

mechanism, the water molecule on the *si* face of PEP is activated by the divalent metal ion and the activated water attacks C2 of PEP forming a carbanion intermediate at C3 of PEP. The C3 of PEP then attacks the carbonyl group of D-A5P. This results in the formation of the linear intermediate (Path C in Figure 1.18).[125]

In contrast to the *E. coli* KDO8P synthase where there is no metal bound, there are several residues that serve as metal-binding ligands at the active site of KDO8P synthase from *A. aeolicus*.[124] These residues are Cys11, His185, Glu222, and Asp233, which have their counterparts in *E. coli* KDO8P synthase (Asn26, His202, Glu239 and Asp250). Three of these four residues (His185, Glu222, and Asp233) are completely conserved in all known metal-dependent and metal-independent KDO8P synthases, whereas Cys is found only in metal-dependent KDO8P synthases and is always substituted by an Asn in metal-independent KDO8P synthases.[86,100,124,126] The metal-coordinated water molecule observed in *A. aeolicus* KDO8P synthase has no counterpart in the *E. coli* KDO8P synthase structure. In addition, His185 is also reported to be necessary for the correct binding of PEP in the active site of *A. aeolicus* KDO8P synthase.[129]

More recently, as noted above, it was demonstrated that metal dependency could be eliminated by a single amino acid replacement, Cys11 to Asn in both *A. aeolicus* and *A. pyrophilus* KDO8P synthases.[126,127] Conversely, replacement of Asn26 by Cys in a metal-independent *E. coli* KDO8P synthase led to metal binding with increased activity

from 6 % to 30 % of wild type in the presence of a metal ion, Mn^{2+}.[126] These results suggest that the absence of the metal ion in the metal-dependent KDO8P synthase is not critical for the enzyme-catalysed reaction. It has been proposed that the metal ion has an important structural role in KDO8P synthase enzymes to maintain the correct orientation of the substrates in the enzyme active site for catalysis. Thus, according to the results from these studies, it has been suggested that Asn in *E. coli* KDO8P synthase, in place of the metal-binding Cys in metal-dependent KDO8P synthases, may also play a similar structural role to the metal ion.

1.3.4. The relationship between DAH7P synthase and KDO8P synthase

Although these two enzymes, DAH7P synthase and KDO8P synthase, are functionally unrelated as described in earlier sections (see section 1.1 and 1.3), they share many mechanistic features. Due to their similarities, many comparisons have been made between DAH7P synthase and KDO8P synthase. Both DAH7P synthase and KDO8P synthase catalyse a reaction between PEP and a phosphorylated monosaccharide, D-E4P for the former to give a seven-carbon sugar product, DAH7P, and D-A5P for the latter to generate KDO8P, an eight-carbon sugar. While there is little primary sequence similarity between the *E. coli* KDO8P synthase and the *E. coli* DAH7P synthase, that is only 13 % of the residues are identical, and 38 % are either identical or substituted conservatively,[62] it is clear that there is a high degree of structural similarity. Both enzymes catalyse the condensation reaction of PEP with a phosphorylated aldolase by a

similar ordered-sequential mechanism where PEP binds first and final sugar product is released last.[53,101] Both reactions involve the cleavage of the C–O bond of PEP instead of P–O cleavage,[51,52,102] with the *si* face of PEP coupling with the *re* face of their respective sugar substrate, D-E4P or D-A5P.[49,107] Moreover, it has been shown that DAH7P synthases and KDO8P synthases have remarkably similar active-site architectures from their X-ray crystal structure determinations.[29,57,73,74,121,124] The results suggest that both PEP and the sugar phosphate substrates bind in similar locations at the active site of both DAH7P and KDO8P synthases, although the sugar phosphate substrates are different lengths. Many key active site residues from both enzymes are in the same relative positions and can be mapped onto their DAH7P synthase counterparts (Table 1.3).

While the similarities are clear, there are two major differences between DAH7P synthase and KDO8P synthase: (i) substrate specificity and (ii) metal requirement. As mentioned in section 1.3.2, DAH7P synthase shows broad substrate specificity accepting five-carbon sugars and 2-deoxyE4P,[74,79,130] whereas KDO8P synthase takes only D-A5P but not four-, other five-, and six-carbon phosphorylated sugars.[83-85] In addition, all characterised DAH7P synthases are known to be metal-dependent, whereas for KDO8P synthases, both metal-dependent and metal-independent enzymes have been characterised.

[81-83,121,124,126] Recent studies have shown that metal-dependent KDO8P synthases can be converted into metal-independent KDO8P synthases by the mutation of the metal-binding Cys to Asn, as mentioned in section 1.3.3.[126,127] It has been suggested that the metal ion is not directly involved in the metal-dependent enzyme-catalysed KDO8P synthase reaction and it may have a different function.[126,127]

Table 1.3.
Equivalent residues in the active site of DAH7P and KDO8P synthases based on 3-dimensional structure analysis

	E. coli DAH7P synthase[29]	*S. cerevisiae* DAH7P synthase[73]	*T. maritima* DAH7P synthase[57]	*P. furiosus* DAH7P Synthase[74]	*A. aeolicus* KDO8P synthase[124]	*E. coli* KDO8P synthase[121]
PEP-Phosphate binding	Ala164 Lys186 Arg234 Arg165	Ala179 Lys201 Arg180 Arg249	Ala185 Lys207 Arg186 Arg237	Ala114 Lys136 Arg115 Arg166	Ala102 Lys124 Arg154 Phe103	Ala116 Lys138 Arg168 Phe117
PEP-Carboxylate binding	Arg92 Lys97[a] Lys186	Arg107 Lys112 Lys201	Arg126 Lys131 Lys207 Gln182	Arg55 Lys60[b] Gln111	Lys41 Lys46 Lys124 Ser43 Gln99	Lys55 Lys60 Lys138
Metal binding	Cys61 His268 Glu302 Asp326	Cys76 His282 Glu316 Asp342	Cys102 His272 Glu298 Asp309	Cys31 His201 Glu227 Asp238	Cys11 His185 Glu222 Asp233	Asn26 His202 Glu239[c] Asp250
D-E4P/ D-A5P Phosphate binding	Arg99 Thr100	Arg114 Thr115	Arg133 Thr134	Arg62 Thr63	Arg49 Ser50	Arg63 Ser64
D-E4P/ D-A5P Hydroxyl group binding		Pro113 (C2-$OH^{D\text{-}E4P}$)[d] Asp342 (C3-$OH^{D\text{-}E4P}$)[d]	Pro 132/ Arg186 (C3-$OH^{D\text{-}E4P}$) Asp309 / Ser308 (C2-$OH^{D\text{-}E4P}$)	Pro61/ Arg115 (C2-$OH^{D\text{-}E4P}$) Asp 238 (C3-$OH^{D\text{-}E4P}$)	 Asp48 / PO_4^- (C1 $^{D\text{-}A5P}$) Cd^{2+} (C2-$OH^{D\text{-}A5P}$ /C3-$OH^{D\text{-}A5P}$) Asn48 (C3-$OH^{D\text{-}A5P}$)	

[a] Lys97 hydrogen bonds to a water that is coordinated to the Mn^{2+} centre.
[b] Note: in this reference,[74] this residue is disordered Lys136.
[c] Note: in this reference,[121] this residue is mislabelled His235.
[d] C2 and C3 hydroxyl groups of D-E4P are inferred to be C1 and C2 in G3P.

1.4. Aim of the project

Although there has been intensive study on the enzymic reactions catalysed by DAH7P and KDO8P synthases, there are a number of questions that still remain:

1. What are the effects of the configuration of the hydroxyl groups of aldose phosphate substrates on the enzyme-catalysed reaction?
2. What are the mechanistic similarities and differences between DAH7P synthase and KDO8P synthases, since D-E4P is a natural substrate for DAH7P synthase but D-R5P, the C2 epimer of D-A5P (a natural substrate for KDO8P synthase) with E4P-like C2 configuration, is not a substrate for KDO8P synthase.[74,79,83-85,130]

Therefore, synthetic molecules, which are stereoisomers of D-E4P, were designed and these compounds were tested as alternative substrates for DAH7P synthase to address some of these issues. The general focus of these studies is to examine the tolerance of DAH7P synthases from *E. coli* and *P. furiosus* and the KDO8P synthase from *N. meningitidis* to changes in the structure of the various phosphorylated monosaccharide substrates.

The aim of this research was to prepare, for the first time, alternative C2 or C3 stereoisomers of the natural substrate D-E4P of DAH7P synthase and alternative C2, C3, or C4 stereoisomers of the natural substrate D-A5P of KDO8P synthase. This is the first systematic study of the tolerance of both enzymes to changes in the C2, C3, or C4 configuration of the aldose phosphate substrate.

The specific goals of this study were:

- To synthesise the diastereoisomers of D-E4P (Figure 1.19): D-threose 4-phosphate (D-T4P) and L-threose 4-phosphate (L-T4P).
- To synthesise D-A5P and the stereoisomers of D-A5P (Figure 1.19): D-xylose 5-phosphate (D-X5P), L-xylose 5-phosphate (L-X5P), D-lyxose 5-phosphate (D-L5P).

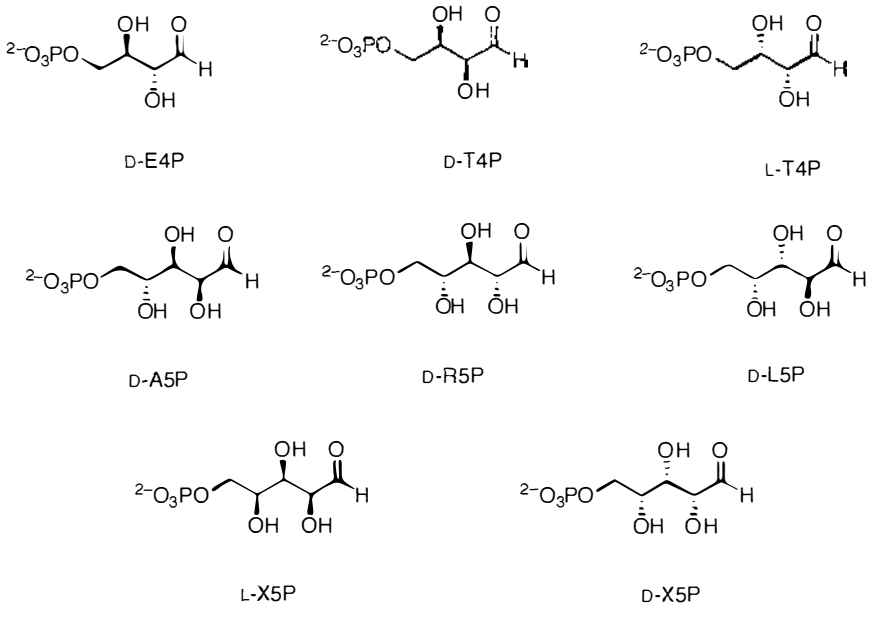

Figure 1.19. Target compounds for DAH7P synthase and KDO8P synthase: Isomers of D-E4P and D-A5P

- To examine the tolerance of DAH7P synthase to changes in C2 or C3 stereochemistry by examining whether these compounds act as alternative substrates for, or as inhibitors of *E. coli* DAH7P(Phe) synthase and *P. furiosus* DAH7P synthase.
- To examine the tolerance of KDO8P synthase to changes in C2, C3, or C4 stereochemistry using *N. meningitidis* KDO8P synthase.

- To characterise the products of the DAH7P synthase and KDO8P synthase reactions where these compounds do act as alternative substrates to D-E4P or D-A5P.

The successful synthesis of the stereoisomers of D-E4P and D-A5P led to an investigation of the tolerance of DAH7P synthase to stereochemical changes at C2 and C3 of D-E4P and of KDO8P synthase to stereochemical changes at C2, C3, or C4 of D-A5P. Kinetic data for the stereoisomers of D-E4P and D-A5P were obtained with *E. coli* and *P. furiosus* DAH7P synthases and with *N. meningitidis* KDO8P synthase, respectively. The products of these reactions, the DAH7P and KDO8P isomers, were characterised by mass spectrometry and NMR spectroscopy. As a result of this success, the mechanistic differences between DAH7P and KDO8P synthase could carefully be compared with respect to metal requirement and to sugar substrate C2 configuration.

Chapter Two

PREPARATION OF AND PRELIMINARY STUDIES WITH D-ERYTHROSE 4-PHOSPHATE AND ITS ANALOGUES

As introduced in the previous chapter, we are interested in how sensitive DAH7P synthase is to structural changes particularly in stereochemistry of the monosaccharide phosphate substrate. This investigation was initiated in order to provide further significant information about the enzyme mechanism at the active sites of DAH7P synthase and KDO8P synthase.

This chapter describes the preparation of, and studies with analogues of the natural substrate for DAH7P synthase, D-E4P. The interaction of these compounds with DAH7P synthase is described in chapter four.

2.1. Preparation, Properties, and Determination of D-E4P

This section describes the properties of D-E4P and its preparation using a previous reported procedure.[131]

2.1.1. Studies with analogues of D-E4P

As mentioned previously in the introduction, there have been few studies on analogues of D-E4P as compared to PEP. Both phosphonate and homophosphonate (Figure 2.1) are known analogues of D-E4P and have been reported to be substrates of *E. coli* DAH7P(Tyr) synthase.[89,132] However, it has been found that the natural substrate D-E4P is a much better substrate for the enzyme. Interesting results from our laboratory studying racemic 2-deoxyE4P, (3*S*)-*2*-deoxyE4P, and 3-deoxyE4P (Figure 2.1) have found that these compounds are accepted as substrates of the enzyme, *E. coli* DAH7P(Phe) synthase.[90,130]

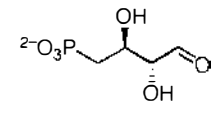

phosphonate

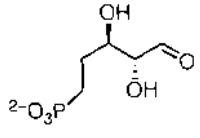

homophosphonate

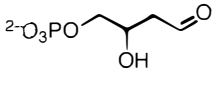

2-deoxyE4P

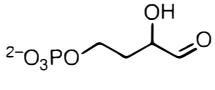

3-deoxyE4P

Figure 2.1. Analogues of D-E4P

The product of the reaction of 2-deoxyE4P with PEP in the DAH7P synthase-catalysed reaction was identified as the expected 5-deoxyDAH7P (Figure 2.2), as the enzyme appears to utilise only one enantiomer of racemic 2-deoxyE4P, the stereoisomer with the same C3 stereochemistry as D-E4P.[90,130]

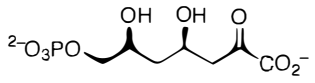

Figure 2.2. 5-DeoxyDAH7P generated from the reaction of PEP with (3*S*)-2-deoxyE4P

Additionally, 2-deoxyE4P was found to be an alternative substrate of *P. furiosus* DAH7P synthase and it was used more efficiently by this enzyme than D-E4P (Table 2.1).[74] 3-DeoxyE4P was also tested with *E. coli* and *P. furiosus* DAH7P synthases and found to be a considerably poorer substrate than 2-deoxyE4P for both enzymes (Table 2.1).[74,90] This work indicates that the C3 hydroxyl group of D-E4P was not essential for catalysis with DAH7P synthase, which is consistent with an acyclic mechanism rather than the cyclic mechanism as discussed in chapter one.

Table 2.1.
Kinetic results from analogues of D-E4P with DAH7P synthases[a]

Analogues of D-E4P	*E. coli* DAH7P(Phe) synthase[90]			*P. furiosus* DAH7P synthase[74]		
	K_M (μM)	k_{cat} (s^{-1})	k_{cat}/K_M ($s^{-1}/\mu M$)	K_M (μM)	k_{cat} (s^{-1})	k_{cat}/K_M ($s^{-1}/\mu M$)
D-E4P	39 ± 4	26 ± 2	670 α 10^{-3}	9 ± 1	1.4 ± 0.1	160 α 10^{-3}
(3*S*)-2-deoxyE4P	410 ± 40	25 ± 3	60 α 10^{-3}	6 ± 1	3.0 ± 0.1	490 α 10^{-3}
(2*R*)-3-deoxyE4P	2680 ± 140	4.5 ± 0.1	2 α 10^{-3}	200 ± 30	27 ± 5	140 α 10^{-3}

[a] DAH7P synthases from both sources were assayed in accordance with previously reported procedures.[74,133]

D-T4P differs from D-E4P in its C2 hydroxyl group configuration, whereas the C3 hydroxyl group of L-T4P is in the opposite configuration to that found at C3 in D-E4P. Due to the different configuration of the C2 and C3 hydroxyl groups, the study of D- and L-T4P will give us significant information as to the tolerance of the enzyme DAH7P synthase to changes in D-E4P, and the role that the C2 and C3 hydroxyl groups play in the normal enzyme-catalysed reaction.

2.1.2. Properties and previous preparations of D-E4P

D-E4P is a notoriously unstable compound in solution and consequently it is difficult to handle.[134] It has been reported that both monomer and dimer forms of D-E4P are found in aqueous solutions and the amount of dimer depends on the D-E4P concentration.[135]

The three major forms of D-E4P identified by NMR spectroscopic studies by Duke *et al.* are dimers of D-E4P in solution (Figure 2.3), which dissociate to monomer forms at relatively low concentrations (< 0.2M).[135] The monomer exists mainly as its hydrate in solution. The monomer of D-E4P would be expected to be the most predominant species in biological assay studies as the D-E4P concentration is relatively low. However, the dissociation rate of the dimer to the monomer is slow. Thus, care has to be taken to ensure that the solution has time to be allowed to equilibrate. As well, D-E4P solutions cannot readily be evaporated to dryness to give solid D-E4P as the molecule dephosphorylates on concentration. This poses particular difficulties with the isolation and purification of this compound.

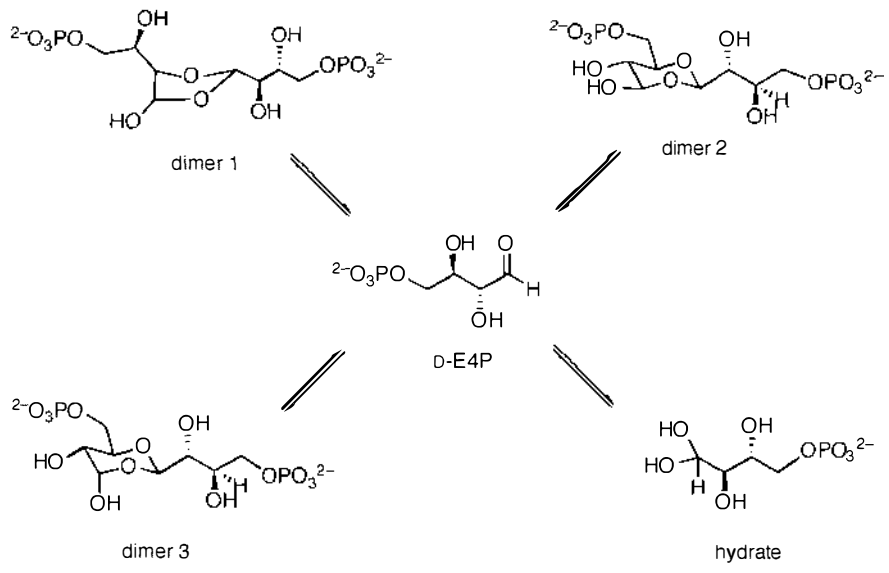

Figure 2.3. Equilibration of D-E4P

Both enzymatic and synthetic methods for the preparation of D-E4P have been reported.[136,137] D-E4P can be formed enzymatically by the enzyme transketolase.[136] In this enzyme-catalysed reaction, D-fructose 6-phosphate (D-F6P) and D-R5P produce D-E4P and sedoheptulonase 7-phosphate (S7P) (Figure 2.4). This is a reversible reaction and therefore, D-E4P is present as well as the other sugar phosphates at equilibrium. It is difficult to purify D-E4P from this complex mixture. However, it is a useful method for the generation of D-E4P when the D-E4P does not need to be isolated.

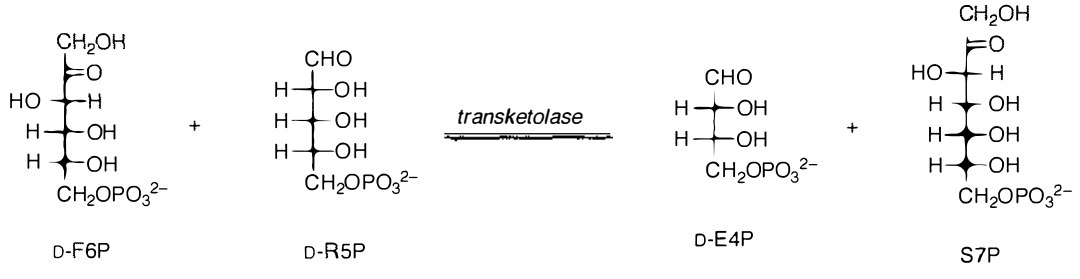

Figure 2.4. Enzymatic synthesis of D-E4P using transketolase

Ballou *et al.* have prepared D-E4P using two different synthetic methods.[137] Both methods produce 4-*O*-trityl-2,3-di-*O*-acetyl-D-erythrose diethyl mercaptal as a key intermediate (Figure 2.5). In method A, 4-*O*-trityl-2,3-di-*O*-acetyl-D-erythrose diethyl mercaptal was synthesised from D-arabinose *via* D-erythrose with an overall yield of 14 %. In method B, 4-*O*-trityl-2,3-di-*O*-acetyl-D-erythrose diethyl mercaptal was prepared from 4,6-*O*-ethylidene-D-glucose *via* 2,4-*O*-ethylidene-D-erythrose in an overall yield of 45 %.

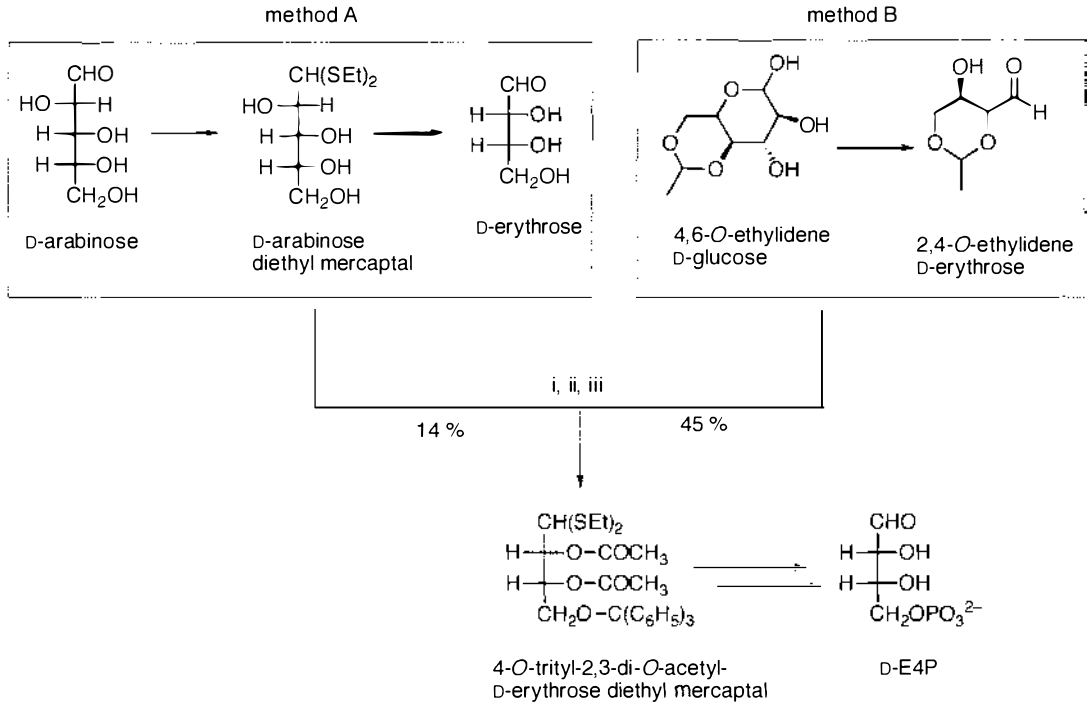

Figure 2.5. Reported scheme for the preparation of D-E4P.[137] i. C_2H_5SH, HCl; ii. $(C_6H_5)_3CCl$, C_5H_5N; iii. $(CH_3CO)_2O$.

D-E4P can also be prepared in high yield (85 %) by oxidative cleavage of D-glucose 6-phosphate (D-Glu6P) with lead tetraacetate (Figure 2.6).[131,138] This is a convenient one step procedure and it is the commonly used method for the synthesis of D-E4P. This

chapter describes the synthesis of D-E4P using this method and the synthesis of D-T4P using D-galactose 6-phosphate (D-Gal6P) as an alternative starting material by an adaptation of this method.

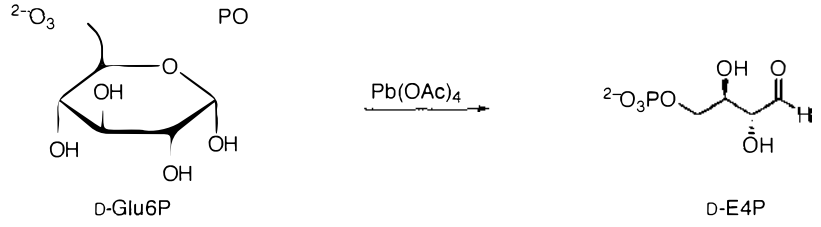

Figure 2.6. Synthesis of D-E4P using lead tetraacetate

2.1.3. Preliminary investigations into the preparation of D-E4P

In these studies, following reported procedures, D-E4P was prepared by oxidation of D-Glu6P with lead tetraacetate (Figure 2.6).[131] Theoretically, two equivalents of lead tetraacetate are required for each equivalent of D-Glu6P to achieve cleavage of the six-carbon sugar to the four-carbon sugar. In accordance with the published method,[131] only 1.7 equivalents of lead tetraacetate were used in order to avoid over-oxidation to D-glyceraldehyde 3-phosphate. After the oxidation of D-Glu6P with lead tetraacetate, the presence of D-E4P was determined using an enzymic assay system involving the enzyme transaldolase (EC 2.2.1.4).

In this assay system, the oxidation of NADH to NAD^+ by G3P dehydrogenase (EC 1.1.99.5) is monitored at 340 nm ($\alpha_{340} = 6.4 \alpha 10^3 M^{-1} cm^{-1}$) after the conversion of D-E4P to dihydroxyacetone phosphate *via* D-glyceraldehyde 3 phosphate catalysed by the

enzymes transaldolase and triose phosphate isomerase (EC 5.3.1.1, Figure 2.7). This enzyme assay system is particularly useful as it allows measurement of D-glyceraldehyde 3-phosphate in the same assay mixture. According to this assay, in our hands, D-E4P was synthesised from D-Glu6P in a 73 % yield.

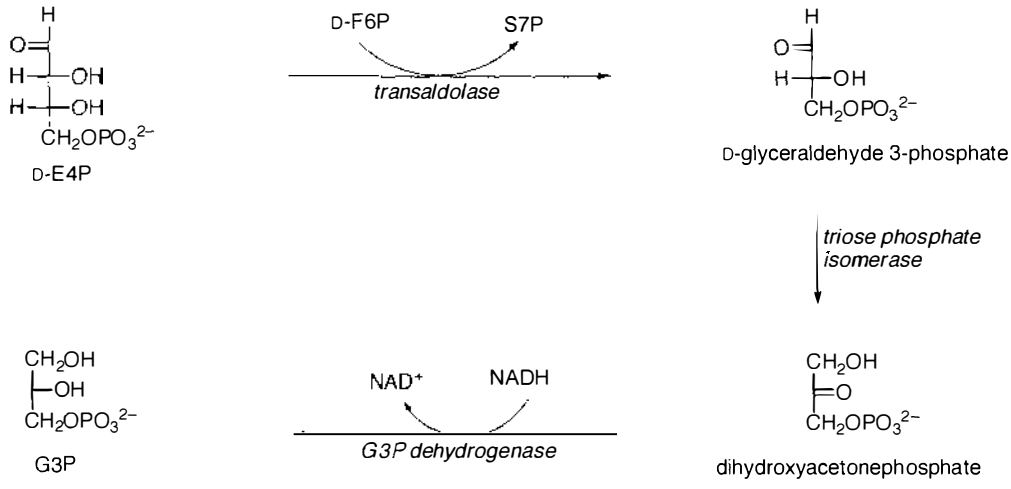

Figure 2.7. A coupled assay system using transaldolase, triose phosphate isomerase, and G3P dehydrogenase

For this study, the presence of D-E4P was also confirmed by using the DAH7P synthase reaction. The loss of PEP was followed on conversion of the two substrates PEP and D-E4P to DAH7P catalysed by *E. coli* DAH7P(Phe) synthase at 232 nm ($\alpha_{232} = 2.8 \alpha 10^3$ M^{-1} cm^{-1}) (Figure 2.8). During the reaction, PEP loses its double bond between C2 and C3 causing the disappearance of absorption at 232nm when the enzyme catalyses the formation of DAH7P. Therefore, with PEP in excess, the loss of absorbance will be proportional to the D-E4P concentration.

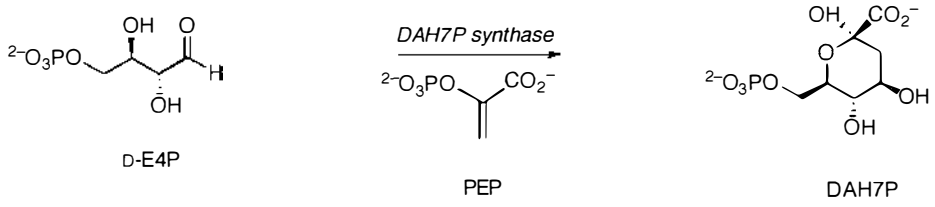

Figure 2.8. Preparation of DAH7P from D-E4P and PEP by the DAH7P synthase-catalysed reaction

To confirm that DAH7P was formed in this enzyme-catalysed reaction, and therefore, that D-E4P was present, two methods were used. The first of these was the thiobarbituric acid assay, which is a colourimetric method for the estimation of 3-deoxyaldulosonic acids.[139] α-Formylpyruvate is generated by periodate oxidative cleavage between C4 and C5 of a 3-deoxyaldulosonic acid (Figure 2.9). α-Formylpyruvate gives rise to a pink colour with thiobarbituric acid and this is spectrophotometrically detected at 549 nm (α_{549} = 1.03 α 10^5 $M^{-1}cm^{-1}$). The enzymic product from the D-E4P generated from D-Glu6P in this assay showed a dark pink colour and absorbed at 549 nm. This result is consistent with the formation of DAH7P from the chemically synthesised D-E4P in the DAH7P synthase-catalysed reaction.

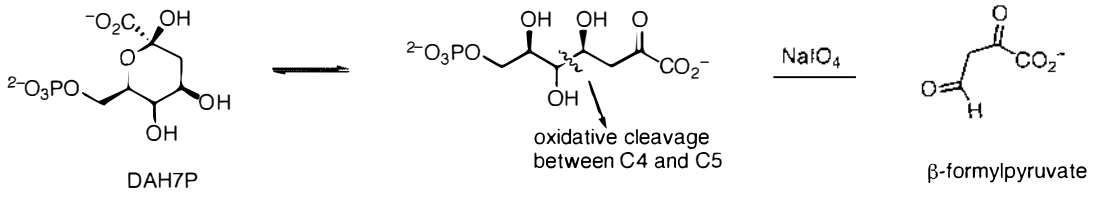

Figure 2.9. Formation of α-formylpyruvate for the thiobarbituric acid assay

The other method to confirm that DAH7P was generated was to employ a coupled assay system using the enzymes 3-dehydroquinate synthase (DHQS, EC 4.6.1.3) and dehydroquinase (DHQase, EC 4.2.1.10), which are the second and third enzymes of the shikimate pathway, respectively. This coupled assay system is followed at 234 nm (α_{234} = 1.2 α 10^4 $cm^{-1}M^{-1}$) where the generation of 3-dehydroshikimate (DHS) can be observed by the absorption of its α,α-unsaturated acid group (Figure 2.10).

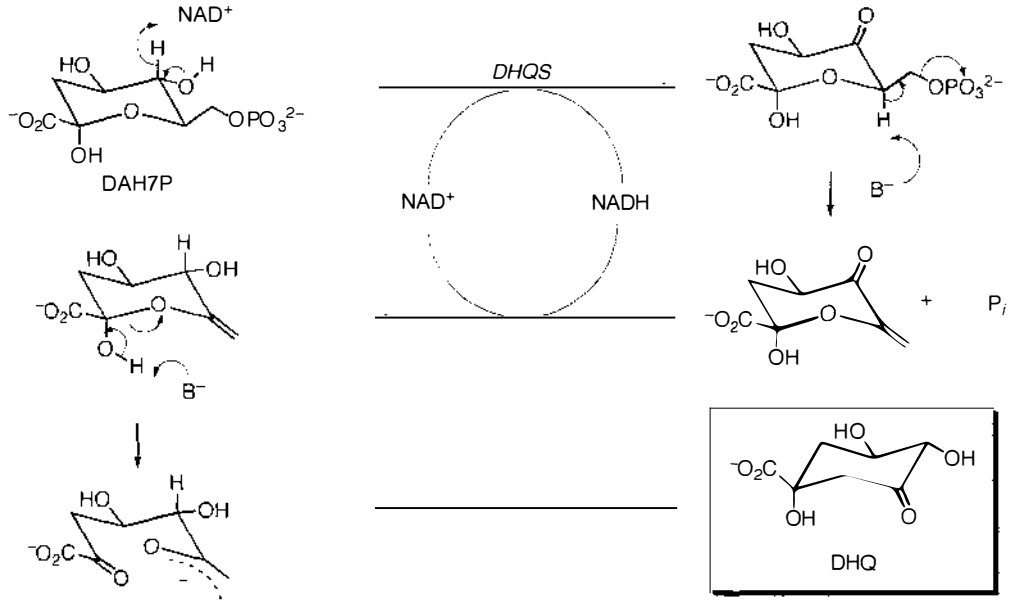

Figure 2.10. Proposed mechanism of DHQS. Taken from Knowles.[140]

The product of the DAH7P synthase reaction gave rise to an increase in absorbance at 234 nm when incubated with DHQS and DHQase in the presence of NAD^+ (catalytic amounts of this cofactor are required by DHQS). This result confirms the presence of DAH7P and therefore, the presence of D-E4P following the oxidation of D-Glu6P by lead tetraacetate. More details of this assay will be discussed in section 2.2.4.

Both of these assays (the thiobarbituric assay and the coupled assay with DHQS and DHQase) were important for testing for the presence of D-T4P and for confirming its ability to act as a substrate for DAH7P synthase despite the C2 configurational change. These results with D-T4P are described in section 2.2.3 and 2.2.4.

2.2. Preparation and Determination of D-T4P

The key goal of this section is the preparation of D-T4P using different starting materials. In this section, the synthesis of D-T4P using both oxidative chemistry from six- or five-carbon sugars (Figure 2.11) and starting with a four-carbon precursor will be introduced.

2.2.1. Preliminary investigations into the preparation of D-T4P from D-Gal6P

As D- and L-T4P are not commercially available, they had to be synthesised. Due to the similarity between D-T4P and D-E4P, it was considered that D-T4P might well be as difficult to handle as D-E4P. Therefore, the same synthetic method that gave rise to D-E4P was considered for the preparation of D-T4P.

As D-E4P could be generated by oxidative cleavage of D-Glu6P following the procedure of Simpson *et al.*,[131] it was considered D-T4P might be able to be produced by adapting this procedure. D-T4P differs from D-E4P by its absolute configuration at C2. Therefore,

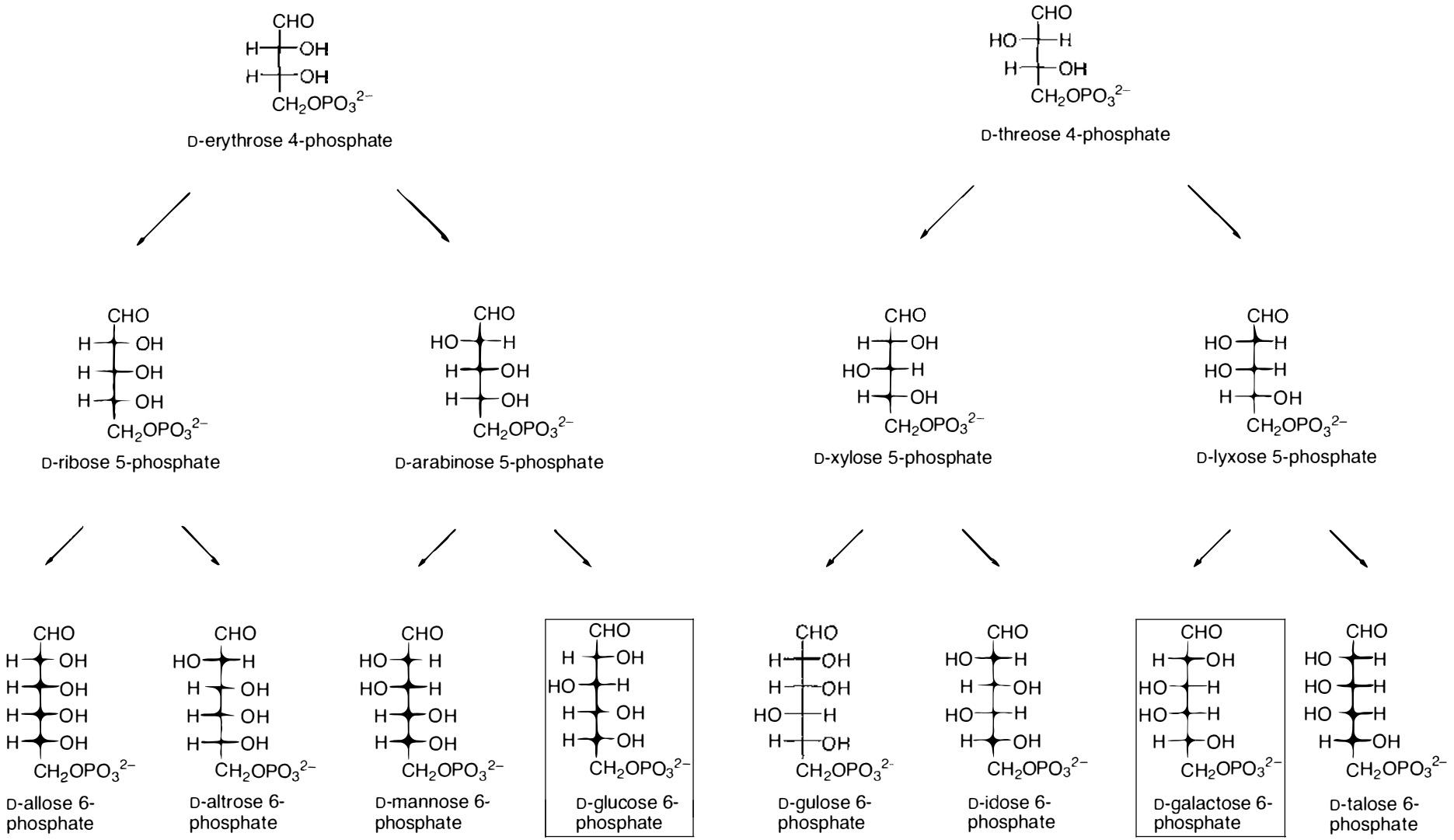

Figure 2.11. Phosphorylated aldoses. D-Glu6P and D-Gal6P used as starting materials for D-E4P and D-T4P, respectively, are in boxes.

there are four possible six-carbon phosphorylated D-aldoses that could be potential starting materials for the generation of D-T4P using the lead tetraacetate cleavage procedure. These are D-gulose 6-phosphate, D-idose 6-phosphate, D-Gal6P, and D-talose 6-phosphate (Figure 2.11). Of these, only D-Gal6P was commercially available at the beginning of this project. Following the method used for the preparation of D-E4P, D-T4P was prepared by oxidation with 1.7 equivalents of lead tetraacetate from D-Gal6P (Figure 2.12). After the oxidative cleavage, the mixture needed to be tested for the production of D-T4P. As with the generation of D-E4P from D-Glu6P, enzyme assays were utilised for this purpose. The D-T4P was confirmed to be an alternative substrate of DAH7P synthase by the observation of the loss of PEP when incubated with *E. coli* DAH7P(Phe) synthase.

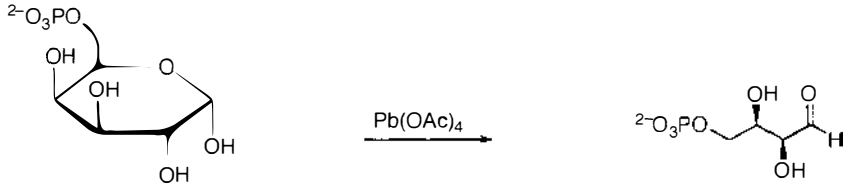

D-Gal6P D-T4P

Figure 2.12. Proposed preparation of D-T4P using lead tetraacetate

2.2.2. Determination of the presence of D-T4P using transaldolase assay

The transaldolase assay was used to determine the presence of D-T4P. Using this method, D-T4P was calculated to be produced in a 19 % yield from D-Gal6P. The concentration of D-T4P was determined by observing the oxidation of NADH at 340 nm

(α_{340} = 6.4 α 10^3 $M^{-1}cm^{-1}$) catalysed by G3P dehydrogenase. D-T4P is converted to G3P *via* D-glyceraldehyde 3-phosphate and dihydroxyacetone phosphate by the enzymes transaldolase and triose phosphate isomerase (Figure 2.7). This result was consistent with the formation of D-T4P from D-Gal6P by cleavage with lead tetraacetate. However, the result from the coupled assay system showed more dramatically increased absorption for the presence of D-glyceraldehyde 3-phosphate than that of produced D-T4P. It suggests that, although D-T4P was successfully synthesised by the oxidative cleavage with lead tetraacetate of D-Gal6P, substantial over-oxidation had occurred.

Analysis of the stereochemistry differences between D-Glu6P and D-Gal6P may explain the low yield of D-T4P in this reaction since the oxidation requires *cis*-diols. Structurally, the α-D-Glu6P pyranose form has only one *cis*-diol between C1 and C2, whereas α-D-Gal6P has two, one between C1 and C2 and the other between C3 and C4 (Figure 2.13). This change in stereochemistry may account for the difference in yield of D-E4P (73 %) and D-T4P (19 %) from D-Glu6P and D-Gal6P, respectively. The presence of a *cis*-diol between C3 and C4 may be the reason for the substantial over-oxidation to D-glyceraldehyde 3-phosphate observed in our synthesis of D-T4P as observed in the coupled assay system as described in section 2.1.3.

Since it was found that D-T4P had been synthesised, the loss of PEP in the presence of *E. coli* DAH7P(Phe) synthase and the D-T4P was followed at 232 nm. This enzyme assay showed time- and enzyme concentration-dependent loss of PEP (Figure 2.14).

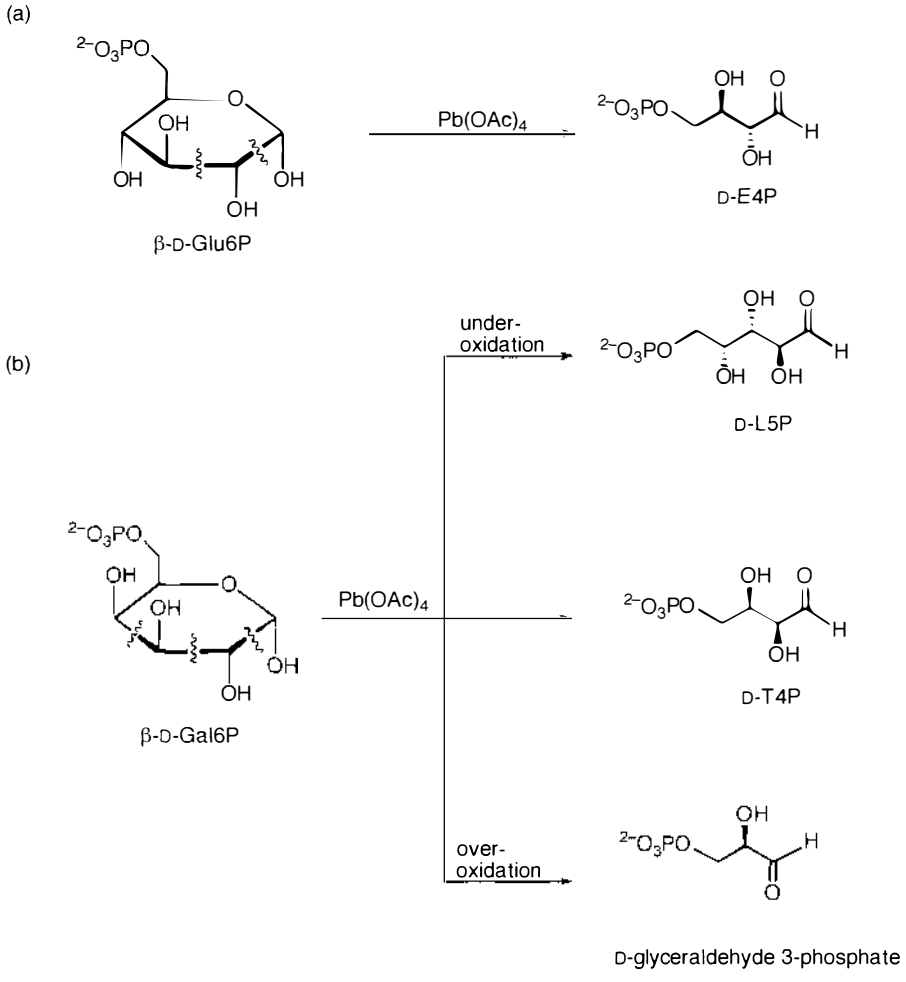

Figure 2.13. Structure of (a) β-D-Glu6P and (b) β-D-Gal6P leading D-E4P and D-T4P, respectively, by oxidative cleavage. The possible side products, D-L5P and D-glyceraldehyde 3-phosphate from under- and over-oxidation from β-D-Gal6P are also shown.

The pattern of the enzyme reaction observed was similar to that observed with D-E4P, suggesting that the enzyme, *E. coli* DAH7P(Phe) synthase, tolerates D-T4P as an alternative substrate. This is a significant result as it indicates that the enzyme is able to accept a substrate with altered C2 stereochemistry. However, the reaction rate of D-T4P was very slow compared to the same enzyme reaction with D-E4P. Although this may

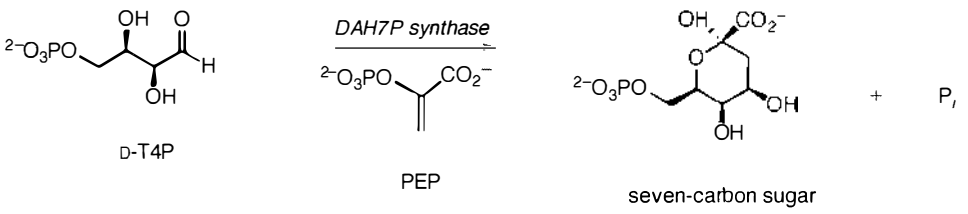

Figure 2.14. Seven-carbon monosaccharide produced by DAH7P synthase with D-T4P and PEP

indicate that D-T4P is a poorer substrate than D-E4P for *E. coli* DAH7P(Phe) synthase, it might also be due to the presence of other monosaccharide sugars, D-glyceraldehyde 3-phosphate and D-L5P, from the over- and under-oxidation of D-Gal6P, respectively (Figure 2.13). In previously published reports, it has been shown that other five-carbon monosaccharides are substrates of *E. coli* DAH7P(Phe) synthase and that D-glyceraldehyde 3-phosphate competes with D-E4P for active-site binding.[79,84] Thus, if D-glyceraldehyde 3-phosphate and D-L5P are in solution with D-T4P, they may compete with each other for the enzyme, thereby slowing the enzyme reaction rate, or it might mean that the loss of PEP we are observed, may not be due to consumption of D-T4P in the mixture. Therefore, it was necessary to check that the loss of PEP in this enzyme assay was due to the consumption of D-T4P only and was not due to the presence of any other monosaccharide sugars. It was confirmed that D-T4P was generated by the examination of the production of 3-deoxy-D-*lyxo*-heptulosonate 7-phosphate (D-DLH7P) by enzymatic reaction with PEP. This was also performed in a number of ways in following sections, closely paralleling the confirmation of DAH7P production from D-E4P and PEP by the enzymatic reaction described in section 2.2.1 above.

2.2.3. Thiobarbituric acid assay

D-DLH7P obtained from the reaction of D-T4P with PEP catalysed by *E. coli* DAH7P(Phe) synthase was subjected to the thiobarbituric acid assay. In the assay, a positive result was observed indicating the formation of a new C–C bond between D-T4P and PEP catalysed by *E. coli* DAH7P(Phe) synthase. The colour of the reaction product, α-formylpyruvate, appeared dark pink similar to that resulting from the assay with DAH7P (Figure 2.9). The absorption of the product was detected at 549 nm. The results indicate that D-DLH7P was present in the reaction product and therefore, an aldehyde cosubstrate must have been present in the D-T4P mixture. It also is a confirmation that the oxidative cleavage of D-Gal6P had been successful.

2.2.4. Coupled enzyme assay using DHQS and DHQase

After the generation of D-DLH7P from the D-T4P mixture and PEP in the enzyme reaction, the product was observed to be an isomer of DAH7P by mass spectrometry showing the same mass as was observed for DAH7P (287.013 for DAH7P; 287.0123 for D-DLH7P from D-T4P).

A coupled assay system using DHQS and DHQase was then used to detect DHQ generation at 234 nm as described in section 2.1.3. However, no DHQ production was observed after the addition of the two enzymes DHQS and DHQase.

Analysis of the mechanism of DHQS could explain the inability of D-DLH7P to act as a substrate for DHQS. DHQS catalyses the cyclisation of DAH7P to give DHQ in the

presence of both a divalent metal ion and NAD^+ (Figure 2.10).[140] In the first step of this reaction, oxidation of the C5 hydroxyl group of DAH7P takes place. The C5 hydroxyl group is restored only after elimination of the phosphate to form the enol ether. As the NAD^+ oxidant only approaches the DAH7P substrate from one side in the active site of DHQS, this enzyme reaction is highly stereospecific. If D-DLH7P had been produced in the DAH7P synthase reaction with D-T4P and PEP, it would not be expected to be a substrate for DHQS as the C5 hydroxyl group is not in the correct configuration (Figure 2.15). Therefore, the negative result from this coupled assay test in combination with the other results is consistent with D-T4P presence and D-DLH7P production. Perhaps more significantly, this result indicates that the loss of PEP observed in the DAH7P synthase reaction is not due to the presence of any D-E4P in the mixture, which may potentially be formed by the epimerisation of D-T4P.

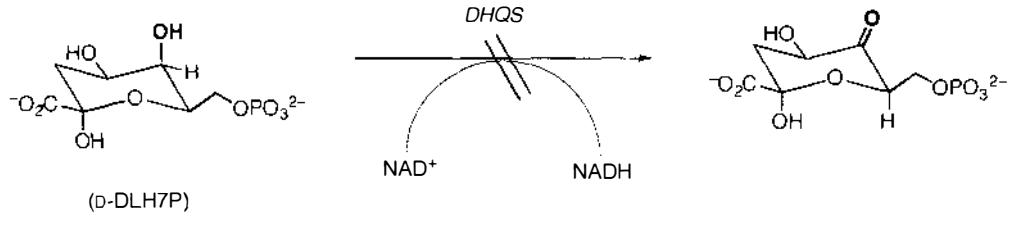

Figure 2.15. Oxidation of D-DLH7P in the first step of the DHQS mechanism

2.3. Synthetic Strategies for the Preparation of D-T4P

Although the formation of D-T4P from D-Gal6P by lead tetraacetate oxidation has been demonstrated, 19 % yield of D-T4P is clearly unsatisfactory, as a mixture of other aldose phosphates is present in this reaction from the over- and under-oxidation (Figure

2.13) of D-Gal6P. Due to that D-T4P cannot be purified from other aldose phosphates, which might be interacting with the enzyme DAH7P synthase, we wanted to investigate more fully whether the oxidation of D-Gal6P could be improved to give higher yields of the desired D-T4P product. However, as D-Gal6P was no longer commercially available after our initial experiments, a chemical synthesis of D-Gal6P was investigated.

2.3.1. Synthesis of D-Gal6P

The synthetic scheme was designed using D-galactose as a starting material to produce D-Gal6P *via* D-galactose diacetonide (Figure 2.16).

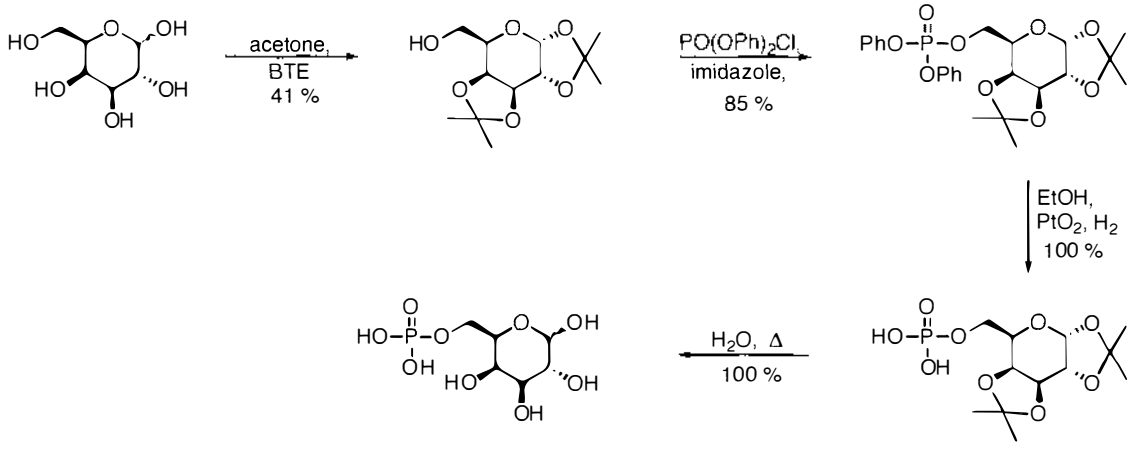

Figure 2.16. Synthetic scheme for the preparation of D-Gal6P

D-Galactose was treated with acetone and boron trifluoride etherate (BTE) to give the 1,2:3,4-diisopropylidene D-galactopyranose (41 %).[141] The modest yield could be due to either an incomplete reaction or the loss of compound during purification. Although the

41 % yield was not very satisfactory, the next step was carried out as the starting material was relatively inexpensive. Following the protection of the hydroxyl groups, the C5 hydroxyl group was phosphorylated using diphenyl chlorophosphate. Hydrogenolysis and cleavage of the diacetonide gave rise to D-Gal6P with overall yield of 35 %.

Hydrogenolysis was carried out in ethanol using a platinum catalyst and the progress of the reaction was followed by thin layer chromatography (tlc). After the starting material was completely consumed, the reaction mixture was filtered and the solvent was evaporated. The D-diacetonide galactose 6-phosphate was then dissolved in water and the solution was heated at 50 °C to cleave the acetal protecting groups. The deprotected final product, D-Gal6P, was then lyophilised and used as a starting material for the synthesis of D-T4P.

Due to the low yield (19 %) of D-T4P from over-oxidation by using 1.7 equivalent of lead tetraacetate when using commercial D-Gal6P as previously observed, four reactions were carried out that 0.85, 1.0, 1.3, or 1.5 of lead tetraacetate equivalents instead of 1.7 equivalent of lead tetraacetate. The yield of D-T4P was determined by using the *E. coli* DAH7P(Phe) synthase-catalysed reaction following the loss of PEP at 232 nm as described in section 2.1.3. The best yield was obtained with 1.5 equivalents of lead tetraacetate (Table 2.2).

Table 2.2.
The yield of D-T4P from synthesised D-Gal6P using various equivalents of lead tetraacetate

Lead tetraacetate	0.85 equiv	1 equiv	1.3 equiv	1.5 equiv
Yield of D-T4P	11 %	20 %	22.5 %	40 %

2.3.2. Synthesis of D-T4P from D-X5P

As the oxidative cleavage using lead tetraacetate had been successful for the preparation of both D-E4P and D-T4P, it was considered that five-carbon sugars rather than six-carbon sugars could be employed as alternative starting materials. Using five-carbon sugars as starting materials involves the cleavage of one carbon rather than two carbons to give rise to the desired four carbon products. As shown in Figure 2.11, there are four five-carbon phosphorylated D-aldoses: D-A5P, D-R5P, D-X5P, and D-L5P. D-A5P and D-R5P are potential starting materials for D-E4P, and D-X5P and D-L5P are possible candidates for D-T4P production. Of these four compounds, only D-R5P and D-A5P are commercially available. As D-R5P is relatively inexpensive compared to D-A5P and it was available in our laboratory, D-R5P was chosen as a starting material to investigate whether five-carbon phosphorylated sugars were indeed suitable starting materials for the oxidative cleavage. D-R5P was oxidised by using 0.85 equivalent of lead tetraacetate in order to produce D-E4P (Figure 2.17). After the oxidative cleavage, the mixture was tested for D-E4P presence. These enzyme assays showed that D-E4P was successfully synthesised with 64 % yield from D-R5P.

This success of the production of D-E4P from D-R5P prompted us to investigate the possibility of the generation of D-T4P from five-carbon phosphate sugars. As neither D-X5P nor D-L5P was commercially available, the synthesis of D-X5P or D-L5P was required. We chose to synthesise D-X5P as this synthesis had been previously reported from the relatively inexpensive starting material, D-xylose. Additionally, D-X5P was also useful for our investigations into the substrate specificity of KDO8P synthase as

described in chapter five. D-X5P was prepared from D-xylose with five steps in 22 % overall yield. This preparation of D-X5P is described in more detail in chapter three.

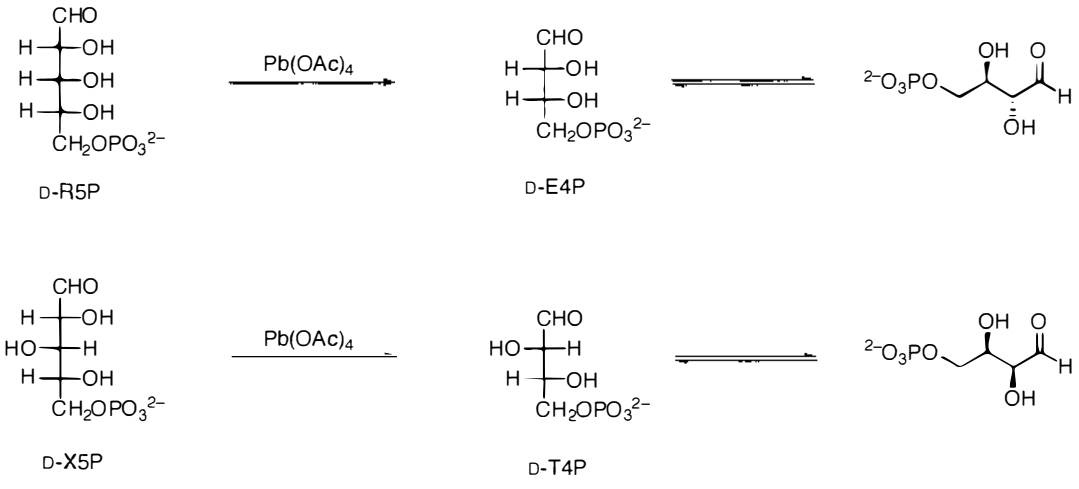

Figure 2.17. Preparation of D-E4P from D-R5P and D-T4P from D-X5P by oxidative cleavage

With D-X5P in hand, various ratios of lead tetraacetate (0.85, 0.7, and 0.5 equivalents) were used for its oxidation to D-T4P. However, none of these reactions produced any D-T4P as analysed by enzyme assay following the loss of PEP at 232 nm. However, as we only had access to limited starting material, D-X5P, and the successful synthesis of D-Gal6P using D-galactose had already been completed, we decided not to investigate this route further. As any product generated in this way would also be expected to be contaminated with other sugar phosphates, it was considered that this oxidative cleavage route was unlikely to give any significant improvement over the oxidation of D-Gal6P.

Although we had been successful in synthesising D-T4P from D-Gal6P, D-glyceraldehyde 3-phosphate and D-L5P are likely contaminants of D-T4P from the over- or under-oxidation of D-Gal6P, respectively. As it is very difficult to separate the D-T4P from these side products, a more efficient synthesis of D-T4P was required. Therefore, two alternative synthetic strategies for D-T4P preparation using two different starting materials, 2,3-*O*-isopropylidene-D-threitol and diethyl tartrate, were investigated.

2.3.3. Synthesis of D-T4P using 2,3-*O*-isopropylidene-D-threitol

The use of 2,3-*O*-isopropylidene-D-threitol was investigated as a possible starting material for the synthesis of D-T4P (Figure 2.18). In this synthetic plan, D-T4P and an

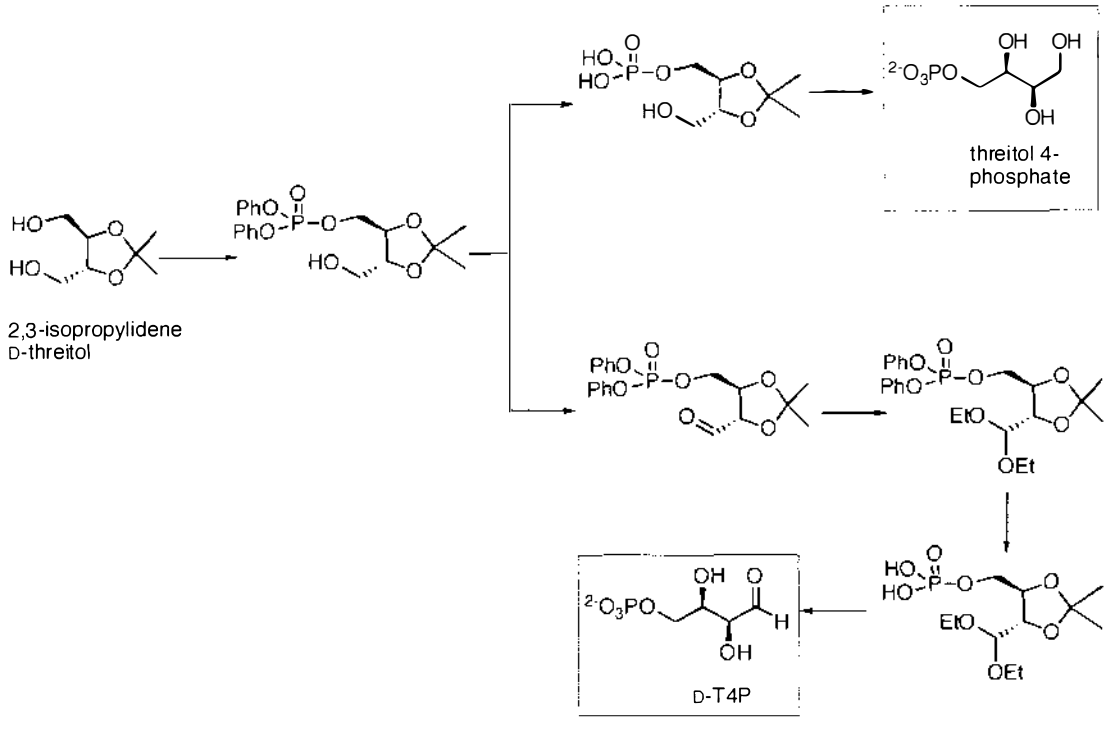

Figure 2.18. Overall scheme of the synthesis of D-T4P and threitol 4-phosphate from 2,3-isopropylidene D-threitol

alternative compound, D-threitol 4-phosphate could be produced using similar chemistry. This reduced version of D-T4P may also be an useful tool for investigating the DAH7P synthase reaction.

The first step in this scheme was the monophosphorylation of 2,3-isopropylidene D-threitol (Figure 2.19). Due to the symmetry of 2,3-isopropylidene D-threitol, monophosphorylated products on either C1 or C4 hydroxyl group are identical. Although phosphorylation of an alcohol has previously been carried out using excess of the diphenyl chlorophosphate (about 1.4 equivalents), only one equivalent was used in this case in order to minimise diphosphorylation. Regardless of this, diphosphorylated product was still observed by tlc. The diphosphorylated product was isolated by column chromatography to give 37 % yield.

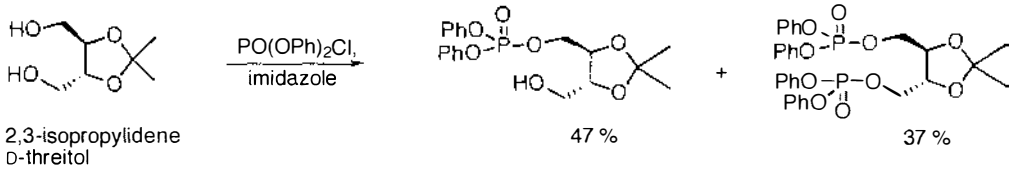

Figure 2.19. Phosphorylation of 2,3-isopropylidene D-threitol

Dess-Martin periodinane is an oxidising reagent used to oxidise a primary alcohol to an aldehyde or a secondary alcohol to a ketone.[142] As the reaction using Dess-Martin periodinane occurs under relatively mild conditions, this reagent was chosen for the next step. Despite using three equivalents of Dess-Martin periodinane for this reaction, a poor yield (22 %) of aldehyde product was obtained (Figure 2.20). The low yield

might be caused by the Dess-Martin periodinane not being fresh or it may have been due to the presence of excess acetic acid in Dess-Martin periodinane, which may cleave the acetal group. However, despite this low yield, the next step, the protection of aldehyde group, was carried out in order to determine whether this proposed synthetic route to D-T4P was likely to be successful.

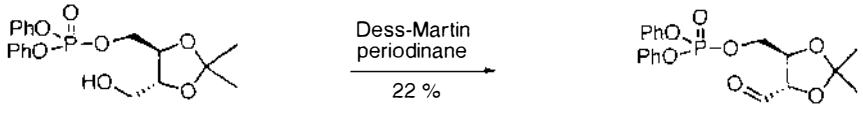

Figure 2.20. Oxidation of primary alcohol to aldehyde using Dess-Martin periodinane

The aldehyde was treated with triethyl orthoformate in the presence of acid (Figure 2.21).[143] However, there was no indication of the formation of diethyl acetal, possibly due to insufficient starting compound (only 32 μmol used), too short a reaction time (1 hour), or cleavage of the other acetal under these conditions. As there was more success with an alternative starting material (see section 2.3.5 below), this route was not investigated any further.

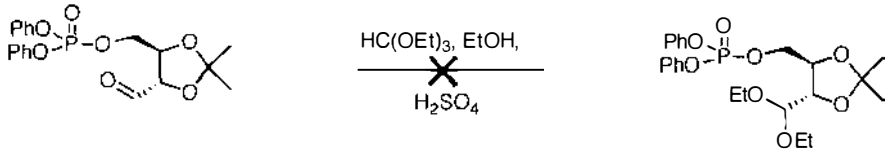

Figure 2.21. Protection of aldehyde

2.3.4. Preparation of D-threitol 4-phosphate

While D-threitol 4-phosphate would not be expected to be a substrate for DAH7P synthase as it lacks the aldehyde functionality, it may be useful as a probe for the active site of DAH7P synthase. The scheme investigated for the production of D-T4P in section 2.3.3 could be readily adapted for the synthesis of this compound.

For the preparation of D-threitol 4-phosphate, phosphorylation of 2,3-isopropylidene D-threitol was followed by hydrogenolysis to remove the phenyl protecting groups (Figure 2.22). Following hydrogenolysis, the acetal protecting group was removed by dissolution in water and heating at 60 °C for about two hours to give the final product D-threitol 4-phosphate (27 %) of a yellow powder. The product was then stored at -20 °C until required for the future investigation.

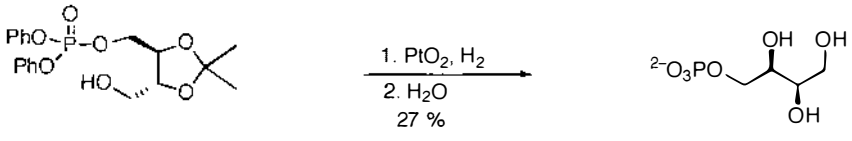

Figure 2.22. Preparation of D-threitol 4-phosphate

2.3.5. Synthesis of D-T4P from D-diethyl tartrate

Following the successful synthesis of D-threitol 4-phosphate, an alternative synthetic scheme was devised for the synthesis of D-T4P using D-tartaric acid as a starting

material (Figure 2.23). Using this scheme, D-T4P was successfully synthesised from D-diethyl tartrate in seven steps with an overall yield of 12 %.

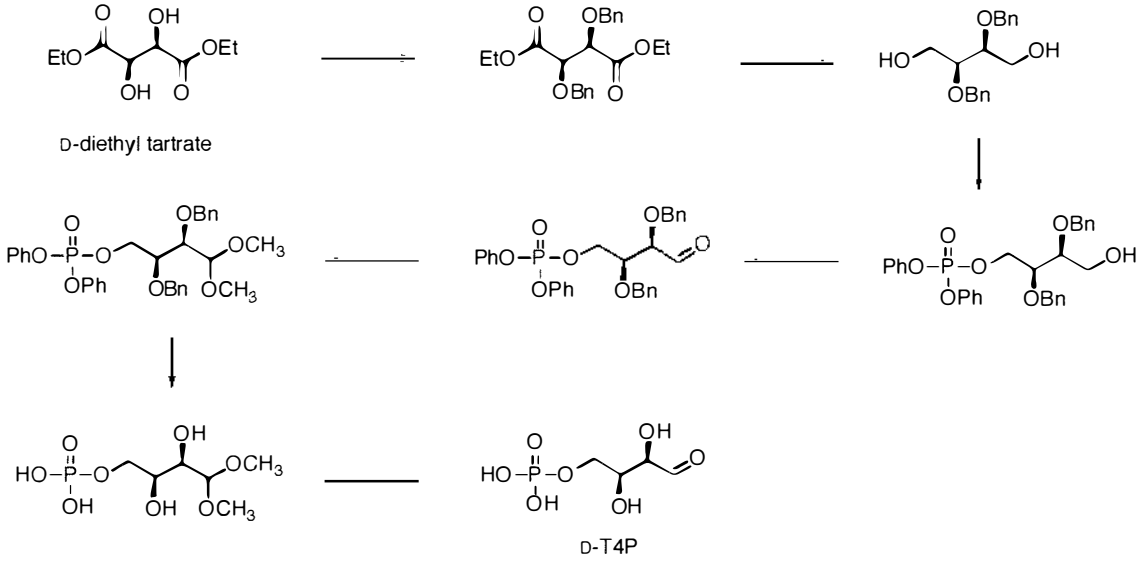

Figure 2.23. New synthetic scheme for D-T4P starting with D-diethyl tartrate

The two hydroxyl groups of D-diethyl tartrate were first protected by benzylation using benzyl bromide and silver oxide with a 97 % yield (Figure 2.24).[144-146]

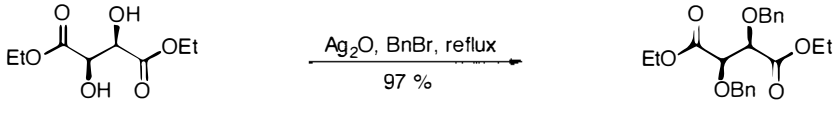

Figure 2.24. Benzylation of D-diethyl tartrate

Dibenzyl-D-diethyl tartrate in ether was then reduced using dry lithium aluminum hydride (LAH) to give the diol in a 76 % yield (Figure 2.25).[147,148] Care with LAH had

to be taken during this reaction as LAH reacts very vigorously with water. LAH was added very slowly into the reaction mixture at 0 °C and the mixture was then refluxed.

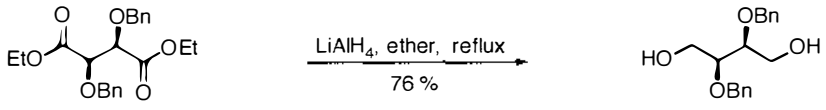

Figure 2.25. Reduction of dibenzyl-D-diethyl tartrate using LAH

Monophosphorylation (48 %) was followed by oxidation using the Dess-Martin periodinane to give the phosphorylated aldehyde (87 %, Figure 2.26).[149]

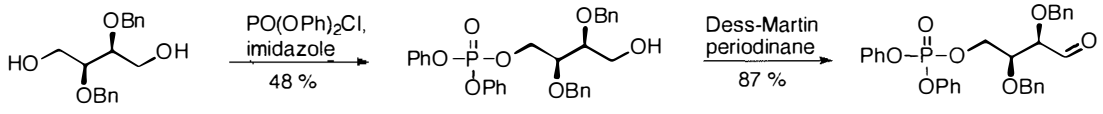

Figure 2.26. Monophosphorylation and oxidation of primary alcohol

The aldehyde group that resulted from the oxidation was then protected as the dimethyl acetal using trimethyl orthoformate (76 %, Figure 2.27).[150] The phenyl esters were removed by hydrogenolysis with H_2 over platinum in methanol. The acetal protecting group was removed by dissolution in water and stirring at room temperature for two days to give rise to the final product D-T4P (51 %, Figure 2.28). The D-T4P was kept in water frozen at -80 °C.

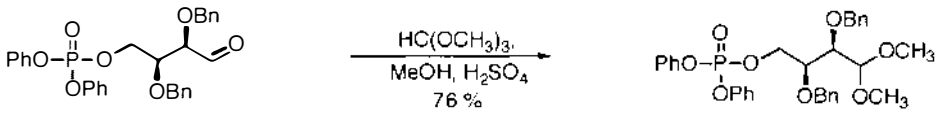

Figure 2.27. Protection of aldehyde

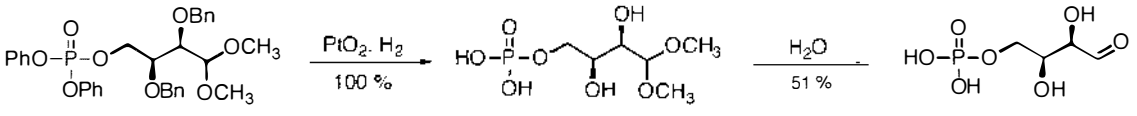

Figure 2.28. Hydrogenolysis and deprotection for the formation of D-T4P

L-T4P was synthesised using the same method as described above for the synthesis of D-T4P from L-diethyl tartrate as the starting material. Similar yields (10 % overall yield) and identical spectra were obtained.

2.4. Conclusion

Following the success of synthesis of D-E4P in 73 % yield from D-Glu6P using the standard literature procedure, this procedure was adapted for the synthesis of D-T4P from D-Gal6P. D-T4P was synthesised *via* lead tetraacetate oxidative cleavage of D-Gal6P. The D-T4P was identified and quantified by enzymatic reactions catalysed by either transaldolase or DAH7P synthase. The yield of the initial oxidation reaction of D-Gal6P was determined to be around 19 %. This low yield appears to be due to substantial over-oxidation to D-glyceraldehyde 3-phosphate. This over-oxidation may result from the presence of a second *cis*-diol between C3 and C4 in the D-

galactopyranose phosphate starting material, which is *trans* configuration in the D-Glu6P form. The low yield of the D-T4P and the presence of other aldehyde phosphates in the product mean that this preparation of D-T4P was not particularly satisfactory for undertaking enzyme kinetic studies. Additionally, after completing these initial studies, it was found that the D-Gal6P was no longer commercially available.

D-Gal6P was synthesised from D-galactose in order to repeat the initial studies of the synthesis of D-T4P using D-Gal6P. D-X5P, a five-carbon phosphorylated sugar, was also synthesised to investigate whether one-carbon cleavage was more efficient than two-carbon cleavage from D-Gal6P. However, although D-X5P was successfully synthesised, there was no sign that D-T4P was prepared from D-X5P by lead tetraacetate oxidation. This is possibly due to the small scale that this reaction was carried out on. With the unsatisfactory yield and the requirement to synthesise the starting material, the oxidative cleavage of D-X5P using lead tetraacetate was not an ideal route for D-T4P generation.

To overcome the problem with oxidative cleavage, a more efficient synthesis of D-T4P was designed from either 2,3-*O*-isopropylidene-D-threitol or D-diethyl tartrate. Unfortunately, D-T4P was not produced from 2,3-*O*-isopropylidene-D-threitol due to the inability to protect the aldehyde group on 2,3-*O*-isopropylidene-D-threitol 4-phosphate. However, by modifying this route, D-threitol 4-phosphate was synthesised, which may be useful as a probe for the active site of DAH7P synthase.

D-T4P was prepared from D-diethyl tartrate in 12 % overall yield. L-T4P was also synthesised from L-diethyl tartrate employing the same method. The detailed study of

the interaction of D- and L-T4P with *E. coli* DAH7P synthase and *P. furiosus* DAH7P synthase is described in chapter four.

Chapter Three

PREPARATION OF D-ARABINOSE 5-PHOSPHATE AND ITS ANALOGUES

3.1. Preparation and Studies of Substrate Analogues of Five-Carbon Sugars

Structural changes to four-carbon monosaccharide phosphate substrates were described in chapter two. This chapter describes the preparation of five-carbon phosphorylated monosaccharides. The interaction of the compounds with KDO8P synthase and DAH7P synthase is discussed in the following chapters.

3.1.1. Previous studies with substrate analogues of D-A5P

While DAH7P synthase is known to be able to utilise five-carbon sugars as well as four-carbon sugars to produce KDO8P,[74,79] KDO8P synthase appears to be much more specific in its substrate selection.[83-85] Four- and five-carbon phosphorylated sugars have been examined as substrates and only natural substrate D-A5P and 2-deoxyR5P were found to be alternative substrates for *E. coli* KDO8P synthase, whereas D-R5P did not appear to be a substrate for the enzyme.[85,97,125] This has provided some insight into the role of the C2 hydroxyl group of the monosaccharide in the condensation reaction since the configuration of the C2 hydroxyl group of D-R5P is opposite to that of D-A5P and 2-deoxyR5P completely lacks the C2 hydroxyl group of D-A5P and D-R5P.

Whereas the importance of the C2 hydroxyl group stereochemistry of D-A5P for KDO8P synthase has been investigated, the importance of the correct stereochemistry at C3 and C4 has not been studied. In early studies, 3-deoxyA5P was prepared and was shown to be neither substrate nor inhibitor for *E. coli* KDO8P synthase.[94] On the other hand, 4-deoxyA5P was shown to be a substrate for this enzyme.[111] D-X5P (C3 epimer of D-A5P) has also been shown not to be a substrate over four decades ago.[151] However, no evidence or data were provided to support this result. Since then, any further investigations for the interactions of the compounds with the alternative configuration of the hydroxyl group at C3 or C4 have not been reported. This lack of information led us to investigate the preparation of alternative diastereoisomers of D-A5P (Figure 3.1). These compounds were prepared by a combination of chemical and enzymatic syntheses and were examined as substrates for *N. meningitidis* KDO8P synthase. This series of analogues have allowed us to investigate the influence of the hydroxyl group configurations at C2, C3, and C4 on the KDO8P-synthase reaction.

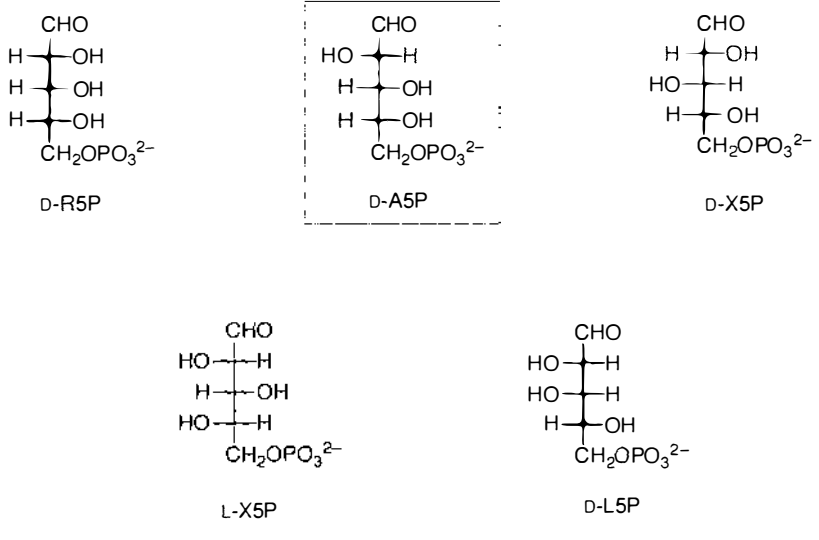

Figure 3.1. Phosphorylated pentoses. D-A5P (boxed) is the natural substrate of KDO8P synthase

3.1.2. Previous preparation of D-A5P

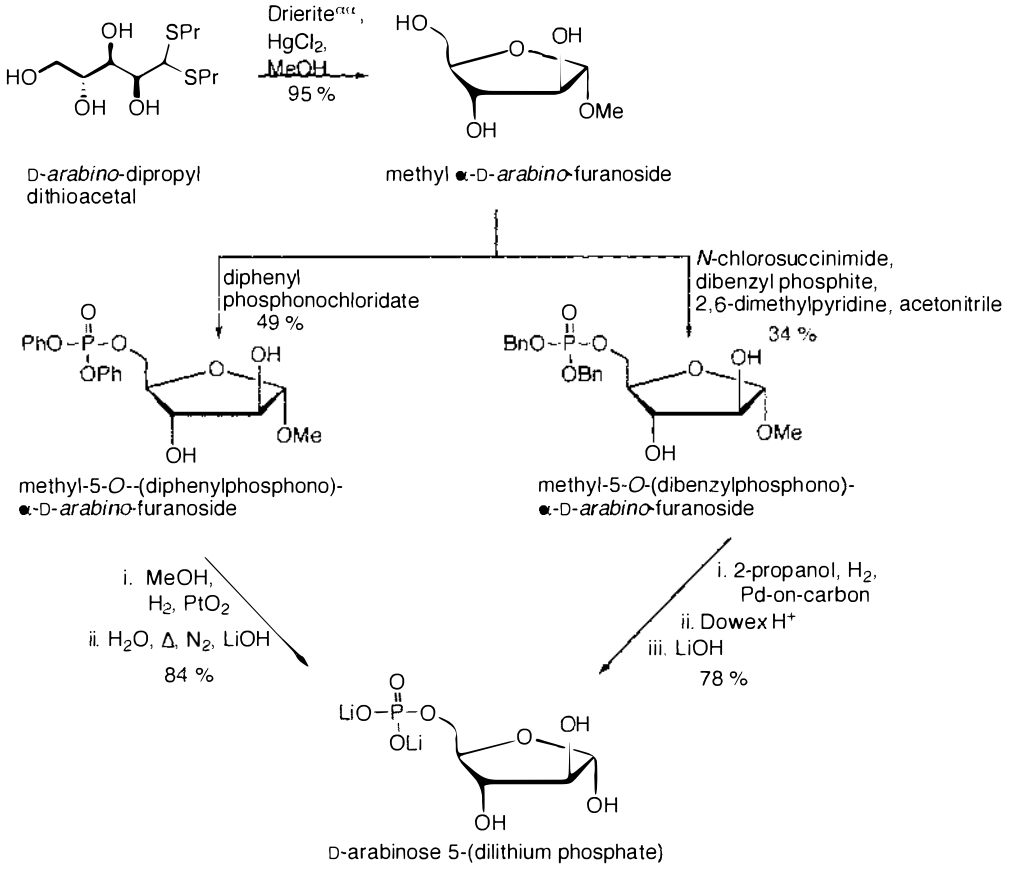

Figure 3.2. Synthetic method for the preparation of D-A5P. Taken from Maehr and Smallheer.[152]

Although D-A5P is commercially available, it is a relatively expensive compound (about USD 10^6/mol). Both enzymatic and chemical syntheses of D-A5P have been previously reported.[151 153] In early studies, D-A5P was prepared synthetically from either oxidative cleavage of D-Glu6P by lead tetraacetate or by synthesis from D-arabinose with polyphosphoric acid.[151] D-A5P was also chemically synthesised by Maehr and Smallheer in 1978 using D-arabinose dipropyl dithioacetal as a starting material (Figure 3.2).[152] D-A5P (89 % yield) has enzymatically been synthesised from D-arabinose using

two enzymes, hexokinase (EC 2.7.1.1) and pyruvate kinase (EC 2.7.11.2).[153] In this coupled enzyme system, hexokinase catalyses the generation of D-A5P from D-arabinose using a catalytic amount of ATP. ATP is generated from ADP by the conversion of PEP to pyruvate catalysed by pyruvate kinase (Figure 3.3).[154]

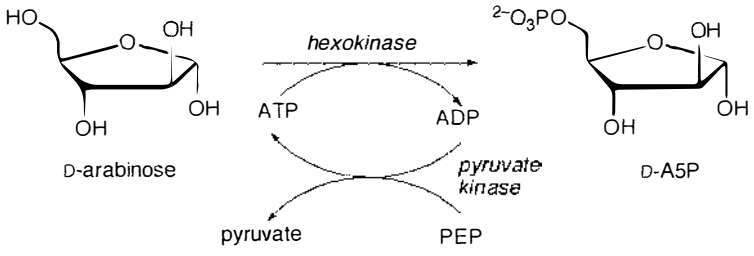

Figure 3.3. Enzymatic synthesis of D-A5P[153]

As the enzymatic synthesis is a most commonly employed and convenient method, this route was chosen for D-A5P production. This chapter describes the synthesis of D-A5P and D-L5P from D-arabinose and D-lyxose, respectively, employing this method. D-X5P and L-X5P were also synthesised chemically using D-xylose and L-xylose, respectively.

3.1.3. Preparation of D-A5P

As the coupled enzyme system using hexokinase is known to be the simplest and easiest procedure as described above,[153] this route was adopted for the preparation of D-A5P. To prepare D-A5P, PEP, ATP, $MgSO_4$, and KCI were added to a solution of D-arabinose in water and the pH of the solution was adjusted to pH 7.65 with 1M NaOH. The reaction was initiated by the addition of pyruvate kinase and hexokinase. The reaction

progress was followed by ^{31}P NMR spectroscopy and complete loss of the PEP from the reaction mixture was observed after 48 hours (Figure 3.4).

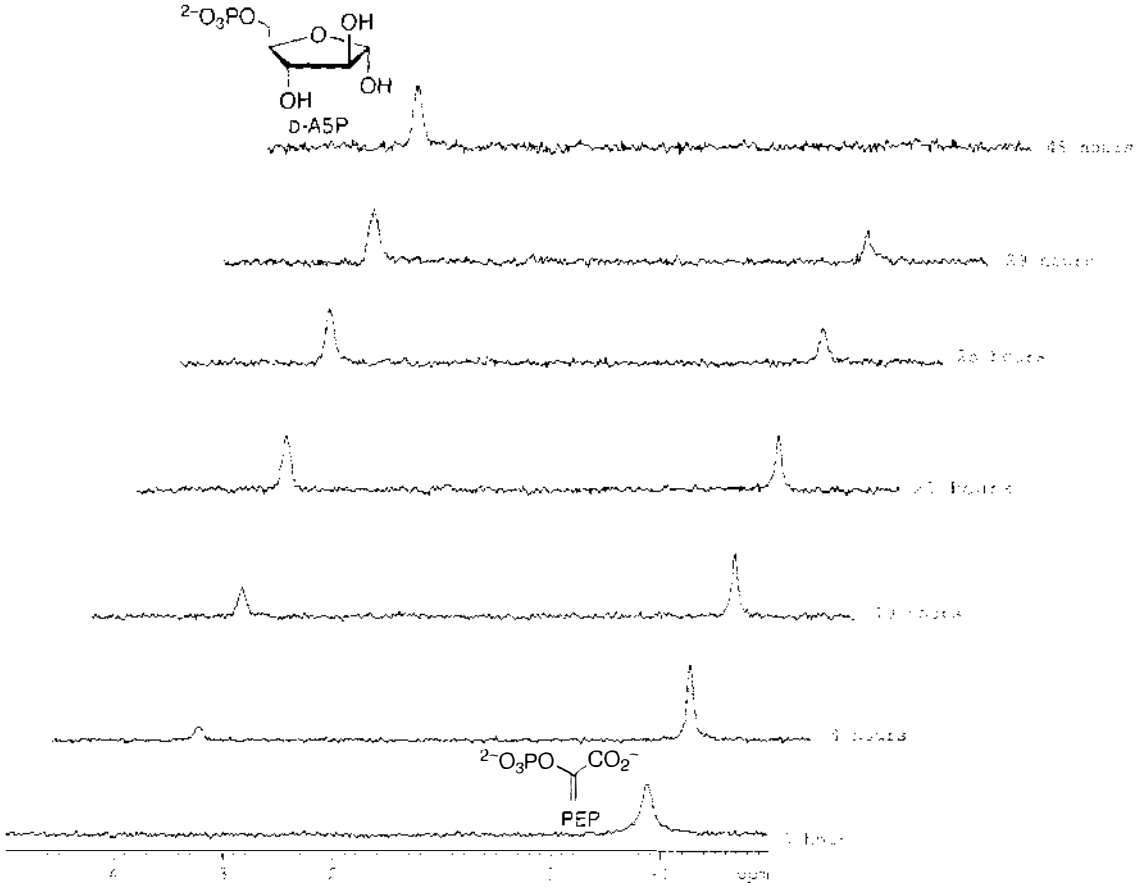

Figure 3.4. Enzymatic formation of D-A5P followed by ^{31}P NMR. The reaction was performed at pH 7.6 and at room temperature.

The impure D-A5P was purified using a SourceQ™ anion exchange column. D-A5P was eluted using a 0-1 M NH_4HCO_3 gradient and fractions containing D-A5P identified by enzymic assay with *N. meningitidis* KDO8P synthase (see chapter five), were pooled and lyophilised giving D-A5P (95 %).

3.1.4. Preparation of D-L5P

As D-arabinose could be readily phosphorylated using hexokinase, this prompted us to investigate whether D-lyxose might also be a substrate for hexokinase. This was preferable to embarking on a multi step synthesis that would require various protecting and deprotecting steps.

According to the studies on the substrate ambiguity of hexokinase, it has been shown that hexokinase catalyses the phosphorylation of D-mannose as effectively as D-glucose, the natural substrate of hexokinase.[155,156] However, D-galactose was not a substrate for the enzyme, suggesting that hexokinase is highly tolerant of configurational changes at C2 and C3 of D-glucose but less tolerant to changes at C4.[157-162] Whereas hexose sugars have been well studied as substrates for hexokinase, the phosphorylation of pentose sugars is less well studied. In 1986, Michalcácová *et al.* reported that five-carbon sugars (D- and L-arabinose, D- and L-ribose, D- and L-xylose, and D- and L-lyxose) were not substrates of yeast hexokinase.[156] However, it was demonstrated in 1988 that D-arabinose was a substrate for the enzyme and D-A5P was synthesised using the coupled enzyme reaction described in section 3.1.2.[153,155] No other five-carbon sugars have been reported to be phosphorylated by hexokinase, other than D-arabinose. It was considered possible that the method used for the preparation of D-A5P could be adapted for D-L5P preparation although D-lyxose has an inverted configuration at C3 relative to D-arabinose (Figure 3.1).

Using the same method used for D-A5P preparation, PEP, ATP, $MgSO_4$, and KCl were added to a solution of D-lyxose in water, and then the pH of the solution was adjusted to

7.65 using 1M NaOH. Both hexokinase and pyruvate kinase were added to initiate the reaction, which was followed by ^{31}P NMR spectroscopy. After 29 hours, evidence for

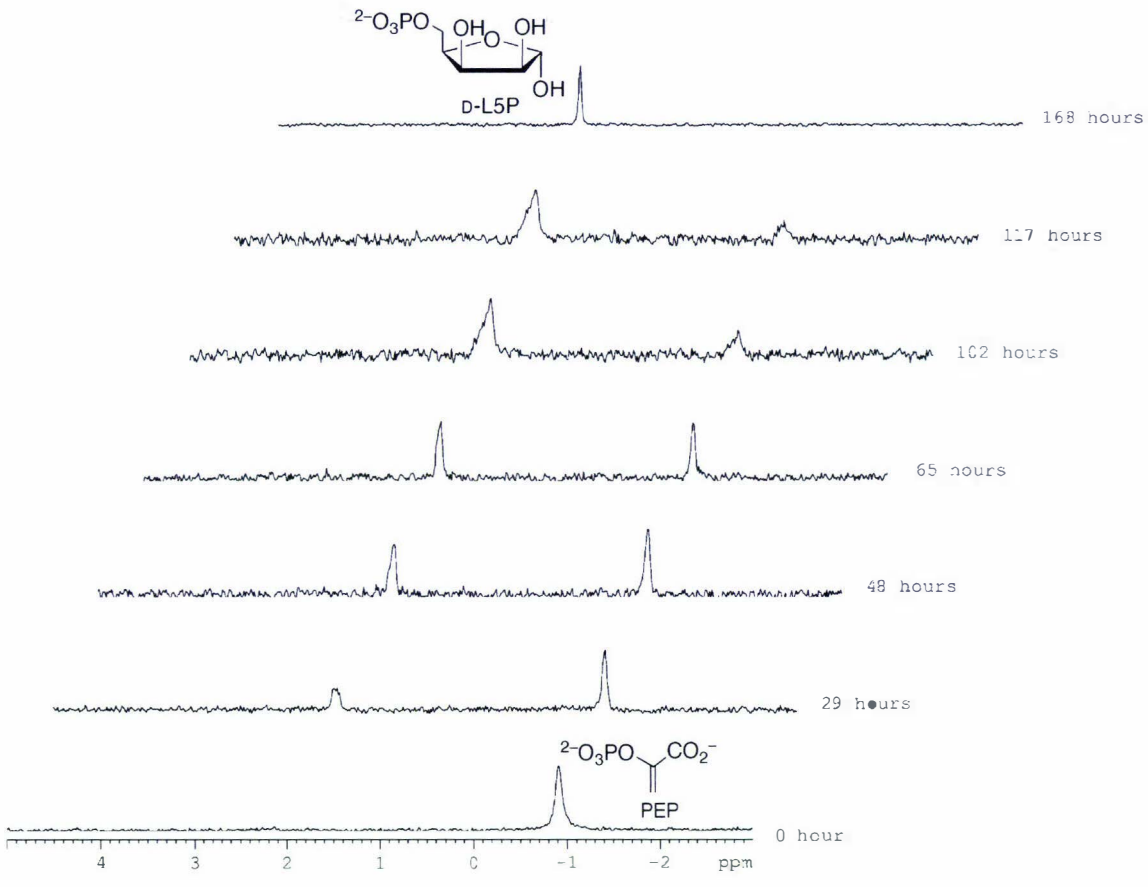

Figure 3.5. Enzymatic formation of D-L5P followed by ^{31}P NMR. The experiment was performed at pH 7.6 and at room temperature.

D-L5P was observed in the ^{31}P NMR spectrum, indicating that D-L5P could be generated from this coupled enzyme reaction (Figure 3.5). However, to complete the phosphorylation of D-lyxose, more than three times the amount of hexokinase and pyruvate kinase were required and the reaction took 3.5 times longer than the

phosphorylation of D-arabinose (Figure 3.5). Thus, although D-lyxose does appear to be a substrate, it is a considerably poorer substrate of hexokinase than D-arabinose.

Analysis of the stereochemistry may explain that D-arabinose is a better substrate for hexokinase than D-lyxose. It has been found that hexokinase reacts well with sugar compounds that have the same configuration at C3 and C4 as D-glucose, the natural substrate of hexokinase.[156] D-Arabinose has same hydroxyl group configuration at both C2 and C3 to C3 and C4 hydroxyl groups of D-glucose. On the other hand, the configuration of the hydroxyl group at C2 of D-lyxose is same as C3 hydroxyl group of D-glucose but C3 hydroxyl group of D-lyxose has the opposite configuration to C4 hydroxyl group of D-glucose. This may explain why D-lyxose was observed to be a poorer substrate for hexokinase than D-arabinose.

To remove the enzymes from the D-L5P mixture after phosphorylation was complete, the solution was filtered through a molecular weight cut off device and the impure D-L5P in the filtrate was purified using a SourceQ™ anion exchange column. Fractions containing D-L5P were confirmed using Bial's reagent, an established method for the detection of pentoses.[163-165] When the purified fractions were tested with Bial's reagent, a green colour appeared where D-L5P was present. Fractions that contained D-L5P were then pooled and lyophilised, giving D-L5P (84 %).

3.1.5. Preparation of D-X5P and L-X5P

As mentioned in chapter two, D- and L-X5P were prepared in order to investigate their usefulness as starting materials for the production of D- and L-T4P. Additionally, these

five-carbon phosphorylated sugars that have alternative stereochemistry to D-A5P are potentially useful alternative substrates for DAH7P or KDO8P synthases in their own right.

D-X5P has the opposite configuration at C2 and C3 (Figure 3.1) as compared to D-A5P. L-X5P, on the other hand, has the same C2 and C3 configuration to D-A5P but is inverted at C4. In early studies, D-X5P was examined with *E. coli* KDO8P synthase and was found not to be an alternative substrate of the enzyme.[151] However, no further investigation has been carried out on the role of C2 and C3 hydroxyl groups with this enzyme. This lack of information on the stereospecificity with KDO8P synthase encouraged us to prepare D- and L-X5P to investigate the tolerance of the enzyme to configurational change at C2, C3, and C4. Both D-X5P and L-X5P were prepared using the same sequence of reactions but with different starting materials, D-xylose for D-X5P and L-xylose for L-X5P.

The preparation of D-X5P is a straightforward synthetic route (Figure 3.6).[166,167] Treatment of D-xylose with acetone gave the 1,2:3,5-bisacetonide. Selective removal of the 3,5-acetonide with dilute hydrochloric acid gave the corresponding 3,5-diol. The C5 hydroxyl group was then selectively phosphorylated and the phenyl esters were removed by hydrogenolysis. In order to give unprotected D-X5P, the partially protected D-X5P was dissolved in water and was heated at 50 °C to remove the 1,2-acetonide. This aqueous solution containing D-X5P was then lyophilised to give D-X5P in 22 % overall yield as analysed by the loss of PEP at 232 nm at 25 °C with *E. coli* DAH7P(Phe) synthase.

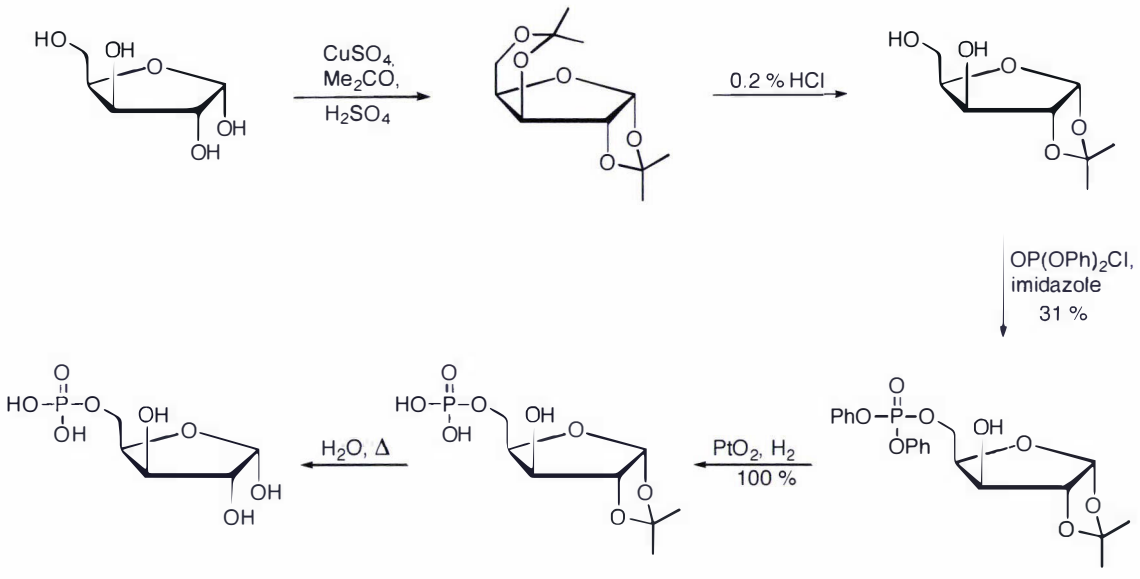

Figure 3.6. Synthesis of D-X5P

L-X5P was also prepared from L-xylose by adopting the same method. L-X5P was obtained with 13 % overall yield. The presence of this compound was detected by monitoring the loss of PEP at 232 nm at 30 °C with *N. meningitidis* KDO8P synthase. More details of how D- and L-X5P interact with *E. coli* DAH7P synthase and *N. meningitidis* KDO8P synthase are provided in chapter five.

3.2. Summary

D-A5P and its stereoisomer, D-L5P, were successfully prepared using hexokinase catalysed phosphorylation. The formation of D-A5P and D-L5P was observed by ^{31}P NMR spectroscopy. The reaction time of D-lyxose was slower than that of D-arabinose, suggesting that D-lyxose might be a poorer substrate for hexokinase than D-arabinose. The D- and L-X5P were generated synthetically from D-xylose and L-xylose, respectively.

Chapter Four

INVESTIGATION INTO THE ENZYME-SPECIFIC REACTION WITH 3-DEOXY-D-*ARABINO*-HEPTULOSONATE 7-PHOSPHATE SYNTHASES USING PHOSPHORYLATED MONOSACCHARIDE ANALOGUES

This chapter describes how diastereomers of the natural substrate D-E4P interact with *E. coli* and *P. furiosus* DAH7P synthases. The synthetic routes that gave rise to these diastereomers were described in chapter two.

4.1. Stereospecific Reaction of Five-Carbon Sugars with *E. coli* DAH7P(Phe) Synthase and *P. furiosus* DAH7P Synthase

As discussed in section 1.2.5, the comparison of sequences and structures has revealed that the subfamily $I\delta_D$ DAH7P synthases are more closely related to the subfamily $I\delta_K$ KDO8P synthases than to the Iδ subfamily of DAH7P synthases.[62] *P. furiosus* DAH7P synthase is from the $I\delta_D$ subfamily and it has been shown that this is likely to be the most closely related DAH7P synthase to the $I\delta_K$ subfamily yet characterised due to its lack of feedback inhibition, its requirement for a divalent metal, and its broad substrate specificity.[74]

Prior to the commencement of these studies, some limited substrate specificity studies had been reported. It was shown that *E. coli* DAH7P(Tyr) synthase was able to accept phosphonate analogues of D-E4P as substrates.[89,132] A range of commercially available

five-carbon-sugars, D-R5P, D-A5P, and 2-deoxyR5P have been tested.[79] This study showed that these compounds acted as alternative substrates of *E. coli* DAH7P(Phe) synthase and the products of the enzymatic reaction were characterised.

During the course of the studies described in this thesis, *P. furiosus* DAH7P synthase was characterised functionally and structurally.[39,74] Also, in parallel studies, 2- and 3-deoxyE4P were synthesised and tested as substrates for *E. coli* and *P. furiosus* DAH7P synthase by another PhD student, Amy Pietersma within our laboratory.[74,90,130] The findings of these studies have direct bearing on the results presented in this thesis and will be presented and discussed in detail in chapter six.

Although a number of studies of the substrate specificity of DAH7P synthase have been reported, the tolerance of DAH7P synthase to configurational changes at C2 or C3 of natural substrate D-E4P has not been studied previously. Additionally, it has been reported that the C2 epimer of D-A5P, D-R5P (with E4P-like C2 configuration) is not a substrate for the KDO8P synthases from *E. coli* and *A. aeolicus*.[83,85,125] As we are interested in the relationship between DAH7P synthase and KDO8P synthase, this observation led us to examine substrate specificity and how important the C2 or C3 configuration is for DAH7P synthase.

4.1.1. Enzymatic reaction of D-T4P and L-T4P with *E. coli* DAH7P(Phe) synthase

D-T4P was synthesised from either D-Gal6P or D-diethyl tartrate, and L-T4P was synthesised from L-diethyl tartrate as described in chapter two. The synthetic D- and L-T4P were tested as alternative substrates for *E. coli* DAH7P(Phe) synthase in a simple

UV assay system. All assays were performed in 50 mM BTP buffer (pH 6.8) and at 25 °C. All buffers and solutions were Chelex-treated, and the enzymic reaction was initiated by the addition of the purified *E. coli* DAH7P(Phe) synthase. The progress of the reaction was monitored by the loss of PEP at 232 nm.

When the D- and L-T4P were incubated with *E. coli* DAH7P(Phe) synthase in the presence of PEP and Mn^{2+}, a time-dependent loss of absorbance at 232 nm was observed. The magnitude of the absorbance decrease and the rate were proportional to the amount of aldehyde substrate added and to the enzyme concentration, respectively. In order to confirm that PEP loss was connected to both the consumption of D- and L-T4P and to the generation of new seven-carbon sugars, the seven-carbon products, D-DLH7P and 3-deoxy L-*xylose*-heptulosonate 7-phosphate (L-DXH7P) from D- and L-T4P, respectively, were prepared on a larger scale. The D-DLH7P and L-DXH7P were then tested with thiobarbituric acid following cleavage with periodate as described in section 2.2.3. This gave a pink colour consistent with the formation of the 3-deoxyaldulosonic acids. Based on these observations, it appears that *E. coli* DAH7P(Phe) synthase tolerates configurational changes at C2 or C3 of natural substrate D-E4P.

4.1.1.1. Determination of kinetic parameters of D-T4P and L-T4P with *E. coli* DAH7P(Phe) synthase

Kinetic parameters for D- and L-T4P were determined by monitoring the loss of PEP as observed at 232 nm. The reaction mixtures, without enzyme were incubated at 25 °C for 5 minutes prior to initiation and the reaction was initiated by the addition of the purified *E. coli* DAH7P(Phe) synthase. The consumption of PEP was monitored and initial rates

were recorded. The steady state kinetic parameters were calculated by fitting data to the Michaelis-Menten equation using Enzfitter$^{\delta}$ (Biosoft, v 2.0). The Michaelis-Menten plots from which these values were calculated are shown in Figure 4.1. A summary of the calculated kinetic parameters is shown in Table 4.1.

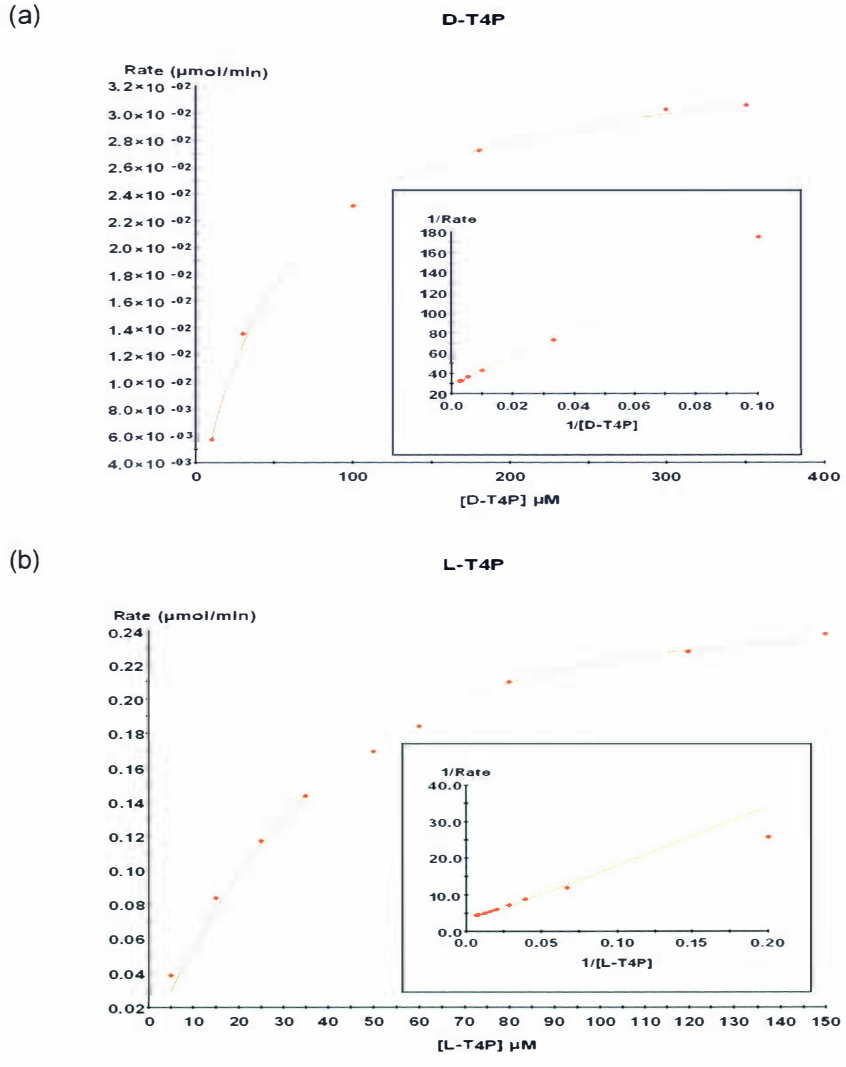

Figure 4.1. Michaelis-Menten plots for the determination of K_M and k_{cat} for (a) D-T4P and (b) L-T4P with *E. coli* DAH7P(Phe) synthase

Table 4.1.
Kinetic parameters of D-T4P and L-T4P with *E. coli* DAH7P(Phe) synthase

	D-E4P[a]	D-T4P[b]	L-T4P[c]
K_M^{PEP} (μM)	2.0 ± 0.2	13 ± 1	9 ± 0.1
$K_M^{monosaccharide}$ (μM)	39 ± 4	390 ± 13	750 ± 10
k_{cat} (s^{-1})	26 ± 2	2.5 ± 0.1	1.5 ± 0.1
$k_{cat} / K_M^{monosaccharide}$ ($s^{-1}/\mu M$)	670 δ 10^{-3}	6 δ 10^{-3}	2 δ 10^{-3}

[a] The kinetic parameters were determined by Dr L. Schofield.[74]
[b] D-T4P synthesised from D-diethyl tartrate was chosen to avoid contaminants from the oxidation that might affect the kinetic results. The kinetic parameters were determined at a concentration of 112 μM of PEP.
[c] The kinetic parameters were determined at a concentration of 126 μM of PEP.

As the kinetic data show, the K_M values for both D- and L-T4P were observed to be at least an order of magnitude higher than that observed for the natural substrate D-E4P. The value for L-T4P was even higher, indicating that this compound does not have as high an affinity for the enzyme. The k_{cat} values found when either D- or L-T4P were used as substrates were about an order of magnitude lower leading to specificity constants approximately two orders of magnitude lower than those found for this enzyme when using D-E4P. In addition, the specificity constant for L-T4P is approximately three times lower than that for D-T4P, suggesting that L-T4P is a poorer substrate than D-T4P for *E. coli* DAH7P synthase.

4.1.2. Enzymatic reaction of D-T4P and L-T4P with *P. furiosus* DAH7P synthase

Synthetic D-T4P and L-T4P were also tested as alternative substrates for *P. furiosus* DAH7P synthase. *P. furiosus* is a hyperthermophile found in deep-sea hydrothermal vents. The expression, purification, and characterisation of *P. furiosus* DAH7P synthase were carried out by Dr Linley Schofield from our group.[39] As *P. furiosus* has an optimum growth temperature of 100 °C, activity assays of *P. furiosus* enzyme should ideally be done close to this temperature. However, due to instability of substrates at higher temperatures, 60 °C was chosen for activity assays. The pH of the buffer was adjusted at 60 °C to pH 6.8. The extinction coefficient of PEP at 60 °C was determined to be 2.6 δ 10^3 M^{-1} cm^{-1} at 232 nm.[39]

All assays were performed in 50 mM BTP buffer (pH 6.8) at 60 °C. All buffers and solutions were Chelex-treated and all assays were initiated by the addition of four-carbon monosaccharide, D- or L-T4P. The reaction was monitored by the loss of PEP at 232 nm. The loss of absorbance in these assays indicated that both D- and L-T4P were accepted as alternative substrates to D-E4P by *P. furiosus* DAH7P synthase.

4.1.2.1. Determination of kinetic parameters of D-T4P and L-T4P with *P. furiosus* DAH7P synthase

For the determination of kinetic parameters for D- and L-T4P with *P. furiosus* DAH7P synthase, the modified continuous assay was used.[39] Initial rates of the assay with the enzyme were recorded and steady-state kinetics parameters were calculated using Enzfitter® (Biosoft, v 2.0). The Michaelis-Menten plots from which these values were

calculated are shown in Figure 4.2. A summary of the kinetic parameters is given in Table 4.2.

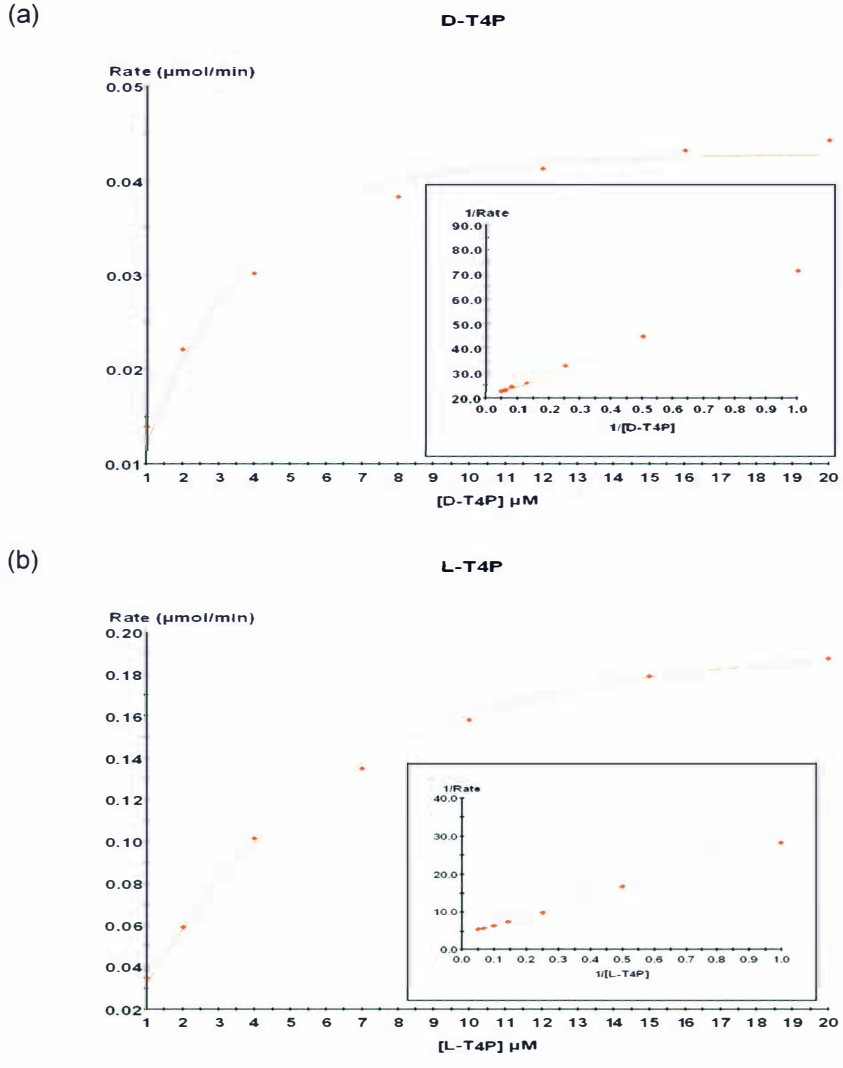

Figure 4.2. Michaelis-Menten plots for the determination of K_M and k_{cat} for (a) D-T4P and (b) L-T4P with *P. furiosus* DAH7P synthase

As the values show, it is clear that D- and L-T4P are alternative substrates for *P. furiosus* DAH7P synthase. In addition, the K_M values for D- and L-T4P with *P. furiosus* DAH7P synthase are more than one order of magnitude lower than those for D- and L-T4P with

E. coli DAH7P(Phe) synthase, and closer to the K_M value for D-E4P. This suggests that D- and L-T4P are better substrates for *P. furiosus* DAH7P synthase than for *E. coli* DAH7P(Phe) synthase.

Table 4.2.
Kinetic parameters of D-T4P and L-T4P with *P. furiosus* DAH7P synthase

	D-E4P[a]	D-T4P[b]	L-T4P[c]
K_M^{PEP} (μM)	93 ± 9	13 ± 1	15 ± 1
$K_M^{monosaccharide}$ (μM)	9 ± 1	21 ± 1	47 ± 3
k_{cat} (s^{-1})	1.4 ± 0.1	2.4 ± 0.1	4.0 ± 0.1
$k_{cat} / K_M^{monosaccharide}$ ($s^{-1}/\mu M$)	160 δ 10^{-3}	110 δ 10^{-3}	85 δ 10^{-3}

[a] The kinetic parameters were determined by Dr L. Schofield.[74]
[b] D-T4P synthesised from D-diethyl tartrate was chosen to avoid contaminants from oxidation that might affect the kinetic results. The kinetic assays were determined at a concentration of 458 μM of PEP.
[c] The kinetic parameters were determined at a concentration of 63 μM of PEP.

4.2. Enzymatic Synthesis of DAH7P and Its Analogues

In order to establish that an aldol-like reaction was involved and that the D-E4P isomers used by DAH7P synthase led to DAH7P isomers, a large-scale enzyme reaction was performed to generate sufficient products for characterisation (Figure 4.3). Although both D- and L-T4P are alternative substrates of both *E. coli* and *P. furiosus* enzymes, *E. coli* DAH7P(Phe) synthase was used for the large-scale enzyme reaction due to instability of D-T4P and L-T4P at 60 °C.

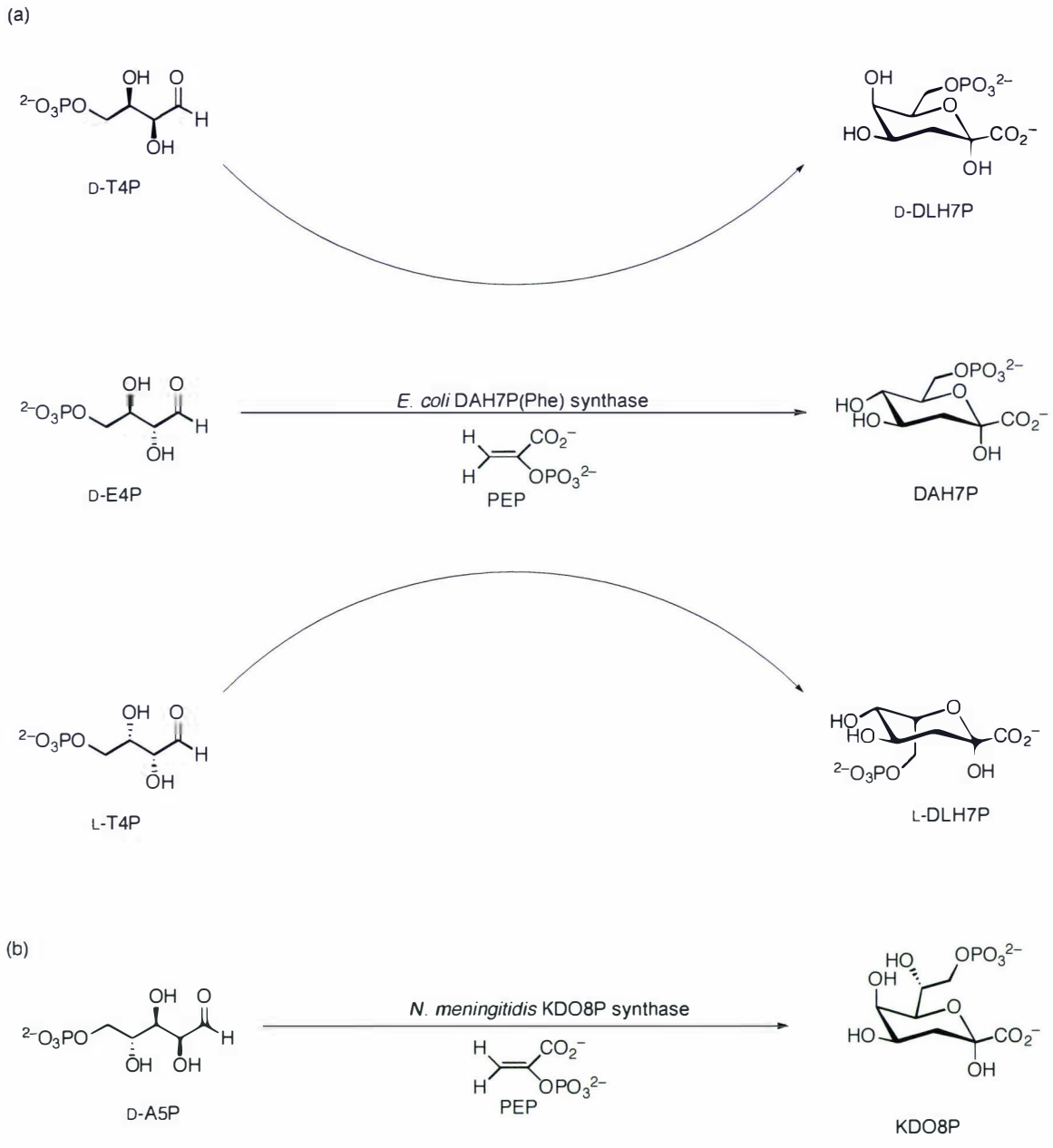

Figure 4.3. Generation of (a) DAH7P and its analogues from four-carbon substrates and PEP using *E. coli* DAH7P(Phe) synthase, and of (b) KDO8P from D-A5P using *N. meningitidis* KDO8P synthase. Products are shown only in the δ-pyranose form for clarity.

4.2.1. Large-scale syntheses and purification

For the generation of DAH7P, D-DLH7P, and L-DXH7P, the aldose phosphate co-substrate, PEP, and $MnSO_4$ were added to reaction mixtures and the pH was adjusted to pH 7. The reactions were initiated by the addition of enzyme and the loss of PEP was monitored at 270 nm. A higher wavelength than the δ_{max} for PEP was used to keep the absorbance measurements within the linear range of the spectrophotometer.

After the loss of PEP had ceased, the enzyme was removed by ultracentrifugation. The products were then purified by anion-exchange chromatography (SourceQ™, Amersham) eluting with an ammonium bicarbonate gradient. The fractions were tested with thiobarbituric acid assay to identify the presence of DAH7P, D-DLH7P, and L-DXH7P. Fractions that tested positive in this test were then pooled, lyophilised, and stored in the freezer at -80 °C prior to NMR and mass spectral analysis. Products were analysed by high resolution ESI (negative ion mode). The spectra showed peaks with the same mass as DAH7P (287.013 for DAH7P; 287.0123 for D-DLH7P; 287.0168 for L-DXH7P), indicating that the products formed by reaction of PEP with the D- or L-T4P mixtures are isomers of DAH7P.

As shown on Figure 4.4, the ^{1}H NMR spectra of the products were difficult to analyse as expected due to the presence of more than one anomer of the products. Therefore, the spectra were assigned by comparison to the data reported for DAH7P and KDO8P.[79,96,108,168] For comparison, DAH7P and KDO8P were also prepared by the enzymatic reaction using *E. coli* DAH7P(Phe) synthase with PEP and D-E4P and using

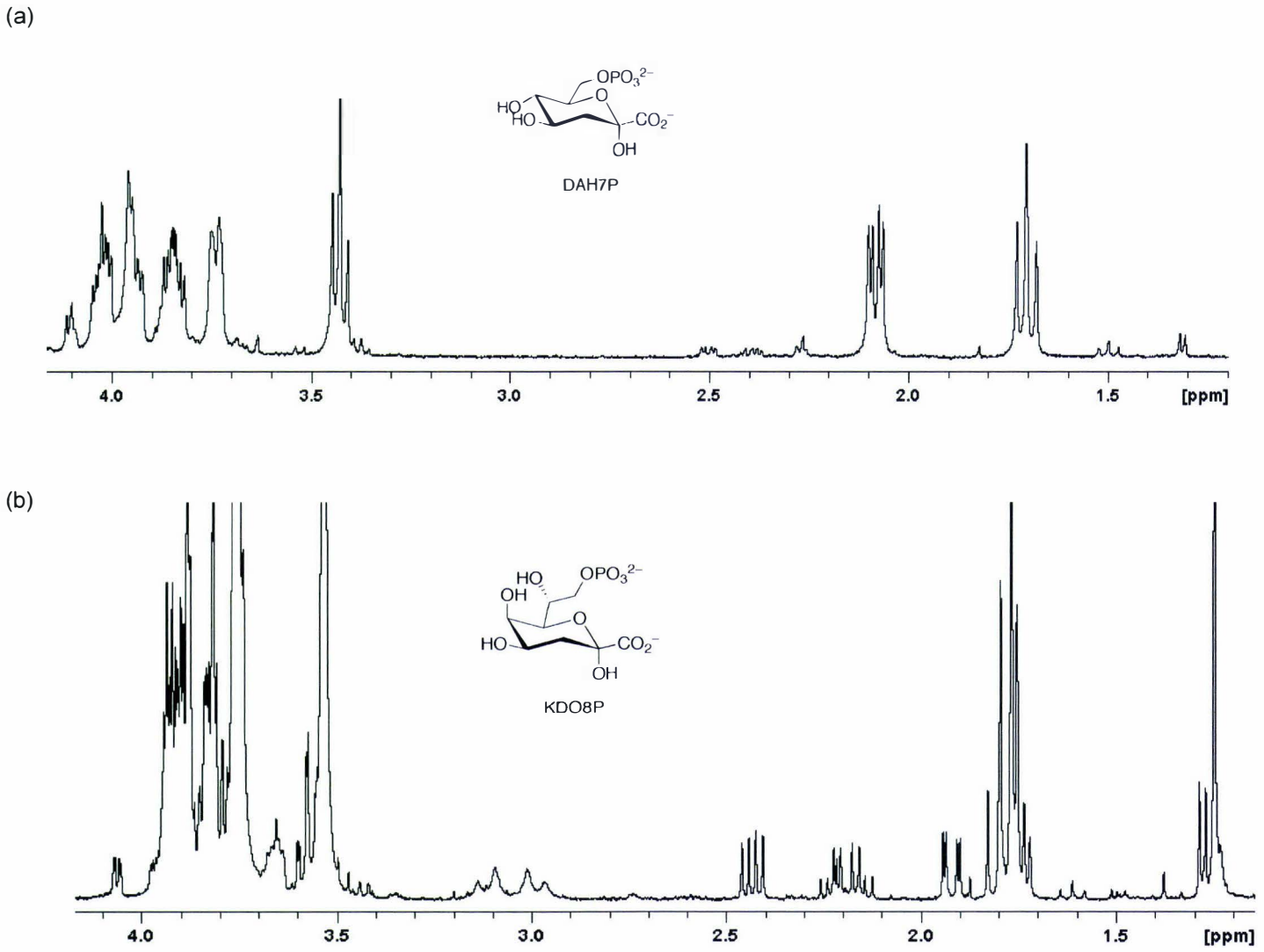

Figure 4.4. ^{1}H NMR spectra of purified (a) DAH7P and (b) KDO8P. The structures of seven- and eight-carbon sugars are only shown in δ-pyranose forms for clarity.

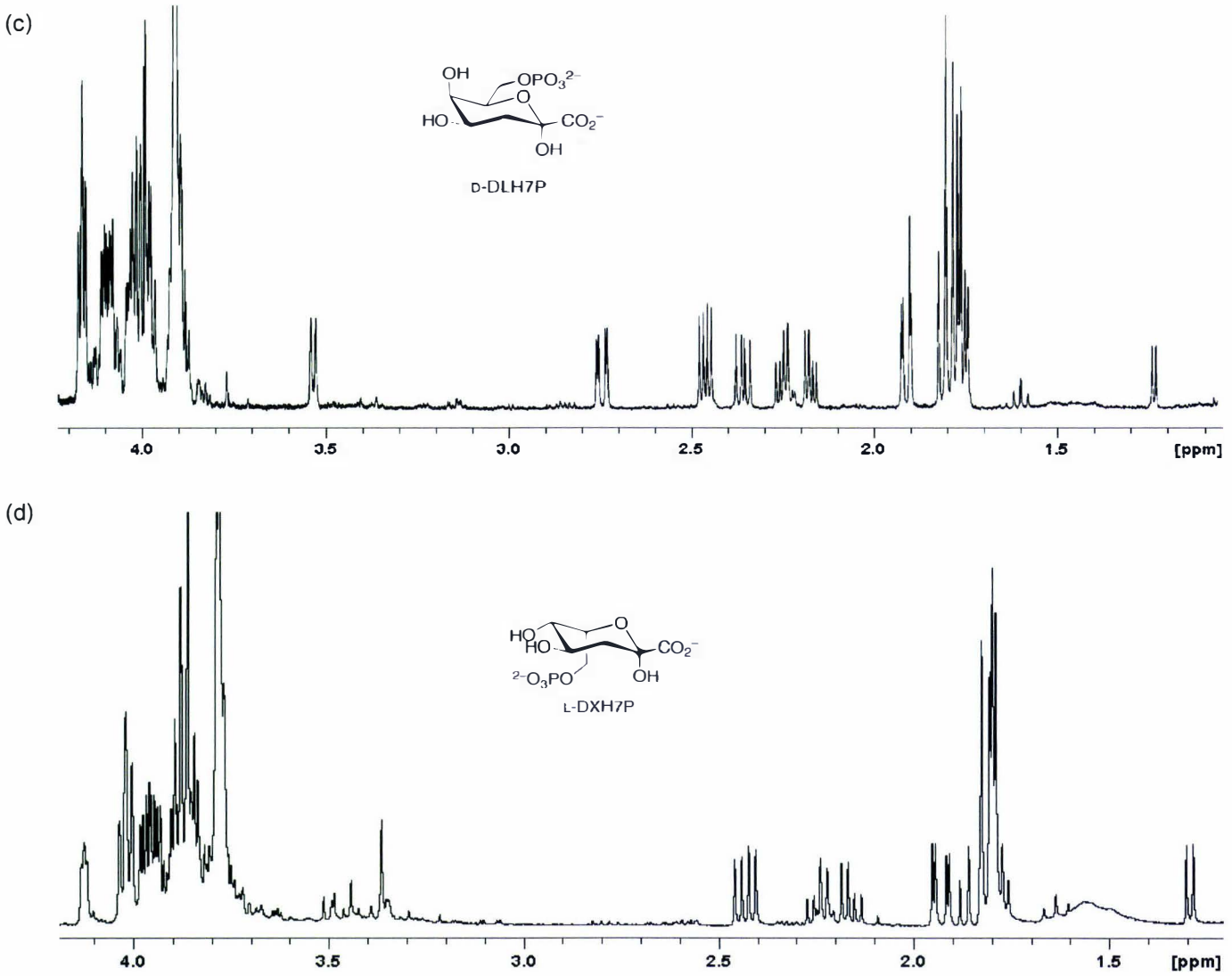

Figure 4.4 continued. ^{1}H NMR spectra of purified (c) D-DLH7P and (d) L-DXH7P. The structures of seven- and eight-carbon sugars are only shown in δ-pyranose forms for clarity.

N. meningitidis KDO8P synthase with PEP and D-A5P. Purified DAH7P and KDO8P were also analysed by high-resolution ESI and NMR spectroscopy and the results showed the expected masses (287.013 for DAH7P; 317.0277 for KDO8P) and spectra (Figure 4.4) to the reference compounds.[79,96,108,168] The spectra of D-DLH7P and L-DXH7P were assigned by comparison to the DAH7P and KDO8P spectra. An NMR software prediction program (ACD/NMR predictor software, v.8.10) was also used to check assignments.

The major ring isomer of DAH7P is the δ-pyranose form. The ^{1}H NMR spectrum of DAH7P showed clearly two major peaks at 1.71 and 2.09 ppm (Figure 4.4) corresponding to the two geminal protons at C3 (Figure 4.5). The coupling constants of 13.2 and 13.2 Hz from the 1.71 ppm peak, and 13.2 and 5.6 Hz from the 2.09 ppm peak showed that these represent H_{3ax} and H_{3eq}, respectively (Figure 4.6). The interpretation is consistent with both NMR prediction and the other published assignments for DAH7P.[130] This can be used as a reference of H_{3ax} and H_{3eq} position to pyranose ring form of other seven- or eight-carbon ring compounds. Other small peaks in the spectrum of DAH7P are attributed to the presence of small amounts of the δ-pyranose and δ- and δ-furanose forms of DAH7P.

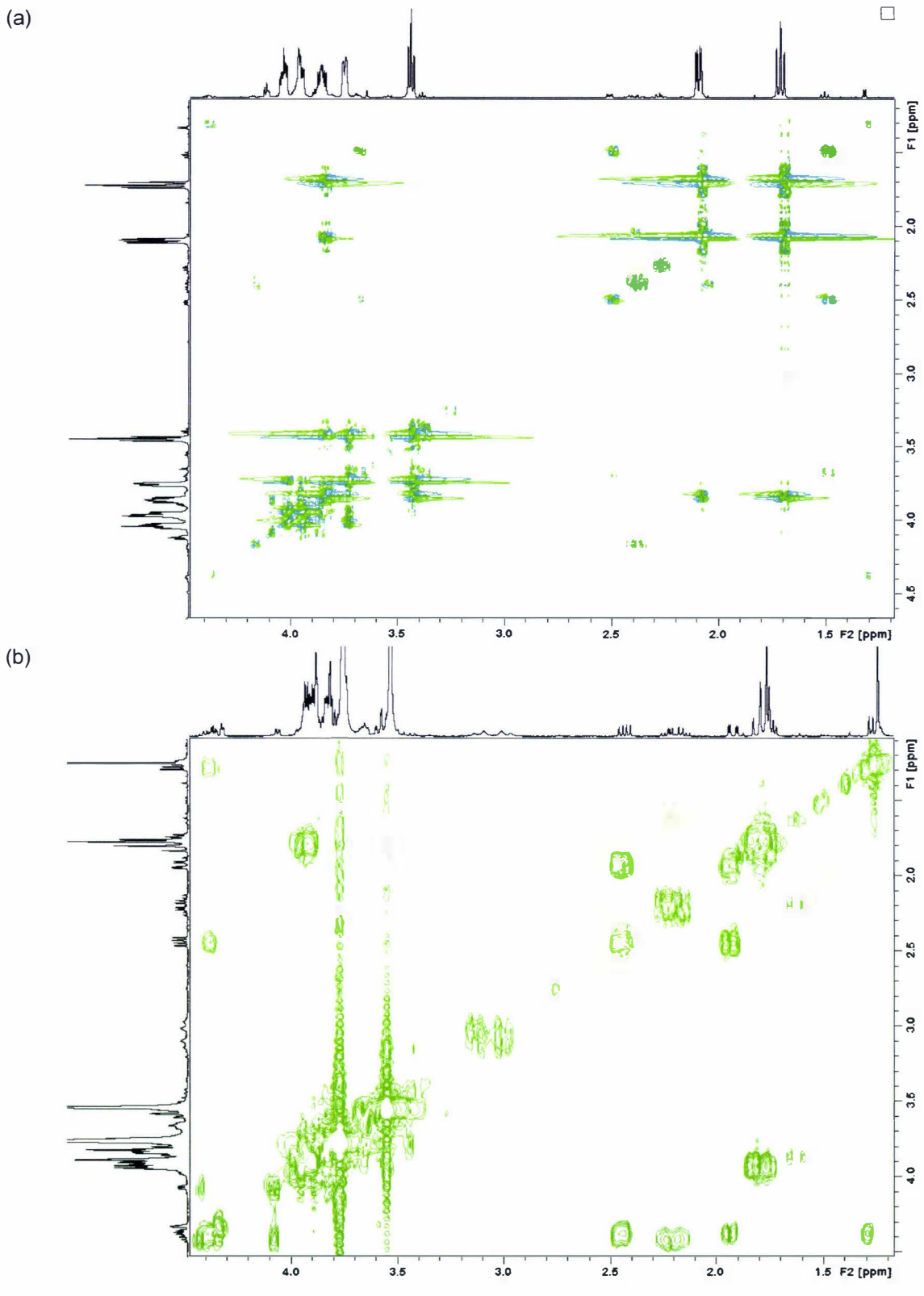

Figure 4.5. COSY spectra of (a) D-DAH7P and (b) KDO8P showing geminal and vicinal couplings

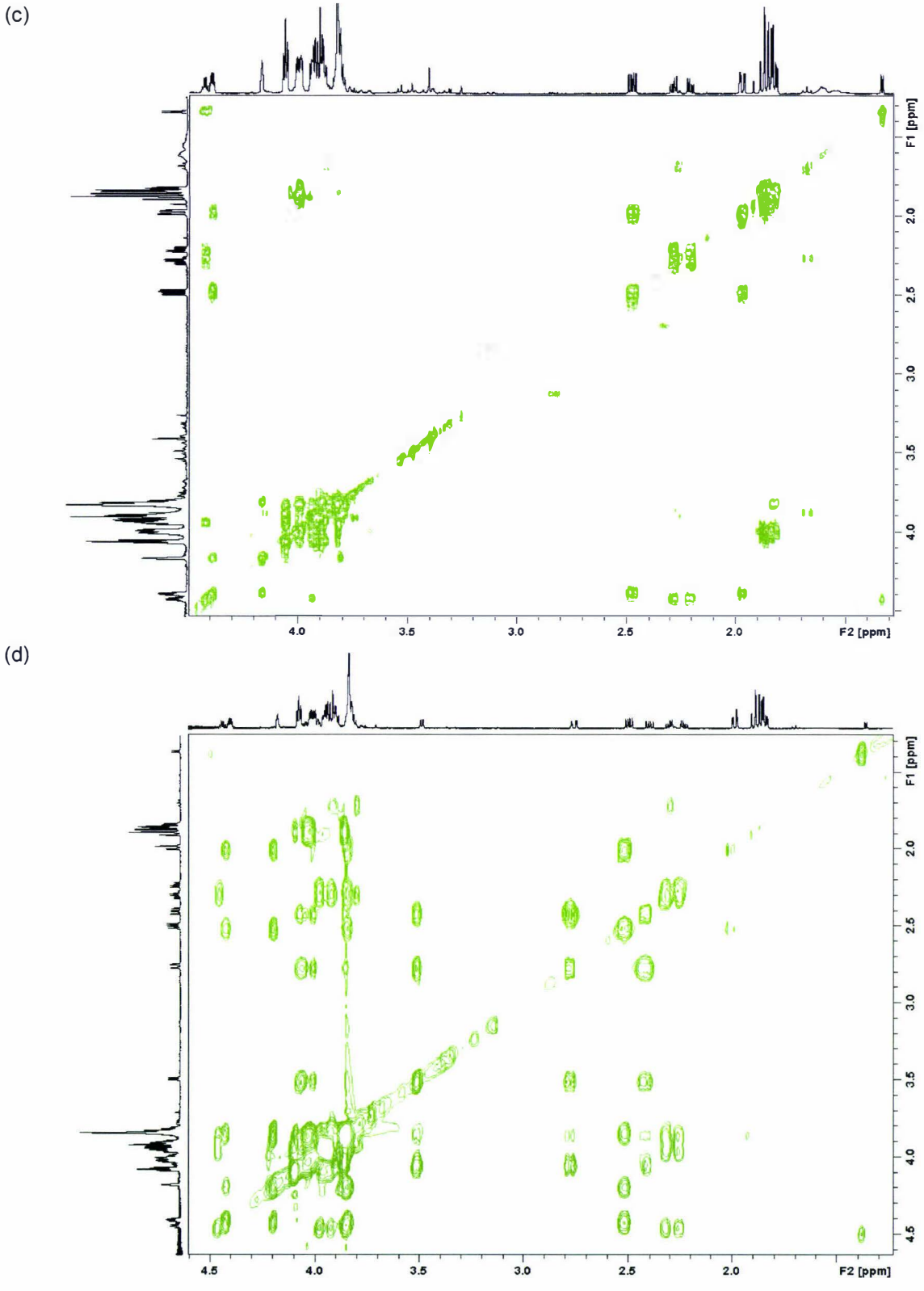

Figure 4.5 continued. COSY spectra of (c) L-DXH7P and (d) D-DLH7P showing geminal and vicinal couplings

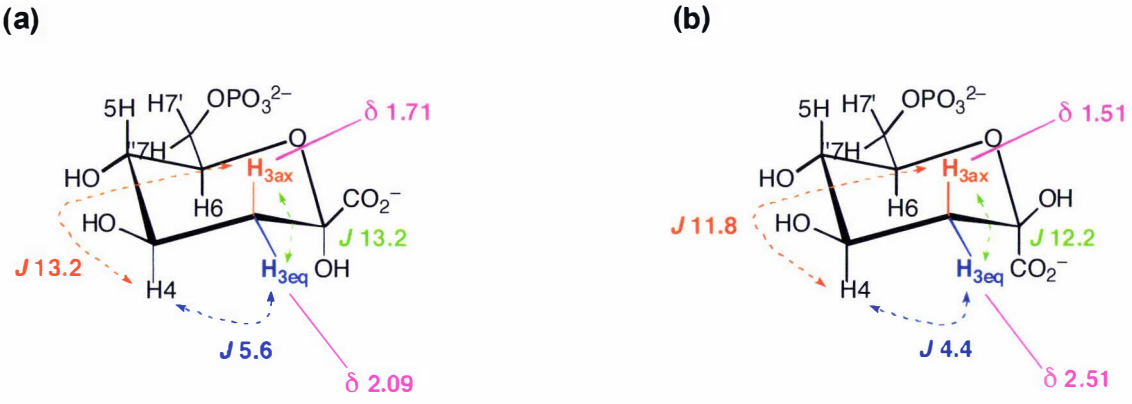

Figure 4.6. Assignment of H3 protons of (a) δ-pyranose and (b) δ-pyranose of DAH7P. δ: ppm; *J*: Hz

The key difference between KDO8P and DAH7P that is expected to influence anomer distribution is the alternative configuration at C5. This decreases the stability of the δ-pyranose relative to alternative δ-pyranose, and δ- and δ-furanose forms of KDO8P. Consequently, in the spectrum of KDO8P, four sets of geminal protons are observed between 1.5 and 2.8 ppm (Figure 4.5).

Somewhat confusingly, the KDO8P ^{1}H NMR spectrum has been assigned in a number of different ways in the published literature.[79,96,107,108] In these analyses, the assignments for the δ- and δ-pyranose forms are consistent; however, there appears to be some disagreement regarding the assignment of the furanose forms. Baasov and Jacob, and Kohen *et al.* assigned the two peaks at 1.9 and 2.4 ppm to the H3 protons of the δ-furanose form, and the 2.12 and 2.2 ppm peaks to the H3 protons of the δ-furanose form (Table 4.3).[96,107] Dotson *et al.* assigns these peaks the other way around (Table 4.3).[108]

Table 4.3.
The assigned C3 protons of the δ- and δ-isomers of KDO8P from ^{1}H NMR chemical shifts with coupling constants given in brackets

Reference	Pyranose δ (*J* Hz)				furanose δ (*J* Hz)			
	δ-pyranose		δ-pyranose		δ-furanose		δ-furanose	
	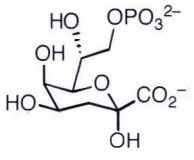		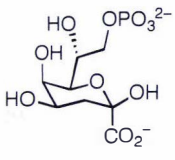		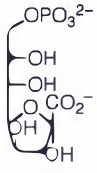		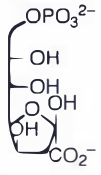	
Dotson[108]	H_{3eq} 1.7	H_{3ax} 1.8	H_{3ax} 1.6	H_{3eq} 2.12	H_{3ax} 2.15	H_{3eq} 2.2	H_{3ax} 1.9 (14.5, 3.0)	H_{3eq} 2.4 (14.5, 7.5)
Baasov and Jacob,[96] Kohen[107]	H_{3eq} 1.7 (13.4, 6.6)	H_{3ax} 1.76 (13.4, 12.9)	H_{3ax} 1.58 (13.4, 12.4)	H_{3eq} 2.15 (13.4, 5.6)	H_{3ax} 2.4 (14.2, 7.2)	H_{3eq} 1.89 (14.2, 3.2)	H_{3ax} 2.12 (13.3, 7.0)	H_{3eq} 2.2 (13.4, 7.0)

In another analysis, Sheflyan *et al.* assigned the peaks at 2.24 and 2.33 ppm correspond to the H3 protons of an undefined furanose form and the peaks at 2.02 and 2.52 ppm to H3 protons of a lactone form of KDO8P.[79] Due to the problems in the assignment of δ- and δ-furanose forms in the published spectra of KDO8P, NMR prediction software was used to help assigning the furanose forms. However, the NMR prediction software (ACD/NMR predictor software, v 8.10) did not distinguish between δ- and δ-forms, predicting a pair of peaks at 1.78 and 2.16 ppm for pyranose forms, and at 2.04 and 2.52 ppm for furanose forms. To assign the spectrum of KDO8P (and those of the other similar sugars), we have tentatively followed the assignments of Baasov and Jacob, and Kohen *et al.* (Figure 4.7).[96,107]

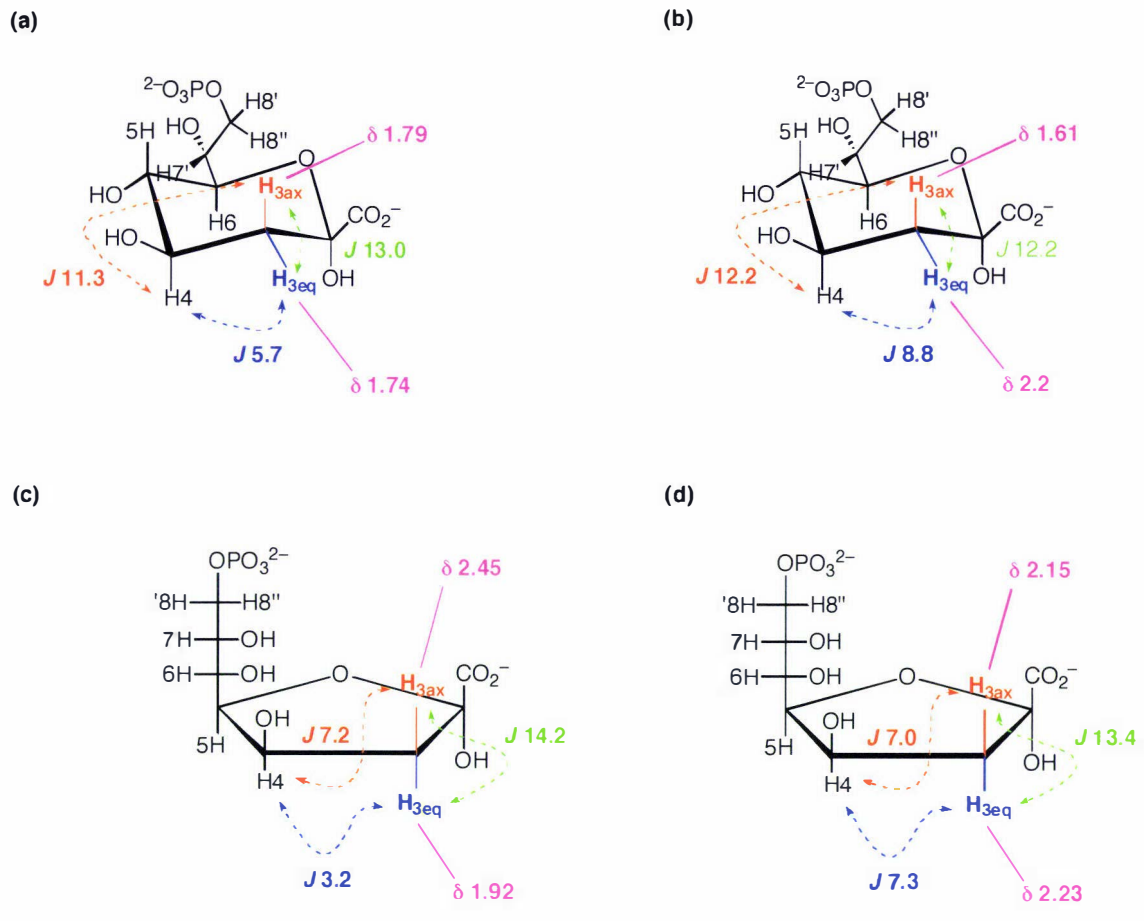

Figure 4.7. Assignment of H3 protons from (a) δ-pyranose, (b) δ-pyranose, (c) δ-furanose, and (d) δ-furanose of KDO8P. δ: ppm; *J*: Hz

Due to the similarity between KDO8P and D-DLH7P with respect to the configuration at C5, we considered that D-DLH7P was likely to share a similar anomeric distribution to KDO8P. Therefore, the spectrum of KDO8P, tentatively assigned, can be used to help assign the spectrum of D-DLH7P. Essentially, for this compound, four similar sets of diastereotopic protons were observed as identified with 1D NMR spectrum (Figure 4.4) and 2D COSY NMR spectrum (Figure 4.5). These resonances can be assigned to the δ- and δ-pyranose, and δ- and δ-furanose forms of D-DLH7P. In addition, the presence of one more set of geminal protons at 2.4 and 2.76 ppm was observed (Figure

4.5). The coupling constants of these signals are consistent to the values predicted by NMR prediction software for a lactone form of D-DLH7P (Figure 4.8).

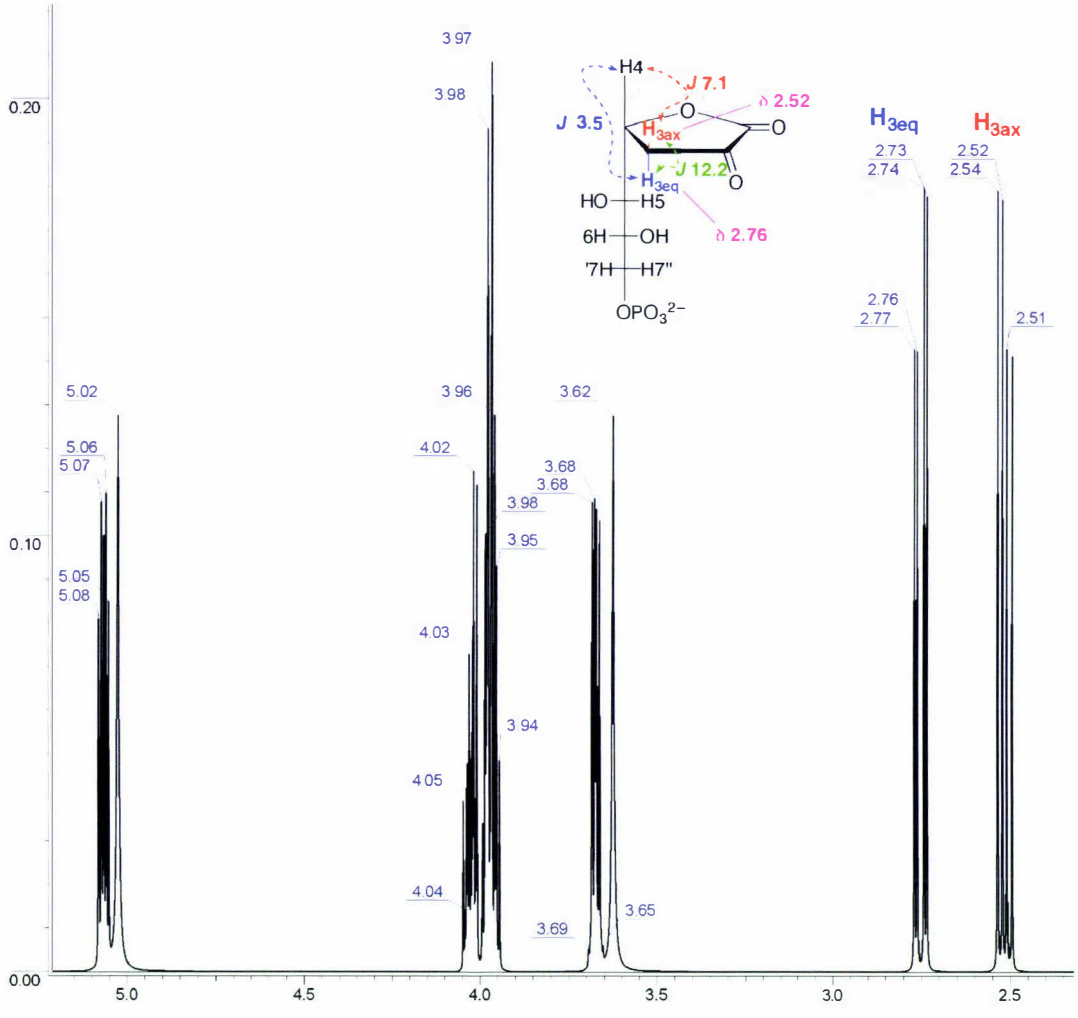

Figure 4.8. Assignment of lactone form of D-DLH7P and the calculated spectrum from NMR prediction software. δ: ppm; *J*: Hz

L-T4P is the C3 epimer of D-E4P; therefore, the reaction product L-DXH7P will have the alternative configuration at C6. Thus, relative to DAH7P, there would be expected to be less preference for a single anomer of this compound. The ^{1}H and 2D COSY NMR spectra of L-DXH7P showed also four sets of geminal protons in the region between 2.5 and 2.8 ppm (Figure 4.5). These have been assigned to δ- and δ-pyranose, and δ- and

δ-furanose forms (Figure 4.9). The coupling constants and chemical shifts of these signals are in line with values predicted by NMR prediction software (Table 4.4). The assignment of C3 protons of, and chemical shifts and coupling constants for DAH7P, D-DLH7P, and L-DXH7P are shown in Figure 4.9 and Table 4.4.

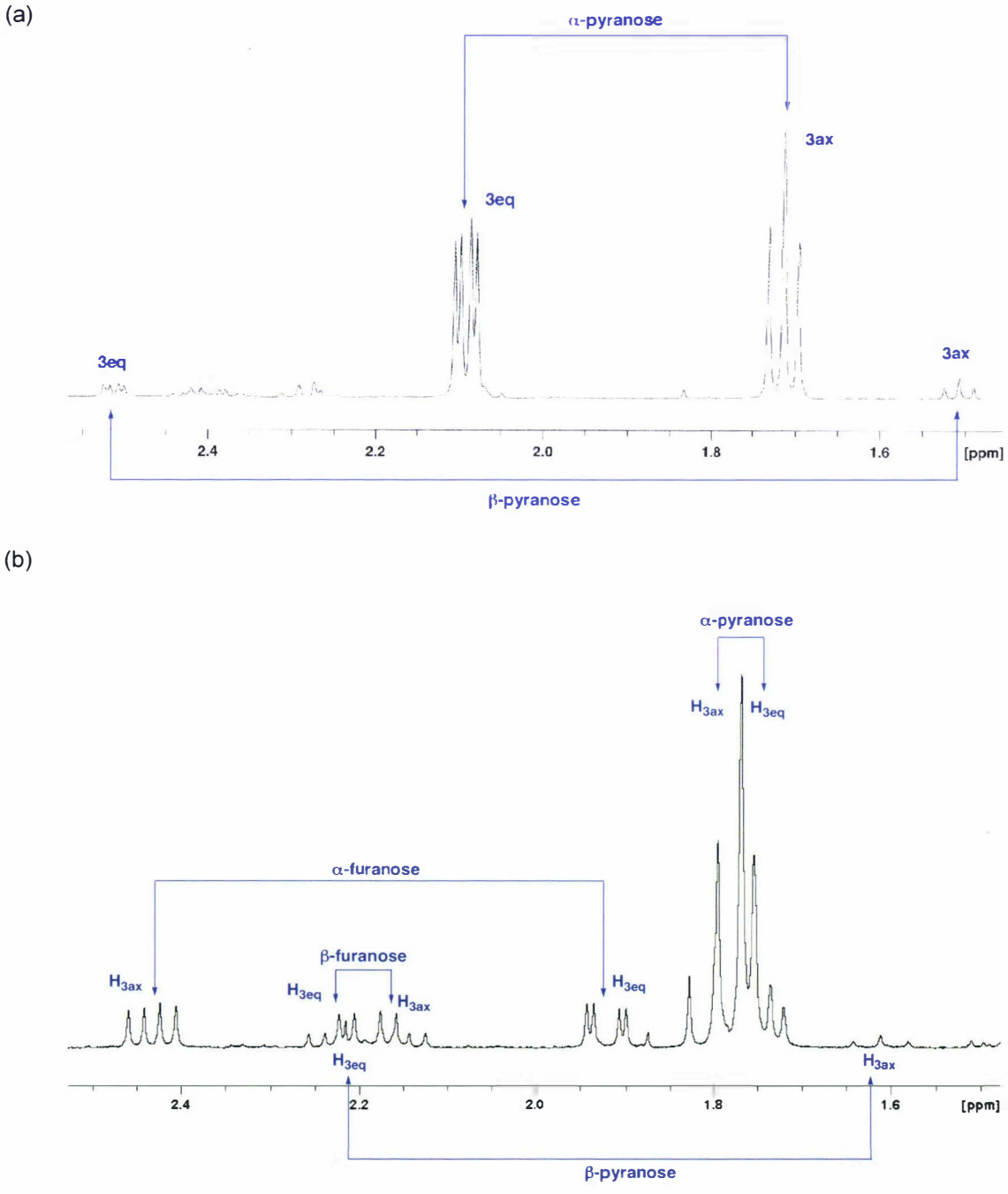

Figure 4.9. Assigned ^{1}H NMR peaks for H3 protons of (a) DAH7P and (a) KDO8P between 1.5 and 2.8 ppm

(c)

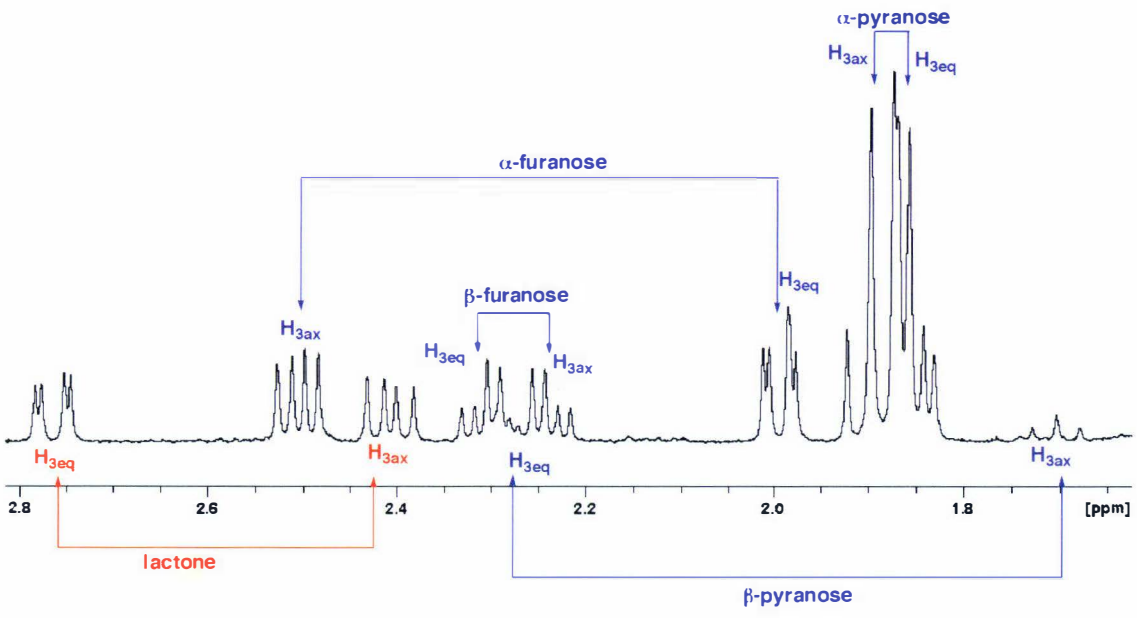

(d)

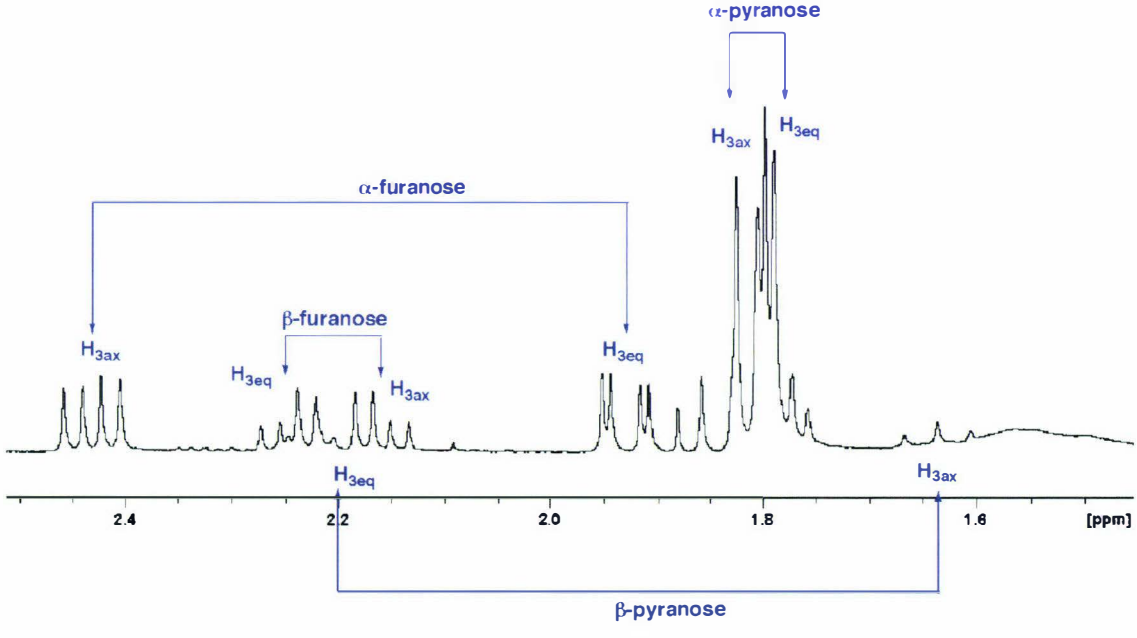

Figure 4.9 continued. Assigned ^{1}H NMR peaks for H3 protons of (c) D-DLH7P and (c) L-DXH7P between 1.5 and 2.8 ppm

Table 4.4.
^{1}H NMR chemical shifts and coupling constants for H3 protons of DAH7P, KDO8P, L-DXH7P, and D-DLH7P

	α-pyranose δ (*J* Hz)	β-pyranose δ (*J* Hz)	α-furanose δ (*J* Hz)	β-furanose δ (*J* Hz)
DAH7P	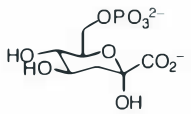 H_{3ax}: 1.71(13.2, 13.2) H_{3eq}: 2.09(13.2, 5.6)	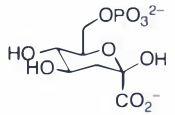 H_{3ax}: 1.51(12.2, 11.8) H_{3eq}: 2.51(12.2, 4.4)	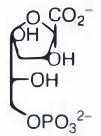	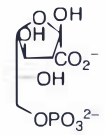
KDO8P	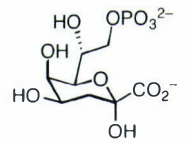 H_{3ax}: 1.79(13.0, 11.3) H_{3eq}: 1.74(13.0, 5.7)	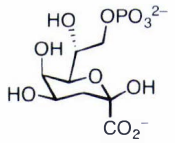 H_{3ax}: 1.61(12.2, 12.2) H_{3eq}: 2.20(12.2, 8.8)	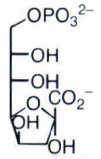 H_{3ax}: 2.45(14.2, 7.2) H_{3eq}: 1.92(14.2, 3.2)	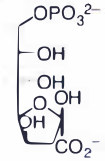 H_{3ax}: 2.15(13.4, 7.0) H_{3eq}: 2.23(13.4, 7.3)
L-DXH7P	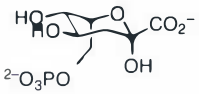 H_{3ax}: 1.87(12.8, 12.5) H_{3eq}: 1.83(12.8, 5.1)	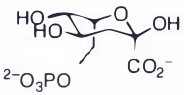 H_{3ax}: 1.68(12.4, 12.4) H_{3eq}: 2.26(12.4 5.0)	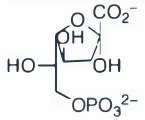 H_{3ax}: 2.48(14.3, 7.4) H_{3eq}: 1.97(14.3, 3.3)	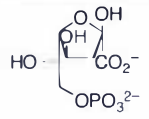 H_{3ax}: 2.21(13.7, 6.5) H_{3eq}: 2.29(13.7, 7.0)
D-DLH7P	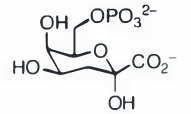 H_{3ax}: 1.89(12.9, 12.4) H_{3eq}: 1.84(12.9, 6.1)	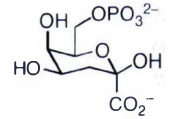 H_{3ax}: 1.69(12.4, 12.4) H_{3eq}: 2.27(12.4, 4.5)	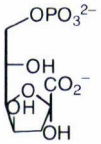 H_{3ax}: 2.5(14.2, 7.1) H_{3eq}: 1.99(14.2, 2.9)	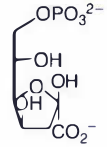 H_{3ax}: 2.23(13.6, 6.8) H_{3eq}: 2.30(13.6, 7.1)

ax and eq refer to the axial and equatorial positions in the pyranose anomers.

4.3. Summary

To investigate the role of the configurations at the C2 and C3 hydroxyl groups of D-E4P in the enzymatic reaction, the C2 and C3 isomers (D- and L-T4P) of D-E4P were tested with *E. coli* DAH7P(Phe) synthase and *P. furiosus* DAH7P synthase. Both D-E4P analogues were found to be alternative substrates for the *E. coli* DAH7P(Phe) synthase and the *P. furiosus* DAH7P synthase. Therefore, the configurations of the hydroxyl groups at C2 and C3 are not critical for the enzymatic reaction. Although the enzymes accepted both alternative substrates, the kinetic data indicated that D- and L-T4P were better substrates for *P. furiosus* DAH7P synthase than for *E. coli* DAH7P(Phe) synthase. Furthermore, both enzymes preferred D-T4P to L-T4P. These observations are consistent with recent results using 2- and 3-deoxyE4P with these enzymes.[90,130] The implications of these findings on reaction mechanism and a comparison to KDO8P synthase are discussed in chapter six.

D-DLH7P and L-DXH7P were prepared from the enzyme-catalysed reaction of D- and L-T4P with PEP and *E. coli* DAH7P(Phe) synthase. The NMR spectra of D-DLH7P and L-DXH7P were assigned (Figure 4.9), based on previously assigned spectra of DAH7P and KDO8P showing four sets of geminally coupled systems for the H3 protons (Figure 4.5) from δ- and δ-pyranose, and δ- and δ-furanose forms between 1.5 and 2.8 ppm. An additional set of geminal protons was observed in the D-DLH7P spectrum, which has been tentatively assigned as the lactone form (Figure 4.9).

Chapter Five

PROBING THE ROLE OF HYDROXYL GROUPS IN 3-DEOXY D-*MANNO*-OCTULOSONATE 8-PHOSPHATE SYNTHASE

This chapter describes the interaction between stereoisomers of D-A5P and *N. meningitidis* KDO8P synthase. The preparation of the diastereomers of D-A5P has been described in chapter three.

5.1. Stereospecific Reaction of Substrate Analogues with KDO8P Synthase

A number of studies of KDO8P synthase with D-A5P analogues have already been reported. The five-carbon sugars, D-R5P, D-A5P, 4-deoxyA5P, 3-deoxyA5P, and 2-deoxyR5P, have been investigated as substrates for KDO8P synthase from *E. coli*.[83-85,94,101,111] 4-DeoxyA5P was found to be an alternative substrate, consistent with the enzyme using the acyclic form of D-A5P.[111] 3-DeoxyA5P was found to be neither a substrate nor a inhibitor.[94] Additionally, 2-deoxyR5P has been reported to be a very poor substrate for the *E. coli* KDO8P synthase (K_M = 50 μM).[85] The C2 epimer of D-A5P, D-R5P, does not act as a substrate for either metal-dependent or metal-independent KDO8P synthases.[83-85,125]

A structural study of the *A. aeolicus* KDO8P synthase in complex with D-R5P has been reported.[125] In this structure, a water molecule, which is coordinated to the metal ion and

C2 hydroxyl group of D-A5P (in the presence of D-A5P), is observed to be missing when the enzyme binds D-R5P. The ineffectiveness of D-R5P as a substrate was attributed to the displacement of this water molecule. However, as metal-dependency can be eliminated by a single mutation of the metal-binding Cys to an Asn,[126,127] it would appear that this water molecule is unlikely to be an essential nucleophile in the catalytic mechanism. More details of the role of the metal ion in KDO8P synthase are discussed in chapter six.

Although the substrate specificity of KDO8P synthase has been investigated to some extent, there have been no complete studies using alternative stereoisomers of D-A5P with the enzyme. In this chapter, the specific roles that the C2, C3, and C4 hydroxyl groups of D-A5P play in the KDO8P synthase reaction are addressed by investigating how D-A5P diastereomers interact with *N. meningitidis* KDO8P synthase. For these studies, the previously prepared D-A5P diastereomers (Figure 5.1), described in chapter three, were examined.

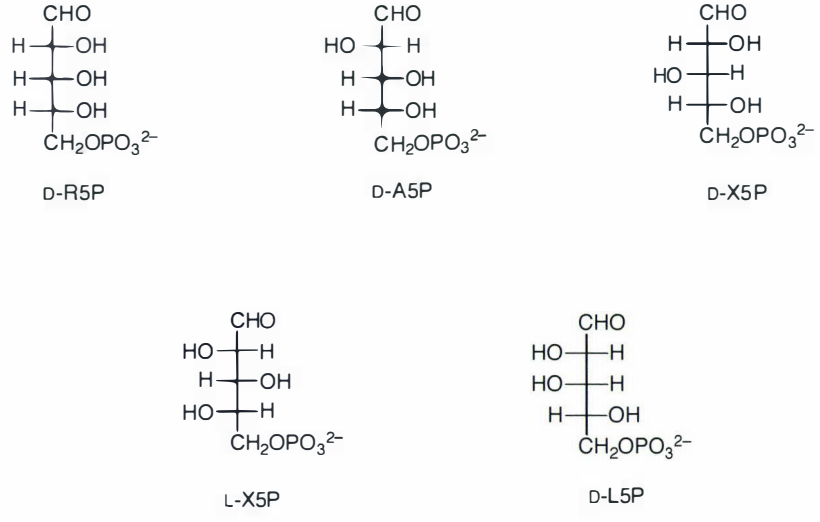

Figure 5.1. D-A5P, the natural substrate of KDO8P synthase and its diastereomers

In order to investigate the abilities of these compounds to act as substrates for KDO8P synthase, the expression, purification, and characterisation of KDO8P synthase from *N. meningitidis* were carried out by Dr Fiona Cochrane from our laboratory.[128] This enzyme has 68.3 % sequence identity with *E. coli* KDO8P synthase, and, like the *E. coli* enzyme, does not require metal for activity.

5.2. Enzymatic Reaction of Five-carbon Sugars with *N. meningitidis* KDO8P Synthase

D- and L-X5P were synthetically prepared from D-xylose and L-xylose, respectively, and D-A5P and D-L5P were generated enzymatically as described in chapter three. These compounds were tested as alternative substrates for *N. meningitidis* KDO8P synthase using the simple UV assay system. All assays were performed in 50 mM BTP buffer. The pH of the buffer was adjusted to 7.4 at 30 °C. The compounds were incubated with PEP at 30 °C for five minutes prior to the reaction being initiated by the addition of purified *N. meningitidis* KDO8P synthase. The reaction was monitored by the loss of PEP at 232 nm. In the presence of PEP, a time-dependent loss of absorbance at 232 nm was observed when D-A5P or L-X5P, which has the same stereochemistry at C2 and C3 as D-A5P, was used. On the other hand, no absorbance loss of PEP was seen in the presence of D-R5P, D-X5P, or D-L5P. These observations suggest that D-R5P, D-X5P, and D-L5P are not substrates of *N. meningitidis* KDO8P synthase, whereas L-X5P is a substrate for the enzyme. This result indicates that the correct C2 and C3 hydroxyl group configurations are essential for the enzyme-catalysed reaction with PEP, but that the configuration at C4 is less important.

These five-carbon compounds were also tested to demonstrate whether they could act as substrates for *E. coli* DAH7P(Phe) synthase, and it was found that D-R5P, and D- and L-X5P were poor substrates for *E. coli* DAH7P(Phe) synthase. Since the reaction rates for the D- and L-X5P were very low even in high concentration of these compounds (34 mM for D-X5P; 30 mM for L-X5P) and of the *E. coli* DAH7P(Phe) synthase (0.7 μM), the enzyme assay system was too inaccurate to investigate kinetic parameters, and the products from D- and L-X5P were unable to be isolated and characterised. On the other hand, D-R5P was shown to be a considerably better substrate than D- and L-X5P. These initial observations suggest that D- and L-X5P are much poorer substrates than D-R5P for *E. coli* DAH7P(Phe) synthase.

5.3. Determination of Kinetic Parameters of Substrate Analogues with *N. meningitidis* KDO8P Synthase

Kinetic parameters for D-A5P and L-X5P were determined by monitoring the loss of PEP at 232 nm using a continuous absorbance assay. The reaction mixtures, without enzyme, were incubated at 30 °C for five minutes and the reaction was initiated by the addition of the purified *N. meningitidis* KDO8P synthase. Consumption of PEP was monitored and initial rates were recorded.

The steady-state kinetic parameters were calculated by fitting data to the Michaelis-Menten equation using Enzfitter[β] (Biosoft, v 2.0). A summary of the kinetic parameters is shown in Table 5.1 and the Michaelis-Menten plots from which these values were calculated are provided in Figure 5.2. As the kinetic data show, L-X5P is an alternative substrate for *N. meningitidis* KDO8P synthase.

Table 5.1.
Kinetic parameters of D-A5P and L-X5P with *N. meningitidis* KDO8P synthase

	D-A5P[a]	L-X5P[a]
K_M^{PEP} (μM)	< 1	2.5 ± 0.1
$K_M^{monosaccharide}$ (μM)	12 ± 1	57 ± 2
k_{cat} (s^{-1})	2.7 ± 0.6	1.1 ± 0.1
$k_{cat}/K_M^{monosaccharide}$ ($s^{-1}/\mu M$)	225 β 10^{-3}	19 β 10^{-3}

[a] The kinetic parameters were determined at a concentration of 160 μM PEP.

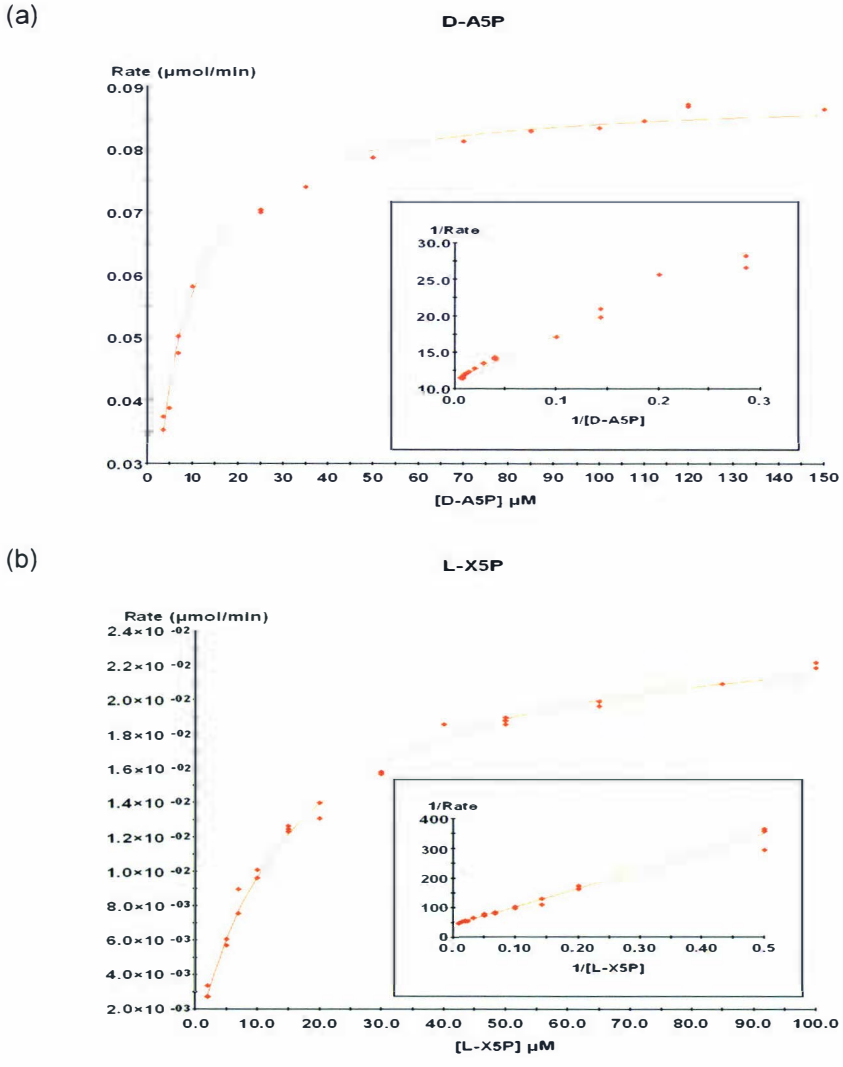

Figure 5.2. Michaelis-Menten plots for the determination of K_M and k_{cat} for (a) D-A5P and (b) L-X5P with *N. meningitidis* KDO8P synthase

5.4. Enzymatic Synthesis of KDO8P and Its Analogues

In order to confirm that PEP loss was connected to the consumption of D-A5P and L-X5P in the KDO8P synthase reaction and to the generation of the expected new eight-carbon sugars (Figure 5.3), KDO8P and 3-deoxy-L-*gulo*-octulosonate 8-phosphate (L-DGO8P) were prepared on a large-scale. 3-Deoxy D-*altro*-octulosonate 8-phosphate (D-DAO8P) was also generated using D-R5P with PEP and *E. coli* DAH7P(Phe) synthase

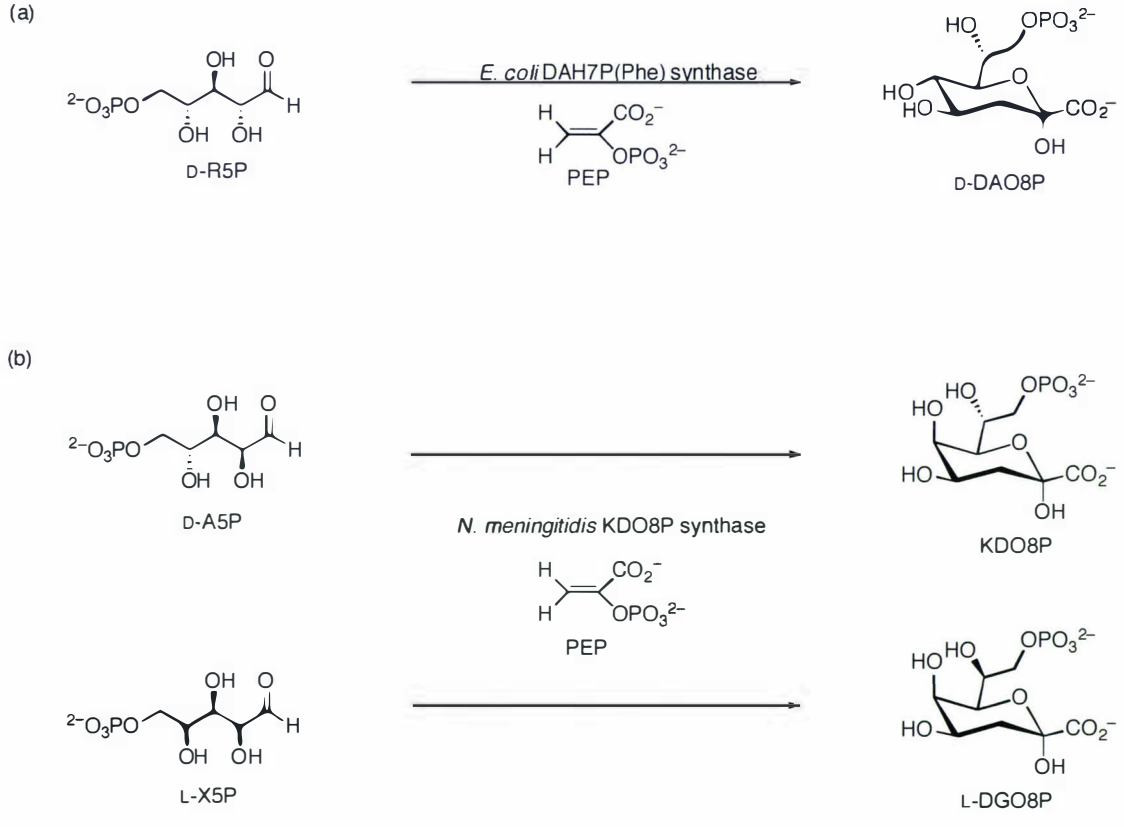

Figure 5.3. Generation of KDO8P and its analogues from alternative substrates of (a) *E. coli* DAH7P(Phe) synthase and (b) *N. meningitidis* KDO8P synthase. Only β-pyranose forms are shown for clarity

since D-R5P is not a substrate of *N. meningitidis* KDO8P synthase. The KDO8P, D-DAO8P, and L-DGO8P were then tested with thiobarbituric acid (as described in section 2.2.3) and the assays gave positive results for the products KDO8P, D-DAO8P, and L-DGO8P.

5.4.1. Large-scale syntheses and purification

In order to establish that KDO8P isomers were generated from an aldol-like reaction between the D-A5P isomers and PEP by KDO8P synthase, sufficient quantities of the products were required for their more detailed characterisation (Figure 5.3). To generate KDO8P and its isomers, L-DGO8P and D-DAO8P, large-scale enzymatic reactions were performed using either the metal-independent *N. meningitidis* KDO8P synthase or *E. coli* DAH7P(Phe) synthase. The reactions were initiated by the addition of enzyme and the loss of PEP was monitored at 270 nm. A higher wavelength than the β_{max} for PEP was used to keep the absorbance measurements within the linear range of the spectrophotometer. After all the PEP was consumed, the enzyme was removed by ultracentrifugation and then the products were purified by anion-exchange chromatography (SourceQ™, Amersham) using an ammonium bicarbonate gradient. Fractions were tested with thiobarbituric acid assay following periodate cleavage to identify the presence of the eight-carbon sugars, then pooled, lyophilised, and stored in the freezer at -80 °C prior to NMR and mass spectral analysis. The high-resolution ESI showed that D-DAO8P and L-DGO8P have the same mass as KDO8P (317.0277 for KDO8P; 317.0275 for D-DAO8P; 317.0273 for L-DGO8P), indicating that the products formed by reaction of PEP with the D-R5P or L-X5P are isomers of KDO8P.

Since the cyclic form of D-DAO8P has the same configuration as DAH7P, we considered that D-DAO8P was likely to share a similar anomeric distribution to DAH7P. As predicted, the ^{1}H spectrum of D-DAO8P clearly showed two major peaks at 1.65 and 2.0 ppm corresponding to the two geminal protons on C3 (Figure 5.4). The coupling constants of 12.7 and 12.4 Hz, and 12.7 and 5.0 Hz associated with peaks at 1.65 ppm and 2.0 ppm, respectively, were similar to those observed for the β-pyranose form of DAH7P. This suggests that those two signals, 1.65 and 2.0 ppm, represent respectively, H_{3ax} and H_{3eq} from D-DAO8P in its β-pyranose form. There were small signals at 1.43 and 2.42 ppm that are assigned as H_{3ax} and H_{3eq} from the β-anomer due to their similar coupling constants (Table 5.2). This interpretation is consistent with both the result of the NMR software prediction program (ACD/NMR predictor software, v.8.10) and the other published assignments for D-DAO8P.[96,107]

The only difference between L-DGO8P and KDO8P is at a stereocentre that is not included in pyranose or furanose ring forms. Therefore, the anomer distribution of L-DGO8P would be expected to be similar to that of KDO8P. In the spectrum of L-DGO8P, four sets of geminal protons are observed between 1.5 and 2.8 ppm (Figure 5.5). As the ^{1}H NMR spectrum of L-DGO8P appeared to be similar to that of KDO8P, the spectrum of L-DGO8P was assigned by comparison to the KDO8P spectrum and by using the NMR prediction program to check the assignments. The assignment of the C3 protons of, and chemical shifts and coupling constants for, D-DAO8P and L-DGO8P are shown in Figure 5.6 and Table 5.2.

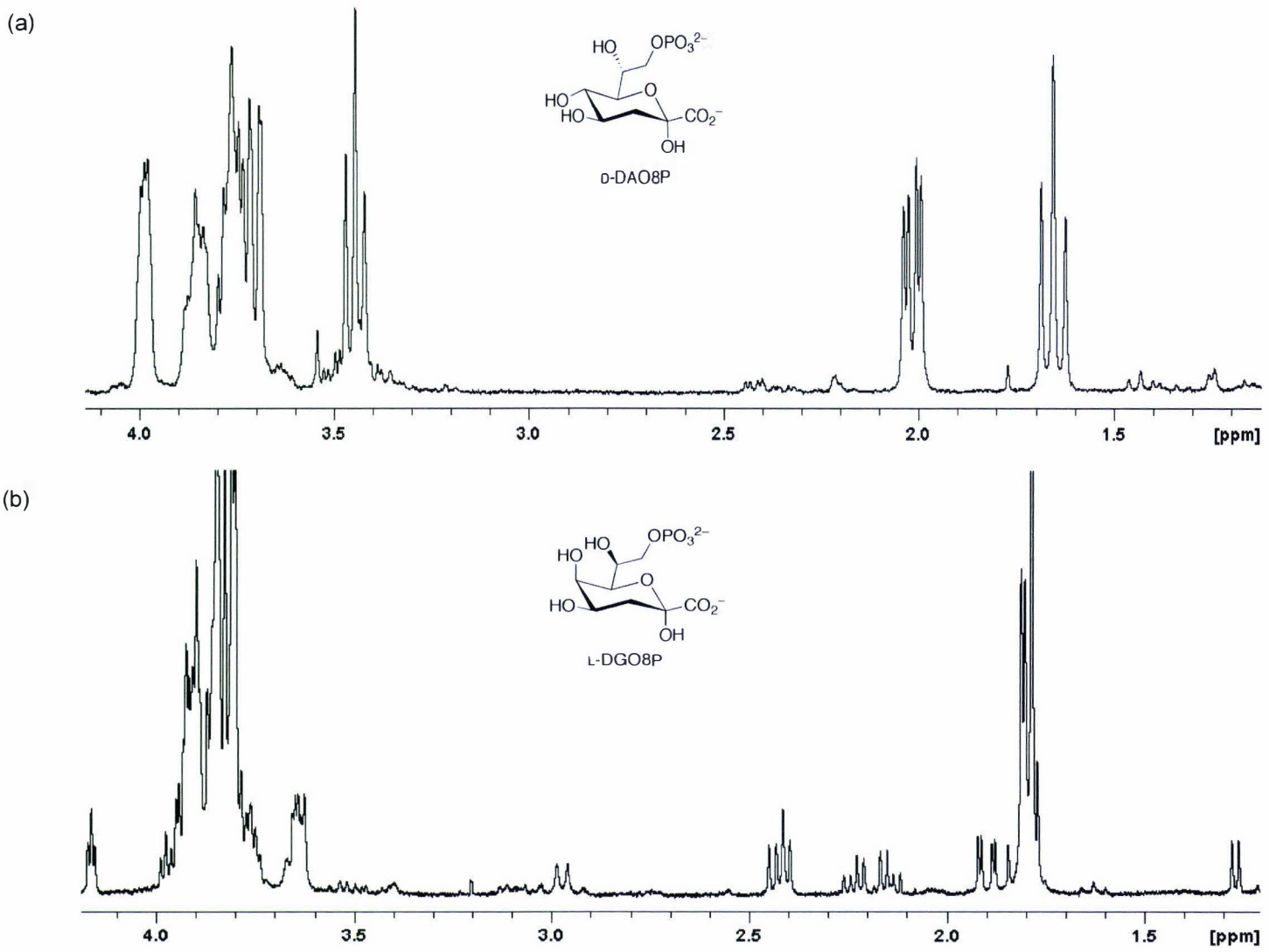

Figure 5.4. ^{1}H NMR spectra of isolated (a) D-DAO8P and (b) L-DGO8P. The structures of eight-carbon sugars are only shown in β-pyranose forms for clarity.

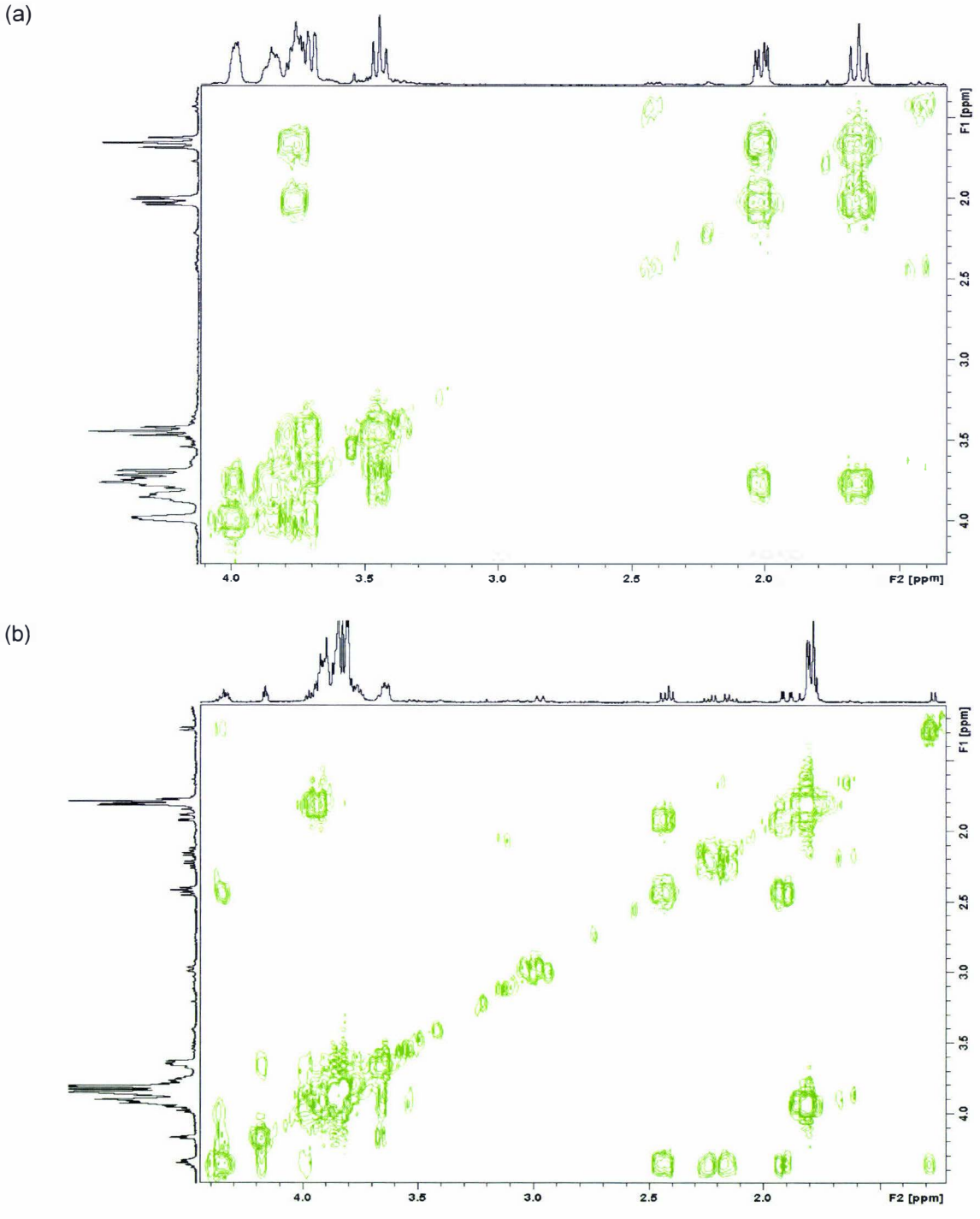

Figure 5.5. COSY spectra of (a) D-DAO8P and (b) L-DGO8P showing geminal and vicinal couplings

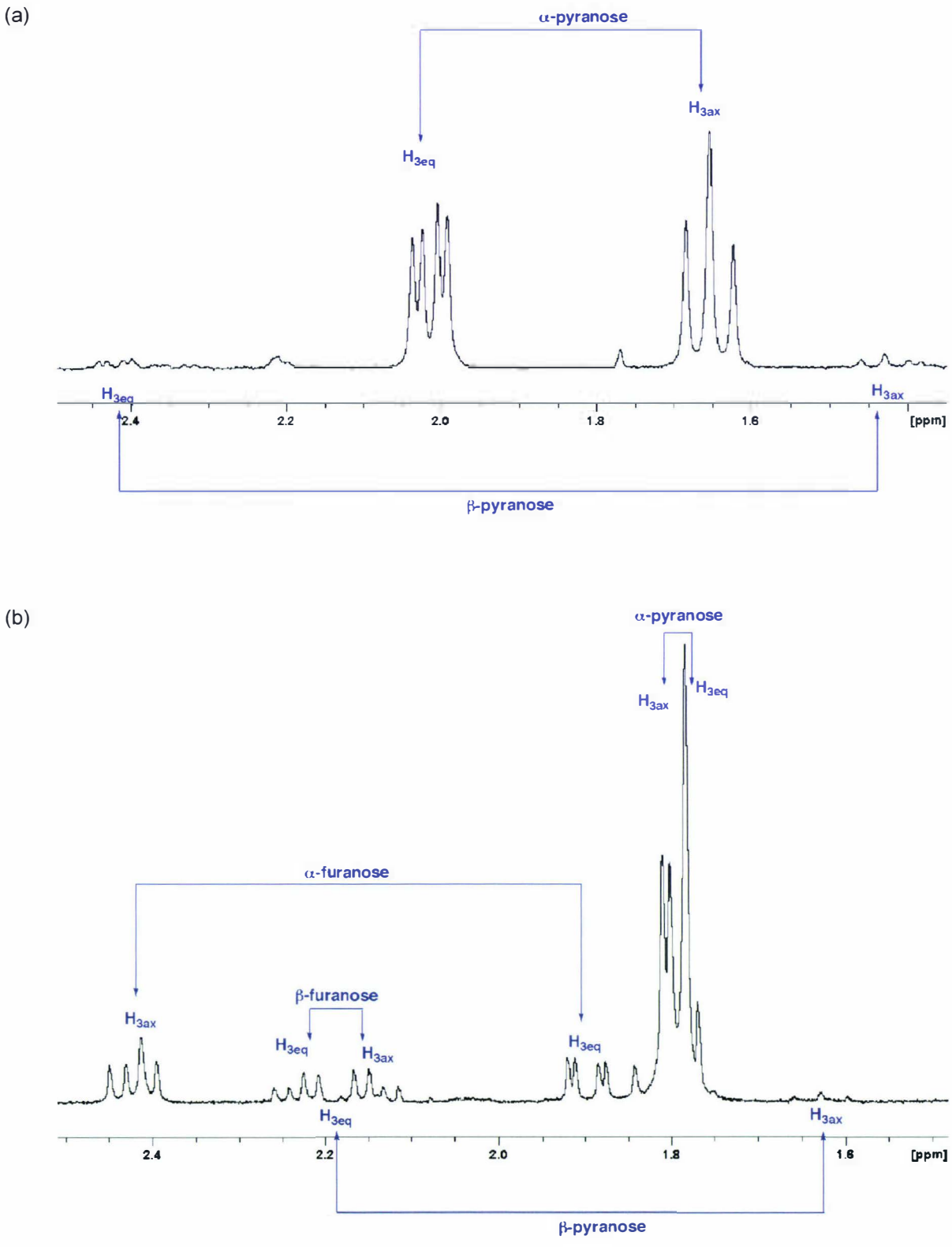

Figure 5.6. Assigned ^{1}H NMR peaks for H3 protons of (a) D-DAO8P and (b) L-DGO8P between 1.4 and 2.5 ppm

Table 5.2.
^{1}H NMR chemical shifts and coupling constants for H3 protons of D-DAO8P and L-DGO8P

	α-pyranose δ (J Hz)	β-pyranose δ (J Hz)	α-furanose δ (J Hz)	β-furanose δ (J Hz)
D-DAO8P	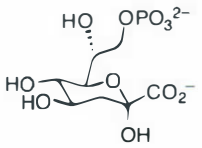	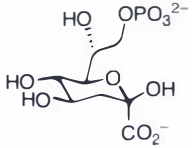	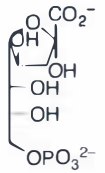	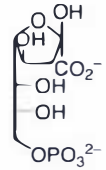
	H_{3ax}: 1.65(12.7, 12.4) H_{3eq}: 2.0(12.7, 5.0)	H_{3ax}: 1.43(12.3, 12.3) H_{3eq}: 2.42(12.3, 4.48)		
L-DGO8P	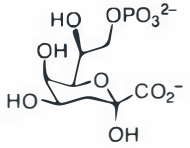	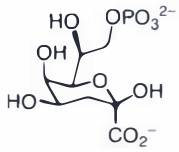	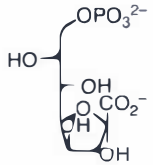	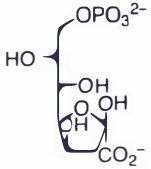
	H_{3ax}: 1.81(12.3, 10.5) H_{3eq}: 1.79(12.3, 4.7)	H_{3ax}: 1.61(12.3, 12.3) H_{3eq}: 2.18[a]	H_{3ax}: 2.42(14.3, 7.4) H_{3eq}: 1.9(14.3, 3.4)	H_{3ax}: 2.14(13.5, 7.0) H_{3eq}: 2.23(13.5, 6.8)

ax and eq refer to the axial and equatorial orientation in the pyranose and furanose anomers.
[a] Due to being the peak either hidden or overlapped, the coupling constant for this peak was not calculated. However, the geminal coupling from this peak was clearly shown.

5.5. Summary

To investigate the roles of C2, C3, and C4 hydroxyl groups in the enzymatic reaction, the isomers of D-A5P, the natural substrate of KDO8P synthase, D-R5P, D-X5P, L-X5P, and D-L5P were tested with *N. meningitidis* KDO8P synthase. It was demonstrated that L-X5P is an alternative substrate for *N. meningitidis* KDO8P synthase, but D-R5P, D-X5P, and D-L5P are not substrates for this enzyme. These observations suggest that correct C2 and C3 hydroxyl group configurations are critical for enzyme reaction but that the C4 hydroxyl group configuration is not important. The roles of the C2 and C3 hydroxyl groups in the KDO8P synthase reaction mechanism, and the roles of these hydroxyl groups in KDO8P and DAH7P synthase reactions are discussed in chapter six.

D-DAO8P was prepared from D-R5P with PEP and *E. coli* DAH7P(Phe) synthase as D-R5P is not a substrate of *N. meningitidis* KDO8P synthase. L-DGO8P was generated from the prepared L-X5P with PEP catalysed by *N. meningitidis* KDO8P synthase. Both eight-carbon sugars were isolated and characterised by NMR spectroscopy and mass spectrometry. As predicted, the ^{1}H NMR spectrum of D-DAO8P was similar to that of DAH7P, and the spectrum for L-DGO8P was similar to that of KDO8P.

Chapter Six

MECHANISTIC INSIGHT INTO 3-DEOXY D-*ARABINO*-HEPTULOSONATE 7-PHOSPHATE SYNTHASE AND 3-DEOXY D-*MANNO*-OCTULOSONATE 8-PHOSPHATE SYNTHASE

This chapter discusses the specificity of DAH7P synthase and KDO8P synthase to sugar substrates with configurational changes, and proposes previously unrecognised mechanistic differences between these two enzymes.

6.1. Introduction

DAH7P synthase and KDO8P synthase are two functionally unrelated enzymes that share many mechanistic and structural features. Both enzymes catalyse the condensation of PEP with a phosphorylated aldose by a similar ordered-sequential mechanism in which PEP binds first and the seven- or eight-carbon sugar phosphate is released last (Figure 1.4).[53-55,101] Both reactions also involve the cleavage of the C–O bond of PEP and are highly stereospecific with the *si* face of PEP coupling with the *re* face of their respective sugar aldehydes.[49,50,103-106] Additionally, X-ray crystal structures of DAH7P synthases have been found to be remarkably similar to those of KDO8P synthases.[29,57,73,74,121,124,126] Based on these similarities, the phylogenetic relationship between DAH7P synthase and KDO8P synthase has recently received attention.[62,67,68,169] Two types of DAH7P synthase have been identified based on molecular mass and sequence.[66] The type I enzymes are a broad family of 3-deoxyald-2-ulosonate phosphate

synthases that includes the KDO8P synthases.[74] This group is also divided into two subfamilies, Iα and Iβ.[62] Currently, only DAH7P synthases are known in subfamily Iβ, whereas subfamily Iα contains both DAH7P synthases ($I\alpha_D$) and KDO8P synthases ($I\alpha_K$).[68]

Although the similarities are clear between DAH7P and KDO8P synthases, differences between the two enzymes are also apparent. The differences between DAH7P synthase and KDO8P synthase are in metal requirement, and in the sugar substrate C2 configuration (Figure 6.1). All known DAH7P synthases are metalloenzymes, whereas subfamily $I\alpha_K$ contains both metalloenzymes and non-metalloenzymes as exemplified by the *A. aeolicus* metal-dependent and *E. coli* metal-independent KDO8P synthases, respectively.[81-83]

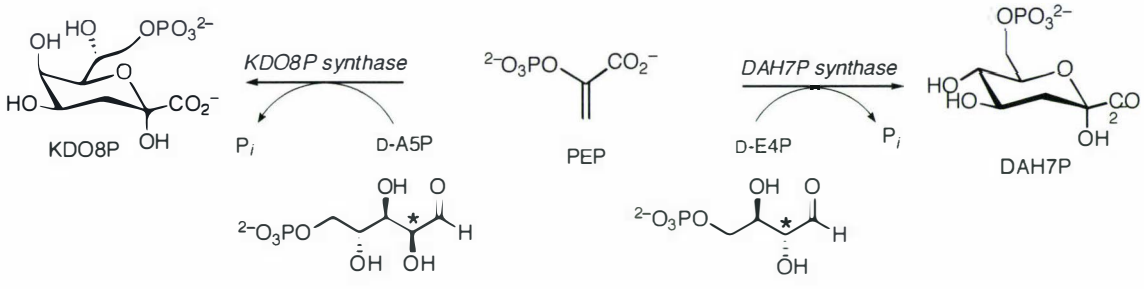

Figure 6.1. Enzymatic reaction of DAH7P synthase and KDO8P synthase. Note stereochemical difference at C2

Previous studies to those presented in this thesis had suggested that DAH7P synthases were somewhat ambivalent to sugar substrate C2 configuration by accepting not only the natural substrate D-E4P but also a variety of five carbon phosphorylated sugars

including those with inverted stereochemistry at C2, such as D-A5P.[74,90,130] On the other hand, KDO8P synthases appeared to be more sensitive to having the correct stereochemistry at this position, as the enzyme takes the natural substrate D-A5P but not D-R5P (E4P-like, the C2-epimer of D-A5P) (Figure 6.1).[83-85,125]

6.2. Substrate Specificity of DAH7P Synthase

Substrate configuration changes in the DAH7P synthase-enzymatic reaction were investigated as part of these studies. D- and L-T4P (C2 and C3 epimers of D-E4P, respectively) were synthesised and tested with *E. coli* DAH7P(Phe) synthase and *P. furiosus* DAH7P synthase. As described in chapter four, both DAH7P synthases were able to accept D- and L-T4P as alternative substrates to D-E4P (Table 1). For the type I× *E. coli* DAH7P synthase, a significant increase in the K_M values were recorded with both substrates, whereas D- and L-T4P were utilised with a comparable catalytic efficiency to the natural substrate D-E4P for *P. furiosus* DAH7P synthase (type $I\times_D$). The seven-carbon phosphorylated sugar products of the enzymatic reactions for both D- and L-T4P were isolated and characterised by both NMR spectroscopy and mass spectrometry. The seven-carbon products from D- and L-T4P were identified as the expected 3-deoxy D-*lyxo* heptulosonate 7-phosphate (D-DLH7P) and 3-deoxy L-*xylo* heptulosonate 7-phosphate (L-DXH7P), respectively.

Table 6.1.
Kinetic parameters of *E. coli* DAH7P(Phe) synthase and *P. furiosus* DAH7P synthase with different monosaccharides

Monosaccharides	*E. coli* DAH7P(Phe) synthase			*P. furiosus* DAH7P synthase		
	K_M (μM)	k_{cat} (s^{-1})	k_{cat} / K_M (s^{-1}/μM)	K_M (μM)	k_{cat} (s^{-1})	k_{cat} / K_M (s^{-1}/μM)
D-E4P[a] 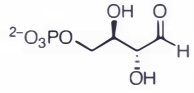	39 ± 4	26 ± 2	670 × 10^{-3}	9 ± 1	1.4 ± 0.1	160 × 10^{-3}
2-deoxyE4P[b] 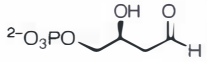	410 ± 40	25 ± 3	60 × 10^{-3}	6 ± 1	3.0 ± 0.1	490 × 10^{-3}
3-deoxyE4P[c] 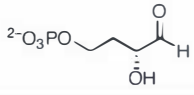	2680 ± 140	4.5 ± 0.1	2 × 10^{-3}	200 ± 30	27 ± 5	140 × 10^{-3}
D-T4P 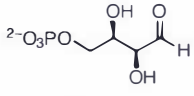	390 ± 13	2.5 ± 0.1	6 × 10^{-3}	21 ± 1	2.4 ± 0.1	110 × 10^{-3}
L-T4P 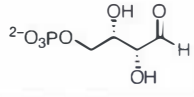	750 ± 10	1.5 ± 0.1	2 × 10^{-3}	47 ± 3	4.0 ± 0.1	85 × 10^{-3}
D-A5P[d] 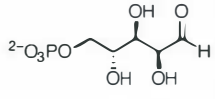	30	0.054	1.8 × 10^{-3}	2700 ± 200	1.1 ± 0.1	0.40 × 10^{-3}
D-R5P[d] 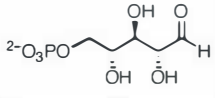	6000	0.72	0.12 × 10^{-3}	1580 ± 110	2.5 ± 0.1	1.6 × 10^{-3}
2-deoxyR5P[d] 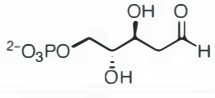	6800	0.46	0.07 × 10^{-3}	2500 ± 150	1.7 ± 0.1	0.69 × 10^{-3}

[a] Kinetic parameters for D-E4P with *P. furiosus* DAH7P synthase were determined by Dr L. Schofield.[74]
[b] Kinetic parameters for 2-deoxyE4P with *P. furiosus* DAH7P synthase were determined by Dr L. Schofield[74] and for 2-deoxyE4P with *E. coli* DAH7P(Phe) synthase by Amy Pietersma.[130]
[c] Kinetic parameters for 3-deoxyE4P with *P. furiosus* DAH7P synthase and *E. coli* DAH7P(Phe) synthase were determined by Amy Pietersma.[90]
[d] Kinetic parameters for the five-carbon sugars with *E. coli* DAH7P synthase are calculated from reference[79] and with *P. furiosus* DAH7P synthase are determined by Dr L. Schofield.[74]

These results were directly comparable with those for D- and L-T4P in terms of the importance of C2 and C3 configuration in the enzymatic reaction. The results with D- and L-T4P, and with 2- and 3-deoxyE4P suggest that both enzymes can tolerate configurational changes to or the removal of either C2 or C3 hydroxyl groups from the substrate, and that the enzymes can utilise D-E4P analogues as alternative substrates. These observations suggest that the C2 or C3 hydroxyl groups do not play a critical role in the DAH7P synthase-enzymatic reaction. It has also been reported that *E. coli* DAH7P synthase was able to accept the five-carbon sugars D-A5P, D-R5P, and 2-deoxyR5P as substrates, showing that DAH7P synthase can also utilise five carbon sugars with variations at the C2 position.[74,79]

6.3. Substrate Specificity of KDO8P Synthase

As part of these studies, the tolerance of KDO8P synthase with respect to configuration changes at the C2, C3, or C4 positions was also investigated. D-L5P and L-X5P were synthesised, and these compounds, together with commercial D-R5P (C3, C4, and C2 stereoisomers of D-A5P, respectively), were examined as substrates for the metal-independent KDO8P synthase from *N. meningitidis*.

As presented in chapter five, the results showed that while D-R5P and D-L5P were not substrates, L-X5P was a substrate for *N. meningitidis* KDO8P synthase (Table 6.2). These observations were consistent with the results from Howe *et al.*[85] that D-R5P was not a substrate of *E. coli* KDO8P synthase. These results indicate that the correct configuration at both positions C2 and C3 is essential for catalysis by KDO8P synthase, but that the alternative configuration at C4 can be accommodated by this enzyme.

Table 6.2.
Kinetic parameters of five-carbon sugars with *N. meningitidis* KDO8P synthase

Five-carbon sugar phosphates	*N. meningitidis* KDO8P synthase			*E. coli* KDO8P synthase[85]		
	K_M (μM)	k_{cat} (s^{-1})	k_{cat} / K_M (s^{-1}/μM)	K_M (μM)	k_{cat} (s^{-1})	k_{cat} / K_M (s^{-1}/μM)
D-A5P 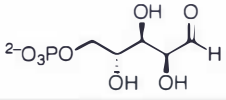	12 ± 1	2.7 ± 0.6	225 × 10^{-3}	19 ± 4	6.8 ± 0.5	358 × 10^{-3}
D-R5P 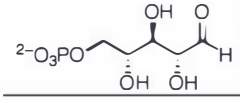	NS [a]			829 ± 54	0.0188 ± 0.0036	227 × 10^{-7}
2-deoxyR5P[b] 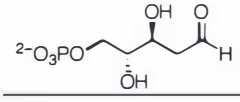	230 ± 20	0.13 ± 0.01	0.6 × 10^{-3}	50 ± 8	0.12 ± 0.05	2.4 × 10^{-3}
D-L5P 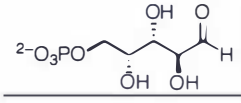	NS [a]					
L-X5P 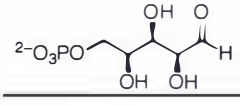	57 ± 2	1.1 ± 0.1	19 × 10^{-3}			

[a] Not a substrate.
[b] The kinetic data were measured by Amy Pietersma.[170]

In earlier experiments reported by others, the interactions of deoxy analogues (2-deoxyR5P, 3-deoxyA5P, and 4-deoxyA5P, Figure 6.2) with *E. coli* KDO8P synthase were studied.[94,111] 4-DeoxyA5P was found to be a substrate (but a poor one), while 2-deoxyR5P and 3-deoxyA5P were neither substrates nor inhibitors for the enzyme. However, a more recent study suggested that 2-deoxyR5P may indeed be an extremely

poor substrate for the enzyme with two orders of magnitude lower catalytic efficient than D-A5P (Table 6.2).[85,128] 2-DeoxyR5P was also tested as a substrate for the KDO8P synthase from *N. meningitidis* showed results of approximately 20 times higher K_M and lower k_{cat} than that of D-A5P (Table 6.2). These results from both *E. coli* and *N. meningitidis* KDO8P synthases demonstrated that 2-deoxyR5P was a very poor substrate. This is consistent with the results presented in this thesis using D-L5P and L-X5P where C2 and C3 hydroxyl group configuration is crucial but C4 hydroxyl group is not important in the KDO8P synthase-enzymatic reaction (Figure 6.2), whereas the DAH7P synthase reaction is ambivalent to changes at these positions.

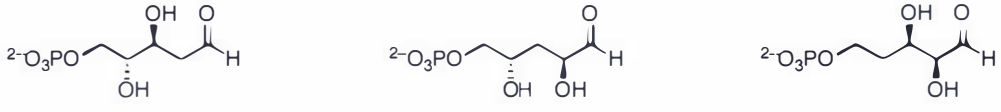

2-deoxyR5P 3-deoxyA5P 4-deoxyA5P

Figure 6.2. Deoxy analogues of D-A5P

6.4. Modelling Studies of DAH7P Synthase

Recent modelling of D-E4P has been reported based on the binding of G3P to *S. cerevisiae* DAH7P(Tyr) synthase and the proposed coordination of D-E4P in *T. maritima* DAH7P synthase (Figure 6.3).[57,73] Both models have suggested that the carbonyl oxygen of D-E4P coordinates to the metal ion and that the C2 and C3 hydroxyl

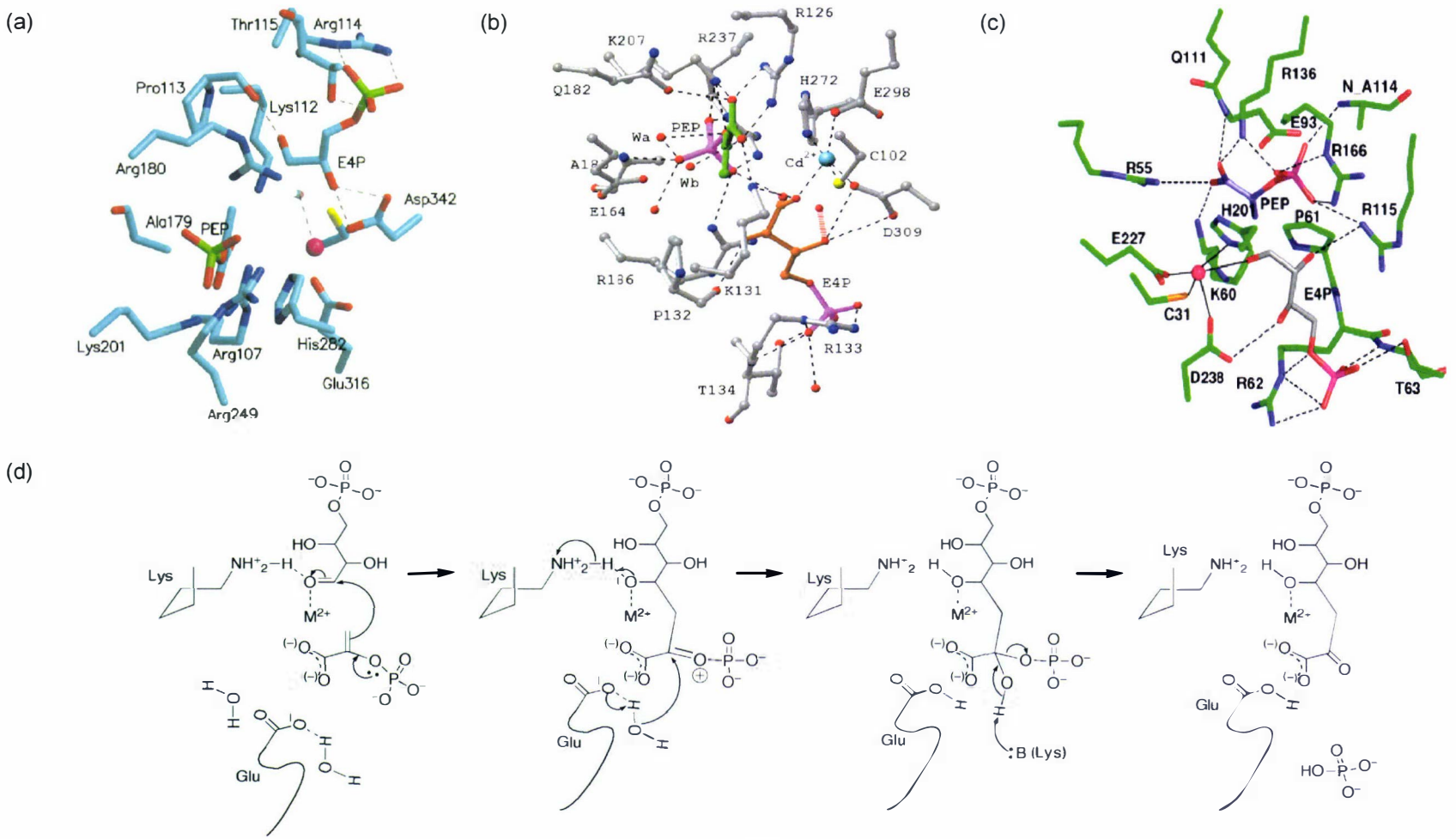

Figure 6.3. (a) Modelled D-E4P in the active site of the *S. cerevisiae* DAH7P(Tyr) synthase–PEP–G3P–Co^{2+} complex after replacement of G3P by D-E4P, taken from König *et al.*,[73] (b) conformation of D-E4P in the active site of *T. maritima* DAH7P synthase–PEP-D-E4P–Cd^{2+}, taken from Shumilin *et al.*,[57] (c) metal ion–PEP–D-E4P–binding ligand in the *P. furiosus* DAH7P synthase active site, taken from Schofield *et al.*,[74] note that R136 is mislabelled and should read K136, and (d) catalytic mechanism of DAH7P synthase based on the proposed binding of D-E4P to *T. maritima* DAH7P synthase, taken from Shumilin *et al.*[57]

groups of D-E4P interact with Pro and Asp residues, respectively; Pro113 and Asp342 in *S. cerevisiae* DAH7P(Tyr) synthase and Pro132 and Asp309 in *T. maritima* DAH7P synthase (Figure 6.3). The Pro is found in the absolutely conserved Lys**Pro**ArgThr motif of DAH7P synthase and the Asp is a metal-binding ligand also absolutely conserved in all DAH7P synthases. Moreover, the modelling studies suggest that the key event in the DAH7P synthase-catalytic mechanism is coordination to the metal ion by the carbonyl oxygen of D-E4P and that interactions of Pro and Asp with the C2 and C3 hydroxyl groups may help to orientate D-E4P in order to improve reactivity. These results are also supported by the study of substrate specificity and structure of *P. furiosus* DAH7P synthase.[74] In the *P. furiosus* DAH7P synthase structure (Figure 6.3), this conserved Pro (Pro61 of the Lys**Pro**ArgThr motif) adopts two different conformations in each of the two subunits of the asymmetric unit. In one subunit, as observed exclusively for *E. coli* DAH7P synthase, this residue points towards the predicted position of the C2 hydroxyl group. In the second, this residue clearly adopts another conformation where the main chain carbonyl of this residue points away from the predicted binding site of D-E4P. This flexibility may explain why *P. furiosus* DAH7P synthase is more tolerant to configurational changes at C2 than *E. coli* DAH7P synthase.[74] Both D-T4P and 2-deoxyE4P were better substrates for this *P. furiosus* DAH7P synthase relative to natural substrate D-E4P with 2-deoxyE4P being even more efficiently utilised than D-E4P by this enzyme.

On the other hand, removing or inverting the C3 hydroxyl group has a far greater influence on the reaction for both *E. coli* and *P. furiosus* DAH7P synthases. This model for the DAH7P synthase reaction suggests that the key role of the enzyme is activation of the aldehyde functionality to nucleophilic attack by coordination to the metal ion. In

the modelled structures of the D-E4P-enzyme complex, the Asp metal-binding ligand (Asp326 in *E. coli* DAH7P synthase and Asp238 in *P. furiosus* DAH7P synthase) is also hydrogen bonded to the C3 hydroxyl group of D-E4P in both enzymes. This interaction would be expected to help both to position Asp and D-E4P, and to influence indirectly the metal ion reactivity, thereby improving the electrophilicity of the aldehyde carbon. Therefore, the sensitivity to changes at C3 can be understood with regard to this proposed mechanism for the DAH7P synthase reaction.

6.5. Comparison of the Active Sites of DAH7P and KDO8P Synthases

Since the structures of DAH7P synthases and KDO8P synthases have been determined, a careful comparison of the active site of the two enzymes has revealed many structural similarities in substrate binding (Table 1.2).[29,57,73,74,121,124] The majority of residues (Ala, Lys, and Arg) that interact with PEP and with the co-substrate are conserved in the active sites of both DAH7P and KDO8P synthase. Although all known DAH7P synthases require a divalent metal for catalysis and both metal-dependent and metal-independent KDO8P synthases have been characterised, the metal-binding site is also similar in DAH7P synthases and metal-dependent KDO8P synthases. In the metal-independent KDO8P synthase, the metal-binding site is filled with an Asn side chain in place of the metal binding Cys. However, there are three absolutely conserved substitutions to residues interacting directly with either PEP or the aldose phosphate substrate (Figure 6.4) that distinguish DAH7P synthases from KDO8P synthases:

i) Arg binds the PEP carboxylate in DAH7P synthases, whereas Lys is found in KDO8P synthases (eg, Arg92 in *E. coli* DAH7P synthase and Lys55 in *E. coli* KDO8P synthase);

ii) an Arg in the PEP phosphate-binding site in DAH7P synthases is substituted by Phe in KDO8P synthases (eg, Arg165 in *E. coli* DAH7P synthase and Phe117 in *E. coli* KDO8P synthase);

iii) in the aldose phosphate binding site, a Pro to AlaAsn substitution is found in the absolutely conserved Lys**Pro**ArgThr motif of DAH7P synthases, creating an equivalent conserved Lys**AlaAsn**ArgSer motif in KDO8P synthases (eg, Pro98 in *E. coli* DAH7P synthase and Ala61Asn62 in *E. coli* KDO8P synthase).

Substitution of the positively charged Arg in DAH7P synthases by the hydrophobic Phe (change is shown in figure 6.4) in KDO8P synthases eliminates a salt bridge to the PEP phosphate that is found in DAH7P synthase and increases the hydrophobicity in the vicinity of the PEP phosphate group in KDO8P synthase. Modelling and structural studies suggest that this allows the aldehyde functionality of D-A5P in KDO8P synthase to be positioned differently to how D-E4P is positioned in DAH7P synthase. This also may allow PEP to be bound to KDO8P synthase in its dianionic rather than the trianionic form.[57,75,122,126] Therefore, in KDO8P synthase, the phosphate moiety of PEP may hydrogen-bond to the aldehydic oxygen of D-A5P.

The second key substitution (Lys**AlaAsn**ArgSer rather than Lys**Pro**ArgThr) provides an additional binding contact for D-A5P ensuring correct placement of the aldehyde moiety in KDO8P synthase close to the PEP phosphate moiety. The key chemical event in these condensation reactions is attack by C3 of PEP on the aldehyde group of co-substrate D-A5P. In all reported metal-dependent KDO8P synthase structures,[124-126] the metal (when

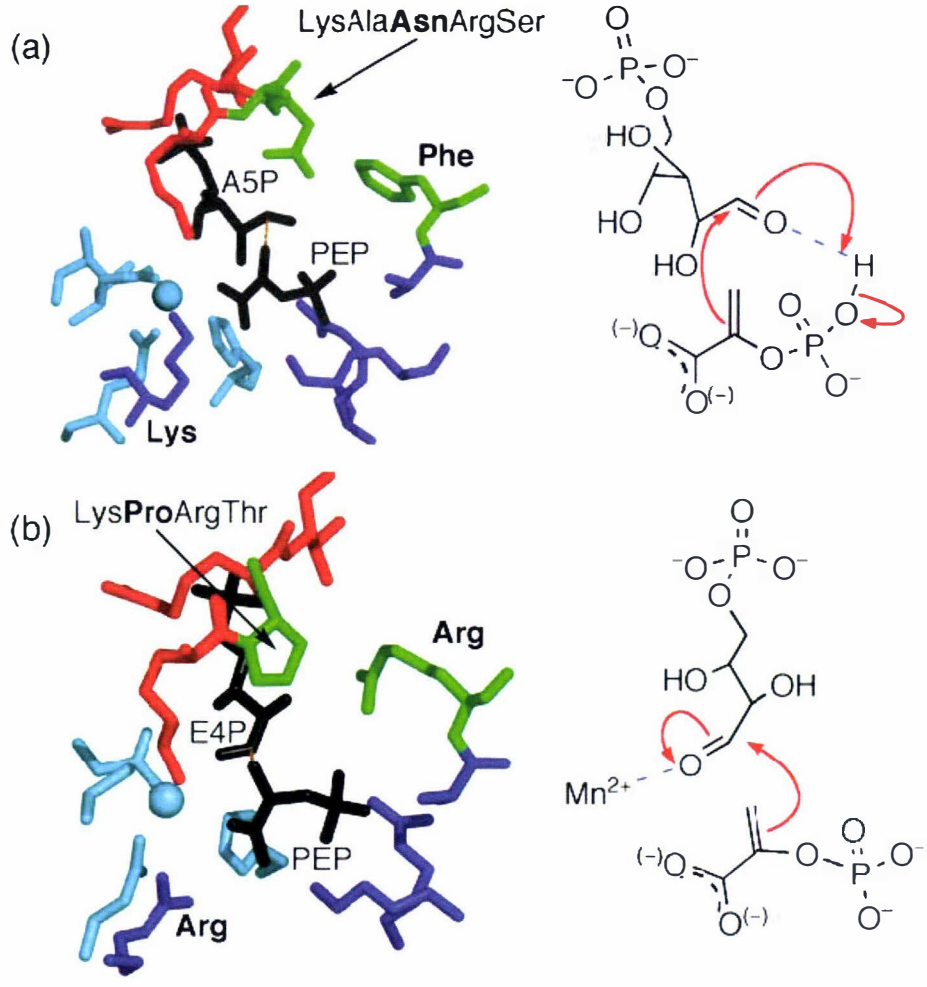

Figure 6.4. Comparison of active sites and proposed (partial) reaction mechanisms for (a) *A. aeolicus* KDO8P synthase and (b) *P. furiosus* DAH7P synthase with D-E4P. D-E4P has been modelled into this structure based on the observed binding of G3P to *S. cerevisiae* DAH7P(Tyr) synthase[73] and the proposed binding of D-E4P to *T. maritima* DAH7P synthase.[57] The key changes discussed in the text are highlighted in green. Metal and metal ligands are in cyan and PEP ligands are shown in blue. Substrates, PEP and D-A5P (or D-E4P) are shown in black

present) appears to be too far from the aldehyde functionality (~ 6 Å) to be involved in electrophilic activation as a Lewis acid catalyst. Moreover, it has recently been reported that the metal dependency can be removed in metal-dependent KDO8P synthases (from *A. pyrophilus* and *A. aeolicus)* by mutation of Cys11 to Asn (Cys11Asn).[126,127] The mutant retains about 10 % of the wild-type maximal activity in the absence of metal ions (Table 6.3). Also, a metal-independent KDO8P synthase (from *E. coli*) can be

converted partially to a metal-dependent KDO8P synthase by mutation of Asn26 to Cys (Asn26Cys, Table 6.3). In the absence of metal ions, Asn26Cys mutant has about 6 % of wild-type activity.

Table 6.3.
Specific activity of the wild-type and mutant KDO8P synthases from *E. coli*, *A. pyrophilus*, and *A. aeolicus*.

	wild-type as purified	EDTA-treated wild-type	Asn26Cys as purified	EDTA-treated Asn26Cys	Cys11Asn as purified	EDTA-treated Cys11Asn
E. coli[a] (unit/mg)	12.0 ± 0.1		0.14 ± 0.01	0.73 ± 0.06		
A. pyrophilus[a] (unit/mg)	3.2 ± 0.3	0.03 ± 0.01 8.0 ± 0.7 (added Cd^{2+})			0.8 ± 0.1	0.8 ± 0.1 1.2 ± 0.1 (added Cd^{2+})
E. coli[b] (unit/mg)	12.28	12.72	0.07	0.17		
A. aeolicus[b] (unit/mg)	1.88	0.08			1.47	1.65

[a] The specific activity of KDO8P synthases from *E. coli* and *A. pyrophilus* as determined by Shulami *et al.*[126]
[b] The specific activity of KDO8P synthases from *E. coli* and *A. aeolicus* as determined by Li *et al.*[127]

However, this activity can be increased to about 30 % of wild-type activity by the addition of Mn^{2+} or Cd^{2+} (Table 6.4).[126] That metal-dependency can be switched on and off by a single mutation indicates that the metal ion is not directly involved in the KDO8P synthase-catalysed reaction, supporting a mechanism where the metal ion plays a dispensable role in KDO8P synthase.

Table 6.4.
Kinetic parameters of the wild-type and mutant KDO8P synthases from *E. coli* and *A. pyrophilus*.[126]

	E. coli				*A. pyrophilus*		
	wild-type	EDTA-treated Asn26Cys	EDTA-treated Asn26Cys		wild-type		EDTA-treated Cys11Asn
			+ Mn^{2+}	+ Cd^{2+}	Mn^{2+}	Cd^{2+}	
k_{cat} (s^{-1})	6.1 ± 0.6	0.36 ± 0.04	1.9 ± 0.1	1.9 ± 0.1	9.0 ± 0.8	6.0 ± 0.8	0.42 ± 0.03
$K_M^{D\text{-}A5P}$ (μM)	20 ± 2	75 ± 11	70 ± 9	110 ± 14	67 ± 6	18 ± 2	140 ± 12
$k_{cat} / K_M^{D\text{-}A5P}$ ($s^{-1}/\mu M^{-1}$)	0.3	0.005	0.03	0.02	0.13	0.33	0.003

Metal binding has also been studied in the DAH7P synthase from *P. furiosus* by mutating Cys31 to Asn.[170] In this study, the Cys31Asn mutant of *P. furiosus* DAH7P synthase showed no detectable enzymic activity with or without EDTA, or added Mn^{2+}. These observations are in contrast to the equivalent mutations in the metal-dependent KDO8P synthases, showing that the metal ion is critical for the catalytic reaction of DAH7P synthase. These findings are entirely consistent with a mechanism for KDO8P synthase involving activation by protonation (Brønsted acid catalysis). In such a mechanism, the activation and positioning of the aldehyde moiety is more delicately choreographed than in the proposed DAH7P synthase mechanism. For KDO8P synthase, the C2 hydroxyl group plays a critical role *via* coordination either to a metal ion or to an Asn side chain (most likely *via* an intermediate water), and therefore the

dihedral angle about the C1–C2 bond of D-A5P is controlled. This mechanism is entirely consistent with the substrate specificity presented in this thesis by altering the configuration of C2 of D-A5P. As shown by the results of *N. meningitidis* KDO8P synthase, the configurational change at C2 of D-A5P disrupts the substrate binding and orientation, such that the KDO8P synthase is unable to utilise D-R5P and is only able to utilise 2-deoxyR5P (or 2-deoxyA5P) as a very poor substrate. On the other hand, DAH7P synthases have been shown to tolerate configurational changes at both the C2 and C3 positions. In both enzymatic reactions, the *si* face of PEP attacks the *re* face side of the aldose co-substrate forming the oxocarbenium intermediate (or transition state). Then, a water molecule located on the *re* face of PEP, observed in both DAH7P synthase and KDO8P synthase structures, attacks the intermediate giving acyclic hemiketal biphosphate.

It should be noted that the X-ray crystal structure of *A. aeolicus* KDO8P synthase in complex with D-R5P has also been solved.[125] When D-R5P was bound, a water molecule coordinated to a metal ion is not present and the C2 hydroxyl group takes its place. This missing water molecule was proposed at that time to act as the nucleophilic water in the catalytic mechanism, and its absence was used to explain the lack of reactivity of D-R5P. However, a direct catalytic role for the divalent metal ion in water activation has been largely discounted as metal-independent KDO8P synthases can be created by a single Cys to Asn mutation.[126,127] What is clear from these structures, however, is that the carbonyl functionality in D-R5P adopts a significantly different orientation in KDO8P synthase compared to DAH7P synthase, but entirely consistent with the prediction that appropriate interaction with the C2 hydroxyl group is vital for addition of C3 of PEP to the carbonyl of D-A5P. The ability of 2-deoxyR5P to act as an

alternative, yet poor, substrate for KDO8P synthase is consistent with a greater likelihood of this analogue accessing the reactive conformation.

Although D-E4P and D-A5P have the same configuration at C3, the results from the present study indicate that the role of the C3 hydroxyl group is different in DAH7P synthases and KDO8P synthases. Whereas L-T4P (C3 epimer of D-E4P) was a substrate for both *E. coli* and *P. furiosus* DAH7P synthases, D-L5P (C3 epimer of D-A5P) did not act as a substrate for *N. meningitidis* KDO8P synthase but L-X5P (C4 epimer of D-A5P) did. These results suggest that the correct C3 configuration is not essential in the DAH7P synthase-catalysed reaction, whereas it is critical in the KDO8P synthase-reaction mechanism, and that the correct C4 configuration is not essential for the KDO8P synthase-enzymatic reaction. This study indicates that the C3 hydroxyl group in D-A5P may also be directly involved in the KDO8P synthase reaction by controlling the dihedral angle about the C1–C2 bond of D-A5P to position the aldehyde moiety to be attacked by C3 of PEP. The structure with D-A5P bound to the *A. aeolicus* metal-dependent KDO8P synthase shows that the C3 hydroxyl group hydrogen bonds to the Asn residue.[126] This residue is part of the Lys**AlaAsn**ArgSer conserved motif that is essential for placement of the aldehyde functionality of D-A5P in the mechanism for KDO8P synthase proposed in this thesis. Therefore, the C3 hydroxyl group is also intimately involved in the correct positioning of the aldehyde group of D-A5P and any changes at this position would be expected to greatly influence the reaction. On the other hand, the changes at the C4 hydroxyl group have a relatively minor influence on the enzymic reaction as there is no direct interaction with this hydroxyl group and the residues that determine placement of the carbonyl carbon.[123,126]

Likewise, this analysis would also appear to account for the recently reported disparity in behaviour with (*E*)-3-fluoroPEP and (*Z*)-3-fluoroPEP between KDO8P synthases (from *A. pyrophilus* and *E. coli*) and DAH7P synthase.[171] That study has found that the overall stereochemistry for both metal-dependent (from *A. pyrophilus*) and metal-independent (from *E. coli*) KDO8P synthase are identical and that both KDO8P synthases prefer (*E*)-3-fluoroPEP to (*Z*)-3-fluoroPEP (the relative k_{cat}/K_M ratio being 100 and 33, respectively, Table 6.5). However, there is little difference between the reactivity of (*E*)-3-fluoroPEP and (*Z*)-3-fluoroPEP with DAH7P synthase (the k_{cat}/K_M being ~ 7×10^{-3} $s^{-1}/\mu M$, Table 6.5). The results from this study also suggest that the metal is not important in the KDO8P synthase-catalytic reaction and that there is a mechanistic difference between KDO8P synthase and DAH7P synthase.

Table 6.5.
Steady-state kinetic parameters for *A. pyrophilus* KDO8P synthases, *E.coli* KDO8P synthases, and *E. coli* DAH7P synthase. Taken from Furdui *et al.*[171]

	A. pyrophilus KDO8P synthase			*E. coli* KDO8P synthase			*E. coli* DAH7P synthase		
	PEP	(*E*)-3-fluoroPEP	(*Z*)-3-fluoroPEP	PEP	(*E*)-3-fluoroPEP	(*Z*)-3-fluoroPEP	PEP	(*E*)-3-fluoroPEP	(*Z*)-3-fluoroPEP
k_{cat} (s^{-1})	9 ± 0.2	1 ± 0.1	1.1 ± 0.02	4.5 ± 0.2	0.5 ± 0.05	0.3 ± 0.04	32	–	–
$K_M^{D\text{-}A5P}$ (μM)	26 ± 1.3	4.7 ± 0.3	500 ± 60	5 ± 0.05	1.9 ± 0.3	32 ± 9	9	–	–
$k_{cat}/K_M^{D\text{-}A5P}$ ($s^{-1}/\mu M^{-1}$)	0.3	0.2	0.002	0.9	0.3	0.009	3.55	0.0069	0.007

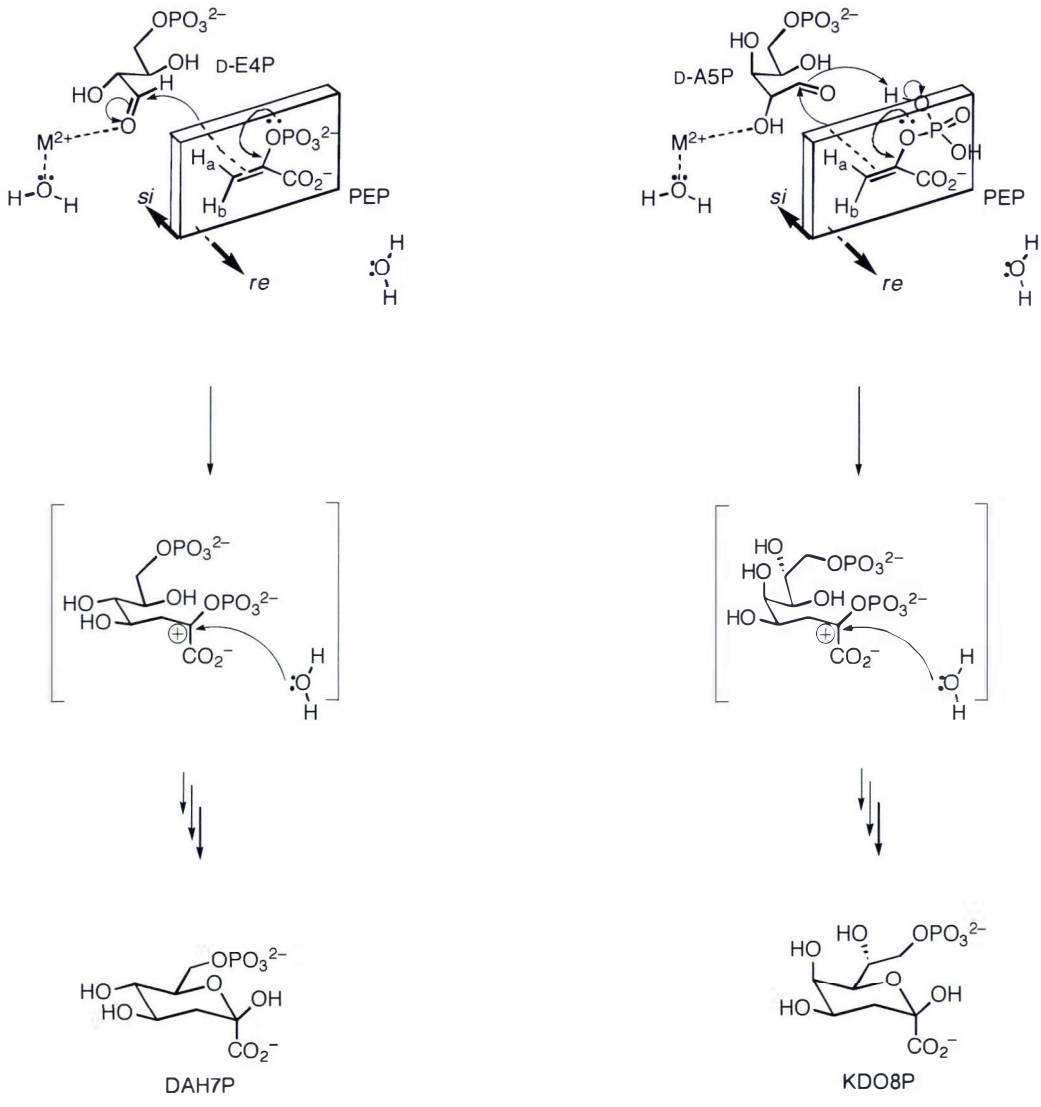

Figure 6.5. Proposed mechanism for DAH7P synthase by Lewis acid catalysis and for KDO8P synthase by protic acid catalysis

As explained earlier in this section, the metal plays a structural role and the reaction is activated by a protonation of the carbonyl of D-A5P (protic acid catalysis) in the new proposed model for the KDO8P synthase mechanism (Figure 6.5). When the divalent metal is absent in KDO8P synthase, the metal-binding ligand Cys is replaced by Asn and this residue plays the same structural role as Cys. Thus, there is no mechanistic difference between metal-dependent and metal-independent KDO8P synthases. A

mechanism for DAH7P synthase has also been proposed based on the findings of (i) the tolerance of DAH7P synthase for change in stereochemistry at the C2 position of its natural substrate, and (ii) the requirement of a divalent metal ion for the DAH7P synthase-catalytic reaction. In this mechanism, the reaction is activated by coordination of metal–carbonyl of D-E4P (Lewis acid catalysis) and therefore, the metal ion has a critical role in this reaction of DAH7P synthase. Thus, contrary to what has been proposed in earlier studies, there is no real mechanistic difference between metal-dependent and metal-independent KDO8P synthase, but there is a mechanistic difference between DAH7P synthase and KDO8P synthase.

6.6. Summary

Identification of key mechanistic similarities, the discovery of metal-dependent KDO8P synthases, and phylogenetic analysis have led to the assumption that a common mechanism applies to these two related enzyme-catalysed reactions. Although many similarities between DAH7P synthase and KDO8P synthase have been shown mechanistically and structurally, the results from this study together with those of other studies suggest that there is a fundamental mechanistic difference between the two enzymes: DAH7P synthases use metal for the activation of their aldose phosphate structure (Lewis acid catalysis) whereas KDO8P synthases use protonation (Brønsted acid catalysis) for activation. This difference in catalytic mechanism gives rise to entirely different substrate specificity profiles for the two enzymes as revealed by the studies presented in this thesis. The present study, together with a reinterpretation of existing substrate specificity and structural data suggests that the evolutionary processes that led to altered substrate specificity also gave rise to different mechanisms of

catalysis. Consequently, the divalent metal ion on which some KDO8P synthases rely for catalytic activity plays an altered and dispensable role in the enzyme-catalysed reaction. Its presence, however, in some enzymes, albeit as an evolutionary carry-over provides further evidence for a common DAH7P synthase-like ancestor for this enzyme family.

6.7. Future Studies

The studies in this thesis have suggested that there are fundamental mechanistic differences in the way that KDO8P synthase and DAH7P synthase process their aldehydic substrates. Based on this finding, we have proposed that the mechanistic differences between the two enzymes are associated with conserved changes to two amino acid motifs in each enzyme class. However, in order to test this proposal and to understand more fully the evolutionary relationship between these two enzymes, further investigations are required. The obvious experiments are to make mutants of the *P. furiosus* DAH7P synthase to convert this metal-dependent enzyme to a metal-dependent KDO8P synthase, as this type $I\times_D$ DAH7P synthase appears to be the closest to the type $I\times_K$ KDO8P synthase subfamily. To introduce the conserved metal-dependent KDO8P synthase motifs to the *P. furiosus* DAH7P synthase, the following minimum changes are required:

i) Mutation of the conserved Arg in the PEP phosphate-binding site of DAH7P synthases to Phe, which is conserved in all KDO8P synthases;

ii) Mutation of the conserved Pro of Lys**Pro**ArgSer motif in the aldose phosphate-binding site of DAH7P synthases to AlaAsn of conserved Lys**AlaAsn**ArgSer motif of KDO8P synthases.

It is highly likely that there are other secondary sequence differences in addition to the changes noted above that have occurred with the evolution of KDO8P synthase activity from an ancestral DAH7P synthase. Therefore, careful structural and sequence analysis of both mutant and native proteins will also be needed to help to unravel the evolution of KDO8P synthases. A combination of these studies and an investigation into the ability of the active site of these enzymes to accept modified substrates, such as the studies presented in this thesis, will help unravel the evolutionary relationship between these two enzymes.

Chapter Seven

EXPERIMENTAL

7.1. General Procedure

Solvents

All organic solvents were freshly distilled before use. Dichloromethane was distilled from calcium hydride. Diethyl ether was dried with sodium hydroxide. THF was distilled from sodium wire. Analytical grade acetone, methanol, and ethanol were used as supplied from commercial sources.

Reagents

All chemical reagents used for experiments were purchased from commercially available sources and used as supplied.

Silver oxide (AgO_2) was freshly prepared following the published procedure (Organic synthesis collective. V5. 386-392)[172] before use.

Dess-Martin periodinane prepared according to the literature[142] by Dr Matthias Rost or Scott Walker. Dess-Martin periodinane was dried in a desiccator over night prior to use.

Chromatography

Analytical thin layer chromatography (tlc) was performed on Merck Silica Gel 60 F254 aluminum-backed sheets. Spots on plates were visualised under UV (254 nm) followed by staining with aqueous potassium permanganate.

Flash column chromatography was carried out on Scharlau silica gel 60, 230 – 400 mesh. Chromatographic solvents, ethyl acetate and hexane, were distilled prior to use.

Reactions and Work-up

All reactions were performed under an inert atmosphere of dry nitrogen (N_2), argon (Ar), or hydrogen (H_2) unless otherwise stated. Crude organic extracts were dried with anhydrous magnesium sulfate. Evaporations were carried out on a rotary evaporator with a bath temperature, less than 40 °C unless otherwise stated.

NMR spectroscopy

^{1}H NMR spectra were obtained on a Bruker Avance$^{\alpha}$ 400 MHz or Bruker Avance$^{\alpha}$ 500 MHz instrument utilising a QNP probe and QXI probe, respectively, or Bruker Avance$^{\alpha}$ 700 MHz instrument utilising a QNP and QXI probes. All spectra were recorded in deuterated solvents as indicated. When the sample was dissolved in D_2O the spectra were referenced to HOD at 4.7 ppm.

^{13}C NMR spectra were obtained on either a Bruker Avance$^{\alpha}$ 400 MHz operating at 100.613 MHz or a Bruker Avance$^{\alpha}$ 500 MHz instrument opening at 125.758 MHz.

^{31}P spectra were recorded on a Bruker Avance$^{\alpha}$ 400 MHz operating at 161.975 MHz.

All signal assignments were consistent with the appropriate 2D NMR experiments ($^{1}H/^{1}H$ COSY and $^{1}H/^{13}C$ HMQC).

Mass Spectrometry

High-resonance mass spectrometry was carried out by either the Department of Chemistry at the University of Auckland on a VG-70SE High-resonance mass spectrometry or the Department of Chemistry at the University of Canterbury on a Micromass LCT.

Low-resolution electrospray ionisation mass spectrometry was carried out on a Micromass spectrometer, utilising a Waters 2790 Separation unit for loading.

UV-Visible Spectrophotometer

UV-Vis spectrophotometry was performed on a Varian Cary® 1 UV-Vis spectrophotometer at 25 °C, 30 °C, or 60 °C as indicated, controlled by a Cary temperature controller using 1 cm path length quartz cells.

7.2. General Biochemical Method

Buffers

Chemicals used for buffer preparation were purchased from commercially available sources.

BTP buffers were prepared by adjusting the pH with concentrated HCl. The following buffers were used in standard assays for the following enzymes:

E. coli DAH7P(Phe) synthase – 50 mM BTP, 10 μM EDTA, pH 6.8 at 25 °C

P. furiosus DAH7P synthase – 50 mM BTP, 10 μM EDTA, pH 7.24 at 60 °C

N. meningitidis KDO8P synthase – 50 mM BTP, pH 7.0 at 30 °C

Enzymes

Transaldolase, triose phosphate isomerase, and G3P dehydrogenase were purchased from Sigma Chemical Company.

Purified *E. coli* DAH7P(Phe) synthase and *P. furiosus* DAH7P synthase were kindly supplied by Dr Linley Schofield. The *P. furiosus* DAH7P synthase was purified and characterised by Dr Linley Schofield.[39] The *N. meningitidis* KDO8P synthase was cloned by Dr Mark L. Patchett, and expressed, purified, and characterised by Dr Fiona Cochrane. These enzymes were kept in aliquots by flash freezing in liquid nitrogen and stored at -80 °C.

Determination of protein concentration

Protein concentrations were determined by Bradford's assay.[173] Using BSA (bovine serum albumin) as standard solutions (0.05, 0.1, 0.2, and 0.4 mg/mL), the assays were carried out by taking standard solutions (100 μL) and by adding the Bradford reagent (1 mL) to diluted unknown samples. The standard solutions and unknown samples were allowed to stand for 10 minutes, and the absorbance reading was then taken of all the standards and samples at 595 nm. The reading was corrected against a blank solution made by milliQ water (100 μL). The concentrations of the unknown samples were determined from a standard plot.

Enzyme assays – general conditions

All enzyme assays were performed in 1 mL, 1 cm path length, quartz cuvettes. All buffer solutions and reagents were treated with Chelex 100 resin (Bio-Rad) to remove metal ions. Solutions were filtered with through a 0.45 μm membrane to remove the

Chelex resin and any particulate matter prior to use. The assays were carried out at 25 °C for *E. coli* DAH7P(Phe) synthase and at 60 °C for *P. furiosus* DAH7P synthase. The assays with *N. meningitidis* KDO8P synthase were carried out using similar conditions except the treatment with Chelex was omitted and the temperature at which the assays were performed was 30 °C. One unit of activity is defined as the loss of 1 μmol of PEP per min at the stated temperature.

Standard enzyme assay for *E. coli* DAH7P(Phe) synthase, *P. furiosus* DAH7P synthase, and *N. meningitidis* KDO8P synthase

PEP was prepared by dissolving a weighed amount in a measured volume of milliQ water. The pH of D-E4P, prepared by lead tetraacetate by oxidation cleavage, was adjusted to around pH 7.0 and the D-E4P solution was kept in the room temperature for 2 hours in order to ensure that D-E4P was in its monomeric form. An accurate concentration value was determined by measuring the loss PEP when D-E4P was limiting, these assays were carried out in duplicate.

Standard assay conditions for *E. coli* DAH7P(Phe) synthase:

E. coli DAH7P(Phe) synthase	0.15 U
PEP	150 μM
D-E4P	250 μM
$MnSO_4$	100 μM

Enzyme assays were monitored at 232 nm ($\alpha_{232} = 2.8 \alpha 10^3 M^{-1}cm^{-1}$). The standard assay reaction mixture except enzyme was incubated at 25 °C for 5 minutes and initiated by adding enzyme.

Standard assay conditions for *P. furiosus* DAH7P synthase:

P. furiosus DAH7P synthase	0.018 U
PEP	160 μM
D-E4P	250 μM
$MnSO_4$	100 μM

Enzyme assays were monitored at 232 nm (α_{232} = 2.6 α 10^3 $M^{-1}cm^{-1}$) and initiated by the addition of phosphorylated sugar. The standard assay mixture, except for the phosphorylated sugar, was incubated at 60 °C for 6 minutes before the assay was initiated.

Standard assay conditions for *N. meningitidis* KDO8P synthase:

N. meningitidis KDO8P synthase	0.016 U
PEP	160 μM
D-A5P	200 μM

Enzyme assays were monitored at 232 nm (α_{232} = 2.8 α 10^3 $M^{-1}cm^{-1}$) and initiated by adding enzyme. The standard assay mixture except enzyme was incubated at 30 °C for 6 minutes before the assay.

Thiobarbituric acid assay[79,139]

Thiobarbituric acid assay reagents:

25 mM sodium periodate ($NaIO_4$) in 0.125 N H_2SO_4

Sodium metaarsenite ($NaAsO_2$) 2 wt %/vol in 0.5 N HCl

Thiobarbituric acid solution (0.36 wt %/vol, pH 9 adjusted with NaOH)

The enzyme mixture (100 μL) was mixed with water (50 μL) and $NaIO_4$ (100 μL in 0.125N H_2SO_4) and the mixture was heated at 60 °C for 1 hour. The excess oxidising agent was reduced by the addition of $NaAsO_2$ (200 μL). Following the disappearance of the yellow colour, thiobarbituric periodate solution (1 mL) was added and the reaction mixture was then heated at 100 °C for 10 minutes. While the sample was cooling down the absorbance of sample was measured at 549 nm ($\alpha_{549} = 1.03 \alpha 10^5 M^{-1} cm^{-1}$).

7.3. Experimental for Chapter Two

Titration of lead tetraacetate

A standard solution of sodium thiosulfate (0.02 M) was prepared for the titration. Lead tetraacetate (0.4 g) was dissolved in glacial acetic acid (20 mL). A potassium iodide solution (250 mL) was also prepared with potassium iodide (25 g) and sodium acetate (125 g). Lead tetraacetate solution (1 mL) was placed in a 500 mL beaker and potassium iodide reagent (15 mL) was added. The iodine liberated by the lead tetraacetate was titrated with sodium thiosulfate (0.02 M) and the endpoint was measured. This titration was performed in triplicate.

Preparation of D-E4P[131]

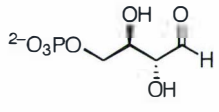

D-Glu6P (0.34 g, 1 mmol) was moistened with water (2 mL) and glacial acetic acid (5 mL) was added to the reaction mixture. Sulfuric acid (3 M, 0.17 mL) and glacial acetic acid (245 mL) were then added to the reaction mixture. A mixture containing sulfuric acid (3 M, 0.6 mL), glacial acetic acid (40 mL), and lead tetraacetate (1.7 mmol) was prepared before use, and added dropwise to the D-Glu6P solution over 30 minutes with vigorous stirring. The reaction mixture was then filtered through a Celite pad. The Celite was washed three times with water (100 mL) and the filtrate was concentrated until the volume of the solution reached approximately 20 mL. The concentrate was then extracted continuously with ether for 15 hours and the volume of the aqueous solution was reduced *in vacuo* to give final volume of 25 mL. This solution was stored in the refrigerator or frozen at -20 °C without further purification.

Preparation of D-T4P

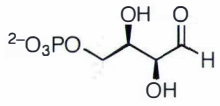

Glacial acetic (2.5 mL) was added to D-Gal6P (0.5 mmol) moistened with 1 mL of water. Sulfuric acid (3 M, 0.085 mL) was added followed by glacial acetic acid (122.5 mL) with stirring. A prepared solution containing sulfuric acid (3 M, 0.3 mL), glacial acetic acid (20 mL), and lead tetraacetate (0.85 mmol) was added dropwise to the rapidly stirring D-Gal6P solution for 30 minutes. The reaction mixture was filtered through a Celite pad and the Celite was washed with water (3 α 100 mL). The filtrate was concentrated until the volume of the solution reached approximately 20 mL. The concentrate was then extracted with ether for 15 hours. The ether dissolved in the

aqueous layer was evaporated to give final volume of 21 mL. This solution was stored in the refrigerator or frozen at -20 °C without further purification.

Synthesis of 1,2:3,4-bis-*O*-(1-methylethylidene)-D-galactopyranose[141]

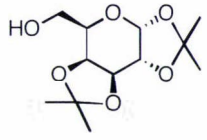

BTE (0.5 ml, 3.95 mmol) was added to D-α-galactose (20 g, 0.11 mol) dissolved in acetone (AR, 400 mL) under Ar and the reaction mixture was refluxed for 14 hours. The mixture was then cooled down to -10 °C and $NaHCO_3$ (0.5 %, 10 mL) was added. The solvent was removed *in vacuo* to give an oily residue. The residue was diluted with H_2O (50 mL) and the aqueous layer was extracted four times with CH_2Cl_2 (50 mL). The concentrated residue was purified by passage through a silica block (3:2, hexane: EtOAc) to give 1,2:3,4-bis-*O*-(1-methylethyledene)-D-galactopyranose (12 g, 41 %) of a colorless syrup.

R_F (hexane:EtOAc, 1:1) = 0.5.

^1H NMR (400 MHz, $CDCl_3$): α 5.43 (d, *J* = 5.0 Hz, 1H), 4.49 (dd, *J* = 5.6, 2.4 Hz, 1H), 4.26 (dd, *J* = 7.4, 2.4 Hz, 1H), 4.15 (dd, *J* = 5.6, 1.8 Hz, 1H), 3.59 – 3.70 (m, 2H), 3.74 (m, 1H), 2.8 (br, s, 1H), 1.37 (s, 3H), 1.32 (s, 3H), 1.29 (s, 6H) ppm. ^{13}C NMR (100.613 MHz, $CDCl_3$): α 24.7, 25.3, 26.2, 26.3, 62.2, 68.7, 70.9, 71.0, 71.7, 96.6, 109.0, 109.7 ppm.

Synthesis of 1,2:3,4-bis-*O*-(1-methylethyledene)-6-(diphenyl phosphate)-α-D-galactopyranose

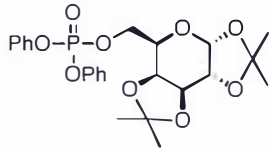

Imidazole (12.53 g, 0.18 mol) and diphenylchlorophosphate (13.3 mL, 64.4 mmol) were added to 1,2:3,4-bis-*O*-(1-methylethyledene)-D-galactopyranose (12 g, 46 mmol) dissolved in dry CH_2Cl_2 (130 mL) at 0 °C. The reaction mixture was stirred under N_2 for 1 day. The reaction was stopped by the addition of H_2O (200 mL), 10 % HCl (100 mL), and CH_2Cl_2 (200 mL) to the reaction mixture. The aqueous layer was extracted three times with CH_2Cl_2 (200 mL). The combined extracts were washed with saturated aqueous $NaHCO_3$ (100 mL), H_2O (100 mL), and saturated aqueous NaCl (100 mL), and concentrated. Purification by flash chromatography (2:1, hexane:EtOAc) gave 1,2:3,4-bis-*O*-(1-methylethyledene)-6-(diphenyl phosphate)-α-D-galactopyranose (19.4 g, 85 %) as a colourless syrup.

R_F (hexane:EtOAc, 1:1) = 0.73.

m/z (+ve FAB) $(M+H)^+$ $C_{24}H_{30}O_9P$, cal. 493.16275, found. 493.16278.

^{1}H NMR (400 MHz, $CDCl_3$): α 7.22 (m, 10H) 5.5 (d, *J* = 4.9 Hz, 1H), 4.56 (dd, *J* = 5.6, 2.4 Hz, 1H), 4.32 – 4.42 (m, 2H), 4.36 (dd, *J* = 7.4, 2.4 Hz, 1H), 4.19 (dd, *J* = 6.3, 1.6 Hz, 1H), 4.08 (t, *J* = 6.3 Hz, 1H), 1.44 (s, 3H), 1.40 (s, 3H), 1.28 (s, 6H) ppm. ^{13}C NMR (100.613 MHz, $CDCl_3$): α 24.8, 25.4, 26.3, 26.4, 67.1, 67.9, 70.8, 70.9, 71.0, 96.6, 109.3, 110.0, 120.5, 125.7, 128.0, 128.6, 130.1, 150.9 ppm.

Synthesis of 1,2:3,4-bis-*O*-(1-methylethyledene)-6-(dihydrogenphosphate)-α-D-galactopyranose

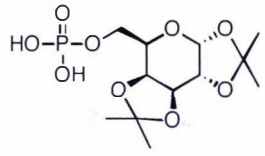

To dissolved 1,2:3,4-bis-*O*-(1-methylethyledene)-6-(diphenyl phosphate)-α-D-galactopyranose (3.1 g, 6.28 mmol) in ethanol (99.9 % Abs, 50 mL), PtO_2 (0.3 g, 1.3 mmol) was added. The reaction mixture was then allowed to stir overnight under complete H_2 atmosphere at room temperature. The reaction mixture was filtered and solvent was evaporated *in vacuo* to give 1,2:3,4-bis-*O*-(1-methylethyledene)-6-(dihydrogenphosphate)-α-D-galactopyranose (2.1 g, 100 %).

m/z (-ve ESMS) $(M-H)^-$ $C_{12}H_{20}O_9P$, cal. 339.95, found. 338.99.

^{1}H NMR (400 MHz, $CDCl_3$): α 5.48 (d, *J* = 5 Hz, 1H), 4.58 (dd, *J* = 5.6, 2.3 Hz, 1H), 4.28 (m, 1H), 4.27 (m, 1H), 4.07 (dd, *J* = 14.1, 7.9 Hz, 2H), 4.02 (t, *J* = 5.2 Hz, 1H), 1.47 (s, 3H), 1.39 (s, 3H), 1.28 (s, 6H) ppm. ^{13}C NMR (100.613 MHz, $CDCl_3$): α 24.7, 25.3, 26.2, 26.3, 65.7, 67.3 (3C), 70.9, 96.6, 109.5, 110.0 ppm.

Synthesis of D-Gal6P

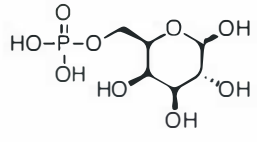

Dissolved 1,2;3,4-*O*-diisopropylidene-D-6-phospho galactopyranose (2.1 g, 6.2 mmol) in H_2O (20 mL) was stirred at 50 °C for two days. After the deprotection was complete

observed by disappearance of the acetonide groups by ^{1}H NMR spectroscopy, the solution was lyophilised without further purification to give D-Gal6P as a white powder (1.6 g, 100 %).

m/z (-ve ESI) $(M-H)^-$ $C_6H_{13}O_9P$, cal. 259.0219, found. 259.0218.

Synthesis of 2,3-*O*-isopropylidene-diphenylphospho-4-hydroxyl-D-threitol

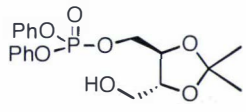

2,3-*O*-Isopropylidene-D-threitol (50 mg, 0.3 mmol) was dissolved in 1 mL of CH_2Cl_2 under N_2 at 0 °C. Imidazole (1.24 mmol) and diphenylchlorophosphate (0.3 mmol) were added, and the reaction was stirred for 1.5 hours under N_2. The reaction mixture was quenched by the addition of H_2O (2.5 mL) and 10 % HCl (2.5 mL). The aqueous layer was then extracted with CH_2Cl_2, and the combined extracts were washed with saturated aqueous $NaHCO_3$, H_2O, and saturated aqueous NaCl. Concentration of the washed organic extracts gave an oil. Column chromatography (1:1, EtOAc:hexane) gave a colourless oil (56.8 mg, 62.3 %).

R_F (hexane:EtOAc, 1:1) = 0.2.

^{1}H NMR (400 MHz, $CDCl_3$): α 7.24 (m, 10H), 4.33 (m, 2H), 4.1 (qd, *J* = 4.5 Hz, 1.1 Hz, 1H), 3.94 (q, *J* = 4.1 Hz, 1H), 3.72 (dd, *J* = 12.0, 4.2 Hz, 1H), 3.59 (dd, *J* = 12, 4.2 Hz, 1H), 3.24 (br, s, 1H), 1.36 (s, 3H), 1.32 (s, 3H) ppm. ^{13}C NMR (100.613 MHz, $CDCl_3$): α 27.2, 27.4, 30.7, 62.2, 68.4 (d, *J* = 5.9 Hz), 76.0 (d, *J* = 7.8 Hz), 77.8, 120.5, 126.0, 130.3, 150.7 ppm.

Synthesis of 2,3-*O*-isopropylidene-diphenylphospho-4-oxo-D-threitol[142]

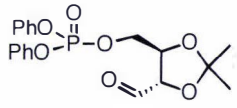

Dess-Martin periodinane (0.27 mmol) was added to the 2,3-*O*-isopropylidene-diphenylphosphono-4-hydroxyl-D-threitol (20 mg, 68 μmol) dissolved in CH_2Cl_2 (1 mL) and the reaction was stirred overnight at 0 °C. Dess-Martin periodinane was then filtered and washed with CH_2Cl_2 (15 mL). The filterate was washed with saturated aqueous Na_2SO_3, H_2O, and brine, and concentrated *in vacuo*. The residual oil was purified by column chromatography (2:1, hexane:EtOAC) to give 2,3-*O*-isopropylidene-diphenylphospho-4-oxo-D-threitol (4.6 mg, 23 %).

R_F (hexane:EtOAc, 1:1) = 0.5.

^{1}H NMR (400 MHz, $CDCl_3$): α 9.72 (s, 1H), 7.5 (m, 10H), 4.34 (qd, *J* = 4.5, 1.7 Hz, 2H), 4.09 (qd, *J* = 4.5, 1.1 Hz, 1H), 3.94 (q, *J* = 4.1 Hz, 1H), 1.37 (s, 3H), 1.32 (s, 3H) ppm. ^{13}C NMR (100.613 MHz, $CDCl_3$): α 27.1, 27.1, 30.7, 68.4, 76.1, 81.0, 120.5, 126.0, 130.3, 150.7, 201.1 ppm.

Synthesis of D-threitol 4-phosphate

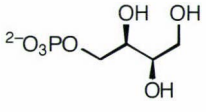

PtO_2 (0.2 mmol) was added to 2,3-*O*-isopropylidene-diphenylphospho-4-hydroxyl-D-threitol (30 mg, 0.1 mmol) dissolved in EtOH (5 mL). The reaction mixture was stirred

under H_2 for two days. The reaction was then filtered, and the solvent was evaporated to give a colourless oil. The oil was then dissolved in water (2 mL) and heated at 60 °C for 1 hour. The reaction mixture was concentrated *in vacuo* to give D-threitol 4-phosphate (5.5 mg, 27 %).

^{1}H NMR (400 MHz, D_2O): α 3.77 (m, 2H), 3.64 (qd, *J* = 6.4, 3.6 Hz, 1H), 3.54 (q, *J* = 4.2 Hz, 1H), 3.48 (dd, *J* = 12.8, 4.3 Hz, 1H), 3.40 (dd, *J* = 13.1, 5.7 Hz, 1H) ppm. ^{13}C NMR (100.613 MHz, D_2O): α 62.7, 67.0, 70.3 (d, *J* = 5.4 Hz), 71.8 (d, *J* = 8.0 Hz) ppm.

Synthesis of diethyl (2*R*,3*R*)-bis(benzyloxy)tartrate[144-146]

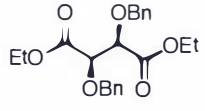

D-Diethyl tartrate (8.6 mL, 0.05 mol) was dissolved in CH_2Cl_2 (100 mL) and BnBr (17.82 mL, 0.15 mol), AgO_2[172] (24.7 g, 0.106 mol), and KI (1.66 mg, 0.01 mol) were added. The reaction mixture was refluxed under Ar for 1 hour and filtered over a Celite pad. The filtrate was then washed with water and dried. The solvent was then removed *in vacuo* to give an oily residue. The residual oil was purified by column chromatography on silica gel (5:1, hexane:EtOAc) to give diethyl (2*R*,3*R*)-bis(benzyloxy)tartrate as a colourless oil (18.9 g, 97 %).

R_F (hexane:EtOAc, 1:1) = 0.89.

^{1}H NMR (400 MHz, $CDCl_3$): α 7.3 (m, 10H), 4.89 (d, *J* = 9.6 Hz, 2H), 4.48 (d, *J* = 9.6 Hz, 2H), 4.42 (s, 2H), 4.23 (dt, *J* = 8.5, 5.7 Hz, 2H), 4.10 (dt, *J* = 8.5, 5.7 Hz, 2H), 1.21

(t, J = 5.7 Hz, 6H) ppm. ^{13}C NMR (125 MHz, $CDCl_3$): α 14.1, 61.3, 73.2, 78.4, 128.0, 128.3, 128.4, 137.0, 169.2 ppm.

Synthesis of (2*S*,3*S*)-2,3-bis(benzyloxy)-1,4-butanediol[147,148]

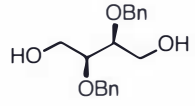

LAH (0.83 g, 21.85 mmol) was suspended in dry ether (20 mL) and added dropwise over 1 hour to diethyl (2*R*,3*R*)-bis(benzyloxy)tartrate (3.95 g, 0.3 mmol) dissolved in dry ether (20 mL) under N_2 at 0 °C. The reaction mixture was then refluxed for 4 hours. Excess LAH was destroyed by sequential addition of H_2O (1 mL), 15 % NaOH (1 mL), and extra H_2O (1 mL) at 0 °C. The reaction mixture was filtered through Celite and the Celite pad was washed with ether. Removal of the solvent *in vacuo* yielded an oil. Column chromatography on silica gel (1:1, hexane:EtOAc) gave (2*S*,3*S*)-2,3-bis(benzyloxy)-1,4-butanediol (2.34 g, 76 %) as a white solid.

R_F (hexane:EtOAc, 1:1) = 0.14.

^{1}H NMR (500 MHz, $CDCl_3$): α 7.4 (m, 10H), 4.65 (s, 4H), 3.85 (d, J = 11.6 Hz, 2H), 3.75 (d, J = 12 Hz, 2H), 3.73 (m, 2H), 2.44 (br, s, 2H).

Synthesis of phosphoric acid, (2*S*,3*S*)-2,3-bis(benzyloxy)-4-hydroxy-butyl diphenyl ester

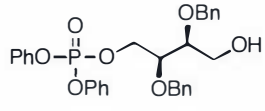

Imidazole (0.82 g, 12 mmol) was added to (2*S*,3*S*)-2,3-bis(benzyloxy)-1,4-butanediol (2.4 g, 8.1 mmol) dissolved in dry CH_2Cl_2 (30 mL) under N_2 at 0 °C. After the imidazole had completely dissolved, diphenylchlorophosphate (0.43 mL, 8.1 mmol) was added and the reaction was then stirred for 4 hours under N_2. The reaction mixture was quenched by adding H_2O (5 mL) and 10 % HCl (5 mL) to the reaction mixture. The organic layer was removed and the aqueous layer was further extracted with CH_2Cl_2. Concentration of the combined organic *in vacuo* extracts gave an oil. Column chromatography (2:3, hexane:EtOAc) gave phosphoric acid, (2*S*, 3*S*)-2,3-bis(benzyloxy)-4-hydroxy-butyl diphenyl ester as a colourless oil (1.2 g, 48 %).

R_F (hexane:EtOAc, 1:1) = 0.54.

m/z (+ve FAB) $(M+H)^+$ $C_{30}H_{29}O_7P_1$, cal. 535.18857, found. 535.18912.

^{1}H NMR (400 MHz, $CDCl_3$): α 7.3 (m, 20H), 4.66 (d, *J* = 11.6 Hz, 1H), 4.57 (m, 4H), 4.25 (ddd, *J* = 11.0, 6.6, 7.1 Hz, 1H), 3.90 (m, 1H), 3.74 (m, 1H), 3.63 (m, 2H), 2.90 (br s, 1H) ppm. ^{13}C NMR (100 MHz, $CDCl_3$): α 61.0, 68.7 (d, *J* = 6.5 Hz), 72.9, 73.3, 77.8 (d, *J* = 7.3 Hz), 78.4 ppm.

Synthesis of phosphoric acid, (2*R*,3*S*)-2,3-bis(benzyloxy)-4-oxo-butyl diphenyl ester[149]

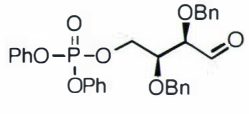

To a stirred solution of phosphoric acid (2*S*,3*S*)-2,3-bis(benzyloxy)-4-hydroxy-butyl diphenyl ester (0.3 g, 0.56 mmol) in dry CH_2Cl_2 (40 mL), Dess-Martin periodinane (0.36 g, 0.84 mmol) was added at room temperature. The reaction mixture was refluxed

for 4 hours and then stirred at room temperature overnight under Ar. Excess periodinane was quenched with ether (45 mL), the mixture was washed with saturated aqueous $Na_2S_2O_3$ (40 mL), saturated aqueous $NaHCO_3$ (40 mL), water (40 mL), and Et_2O (200 mL). The resulting mixture was stirred for 1 hour at room temperature and then extracted three times with ether (80 mL). The combined extracts were washed with water and brine, and concentrated *in vacuo*. The residual oil was purified by column chromatography on silica gel (2:1, hexane:EtOAc) to give phosphoric acid, (2*R*,3*S*)-2,3-bis(benzyloxy)-4-oxo-butyl diphenyl ester (0.26 g, 87 %) as a light yellow syrup.

R_F (hexane:EtOAc, 1:1) = 0.75.

m/z (+ve FAB) $(M+H)^+$ $C_{30}H_{29}O_7P_1$, cal. 533.17292, found. 533.17337.

^{1}H NMR (400 MHz, $CDCl_3$): α 9.63 (s, 1H), 7.3 (m, 20H), 4.69 (d, *J* = 11.8 Hz, 1H), 4.59 (d, *J* = 11.6 Hz, 1H), 4.51 (d, *J* = 11.6 Hz, 1H), 4.47 (d, *J* = 11.6, 1H), 4.42, (m, 2H), 4.05 (m, 1H), 3.89 (d, *J* = 3.8 Hz, 1H) ppm. ^{13}C NMR (100 MHz, $CDCl_3$): α 66.3, 73.5, 73.7, 77.1, 81.9, 120.1, 125.6, 128.2, 129.7, 136.9, 150.4, 202.1 ppm.

Synthesis of phosphoric acid (2*R*,3*S*)-2,3-bis(benzyloxy)-4,4-dimethoxy-butyl diphenyl ester[150]

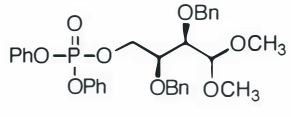

Trimethyl orthoformate (0.124 mL, 1.13 mmol) and H_2SO_4 (0.98 μL, 18.39 μmol) were added to a solution of phosphoric acid, (2*R*,3*S*)-2,3-bis(benzyloxy)-4-oxo-butyl diphenyl ester (60.2 mg, 0.133 mmol) in dry methanol (1 mL). The reaction was stirred overnight at room temperature under argon. The reaction mixture was diluted with ether (10 mL), H_2O (5 mL), and saturated aqueous $NaHCO_3$ (3 mL). The aqueous layer was

extracted three times with 2 mL of Et_2O. The organic extracts were combined and concentrated *in vacuo*. The residual oil was purified by column chromatography on silica gel (2:1, hexane:EtOAC) to give acetal phosphoric acid, (2*R*,3*S*)-2,3-bis(benzyloxy)-4,4-dimethoxy-butyl diphenyl ester (49.7 mg, 76 %) as a colorless oil.

R_F (hexane:EtOAc, 2:1) = 0.49.

m/z (+ve FAB) $(M+H)^+$ $C_{32}H_{35}O_8P_1$, cal. 601.19673, found. 601.19715.

^{1}H NMR (400 MHz, $CDCl_3$): α 7.2 (m, 20H), 4.74 (d, *J* = 11.4, 1H), 4.61 (d, *J* = 11. 4 Hz, 1H), 4.51 (d, *J* = 11.4 Hz, 2H), 4.46 (d, *J* = 6.1 HZ, 1H), 4.30 (m, 2H), 3.88 (ddd, *J* = 8.4, 5.8, 3.5 Hz, 1H), 3.5 (dd, *J* = 6.1, 3.5 Hz, 1H), 3.43 (s, 3H), 3.25 (s, 3H) ppm. ^{13}C NMR (100 MHz, $CDCl_3$) α 54.8, 56.3, 68.1 (d, *J* = 6.6 Hz): 71.7, 73.8, 73.8, 74.5, 77.2 (d, *J* = 8.4 Hz), 77.9, 105.2 ppm.

Synthesis of D-T4P

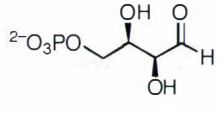

Protected D-T4P phosphoric acid, (2*R*,3*S*)-2,3-bis(benzyloxy)-4,4-dimethoxy-butyl diphenyl ester (49.7 mg, 85.8 μmol) was dissolved in methanol (2 mL) and PtO_2 (19.5 mg, 86 μmol) was added. The mixture was stirred at room temperature overnight under H_2 (atmospheric pressure). The reaction mixture was filtered over Celite and the solvent was removed *in vacuo* to give dimethyl acetal D-T4P (21 mg, 100 %). Dimethyl acetal D-T4P (21 mg, 85.6 μmol) was then dissolved in H_2O and stirred for two days. The progress of the reaction was followed by ^{1}H NMR spectroscopy. After the complete disappearance of the acetal group was observed by ^{1}H NMR spectroscopy, the yield of

D-T4P (43.7 μmol, 51 %) was determined using the DAH7P synthase assay by following the loss of PEP at 232 nm (with D-T4P limiting).

m/z (-ve ESI) $(M-H)^-$ $C_4H_9O_7P_1$, cal. 199.0008, found 199.0009.

Synthesis of L-T4P

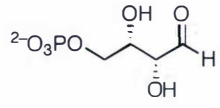

L-T4P (0.12 g, 10 % overall yield) of was prepared starting with L-diethyl tartrate (1 mL, 5.8 mmol) using same method for D-T4P. Intermediate compounds were identified by NMR spectroscopy, and mass spectrometer showed same spectra and masses to that of the intermediate compounds for D-T4P.

m/z (-ve ESI) $(M-H)^-$ $C_4H_9O_7P_1$, cal. 199.0008, found 199.0004.

Alternative enzymic assay system using transaldolase, triose phosphate isomerase, and G3P dehydrogenase

An alternative assay for D-E4P (or D-T4P) involved observing the oxidation of NADH ($\alpha_{340} = 6.2 \alpha 10^3 M^{-1} cm^{-1}$) followed by the conversion of D-E4P (or D-T4P) to G3P *via* D-glyceraldehyde 3-phosphate and dihydroxyacetone phosphate catalysed by the enzymes transaldolase, triose phosphate isomerase, and G3P dehydrogenase (Figure 2.7). EDTA, D-F6P, and NADH solutions were freshly made in 50 mM BTP buffer (pH 6.8). The pH of 1 mL of D-E4P (or D-T4P) solution was adjusted to about pH 7.0 with 1 M of NaOH.

The following assay conditions were used:

EDTA	1 mM
D-F6P	300 μM
NADH	120 μM
Transaldolase	2 U
Triose phosphate isomerase	2 U
G3P dehydrogenase	0.1 U

The reaction mixture except enzymes was incubated at 25 °C for 5 minutes and enzyme assay was monitored at 340 nm. The assay was initiated by the addition of two units of triose phosphate isomerase and followed by the addition of 0.1 U of G3P dehydrogenase. When all G3P had been consumed, two units of transaldolase were then added.

Coupled assay system using DHQase and DHQS

A coupled assay system using unpurified DHQase and DHQS was performed after generating DAH7P and D-DLH7P from the D-E4P and D-T4P, respectively in the DAH7P synthase reaction. The coupled assay reaction was monitored at 234 nm (α_{234} = 1.2 α 10^4 cm^{-1} M^{-1}) following the generation DHS.

The assay solution contained:

$MnSO_4$	100 μM
NAD^+	30 μM
DHQase	5 μL
DHQ synthase	5 μL

A coupled assay reaction mixture contained DAH7P (or D-DLH7P), $MnSO_4$, and NAD^+ in BTP buffer at pH 6.8. The total volume was made up to 1 mL with the buffer. The reaction was initiated by the addition DHQase (5 μL) and DHQS (5 μL), and the absorbance was measured at 234 nm ($\alpha_{234} = 1.2 \alpha 10^4$ cm^{-1} M^{-1}).

7.4. Experimental for Chapter Three

Preparation of D-A5P[153]

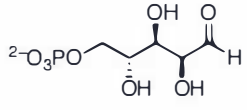

PEP (0.078 g, 0.34 mmol) and ATP (5.5 mg, 10 μmol) were added to D-arabinose (0.05 g, 0.3 mmol) dissolved in H_2O (5 mL). $MgSO_4$ (17 mg, 0.1 mmol) and KCl (7.45 mg, 1 mmol) were then added to this solution and the pH was adjusted to 7.6 with 1 M NaOH. 2-Mercaptoethanol (0.5 μL, 4.1 μmol) and pyruvate kinase (218 U) were added and the reaction was initiated by adding hexokinase (270 U). The reaction mixture was allowed to stir for two days at room temperature and the progress reaction was followed by ^{31}P NMR spectroscopy. After two days, when the complete consumption of PEP was observed by ^{31}P NMR spectroscopy, the enzymes were removed from the solution by filtration (10,000 molecular weight cut off device). The reaction mixture was tested with *N. meningitidis* KDO8P synthase by following the loss of PEP to form the eight-carbon sugar KDO8P. The reaction mixture was then purified by anion exchange. Purification of the D-A5P on a SourceQ™ anion exchange column was performed at 4

°C using a BioLogic Duo-Flow FPLC system (Bio-Rad) with detection at 280 nm and 214 nm. The solution containing D-A5P and buffer solutions were filtered before application to the column. The D-A5P was eluted with a linear gradient of 0-1 M of NH_4HCO_3. The filtered sample was loaded to the column using a 500 μL loop. The flow rate was 0.2 mL/min and 3 mL fractions were collected. The fractions containing D-A5P were identified followed by the loss of PEP using *N. meningitidis* KDO8P synthase. Fractions containing D-A5P were combined, lyophilised, and stored in the -80 °C freezer to yield 73 mg (95 %).

m/z (-ve ESI) $(M-H)^-$ $C_5H_{10}O_8P$, cal. 229.0113, found 229.0119.

^{31}P NMR (161.9675 MHz) 3.400.

Preparation of D-L5P

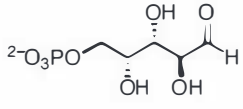

$MgSO_4$ (17 mg, 0.1 mmol) and KCl (7.45 mg, 1 mmol) were added to a reaction mixture containing D-lyxose (0.05 g, 0.3 mmol), PEP (0.078 g, 0.3 mmol), and ATP (5.5 mg, 10 μmol) dissolved in H_2O (5 mL). The pH was adjusted to 7.6 with 1 M NaOH and then 2-mercaptoethanol (0.5 μL, 4.1 μmol) and pyruvate kinase (218 U) were added. The reaction was initiated with adding hexokinase (270 U) and the progress reaction was followed by ^{31}P NMR spectroscopy. After overnight incubation, another pyruvate kinase (109 U), hexokinase (135 U), and $MgSO_4$ (40 mg, 0.34 mmol) were added and the reaction was continued. After two days, additional pyruvate kinase (436 U), hexokinase (540 U), and and $MgSO_4$ (40 mg, 0.34 mmol) were added. The reaction

mixture was left for a further four days. When PEP was ceased, the enzymes were removed for the reaction mixture by filtration (10,000 molecular weight cut-off filtration device). The reaction mixture was tested with Bial's reagent[163-165] to confirm the presence of D-L5P. The reaction mixture was then purified on a SourceQ™ anion exchange column performed at 4 °C using a BioLogic Duo-Flow FPLC system (Bio-Rad) with detection at 280 nm and 214 nm. The solution containing D-L5P filtered previously was eluted with a linear gradient of 0-1 M of filtered NH_4HCO_3. The filtered sample was loaded to the column using a 500 μL loop. The flow rate was 0.2 mL/min and 3 mL fractions were collected. The fractions containing D-L5P were identified with Bial's reagent as described below. Fractions containing of D-L5P were combined, lyophilised, and stored in the -80 °C freezer to yield 58 mg (76 %).

m/z (-ve ESI) $(M-H)^-$ $C_5H_{10}O_8P$, cal. 229.012, found 229.0115.

^{31}P NMR (161.9675 MHz) 1.800.

Bial's reagent assay[163]

Reagents for Bial's assay:

Concentrated HCl	40.7 mL
1 % $FeCl_3$	1 mL
orcinol	0.1 g

Purified fractions were assayed treating with Bial's reagent to determine the presence of D-L5P. All the reagents were combined and the volume was added up to 50 mL. For 100 μL of sample from purified fraction, 500 μL of the reagent was added and the reaction mixture was heated at 100 °C for 10 minutes. The assay gave a green colour in the presence of D-L5P.

Synthesis of (-)-1,2;3,4-*O*-diisopropylidene-α-D-xylofuranose[166,167]

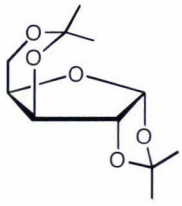

D-Xylose (1 g, 6.67 mmol) was dissolved in acetone (10 mL, AR grade) and $CuSO_4$ (2.12 g, 13.3 mmol), and H_2SO_4 (107 μL, 2 mmol) were added to the reaction mixture. The reaction mixture was allowed to stir vigorously under a calcium chloride drying tube for 28 hours. The mixture was then filtered and the precipitate was washed with acetone (5 mL). The filtrate was treated with aqueous ammonia (160 μL, 28 %) and the precipitate was removed by filtration. The precipitate was washed with acetone (5 mL) and the solvent from the combined filtrates was removed *in vacuo* to give 1,2;3,4-*O*-diisopropylidene-α-D-xylofuranose (1.5 g) of a yellow syrup. Next step was carried out without purification.

^{1}H NMR (400 MHz, $CDCl_3$): α 5.95 (d, *J* = 3.6 Hz, 1H), 4.49 (d, *J* = 3.3 Hz, 1H), 4.30 (s, 1H), 3.98 – 4.13 (m, 3H), 1.45 (s, 3H), 1.40 (s, 3H), 1.34 (s, 3H), 1.28 (s, 3H) ppm.

^{13}C NMR (100.6238 MHz, $CDCl_3$): α 26.6, 27.2, 61.7, 77.5, 78.9, 86.1, 105.3, 112.2 ppm.

Synthesis of (-)-1,2-*O*-isopropylidene-α-D-xylofuranose[166,167]

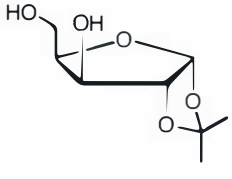

The yellow syrup, 1,2;3,4-*O*-diisopropylidene-α-D-xylofuranose (1.5 g, 6.5 mmol), was dissolved in 7.5 mL of 0.2 % (v/v) HCl and the reaction mixture was then stirred for 25 minutes at room temperature. The reaction was filtered and neutralised to pH 7 – 8 with $NaHCO_3$. The solvent was then evaporated with rotary evaporator to give a yellow slurry. The yellow slurry was washed with 7.5 mL chloroform and filtered. The filtrate was removed in *vacuo* to give 0.95 g of 1,2-*O*-isopropylidene-α-D-xylofuranose of a yellow syrup. Next step was carried out without purification.

^{1}H NMR (400 MHz, $CDCl_3$): α 5.95 (d, *J* = 3.6 Hz, 1H), 4.50 (d, *J* = 3.6 Hz, 1H), 4.30 (s, 1H), 4.01 – 4.14 (m, 2H), 1.46 (s, 3H), 1.29 (s, 3H), ppm. ^{13}C NMR (100.6238 MHz, $CDCl_3$): α 25.3, 25.8, 64.0, 73.9, 80.0, 84.8, 104.8, 113.0 ppm.

Synthesis of (-)-1,2-*O*-isopropylidene-α-D-5-diphenylphospho-xylofuranose

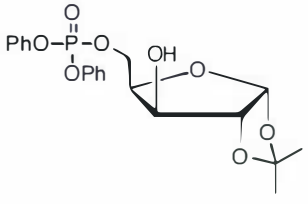

1,2-*O*-Isopropylidene-α-D-xylofuranose (0.95 g, 5 mmol) was dissolved in CH_2Cl_2 (150 mL). Imidazole (1.36 g, 0.02 mol) and diphenylchlorophosphate (1.4 mL, 7 mmol) were added to the reaction mixture at 0 °C. The reaction mixture was stirred under N_2 for 6 hours. The reaction was stopped by adding H_2O (10 mL) and 10 % HCl (10 mL) to the reaction mixture. The aqueous layer was extracted three times with CH_2Cl_2 (50 mL). The combined extracts were washed with saturated aqueous $NaHCO_3$ (20 mL), H_2O (2 α 20 mL), and saturated aqueous NaCl (20 mL), dried with $MgSO_4$, and concentrated.

Purification by flash chromatography (2:3, hexane:EtOAc) gave 1,2-*O*-isopropylidene-α-D-5-diphenylphospho-xylofuranose (0.65 g, 31 %) as a colorless syrup.

R_F (hexane:EtOAc, 1:1) = 0.5.

m/z (+ve FAB) $(M+H)^+$ $C_{20}H_{24}O_8P$, cal. 423.12088, found 423.1208.

^{1}H NMR (400 MHz, $CDCl_3$): α 7.3 (m, 10H), 5.85 (d, *J* = 3.5 Hz, 1H), 4.48 – 4.52 (m, 2H), 4.25 – 4.31 (m, 2H), 4.07 (d, *J* = 1.9 Hz, 1H), 1.45 (s, 3H), 1.27 (s, 3H) ppm. ^{13}C NMR (100.6238 MHz, $CDCl_3$): α 26.2, 26.9, 65.2, 73.8, 78.8, 85.1, 105.0, 111.9, 120.1, 125.8, 128.0, 128.5, 130.0, 150.3 ppm.

Synthesis of (-)-1,2-*O*-isopropylidene-α-D-5-phospho-xylofuranose

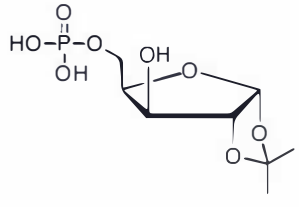

1,2-*O*-Isopropylidene-α-D-5-diphenylphospho-xylofuranose (0.65 g, 1.5 mmol) dissolved in methanol and PtO_2 (0.34 g, 1.5 mmol) was added to the reaction, and the reaction mixture was then stirred overnight under H_2 atmosphere at room temperature. The reaction mixture was then filtered and the solvent was removed *in vacuo* to give 1,2-*O*-isopropylidene-α-D-5-phospho-xylofuranose (0.42 g, 100 %).

^{1}H NMR (400 MHz, $CDCl_3$): α 5.80 (d, *J* = 3.7 Hz, 1H), 4.45 (d, *J* = 3.7 Hz, 1H), 4.19 (m, 1H), 4.07 (d, *J* = 2.8 Hz, 1H), 3.98 – 3.80 (m, 2H), 1.27 (s, 3H), 1.11 (s, 3H) ppm ^{13}C NMR (100.6238 MHz, $CDCl_3$): α 25.3, 25.8, 64.0, 73.9, 79.9, 84.8, 104.8, 113.0 ppm.

Synthesis of D-X5P

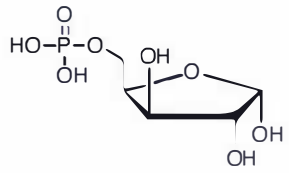

1,2-*O*-Isopropylidene-α-D-5-phospho-xylofuranose (0.42 g, 1.56 mmol) was dissolved in H_2O (15 mL) and stirred for two days at 50 °C. The progress of the reaction was followed by ^1H NMR spectroscopy. After the complete disappearance of the acetonide group was observed by ^1H NMR spectroscopy, the yield of D-X5P (0.26 g, 72 %) was determined by the loss of PEP in general DAH7P synthase assay test explained in section 7.2.

m/z (-ve ESI) $(M-H)^-$ $C_5H_{10}O_8P$, cal. 229.0113, found 229.0113.

Synthesis of L-X5P

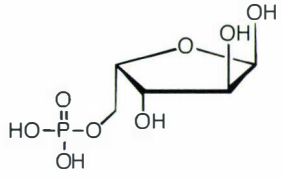

L-X5P (0.2 g, 13 % overall yield) was prepared starting with L-xylose (1 g, 6.67 mmol) following the same procedures for the synthesis of D-X5P. NMR spectra from the intermediate compounds appeared to be same as those recorded for the synthesis of D-X5P.

m/z (-ve ESI) $(M-H)^-$ $C_5H_{10}O_8P$, cal. 229.0113, found 229.0113.

7.5. Experimental for Chapter Four

Kinetic assays for D-T4P and L-T4P with *E. coli* DAH7P(Phe) synthase and *P. furiosus* DAH7P synthase

The continuous assay method follows the disappearance of the double bond of PEP, based on the absorbance at 232 nm of PEP and was modified the assay of Schoner and Herrmann.[44]

Assays for the determination of *E. coli* DAH7P synthase kinetic parameters were performed as previously described.[133] The consumption of PEP was monitored at 232 nm (extinction coefficient at 232 nm of 2.8 α 10^3 M^{-1} cm^{-1} at 25 °C and pH 6.8). Assays were initiated by the addition of the enzyme.

To determine kinetic parameters for PEP the reaction mixture contained:

(i) 2.4 mM D-T4P and 6 – 230 μM PEP

(ii) 2.4 mM L-T4P and 8 – 305 μM PEP

To determine kinetic parameters for D-T4P and L-T4P the reaction mixture contained:

(i) 112 μM PEP and 0.1 – 2.8 mM D-T4P

(ii) 126 μM PEP and 0.1 – 3.0 mM L-T4P

Assays for the determination of *P. furiosus* DAH7P synthase kinetic parameters were performed as previously described.[39] The consumption of PEP was monitored at 232 nm

(extinction coefficient at 232 nm of 2.6 α 10^3 M^{-1} cm^{-1} at 60 °C and pH 6.8). Assays were initiated by the addition of the four-carbon phosphorylated sugar.

To determine kinetic parameters for PEP the reaction mixture contained:

(i) 122 μM D-T4P and 9 – 180 μM PEP

(ii) 300 μM L-T4P and 6 – 231 μM PEP

To determine kinetic parameters for D-T4P and L-T4P reaction mixture contained:

(i) 458 μM PEP and 8 – 160 μM D-T4P

(ii) 63 μM PEP and 4 – 160 μM L-T4P

Large-scale syntheses of DAH7P, D-DLH7P, and L-DXH7P

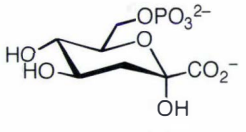

DAH7P

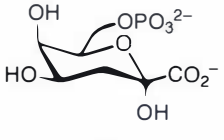

D-DLH7P

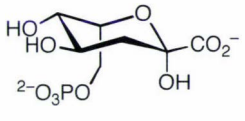

L-DLH7P

Large scale enzymatic reactions were performed using *E. coli* DAH7P(Phe) synthase in order to characterise the products DAH7P, D-DLH7P, and L-DXH7P. For the generation of DAH7P, PEP (28 mg) and D-E4P (21 mg) were dissolved in water (1 mL) and the pH was adjusted to pH 7.0. For the generation of D-DLH7P and L-DXH7P, D-T4P (21 mg)/PEP (23 mg) and L-T4P (18 mg)/PEP, respectively, were dissolved in water (1 mL) and the pH was adjusted to pH 7.0. $MnSO_4$ was added to both reaction mixtures (final concentration of 500 μM). The reactions were initiated by the addition of enzyme (0.7 mg for DAH7P; 0.5 mg for D-DLH7P and L-DXH7P) and the loss of PEP was

monitored for 48 hours at 270 nm. After 48 hours, when the loss of PEP had ceased, the enzyme was removed by ultracentrifugation. The products were then purified by anion-exchange chromatography (SouceQ™, Amersham) using ammonium bicarbonate gradient (0-1 M). The fractions, identified by the presence of DAH7P, D-DLH7P, and L-DXH7P with thiobarbituric periodate, were pooled, lyophilised, and stored in the freezer at -80 °C prior to NMR and mass spectral analysis. The following NMR data for DAH7P, D-DLH7P, and L-DXH7P are partially assigned only for H3. The spectra are shown in appendix 3.

DAH7P: m/z (-ve ESI) $(M-H)^-$ $C_7H_{10}O_{10}P_1$, cal. 287.02, found. 287.013.

^{1}H NMR (700 MHz, D_2O): α-pyranose, 1.71 (dd, *J* = 13.2, 13.2 Hz, 1H, H_{3ax}), 2.09 (dd, *J* = 13.2, 5.6 Hz, 1H, H_{3eq}), α-pyranose α 1.51 (dd, *J* = 12.2, 11.8 Hz, 1H, H_{3ax}), 2.51 (dd, *J* = 12.2, 4.4 Hz, 1H, H_{3eq}), 3.44 (dd, *J* = 9.4, 9.4 Hz, 1H, H_5), 3.75 (d, *J* = 9.4 Hz, 1H, H_6), 3.86, (m, 1H, H_4), 3.89 (m, 1H, H_7), 3.95 (dd, *J* = 11.6, 5.6 Hz, 1H, H_7) ppm.

D-DLH7P: m/z (-ve ESI) $(M-H)^-$ $C_7H_{10}O_{10}P_1$, cal. 287.0168, found 287.0123.

^{1}H NMR (700 MHz, D_2O): α-pyranose, 1.84 (dd, *J* = 12.9, 6.1Hz, 1H, H_{3eq}), 1.89 (dd, *J* = 12.9, 12.4 Hz, 1H, H_{3ax}), α-pyranose α 1.69 (dd, *J* = 12.4, 12.4 Hz, 1H, H_{3ax}), 2.27 (dd, *J* = 12.4, 4.5 Hz, 1H, H_{3eq}), α-furanose 1.99 (dd, *J* = 14.2, 2.9 Hz, 1H, H_{3eq}), 2.5 (dd, *J* = 14.2, 7.1 Hz, 1H, H_{3ax}), α-furanose 2.23 (dd, *J* = 13.6, 6.8 Hz, 1H, H_{3ax}), 2.3, (dd, *J* = 13.6, 7.1 Hz, 1H, H_{3eq}), lactones 2.4, (dd, *J* = 12.2, 7.1 Hz, 1H, H_{3ax}), 2.76 (dd, *J* = 12.2, 3.5 Hz 1H, H_{3eq}) 3.89 (m, 1H,) ppm.

L-DXH7P m/z (-ve ESI) $(M-H)^-$ $C_7H_{10}O_{10}P_1$, cal. 287.0168, found 287.0168.

^{1}H NMR (700 MHz, D_2O): α-pyranose, 1.83 (dd, *J* = 12.8, 5.1Hz, 1H, H_{3eq}), 1.87 (dd, *J* = 12.8, 12.5 Hz, 1H, H_{3ax}), α-pyranose α 1.68 (dd, *J* = 12.4, 12.4 Hz, 1H, H_{3ax}), 2.26 (d, *J* = 12.4, 5.0 Hz, 1H, H_{3eq}), α-furanose 1.97 (dd, *J* = 14.3, 3.3 Hz, 1H, H_{3eq}), 2.48 (dd, *J*

= 14.3, 7.4 Hz, 1H, H_{3ax}), α-furanose 2.21, (dd, *J* = 13.7, 6.5 Hz 1H, H_{3ax}), 2.29 (dd, *J* = 13.7, 7.0 Hz 1H, H_{3eq}) ppm.

Large-scale synthesis of KDO8P

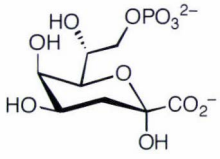

A large scale enzymatic reaction was performed by using *N. meningitidis* KDO8P synthase to generate the product KDO8P from D-A5P. D-A5P (11 mg, 47.3 μmol) was incubated in the presence of PEP (11 mg, 53.4 μmol) in water (1 mL). The pH of the reaction mixture was then adjusted to pH 7.0 and $MnSO_4$ (500 μM) was added. The reaction was initiated by the addition of the *N. meningitidis* KDO8P synthase (0.6 mg) and the loss of PEP was monitored for 8 hours at 270 nm. After 8 hours, when the loss of absorbance had ceased, the enzyme was removed by ultracentrifugation. The products were then purified using anion-exchange chromatography with ammonium bicarbonate gradient (0-1 M) and examined by using thiobarbituric acid assay to identify the presence of KDO8P. The fractions containing KDO8P that tested positive in this thiobarbituric periodate test were then pooled, lyophilised (given 15 mg), and stored in the freezer at -80 °C for NMR analysis and mass spectrum analysis. Following NMR data for KDO8P are partially assigned only for H3. The spectra are shown in appendix 3.

KDO8P: m/z (-ve ESI) $(M-H)^-$ $C_8H_{12}O_{11}P_1$, cal. 317.0274, found 317.0277.

^{1}H NMR (500 MHz, D_2O): α-pyranose, 1.74 (dd, *J* = 13.0, 5.7 Hz, 1H, H_{3eq}), 1.79 (dd, *J* = 13.0, 11.3 Hz, 1H, H_{3ax}), α-pyranose α 1.61 (dd, *J* = 12.2, 12.2 Hz, 1H, H_{3ax}), 2.2 (dd,

J = 12.2, 8.8 Hz, 1H, H_{3eq}), α-furanose 1.92 (dd, J = 14.2, 3.2 Hz, 1H, H_{3eq}), 2.45 (dd, J = 14.2, 7.2 Hz, 1H, H_{3ax}), α-furanose 2.15, (dd, J = 13.4, 7.0 Hz 1H, H_{3ax}), 2.23 (dd, J = 13.4, 7.3 Hz 1H, H_{3eq}) ppm.

7.6. Experimental for Chapter Five

Kinetic assays for D-A5P, L-X5P with *N. meningitidis* KDO8P synthase

Assays for the determination of *N. meningitidis* KDO8P synthase kinetic parameters were performed by the consumption of PEP monitored at 232 nm (extinction coefficient at 232 nm of 2.8 α 10^3 M^{-1} cm^{-1} at 30 °C and pH 7.0). Assays were initiated by the addition of the enzyme.

To determine kinetic parameters for PEP the reaction mixture contained:

(i) 80 μM D-A5P and 1 – 8 μM PEP

(ii) 300 μM L-X5P and 1 – 20 μM PEP

To determine kinetic parameters for phosphorylated monosaccharides the reaction mixture contained:

(i) 160 μM PEP and 2 – 300 μM D-A5P

(ii) 160 μM PEP and 7 – 370 μM L-X5P

The large scale syntheses of D-DAO8P and L-DGO8P

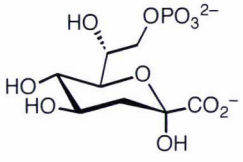

D-DAO8P

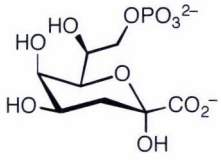

L-DGO8P

A large scale enzymatic reaction was performed by using *E. coli* DAH7P(Phe) synthase for generation of D-DAO8P from D-R5P, and *N. meningitidis* KDO8P synthase to generate the product L-DGO8P from L-X5P. Purchased D-R5P (3 mg, 11 μmol) and synthesised L-X5P (2 mg, 8.7 μmol) were incubated in the presence of PEP (3 mg, 14.5 μmol for reaction with D-R5P; 2 mg, 9.7 μmol for reaction with L-X5P) in water (1 mL). The pH of the reaction mixture was then adjusted to pH 7.0 and $MnSO_4$ (500 μM, final concentration) was added. The reaction was initiated by the addition of the *E. coli* DAH7P(Phe) synthase (2 mg) for reaction with D-R5P, and the *N. meningitidis* KDO8P synthase (0.6 mg) for reaction with L-X5P. The loss of PEP was monitored for 48 hours for L-DGO8P at 270 nm. After 48 hours, when the loss of absorbance had ceased, the enzyme was filtered off by ultracentrifugation. The products were then purified using anion-exchange chromatography with an ammonium bicarbonate gradient (0 - 1 M) and examined by using the thiobarbituric assay to identify the presence of D-DAO8P and L-DGO8P. The fractions that tested positive in this test were then pooled and lyophilised to give D-DAO8P (1.7 mg) and L-DGO8P (1.5 mg). These white solids were stored in the freezer at -80 °C prior NMR and mass spectral analysis. Following NMR data for D-DAO8P and L-DGO8P are partially assigned only for H3. The spectra are shown in appendix 3.

D-DAO8P: m/z (-ve ESI) $(M-H)^-$ $C_8H_{12}O_{11}P_1$, cal. 317.0274, found 317.0275.

^{1}H NMR (400 MHz, D_2O): α-pyranose α 1.65 (dd, *J* = 12.7, 12.4 1H, H_{3ax}), 2.0 (dd, *J* = 12.7, 5.0 Hz, 1H, H_{3eq}), α-pyranose α 1.43 (dd, *J* = 12.3, 12.3 Hz, 1H, H_{3ax}), 2.42 (dd, *J* = 12.3, 4.48 Hz, 1H, H_{3eq}) 3.44 (dd, *J* = 9.5 Hz, 1H, H_5), 3.75 (d, *J* = 10.0 Hz, 1H, H_6), 3.76, (m, 2H, H_4 and H_7), 3.85 (m, 1H, H_8), 3.99 (m, 1H, $H_{8'}$) ppm.

L-DGO8P: m/z (-ve ESI) $(M-H)^-$ $C_8H_{12}O_{11}P_1$, cal. 317.0274, found. 317.0273.

^{1}H NMR (400 MHz, D_2O): α-pyranose, 1.79 (dd, *J* = 12.3, 4.7 Hz, 1H, H_{3eq}), 1.81 (dd, *J* = 12.3, 10.5 Hz, 1H, H_{3ax}), α-pyranose α 1.61 (dd, *J* = 12.3, 12.3 Hz, 1H, H_{3ax}), 2.18 (s, 1H, H_{3eq}), α-furanose 1.9 (dd, *J* = 14.3, 3.4 Hz, 1H, H_{3eq}), 2.42 (dd, *J* = 14.3, 7.4 Hz, 1H, H_{3ax}), α-furanose 2.14, (dd, *J* = 13.5, 7.0 Hz 1H, H_{3ax}), 2.23 (dd, *J* = 13.5, 6.8 Hz 1H, H_{3eq}) ppm.

REFERENCES

1. Bentley, R. The shikimate pathway-A metabolic tree with many branches. *Biochemical and Molecular Biology* **25**, 307-384 (1990).
2. Herrmann, K. M. The Shikimate pathway. *Annual Review Plant Physiology and Plant Molecular Biology* **50**, 473-503 (1999).
3. Roberts, C. W., Roberts, F., Lyons, R. E., Kirisits, M. J., Mui, E. J., Finnerty, J., Johnson, J. J., Ferguson, D. J. P., Coggins, J. R., Krell, T., Coombs, G. H., Milhous, W. K., Kyle, D. E., Tzipori, S., Barnwell, J., Dame, J. B., Carlton, J., and McLeod, R. The shikimate pathway and its branches in apicomplexan parasites. *The Journal of Infectious Diseases* **185**, S25-S36 (2002).
4. Kim, C. G., Krischning, A., Bergon, P., Ahn, Y., Wang, J. J., Shibuya, M., and Floss, H. G. Formation of 3-amino-5-hydroxybenzoic acid, the procedure of mC_7N units in ansamycine antibiotics, by a new variant of the shikimate pathway. *Journal of the American Chemical Society* **114**, 4941-4943 (1992).
5. Jiang, S., and Singh, G. Chemical synthesis of shikimic acid and its analogues. *Tetrahedron* **54**, 4697-47531(998)
6. Fischer, H. O. L., Dangschat, G., Taube, C., Radt, F., and Stettiner, H. Quinic acid and derivatives. II. Constitution and configuration of quinic acid. *Chemistry of Berlin* **65B**, 1009-1031 (1932).
7. Fischer, H. O. L., and Dangschat, G. Quinic acid and derivatives. V. Constitution of shikimic acid. *Helvetica Chimica Acta* **17**, 1200-1207 (1934).

8. Fischer, H. O. L., and Dangschat, G. Quinic acid and derivatives. VI. Degradation of shikimic acid to aconitic acid. *Helvetica Chimica Acta* **18**, 1204-1206 (1935).

9. Fischer, H. O. L., and Dangschat, G. Quinic acid and derivatives. VIII. Configuration of shikimic acid and degradation to glucodesonic acid. (Relation of cyclic plant acids to carbohydrates.). *Helvetica Chimica Acta* **20**, 705-716 (1937).

10. Freudenberg, K., Meisenheimer, H., Lane, J. T., and Plankenhorn, E. Steric series. XXIII. Configuration of the tertiary carbon atom. *Liebigs Annual Chemistry* **543**, 162-171 (1940).

11. Karrer, P., and Link, K. P. Acetyl derivatives of quinic acid. *Helvetica Chimica Acta* **10**, 794-799 (1927).

12. Davis, B. D. Isolation of biochemically deficient mutants of bacteria by penicillin. *Journal of the American Chemical Society* **70**, 4267-4268 (1948).

13. Davis, B. D. Aromatic biosynthesis. I. The role of shikimic acid. *Journal of Biological Chemistry* **191**, 315-325 (1951).

14. Davis, B. D. Aromatic biosynthesis. IV. Preferential conversion, in complete-blocked mutants, of a common precursor of several metabolites. *Journal of Bacteriology* **64**, 729-747 (1952).

15. Weiss, U., and Mingioli, E. S. Aromatic biosynthesis. XV. The isolation and identification of shikimic acid 5-phosphate. *Journal of the American Chemical Society* **78**, 2894-2898 (1956).

16. Salamon, I. I., and Davis, B. D. Aromatic biosynthesis. IX. The isolation of a precursor of shikimic acid. *Journal of the American Chemical Society* **75**, 5567-5571 (1953).

17. Davis, B. D., and Mingioli, E. S. Aromatic biosynthesis. VII. Accumulation of two derivatives of shikimic acid by bacterial mutants. *Journal of Bacteriology* **66**, 129-136 (1953).

18. Levin, J. G., and Sprinson, D. B. Enzymic formation and isolation of 3-enolpyruvyl shikimate 5-phosphate. *Journal of Biological Chemistry* **239**, 1142-1150 (1964).

19. Gibson, F. Chorismic acid; Purification and some chemical and physical studies. *Biochemical Journal* **90**, 256-261 (1964).

20. Srinivasan, P. R., Katagiri, M., and Sprinson, D. B. Conversion of pyruvic acid phosphate and D-erythrose 4-phosphate to 5-dehydroquinic acid. *Journal of Biological Chemistry* **234**, 713-715 (1959).

21. Srinivasan, P. R., and Sprinson, D. B. 2-Keto-3-deoxy-D-*arabo*-heptonic acid 7-phosphate synthetase. *Journal of Biological Chemistry* **234**, 716-722 (1959).

22. Roberts, F., Roberts, C. W., Johnson, J. J., Kyle, D. E., Krell, T., Coggins, J. R., Coombs, G. H., Milhous, W. K., Tzipori, S., Ferguson, D. J. P., Chakrabarti, D., and McLeod, R. Evidence for the shikimate pathway in apicomplexan parasites. *Nature* **393**, 801-805 (1998).

23. Keeling, P. J., Palmer, J. D., Donald, R. H. K., Roos, D. S., Waller, R. F., and McFadded, G. I. Shikimate pathway in apicomplexan parasites. *Nature* **397**, 219-220 (1999).

24. Roberts, C. W., Finnerty, J., Johnson, J. J., Roberts, F., Kyle, D. E., Krell, T., Coggins, J. R., Coombs, G. H., Milhous, W. K., Tzipori, S., Ferguson, D. J. P., Chakrabarti, D., and McLeod, R. Shikimate pathway in apicomplexan parasites. Reply. *Nature* **397**, 220 (1999).

25. Amrhein, N., Deus, B., Gehrke, P., and Steinrucken, H. C. The site of the inhibition of the shikimate pathway by glyphosate. II. Interference of glyphosate with chorismate formation *in vivo* and *in vitro*. *Plant Physiology* **66**, 830-834 (1980).

26. Rogers, S. G. Biotechnology and the soybean. *The American Journal of Clinical Nutrition* **68 (6 Ssuppl)**, 1330s-1332s (1998).

27. Doy, C. H., and Brown, K. D. Control of aromatic biosynthesis; The multiplicity of 7-phospho-2-oxo-3-deoxy-D-*arabino*-heptonate D-erythrose-4-phosphate-lyase (pyruvate-phosphorylating) in *Escherichia coli* W. *Biochemica et Biophysica Acta* **104**, 377-389 (1965).

28. Park, O. K., and Bauerle, R. Metal-catalyzed oxidation of phenylalanine-sensitive 3-deoxy-D-*arainose*-heptulosonate-7-phosphate synthase from *Escherichia coli*: Inactivation and destabilization by oxidation of active-site cysteines. *Journal of Bacteriology* **181**, 1636-1642 (1999).

29. Shumilin, I. A., Kretsinger, R. H., and Bauerle, R. H. Crystal structure of phenylalanine-regulated 3-deoxy-D-*arabino*-heptulosonate 7-phosphate synthase from *Escherichia coli*. *Structure* **7**, 865-875 (1999).

30. Smith, L. C., Ravel, J. M., Lax, S. R., and Shive, W. The control of 3-deoxy-D-*arabino*-heptulosonic acid 7-phosphate synthesis by phenylalanine and tyrosine. *The Journal of Biological Chemistry* **237**, 2566-3570 (1962).

31. Brown, K. D., and Doy, C. H. End-product regulation of the general aromatic pathway in *Escherichia coli* W. *Biochimica et Biophysica Acta* **77**, 170-172 (1963).

32. Jensen, R. A., and Nasser, D. S. Comparative regulation of isoenzymic 3-deoxy-D-*arabino*-heptulosonate 7-phosphate synthase in microorganisms. *Journal of Bacteriology* **95**, 188-196 (1968).

33. Shultz, J., Hermodson, M. A., Garner, C. C., and Herrmann, K. M. The nucleotide sequence of the *aro*F gene of *Escherichia coli* and the amino acid sequence of the encoded protein, the tyrosine-sensitive 3-deoxy-D-*arabino*-hoptulosonate 7-phosphate synthase. *The Journal of Biological Chemistry* **259**, 9655-9661 (1984).

34. Abell, C. Enzymology and molecular biology of the shikimate pathway. *Comprehensive Natural Products Chemistry* **1**, 573-607 (1999).

35. Ogino, T., Garner, C., Markley, J. L., and Herrmann, K. M. Biosynthesis of aromatic compounds: carbon-13 NMR spectroscopy of whole *Escherichia coli*. *Journal of Biological Chemistry* **79**, 5828-5832 (1982).

36. Tribe, D. E., Camakaris, H., and Pittard, J. Constitutive and repressible enzymes of the common pathway of aromatic biosynthesis in *Escherichia coli* K-12: Regulation of enzyme synthesis at different growth rates. *Journal of Bacteriology*, 1085-1097 (1976).

37. Weaver, L. M., and Herrmann, K. M. Cloning of an *aro*F allel encoding a tyrosine-insensitive 3-deoxy-D-*arabino*-heptulosonate 7-phosphate synthase. *Journal of Bacteriology* **172**, 6581-6584 (1990).

38. Hartmann, M., Schneider, T. R., Pfeil, A., Heinrich, G., Lipscomb, W. N., and Braus, G. H. Evolution of feedback-inhibited $(\alpha/\alpha)_8$ barrel isoemzymes by gene duplication and a single mutation. *Proceeding of the National Academy Sciences in USA* **100**, 862-867 (2003).

39. Schofield, L. R., Patchett, M. L., and Parker, E. J. Expression, purification, and characterization of 3-deoxy-D-*arabino*-heptulosonate 7-phosphate synthase from *Pyroccos furiosus*. *Protein Expression and Purification* **34**, 17-27 (2004).

40. Staub, M., and Dénes, G. Purification and properties of the 3-deoxy-D-*arabino*-heptulosonate 7-phosphate synthase(phenylalanine-sensitive) of *Escherichia coli* K-12. I. Purification of enzyme and some of its catalytic properties. *Biochimica et Biophysica Acta* **178**, 588-598 (1969).

41. Staub, M., and Dénes, G. Purification and properties of the 3-deoxy-D-*arabino*-heptulosonate 7-phosphate synthase(phenylalanine-sensitive) of *Escherichia coli* K-12. II. Inhibition of activity of the enzyme with phenylalanine and funtional group-specific reagents. *Biochimica et Biophysica Acta* **178**, 599-608 (1969).

42. Camakaris, J., and Pittard, J. Purification and properties of 3-deoxy-D-*arabino*-heptulosonic acid 7-phosphate synthetase(trp) from *Escherichia coli*. *Journal of Bacteriology*, 590-597 (1974).

43. Simpson, R., J., and Davidson, B. E. Studies on 3-deoxy-D-arabinoheptulosonate-7-phosphate synthetase(phe) from *Escherichia coli* K12. 2. Kinetic properties. *European Journal of Biochemistry*, 501-507 (1976).

44. Schoner, R., and Herrmann, K. M. 3-Deoxy-D-*arabino*-heptulosonate 7-phosphate synthase. Purification, properties, and kinetics of the tyrosine-sensitive isoenzyme from *Escherichia coli*. *The Journal of Biological Chemistry* **251**, 5440-5447 (1976).

45. Jensen, R. A., and Nester, E. W. Regulatory enzymes of aromatic amino acid biosynthesis in *Bacillus subtilis*. I. Purification and properties of 3-deoxy-D-arabino-heptulosonate 7-phosphate synthase. *Journal of Biological Chemistry* **241**, 3365-3372 (1966).

46. Stephens, C. M., and Bauerle, R. Analysis of the metal requirement of 3-deoxy-D-*arabino*-heptulosonate 7-phosphate synthase from *Escherichia coli*. *The Journal of Biological Chemistry* **266**, 20810-20817 (1991).

47. Wu, J., Sheflyan, G. Y., and Woodard, R. W. *Bacillus subtilis* 3-deoxy-D-*arabino*-heptulosonate 7-phosphate synthase revisited: Resolution of two long-standing enigma. *Biochemical Journal* **390**, 583-590 (2005).

48. Webby, C. J., Patchett, M. L., and Parker, E. J. Characterization of a recombinant type II 3-deoxy-D-*arabino*-heptulosonate-7-phosphate synthase from *Helicobacter pylori*. *Biochemical Journal* **390**, 223-230 (2005).

49. Onderka, D. K., and Floss, H. G. Steric course of the chorismate synthetase reaction and the 3-deoxy-D-*arabino*-heptulosonate 7-phosphate (DAHP) synthetase reaction. *Journal of the American Chemical Society* **91**, 5894-5896 (1969).

50. Floss, H. G., Onderka, D. K., and Carroll, M. Stereochemistry of the 3-deoxy-D-*arabino*-heptulosonate 7-phosphate synthase reaction and the chorismate synthase reaction. *The Journal of Biological Chemistry* **247**, 736-744 (1972).

51. DeLeo, A. B., and Sprinson, D. B. Mechanism of 3-deoxy-D-*arabino*-heptulosonate 7-phosphate (DAHP) synthetase. *Biochemical and Biophysical Research Communications* **32**, 873-877 (1968).

52. Nagano, H., and Zalkin, H. Tyrosine-inhibited 3-deoxy-D-*arabino*-heptulosonate 7-phosphate synthetase. Properties of the partially purified enzyme from *Salmonella typhimurium*. *Archives of Biochemistry and Biophysics* **138**, 58-65 (1970).

53. DeLeo, A. B., Dayan, J., and Sprinson, D. B. Purification and kinetics of tyrosine-sensitive 3-deoxy-D-*arabino*-heptulosonic acid 7-phosphate synthase from *Salmonella*. *The Journal of Biological Chemistry* **248**, 2344-2353 (1973).

54. Nimmo, G. A., and Coggins, J. R. The purification and molecular properties of the trypthphan-sensitive 3-deoxy-D-*arabino*-heptulosonate 7-phosphate synthase from *Neurospora crassa*. *Biochemical Journal* **197**, 427-436 (1981).

55. Paravicini, G., Schmidheini, T., and Braus, G. Purification and properties of the 3-deoxy-D-*arabino*-heptulosonate-7-phosphate synthase (phenylalanine-inhibitable) of *Saccharomyces cerevisiae*. *European Journal of Biochemistry* **186**, 361-366 (1989).

56. Wagner, T., Shumilin, I. A., Bauerle, R., and Kretsinger, R. H. Structure of 3-deoxy-D-*arabino*-heptulosonate 7-phosphate synthase from *Escherichia coli*: Comparison of the Mn^{2+} 2-phosphoglycolate and the Pb^{2+} 2-phosphoenolpyruvate complexes and implication for catalysis. *Journal of Molecular Biology* **301**, 389-399 (2000).

57. Shumilin, I. A., Bauerle, R. H., Wu, J., Woodard, R. W., and Kretsinger, R. H. Crystal structure of the reaction complex of 3-deoxy-D-arabino-heptulosonate-7-phosphate synthase from *Thermotoga maritima* refines the catalytic mechanism and indicates a new mechanism of allosteric regulation. *Journal of Molecular Biology* **341**, 455-466 (2004).

58. Ray, J. M., Yanofsky, C., and Bauerle, R. Mutational analysis of the catalytic and feedback site of the tryptophan-sensitive 3-deoxy-D-*arabino*-heptulosonate 7-phosphate synthase of *Escherichia coli*. *Journal of Bacteriology* **170**, 5500-5506 (1988).

59. Stephens, C. M., and Bauerle, R. Essential cysteins in 3-deoxy-D-*arabino*-heptulosonate-7-phosphate synthase from *Escherichia coli*. *The Journal of Biological Chemistry* **267**, 5762-5767 (1992).

60. Sundaram, A. K., Howe, D. L., Sheflyan, G. Y., and Woodard, R. D. Probing the potential metal binding site in *Escherichia coli* 3-deoxy-D-*arabino*-heptulosonate 7-phosphate synthase (phenylalanine-sensitive). *FEBS Letters* **441**, 195-199 (1998).

61. Huisman, O. C., and Kosuge, T. Regulation of aromatic amino acid biosynthesis in higher plants. *The Journal of Biological Chemistry* **249**, 6842-6848 (1974).

62. Subramaniam, P. S., Xie, G., Xia, T., and Jesen, R. A. Subsrate ambiguity of 3-deoxy-D-*manno*-octulosonate 8-phosphate synthase from *Neisseria gonorrhoeae* in the context of its menbership in a protein family containing a subset of 3-deoxy-D-*arabino*-heptulosonate 7-phosphate synthase. *Journal of Bacteriology* **180**, 119-127 (1998).

63. Howe, D. L., Duewel, H. S., and Woodard, R. W. Histidine 268 in 3-deoxy-D-*arabino*-octulosonic acid 7-phosphate synthase plays the same role as histidine 202 in 3-deoxy-D-*manno*-octulosonic acid 8-phosphate synthase. *The Journal of Biological Chemistry* **275**, 40258-40265 (2000).

64. Hedstrom, L., and Abeles, R. 3-Deoxy-D-*manno*-octulosonate-8-phosphate synthase catalyses the carbon-oxygen bond cleavage of phosphenolpyruvate. *Biochemistry and Biophysics of Research Communications* **157**, 816-820 (1988).

65. Sheflyan, Y. G., Duewel, H. S., Chen, G., and Woodard, R. W. Identification of essential histidine residues in 3-deoxy-D-*manno*-octulosonic acid 8-phosphate synthase: Analysis by chemical modification with diethyl pyrocarbonate and site-directed mutagenesis. *Biochemistry* **38**, 14320-14329 (1999).

66. Walker, G. E., Dunbar, B., Hunter, I. S., Nimmo, H. G., and Coggins, J. R. Evidence for a novel class of microbial 3-deoxy-D-*arabino*-heptulosonate synthase in *Streptomyces coelicolor* A3(2), *Streptomyces rimosus*, and *Neurospora crassa*. *Microbiology* **142**, 1973-1982 (1996).

67. Gosset, G., Bonner, C. A., Jensen R. A. Microbuial origine of plant-type 2-keto-3-deoxy-D-*arabino*-heptulosonate 7-phosphate synthase, examplified by the chorismate- and tryptophan-regulated enzyme from *Xanthomonas campestris*. *Journal of Bacteriology* **183**, 4061-4070 (2001).

68. Jensen, R. A., Xie, G., Calhoun, D. H., and Bonner, C. A. The correct phylogenetic relationship of KdsA (3-deoxy-D-*manno*-octulosonate 8-phosphate synthase) with one of two independently evolved classes of AroA (3-deoxy-D-*arabino*-heptulosonate-7-phosphate synthase). *Journal of Molecular Evolution* **54**, 416-423 (2002).

69. Silakowski, B., Kunze, B., and Müller, R. *Stigmatella aurantiaca* Sg a15 carries genes encoding type I and type II 3-deoxy-D-*arabino*-heptulosonate-7-phosphate synthases: Involvement of a type II synthase in aurachin biosynthesis. *Archives of Microbiology* **173**, 403-411 (2000).

70. Webby, C. J., Lott, J. S., Baker, H. M., Baker, E. N., and Parker, E. J. Crystallization and preliminary X-ray crystallographic analysis of 3-deoxy-D-*arabino*-heptulosonate-7-phosphate synthase from *Mycobacterium tuberculosis*. *Acta Crystallographica Section F* **F61**, 403-406 (2005).

71. Shumilin, I. A., Zhao, C., Bauerle, R. H. and Kretsinger R. H. Allosteric inhibition of 3-deoxy-D-*arabino*-heptulosonate-7-phosphate synthase alters the coordination of both substrates. *Journal of Molecular Biology* **320**, 1147-1156 (2002).

72. Shumilin, I. A., Ronald, B., and Kretsinger, R. H. The high-resonance structure of 3-deoxy-D-*arabino*-heptulosonate-7-phosphate synthase reveals a twist in the plane of bound phosphoenolpyruvate. *Biochemistry* **42**, 3766-3776 (2003).

73. König, V., Pfeil, A., Braus, G. H., and Schneider, T. R. Substrate and metal complexes of 3-deoxy-D-*arabino*-heptulosonate-7-phosphate synthase from *Saccharomyces cerevisiae* provide new insights into the catalytic mechanism. *Journal of Molecular Biology* **337**, 675-690 (2004).

74. Schofield, L. R., Anderson, B. F., Patchett, M. L., Norris, G. E., Jameson, G. B., and Parker, E. J. Substrate ambiguity and crystal structure of *Pyrococcus furiosus* DAH7P synthase-An ancestral 3-deoxyald-2-ulosonate-phosphate synthase? *Biochemistry* **44**, 11950-11962 (2005).

75. McCandliss, R. J., Poling, M. D., and Herrmann, K. M. 3-Deoxy-D-*arabino*-heptulosonate 7-phosphate synthase. Purification and molecular characterization of the phenylalanine-sensitive isozyme from *Escherichia coli*. *Journal of Biological Chemistry* **253**, 4259-4265 (1978).

76. Ray, J. M., and Bauerle, R. Purification and properties of tryptophan-sensitive 3-deoxy-D-*arabino*-heptulosonate 7-phosphate synthase from *Escherichia coli*. *Journal of Bacteriology* **173**, 1894-1901 (1991).

77. Shumilin, I. A., Krestinger, R. H., and Bauerle, R. Purification, crystallization, and preliminary crystallographic analysis of 3-deoxy-D-*arabino*-heptulosonate-7-phosphate synthase from *Escherichia coli*. *PROTEINS: Structure, Funtion, and Genetics* **24**, 404-406 (1996).

78. Schnappauf, G., Hartmann, M., Künzler, M., and Braus, G. H. The two 3-deoxy-D-*arabino*-heptulosonate-7-phosphate synthase isoenzymes from *Saccharomyces cerevisiae* show different kinetic modes of inhibition. *Archives of Microbiology* **169**, 517-524 (1998).

79. Sheflyan, Y. G., Howe, D. L., Wilson, T. L., and Woodard, R. W. Enzymatic synthesis of 3-deoxy-D-*manno*-octulosonate 8-phosphate, 3-deoxy-D-*altro*-octulosonate 8-phosphate, and 3.5-dideoxy-D-*gluco*(*manno*)-octulosonate 8-phosphate by 3-deoxy-D-*arabino*-heptulosonate 7-phosphate synthase. *Journal of the American Chemical Society* **120**, 11027-11032 (1998).

80. Wu, J., Howe, D. L., and Woodard, R. W. *Thermotoga maritima* 3-deoxy-D-*arabino*-heptulosonate 7-phosphate (DAHP) synthase: The ancestal eubacterial DAHP synthase? *The Journal of Biological Chemistry* **278**, 27525-27531 (2003).

81. Duewel, H. S., Sheflyan, G. Y., and Woodard, R. W. Functional and biochemical characterization of a recombinant 3-deoxy-D-*manno*-octulosonic acid 8-phosphate synthase from the hyperthermophilic bacterium *Aquifex aeolicus*. *Biochemical and Biophysical Research Communications* **263**, 346-351 (1999).

82. Duewel, H. S., and Woodard, R. W. A metal bridge between two enzyme families. *The Journal of Biological Chemistry* **275**, 22824-22831 (2000).

83. Ray, P. H. Purification and characterization of 3-deoxy-D-*manno*-octulosonate 8-phosphate synthase from *Eschericia coli*. *Journal of Bacteriology* **141**, 635-644 (1980).

84. Sheflyan, Y. G., Sundaram, A. K., Taylor, W. P., and Woodard, R. W. Substrate ambiguity of 3-deoxy-D-*manno*-octulosonate 8-phosphate synthase from *Neisseria gonorrhoeae* revisited. *Journal of Bacteriology* **182**, 5005-5008 (2000).

85. Howe, D. L., Sundaram, A. K., Wu, J., Gatti, D. L., and Woodard, R. W. Mechanistic insight into 3-deoxy-D-*manno*-octulosonate-8-phosphate synthase and 3-deoxy-D-*arabino*-heptulosonate-7-phosphate synthase utilizing phosphorylated monosaccharide analogues. *Biochemistry* **42**, 4843-4854 (2003).

86. Birck, M. R., and Woodard, R. W. *Aquifex aeolicus* 3-deoxy-D-*manno*-2-octulosonic acid-8-phosphate synthase: A new class of KDO 8-P synthase. *Journal of Molecular Evolution* **52**, 205-214 (2001).

87. Parker, E. J. Mechanistic studies of shikimate pathway enzymes. PhD. Thesis. Cambridge University. (1996).

88. Pilch, P. F., and Somerville, R. L. Fluorine-containing analogues of intermediates in the shikimate pathway. *Biochemistry* **15**, 5315-5320 (1976).

89. Le Marechal, P., Froussios, C., Level, M., and Azerad, R. The interaction of phosphonate and homophosphonate analogues of 3-deoxy-D-*arabino*-heptulosonate 7-phosphate with 3-dehydroquinate synthetase from *Escherichia coli*. *Biochemical and Biophysical Research Communications* **92**, 1104-1109 (1980).

90. Pietersma, A. L. unpublished result.

91. Raetz, C. R., and Whitfield, C. Lipopolysaccharide endotoxins. *Annual Review Biochemistry* **71**, 635-700 (2002).

92. Waldstaetten, P., Christian, R., Schulz, G., Unger, F. M., Kosma, P., Kratky, C., and Paulsen, H. Sandoz-Forschungsinst. Synthesis of oligosaccharides containing 3-deoxy-D-*manno*-2-octulopyranosylono (KDO) residues. *Bacterial Lipopolysaccharides* **ACS Symposium 231**, 121-140 (1983).

93. Raetz, C. R. Biochemistry of endotoxins. *Annual Review Biochemistry*, 129-170 (1990).

94. Ray, P. H., Kelsey, J. E., Bigham, E. C., Benedict, C. D., and Miller, T. A. Synthesis and use of 3-deoxy-D-*manno*-octulosonate 8-phosphate (KDO) in *Escherichia coli*. *Bacterial Lipopolysaccharides* **ACS Symposium 231**, 141-169 (1983).

95. Unger, F. M. The chemistry and biological significance of 3-deoxy-D-*manno*-2-octulosonic acid (KDO). *Advanced Carbohydrate Chemisry and Biochemistry* **38**, 323-388 (1981).

96. Baasov, T., and Jakob, A. Anomeric specificity of 3-deoxy-D-*manno*-2-octulosonate 8-phosphate phosphatase from *Escherichia coli*. *Journal of the American Chemical Society* **112**, 4972-4974 (1990).

97. Ray, P. H., and Benedict, C. D. Purification and characterization of a specific 3-deoxy-D-*manno*-octulosonate 8-phosphate phosphatase from *Escherichia coli* B. *Journal of Bacteriology* **142**, 60-68 (1980).

98. Inouye, M. Lipoprotein of the outer membrane of *Escherichia coli*. *Biomembranes* **10**, 141-208 (1979).

99. Krosky, D., Alm, R., Berg, M., Carmel, G., Tummino, P. J., Xu, B., and Yang, W. *Helicobacter pylori* 3-deoxy-D-*manno*-octulosonate-8phosphate (KDO8P) synthase is a zinc-metalloenzyme. *Biochimica et Biophysica Acta* **1594**, 297-306 (2002).

100. Shulami, S., Yaniv, O., Rabkin, E., Shoham, Y., and Baasov, T. Cloning, expression, and biochemical characterization of 3-deoxy-D-*manno*-2-octulosonate-8-phosphate (KDO8P) synthase from the hyperthermophilic bacterium *Aquifex pyrophilus*. *Extremophiles* **7**, 471-481 (2003).

101. Baasov, T., Sheffer-Dee-Noor, S., Kohen, A., Jakov, A., and Belakhov, V. Catalytic mechanism of 3-deoxy-D-*manno*-2-octulosonate-8-phosphate synthase: The use of synthetic analogues to probe the structure of the putative reaction intermediate. *European Journal of Biochemistry* **217**, 991-999 (1993).

102. Hedstrom, L., and Abeles, R. 3-Deoxy-D-*manno*-octulosonate-8-phosphate synthase catalyses the carbon-oxygen bond cleavage of phosphenolpyruvate. *Biochemistry and Biophysics of Research Communications* **157**, 816-820 (1988).

103. Dotson, G. D., Dua, R. K., Clemens, J. C., Woosten, E. W., and Woodard, R. W. Overproduction and one-step purification of *Escherichia coli* 3-deoxy-D-*manno*-octulosonic acid 8-phosphate synthase and oxygen transfer studies during catalysis using isotopic-shifted heteronuclear NMR. *The Journal of Biological Chemistry* **270**, 13698-13705 (1995).

104. Du, S., Plat, D., Belakhov, V., and Baasov, T. First nonenzymatic synthesis of Kdo8P through a mechanism similar to that suggested for the enzyme Kdo8P synthase. *Journal of Organic Chemistry* **62**, 794-804 (1997).

105. Du, S., Tsipori, H., and Baasov, T. Synthesis and evaluation of putative oxocarbenium intermediate mimic in the KDO0P synthase-catalyzed reaction as a tool for the design of potent inhibitors for lipopolysaccharide biosynthesis. *Bioorganic and Medicinal Chemistry Letters* **7**, 2469-2472 (1997).

106. Baasov, T., and Belakhov, V. Towards a new class of synthetic antibacterials acting on lipopolysaccharide biosynthesis. *Drug Development Research* **50**, 416-424 (2000).

107. Kohen, A., Berkovich, R., Belakhov, V., and Baasov, T. Stereochemistry of the KDO8P synthase. An efficient synthesis of the 3-fluoro analogues of KDO8P. *Bioorganic and Medicinal Chemistry Letters* **3**, 1577-1582 (1993).

108. Dotson, G. D., Nanjappan, P., Reily, M. D., and Woodard, R. W. Stereochemistry of 3-deoxyoctulosonate 8-phosphate synthase. *Biochemistry* **32**, 12392-12397 (1993).

109. Sheffer-Dee-Noor, S., and Baasov, T. Insight into the catalytic mechanism of KDO8P synthase: Sythesis and evalution of the isosteric phosphonate mimic of the putative cyclic intermediate. *Bioorganic and Medicinal Chemistry Letters* **3**, 1583-1588 (1993a).

110. Kohen, A., Belakhov, V., and Baasov, T. Towards the synthesis of the putative reaction intermediate in the Kdo8P synthase-catalysed reaction: Synthesis and evaluation of 3-deoxy-D-*manno*-2-octulosonate-2-phosphate. *Tetrahedron Letters* **35**, 3179-3182 (1994).

111. Kohen, A., Jakob, A., and Baasov, T. Mechanistic studies of 3-deoxy-D-*manno*-2-octulosonate-8-phosphate synthase from *Escherichia coli*. *FEBS Letters* **208**, 443-449 (1992).

112. Baasov, T., and Kohen, A. Synthesis, inhibition, and acid-catalyzed hydrolysis studies of model compounds of the proposed intermediate in the Kdo8P-synthase-catalyzed reaction. *Journal of the American Chemical Society* **117**, 6165-6174 (1995).

113. Baasov, T., Tkacz, R., Scheffer-Dee-Noor, S., and Belakhov, V. Catalytic mechanism of 3-deoxy-D-*manno*-2-octulosonate-8-phosphate synthase. *Current Organic Chemistry* **5**, 127-138 (2001).

114. Xu, X., Wang, J., Grison, C., Petek, S., Coutrot, P., Birck, M. R., Woodard, R. W., and Gatti, D. Sructure-based design of novel inhibitors of 3-deoxy-D-*manno*-octulosonate 8-phosphate synthase. *Drug Design and Discovery* **18**, 91-99 (2003).

115. Du, S., Faiger, H., Belakhov, V., and Baasov, T. Towards the development of novel antibiotics: Synthesis and evaluation of a mechanism-based inhibitor of Kdo8P synthase. *Bioorganic and Medicinal Chemistry* **7**, 2671-2682 (1999).

116. Belakhov, V., Dovgolevsky, E., Rabkin, E., Shulami, S., Shoham, Y., and Baasov, T. Synthesis and evaluation of a mechanism-based inhibitor of KDO8P synthase. *Carbohydrate Research* **339**, 385-392 (2004).

117. Benenson, Y., Belakhov, V., and Baasov, T. 1-(Dihydroxyphosphynyl)vinyl phosphate: The phosphonate analogue of phosphoenolpyruvate is a pH-dependent substrate of KDO8P synthase. *Bioorganic and Medicinal Chemistry Letters* **6**, 2901-2906 (1996).

118. Sheffer-Dee-Noor, S., and Baasov, T. A combined chemical-enzymic synthesis of a new phosphoamidate analogue of phosphoenolpyruvate. *Bioorganic and Medicinal Chemistry Letters* **3**, 1615-1618 (1993b).

119. Liang, P. H., Lewis, J., Anderson, K. S., Kohen, A., D'Souza, W. F., Benenson, Y., and Baasov, T. Catalytic mechanism of Kdo8P synthase: Transient kinetic studies and evaluation of a putative reaction intermediate. *Biochemistry* **37**, 16390-16399 (1998).

120. Li, Z., Sau, A. K., Shen, S., Whitehouse, C., Baasov, T., and Anderson, K. S. A snapshot of enzyme catalysis using electrospray ionization mass spectrometry. *Journal of the American Chemical Society* **125**, 9938-9939 (2003).

121. Radaev, S., Dastidar, P., Patel, M., Woodard, R. W., and Gatti, D. L. Structure and mechanism of 3-deoxy-D-*manno*-octulosonate-8-phosphate synthase. *The Journal of Biological Chemistry* **275**, 9476-9484 (2000).

122. Wagner, T., Kretsinger, R. H., Bauerle, R., and Tolbert, W. D. 3-Deoxy-D-*manno*-octulsonate-8-phosphate synthase from *Escherichia coli*. Model of binding of phosphoenolpyruvate and D-arabinose-5-phosphate. *Journal of Molecular Biology* **301**, 233-238 (2000).

123. Asojo, O., Friedman, J., Adir, N., Belakhov, V., Shoham, Y., and Baasov, T. Crystal structures of KDOP synthase in its binary complexes with the substrate phosphoenolpyruvate and with a mechanism-based inhbitor. *Biochemistry* **40**, 6326-6334 (2001).

124. Duewel, H. S., Radaev, S., Wang, J., Woodard, R. W., and Gatti, D. L. Substrate and metal complexes of 3-deoxy-D-*manno*-octulosonate-8-phosphate synthase from *Aquifex aeolicus* at 1.91Å resolution. *The Journal of Biological Chemistry* **276**, 8393-8402 (2001).

125. Wang, J., Duewel, H. S., Woodard, R. W., and Gatti, D. L. Stuructures of *Aquifex aeolicus* KDO8P Synthase in complex with R5P and PEP, and with a bisubstrate inhibitor: Role of active site water in catalysis. *Biochemistry* **40**, 15676-15683 (2001).

126. Shulami, S., Furdui, C., Adir, N., Shoham, Y., Anderson, K. S., and Baasov, T. A reciprotocal single mutation affects the metal requirement of 3-deoxy-D-*manno*-2-octulosonate-8-phosphate (KDO8P) synthases from *Aquifex pyrophilus* and *Escherichia coli*. *The Journal of Biological Chemistry* **279**, 45110-45120 (2004).

127. Li, J., Wu, J., Fleischhacker, A. S., and Woodard, R. W. Conversion of *Aquifex aeolocus* 3-deoxy-D-*manno*-octulosonate 8-phosphate synthase, a metalloenzyme, into a nonmetalloenzyme. *Journal of the American Chemical Society* **126**, 7448-7449 (2004).

128. Cochrane, F. C. unpublised result.

129. Wang, J., Duewel, H. S., Stuckey, J. A., Woodard, R. W., and Gatti, D. L. Function of His185 in *Aquifex aerolicus* 3-deoxy-D-*manno*-octulosonate 8-phosphate synthase. *Journal of Molecular Biology* **324**, 205-214 (2002).

130. Williamson, R. M., Pietersma, A. L., Jameson, G. B., and Parker, E. J. Stereospecific deuteration of 2-deoxy-erythrose 4-phosphate using 3-deoxy-D-*arabino*-heptulosonate 7-phosphate synthase. *Bioorganic and Medicinal Chemistry Letters* **15**, 2339-2342 (2005).

131. Simpson, F. J., Perlin, A. S., and Steben, A. S. Erythrose 4-phosphate. *Methods in Enzymology* **9**, 35-38 (1966).

132. Le Marechal, P., Froussios, C., Level, M., and Azerad, R. Enzymetic properties of phosphonic analogues of D-erythrose 4-phosphate. *Biochemical and Biophysical Research Communications* **92**, 1097-1103 (1980).

133. Parker, E. J., Bulloch, E. M. M., Jameson, G. B., and Abell, C. Substrate deactivation of phenylalanine-sensitive 3-deoxy-D-*arabino*-heptulosonate 7-phosphate synthase by erythrose 4-phosphate. *Biochemistry* **40**, 14821-14828 (2001).

134. Blackmore, P. F., Williams, J. F., and MacLeod, J. K. Dimerization of erythrose 4-phosphate. *FEBS Letters* **64**, 222-226 (1976).

135. Duke, C. D., and MacLeod, J. K. Nuclear magnetic resonance studies of D-erythrose 4-phosphate in aqueous solution. Structures of the major contributing monomeric and dimeric forms. *Carbohydrate Research* **95**, 1-26 (1981).

136. Reimer, L. M., Conley, D. L., Pompliano, D. L., and Frost, J. W. Construction of an enzyme-targeted organo-phosphonate using immobilized enzyme and whole-cell synthesis. *Journal of the American Chemical Society* **108**, 8010-8015 (1986).

137. Ballou, C. E., Fischer, H. O. L., and MacDonald, D. L. The synthesis and properties of D-erythrose 4-phosphate. *Journal of the American Chemical Society* **77**, 5967-5970 (1955).

138. Sieben, A. S., Perlin, A. S., and Simpson, F. J. An improved preparative method for D-erythrose 4-phosphate. *Canadian Journal of Biochemistry* **44**, 663-669 (1966).

139. Aminoff, D. Mothods for the quantitative estimation of *N*-acetylneuraminic acid and their application to hydrolysates of sialomucoids. *Biochemical Journal* **81**, 384-392 (1961).

140. Knowles, J. R. Mechanistic ingenuity in enzyme catalysis: Dehydroquinate synthase. *Aldrichimica Acta* **22**, 59-66 (1989).

141. Pfaff, K. P., Paust, J., and Hartmann, H. Preparation of sugar ketals. Patent. (1987).

142. Dess, D. B., and Martin, J. C. A useful 12-I-5 triacetoxy periodinane (the Dess-Martin Periodinane) for the selective oxidation of primary or secondary alcohols and a variety of related 12-I-5 species. *Journal of the American Chemical Society* **113**, 7277-7287 (1991).

143. Cloux, R., and Schlosser, M. Selective syntheses with organometallics. Part XI. An efficient synthesis of α, α-unsaturated aldehydes by a four-carbon unit extension of Grignard reagents. *Helvetica Chimica Acta* **67**, 1470-1474 (1984).

144. Bouzide, A., and Sauve, G. Highly selective silver(I) oxide mediated monoprotection of symmetrical diols. *Tetrahedron Letters* **38**, 5945-5948 (1997).

145. Bouzide, A., LeBerre, N., and Sauve, G. Silver(I) oxide-mediated facile and practical sulfonylation of alcohols. *Tetrahedron Letters* **42**, 8781-8783 (2001).

146. Bouzide, A., and Sauve, G. Silver(I) oxide mediated highly selective monotosylation of symmetrical diols. Application to the synthesis of polysubstituted cyclic ethers. *Organic Letters* **4**, 2329-2332 (2002).

147. Cunningham Jr, A. F., and Kundig, E. P. An efficient synthesis of both enantiomers of *trans*-1,2-cyclopentanediol and their conversion to two novel bidentate phosphite and fluorophosphinite ligands. *Journal of Organic Chemistry* **53**, 1823-1825 (1988).

148. Nemoto, H., Takamatsu, S., and Yamamoto, Y. An improved and practical method for the synthesis of optical active diethyl tartrate dibenzyl ether. *Journal of Organic Chemistry* **56**, 1321-1322 (1991).

149. Araki, K., Suenaga, K., Sengoku, T., and Uemura, D. Total synthesis of attenols A and B. *Tetrahedron* **58**, 1983-1995 (2002).

150. Chan, T. H., Brook, M. A., and Chaly, T. A simple prodedure for the acetalization of carbonyl compounds. *Synthesis* **3**, 203-205 (1983).

151. Levin, D. H., and Racker, E. Condensation of arabinose 5-phosphate and phosphorylenol pyruvate by 2-keto-3-deoxy-8-phosphooctonic acid synthetase. *The Journal of Biological Chemistry* **234**, 2532-2538 (1959).

152. Maehr, H., and Smallheer, J. Synthesis of D-arabinose 5-phosphate and D-xylose 5-phosphate. *Carbohydrate Research* **62**, 178-184 (1978).

153. Bednarski, M. D., DiCosimo, C. R., Simon, E. S., Stein, P. D., and Shitesides, G. M. Synthesis of 3-deoxy-D-*manno*-2-actulosonate-8-phosphate (KDO-8-P) from D-arabinose: Generation of D-arabinose-5-phosphate using hexokinase. *Tetrahedron Letters* **29**, 427-430 (1988).

154. Hirschbein, B. L., Mazenod, F. P., and Whitesides, G. M. Synthesis of phosphoenolpyruvate and its used in adenosine triphosphate cofactor regeneration. *Journal of Organic Chemistry* **47**, 3765-3766 (1982).

155. Sols, A., De La Fuente, S., Villar-Palasi. C., and Asensio, C. Substrate specificity and some other properties of baker's yest hexokinase. *Biochemica et Biophysica Acta* **30**, 92-101 (1958).

156. Michalcácová, S., Zalibera, L., Sturdik, E., and Liptaj, T. NMR study of monosaccharide phosphorylation by yeast hexokinase. *Biologia* **41**, 1157-1166 (1986).

157. Slotin, L. A. Current methods of phosphorylation of biological molecules. *Synthesis* **11**, 737-752 (1977).

158. Jones, S. S., Rayner, B., Reese, C. B., Ubasawa, A., and Ubasawa, M. Synthesis of the 3'-terminal decaribonucleoside nonaphosphate of yeast alanine transfer ribonucleic acid. *Tetrahedron* **36**, 3075-3085 (1980).

159. Ramirez, F., and Marecek, J. F. Synthesis of phosphodiesters: The cyclic enediol phosphoryl (CEP) method. *Synthesis* **5**, 449-488 (1985).

160. Sonveaux, E. The organic chemistry underlying DNA synthesis. *Bioorganic Chemistry* **14**, 274-325 (1986).

161. Beaucage, S. L., and Iyer, R. P. The synthesis of specific ribonucleotides and unrelated phosphorylated biomolecules by the phosphoramidite method. *Tetrahedron* **49**, 10441-10488 (1993).

162. Stowell, J. K., and Widlanski, T. S. A new method for the phosphorylation of alcohols and phenols. *Tetrahedron Leters* **36**, 1825-1826 (1995).

163. Dotson, G. D. Mechanistic studies on phosphoenolpyruvate-utinising enzyme involved in bacterial cell wall and lipopolysaccharide biosynthesis. PhD. Thesis. Michigan University. (1994).

164. Miller, G. L., Golder, R. H., and Miller, E. E. Determination of pentose. *Analytical Chemistry* **23**, 903-905 (1951).

165. Summer, J. B. The detection of pentose, formaldehyde, and methyl alcohol. *Journal of the American Chemical Society* **45**, 2378-2380 (1923).

166. White, J. D., and Jeffrey, S. C. Synthesis of the tricarbonyl subunit (C8-C19) of rapamycin *via* tandem chan rearrangement-oxidation. *Journal of Organic Chemistry* **61**, 2600-2601 (1996).

167. Wang, Z. X., Wiebe, L. I., Balzarini, J., DeClercq, E., and Knaus, E. E. Chiral Synthesis of 4-[1-(2-deoxy-α-L-ribofuranosyl)] derivatives of 2-substituted 5-fluoroaniline: "Cytosine Replacement" analogues of deoxy-α-L-cytonide. *Journal of Organic Chemistry* **65**, 9214 – 9219 (2000).

168. Sugai, T., Shen, G-J., Ichikawa, Y., and Wong, C-H. Synthesis of 3-deoxy-D-*manno*-2-octulosonic acid (KDO) and its analogues based on KDO adolase-catalyzed reactions. *Journal of the American Chemical Society* **115**, 413-421 (1993).

169. Birck, M. R., Husan, A., Sheflyahn, G. Y., Ganem, B., and Woodard, R. W. Studies on 3-deoxy-D-*manno*-octulosonic acid 8-phosphate synthase using chorosmate mutase inhibitors. *Bioorganic and Medicinal Chemistry Letters* **11**, 2795-2798 (2001).

170. Ahn, M., Pietersma, A. L., Schofield, L. R., and Parker, E. J. Mechanistic divergence of two closely related enzyme-catalysed reaction. *Organic and Biomolecular Chemistry* **3**, 4046-4049 (2005).

171. Furdui, C. M., Sau, A. K., Yaniv, O., Belakhov, V., Woodard, R. W., Baasov, T., and Anderson, K. S. The use of (*E*)- and (*Z*)-phosphoenol-3-fluoropyruvate as mechanistic probes reveals significant differences between the active sites of KDO8P and DAHP synthases. *Biochemistry* **44**, 7326-7335 (2005).

172. Tanabe, M., and Peters, R. H. (*R*, *S*)-Mevalonolactone-2-^{13}C (2H-pyran-2-one-^{13}C, tetrahydro-4-hydroxy-4-methyl-). *Organic Syntheses Collective Volumes* **60**, 386-392 (1981).

173. Bradford, M. M. A rapid and sensitive method for the quantitation of microgram quantities of protein utilizing the principle of protein–dye binding. *Analytical Biochemistry* **72**, 248-254 (1976).

APPENDIX 1

Molecular Nomenclature

The numbering system for DAH7P and KDO8P begins at the carbon atom of carbonyl group and continue through to the phosphate group:

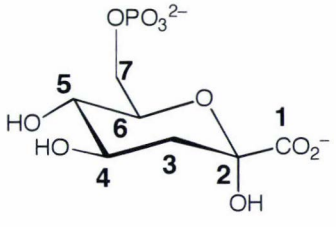

DAH7P

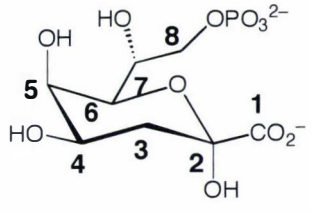

KDO8P

Isomers of DAH7P and KDO8P, which appear in this thesis, have been numbered in the same way.

The numbering used for six-, five-, four-, and three-carbon aldose sugars compounds and their analogues and derivatives in this thesis are numbered in the same way:

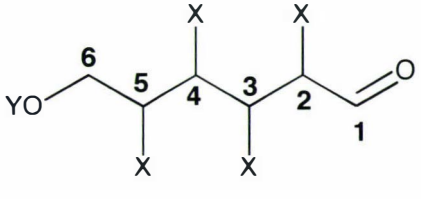

X = H or OH
Y = H or a phosphate moiety

APPENDIX 2

Table of Amino Acids

Amino acid	Symbol	Structure	pK_1 (COOH)	pK_2 (NH_2)	pK_r (R group)
Alanine	**Ala – A**	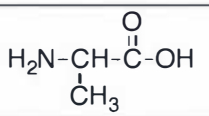	2.4	9.9	
Arginine	**Arg – R**	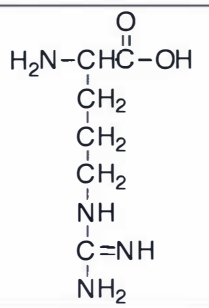	1.8	9.0	12.5
Asparagine	**Asn – N**	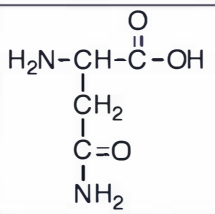	2.1	8.7	
Aspartic acid	**Asp – D**	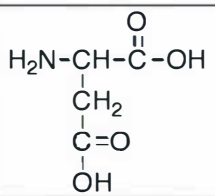	2.0	9.9	3.9
Cysteine	**Cys – C**	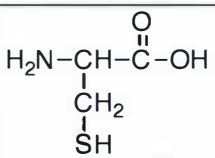	1.9	10.7	8.4
Glutamic acid	**Glu – E**	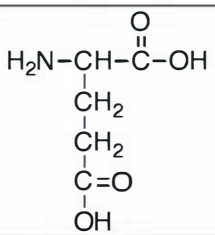	2.1	9.5	4.1

Glutamine	**Gln – Q**	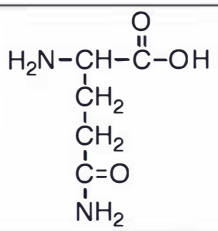	2.2	9.1	
Glycine	**Gly – G**	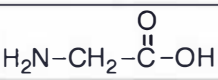	2.4	9.8	
Histidine	**His – H**	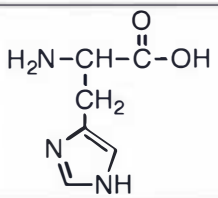	1.8	9.3	6.0
Isoleucine	**Ile – I**	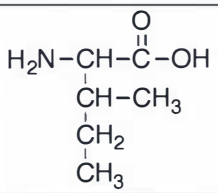	2.3	9.8	
Leucine	**Leu – L**	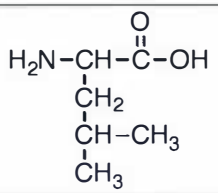	2.3	9.7	
Lysine	**Lys – K**	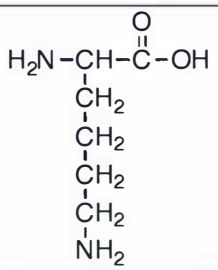	2.2	9.1	10.5
Methionine	**Met – M**	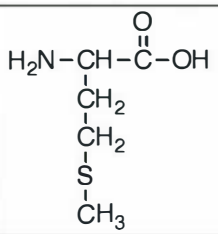	2.1	9.3	
Phenylalanine	**Phe – F**	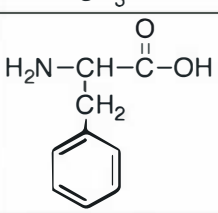	2.2	9.3	
Proline	**Pro – P**	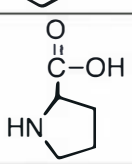	2.0	10.6	

Serine	**Ser – S**	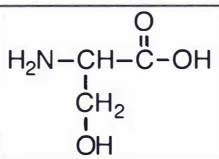	2.2	9.2	
Threonine	**Thr – T**	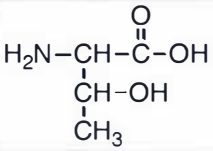	2.1	9.1	
Tryptophan	**Trp – W**	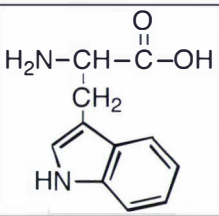	2.5	9.4	
Tyrosine	**Tyr – Y**	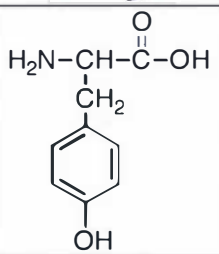	2.2	9.2	10.5
Valine	**Val – V**	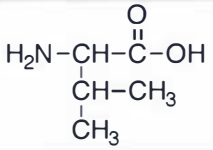	2.4	9.7	

APPENDIX 3

NMR Spectrum for DAH7P, D-DLH7P, L-DXH7P, KDO8P, D-DAO8P, and L-DGO8P

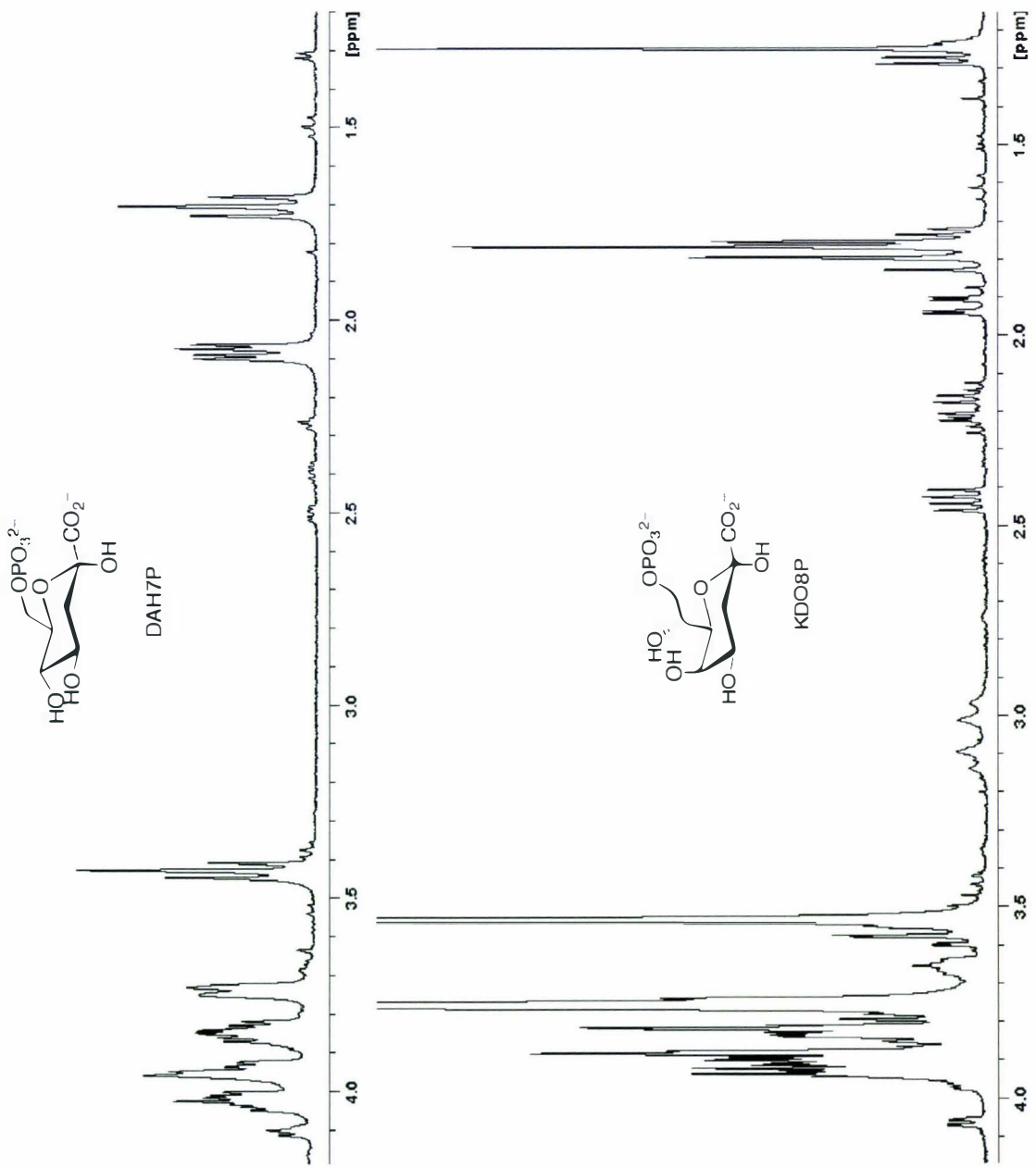

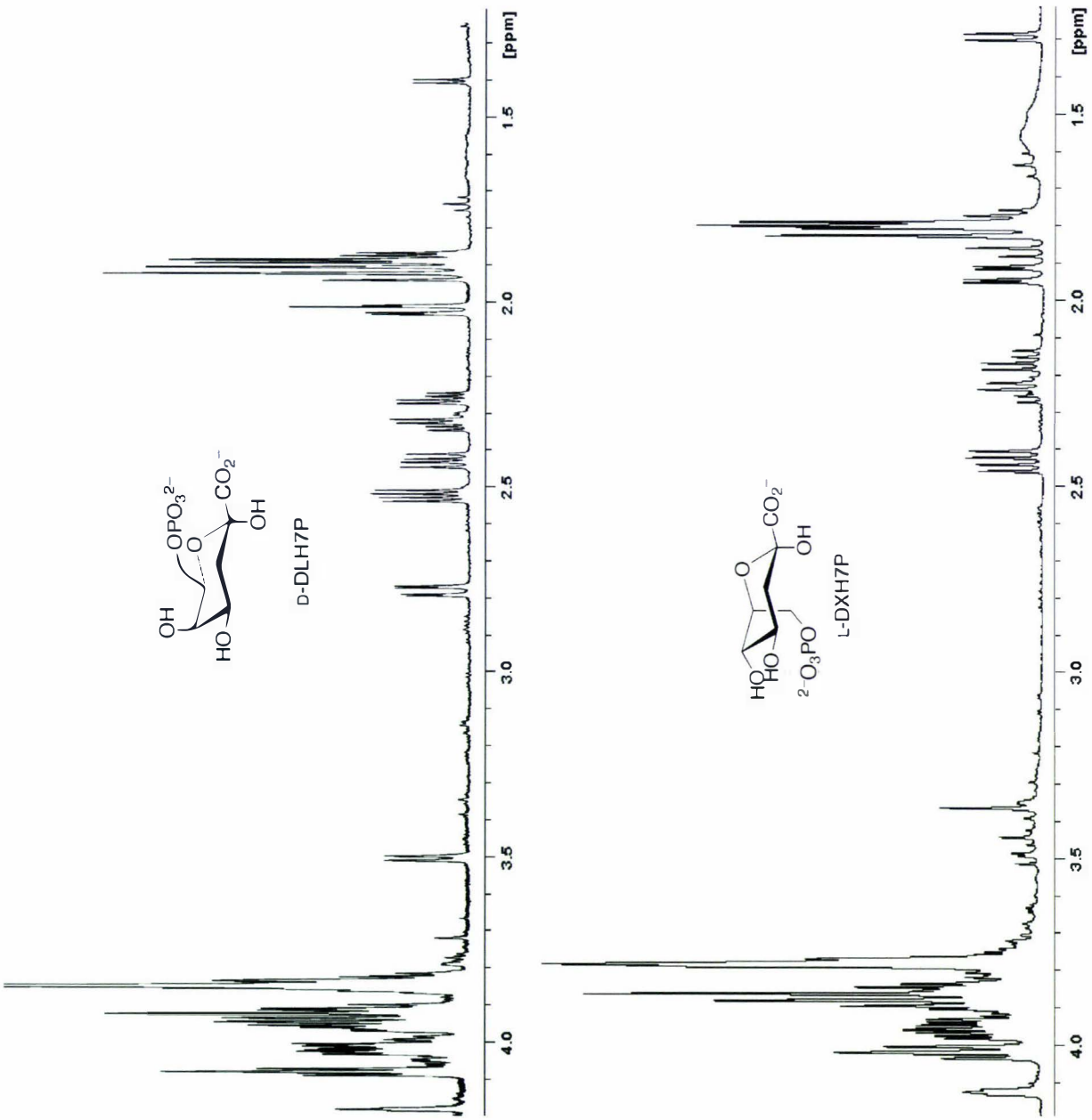
D-DLH7P
L-DXH7P
[ppm]
4.0
3.5
3.0
2.5
2.0
1.5

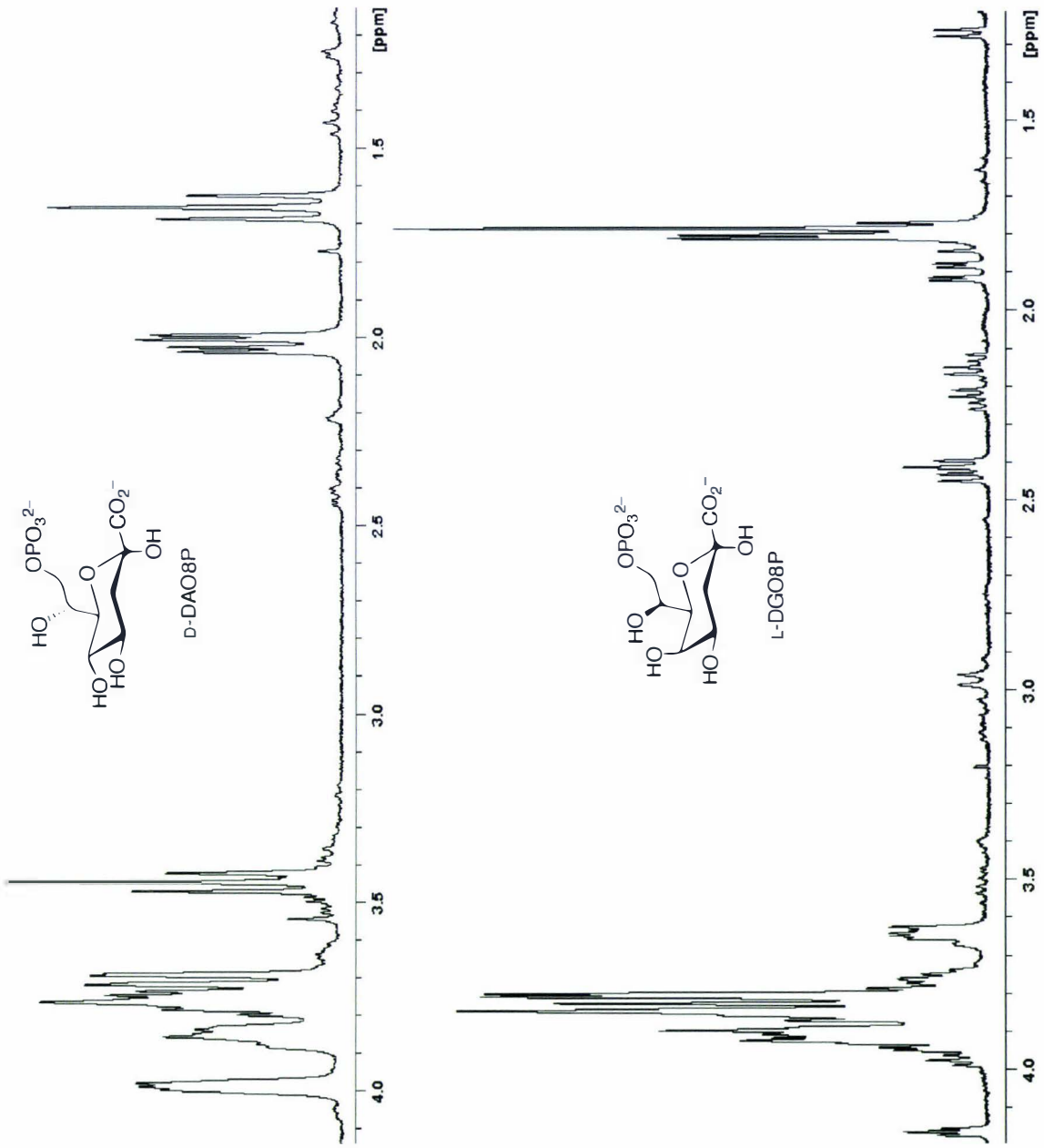
D-DAO8P
L-DGO8P
[ppm]
4.0
3.5
3.0
2.5
2.0
1.5